EINDHOVEN UNIVERSITY OF TECHNOLOGY

Towards the early detection of pregnancy complications using non-invasive assessments of autonomic regulation

Citation for published version (APA):
Bester, M. (2023). *Towards the early detection of pregnancy complications using non-invasive assessments of autonomic regulation*. [Phd Thesis 1 (Research TU/e / Graduation TU/e), Electrical Engineering]. Eindhoven University of Technology.

Document status and date:
Published: 30/06/2023

Document Version:
Publisher's PDF, also known as Version of Record (includes final page, issue and volume numbers)

Please check the document version of this publication:

• A submitted manuscript is the version of the article upon submission and before peer-review. There can be important differences between the submitted version and the official published version of record. People interested in the research are advised to contact the author for the final version of the publication, or visit the DOI to the publisher's website.
• The final author version and the galley proof are versions of the publication after peer review.
• The final published version features the final layout of the paper including the volume, issue and page numbers.

Link to publication

General rights
Copyright and moral rights for the publications made accessible in the public portal are retained by the authors and/or other copyright owners and it is a condition of accessing publications that users recognise and abide by the legal requirements associated with these rights.

• Users may download and print one copy of any publication from the public portal for the purpose of private study or research.
• You may not further distribute the material or use it for any profit-making activity or commercial gain
• You may freely distribute the URL identifying the publication in the public portal.

If the publication is distributed under the terms of Article 25fa of the Dutch Copyright Act, indicated by the "Taverne" license above, please follow below link for the End User Agreement:

www.tue.nl/taverne

Take down policy
If you believe that this document breaches copyright please contact us at:

openaccess@tue.nl

providing details and we will investigate your claim.

Download date: 05. Oct. 2023

Towards the early detection of pregnancy complications using non-invasive assessments of autonomic regulation

Maretha Bester

Towards the early detection of pregnancy complications using non-invasive assessments of autonomic regulation

Maretha Bester

Title:
Towards the early detection of pregnancy complications using non-invasive assessments of autonomic regulation

Author:
Maretha Bester

Cover design and layout by:
Annika Felder

Printed by:
Ipskamp printing

ISBN: 978-90-386-5791-2

This work was performed within the framework of the Eindhoven MedTech Innovation Center (e/MTIC) in collaboration with the Eindhoven University of Technology, Máxima Medical Center (Veldhoven) and Philips Research (Eindhoven).

© Maretha Bester, Eindhoven, the Netherlands, 2023. All rights reserved

Towards the early detection of pregnancy complications using non-invasive assessments of autonomic regulation

THESIS

ter verkrijging van de graad van doctor aan de Technische Universiteit Eindhoven, op gezag van de rector magnificus prof.dr. S.K. Lenaerts, voor een commissie aangewezen door het College voor Promoties, in het openbaar te verdedigen op vrijdag 30 juni 2023 om 16:00 uur

door

Maretha Bester

geboren te Paarl, Zuid-Afrika

Dit proefschrift is goedgekeurd door de promotoren en de samenstelling van de promotiecommissie is als volgt:

Voorzitter:	prof. dr. ir. M.J. Bentum
Promotoren:	prof. dr. ir. M. Mischi
	dr. ir. R. Vullings
Copromotor:	dr. J.O.E.H. van Laar
Promotiecommissieleden:	prof. dr. M.G. Signorini (Politecnico di Milano)
	prof. dr. ir. C. van Pul
	dr. A. Georgieva (University of Oxford)
Adviseur:	dr. ir. R. Joshi (Philips Research, Eindhoven)

Het onderzoek of ontwerp dat in dit proefschrift wordt beschreven is uitgevoerd in overeenstemming met de TU/e Gedragscode Wetenschapsbeoefening.

Executive summary

Executive summary

Every year, 15% of the over 100 million women who become pregnant will develop a type of complication. These pregnancy complications, such as hypertensive disorders of pregnancy and gestational diabetes, not only have detrimental effects during the period of pregnancy but also increase the risk for both the mother and offspring for future diseases. A barrier to reducing the impact of these complications is that they are typically detected after the ideal window for clinical intervention has passed. Efforts to develop improved screening tools are hampered by the unknown etiology of these complications. However, although the origins of pregnancy complications are largely unknown, it is known that women with pregnancy complications have altered autonomic nervous system (ANS) activity compared to those with healthy pregnancies, even as early as the first trimester. Subsequently, assessing maternal autonomic activity may aid in detecting deteriorations in maternal health before the onset of typical symptoms of complications. Furthermore, the technology needed to non-invasively track maternal autonomic regulation is already available. This can be done by assessing heart rate variability (HRV) with wearable heart rate (HR) monitors such as smartwatches using photoplethysmography (PPG), as the ANS regulates HR. However, while the technology may exist, the clinical proof points and physiological insight necessary to implement such a monitoring solution does not. The aim of this thesis is to comprehensively investigate non-invasive measures of maternal autonomic activity and factors that may influence it. In doing so, we address multiple research gaps to move us closer to implementing assessments of autonomic regulation for the early detection of pregnancy complications.

In Section I, *Maternal autonomic regulation during healthy pregnancy,* we show that there are large differences in HRV between pregnant and non-pregnant women and, as a result, assumptions of autonomic activity based on research in non-pregnant women cannot be readily applied to the pregnant population. Additionally, we demonstrate that HRV features capturing non-linear aspects of HR and autonomic responsiveness may be particularly useful in assessing maternal health. Moreover, we determine that assessing features describing the PPG pulse wave, which reflect the autonomically modulated vascular tone and can be extracted from PPG measurements in addition to HRV, provides complimentary value in assessing maternal physiology. Furthermore, we demonstrate that longitudinal assessments of maternal autonomic activity may benefit from focusing on data from a specific sleep stage (for example, deep sleep). Tracking autonomic activity per sleep stage would allow for repeatability between

measurements obtained on different nights. In addition, this may elucidate physiological differences which would remain obscured when assessing autonomic activity based on either an entire night's recording or a time-specific measurement moment.

Next, in Section II, *Factors influencing maternal autonomic regulation during healthy pregnancy*, we investigate which factors – apart from pregnancy complications – may be influencing maternal HRV during pregnancy. We show that maternal HRV changes with progressing gestational age, with identifiable trends such as a sharp decrease in parasympathetic activity at the transition of the second to the third trimester. Furthermore, we determine that maternal characteristics such as age and breathing rate also significantly impact maternal HRV. Ultimately, this section demonstrates that personalized tracking of trends in maternal HRV across pregnancy would be better suited to identifying abnormalities than spot measurements at antenatal appointments.

To characterize the autonomic abnormalities which are indicative of pregnancy complications also necessitates addressing factors that potentially confound autonomic measurements in such complicated pregnancies. In Section III, *The effect of corticosteroids on maternal autonomic regulation in complicated pregnancies,* we address the impact of these routinely administered obstetric medications, which are known to affect fetal HRV, on non-invasive measures of maternal autonomic activity. Based on a secondary analysis as well as a dedicated, prospective study, we show that corticosteroids increase maternal HR, decrease HRV features linked to parasympathetic activity, and have a vasoconstricting effect as reflected by features describing the PPG pulse wave. Consequently, this work demonstrates that studies investigating maternal autonomic regulation in complicated pregnancies should perform measurements before or sufficiently long after corticosteroid administration.

To end, we investigate aspects of autonomic regulations that may offer unique physiological insights and could play a future role in evaluating perinatal health. In Section IV, *Coupling between physiological systems during pregnancy,* we investigate two coupling relationships – i.e., fixed relationships between organ systems – during pregnancy. We first demonstrate that cardiorespiratory coupling is weaker in healthy pregnant women when compared to their non-pregnant counterparts, likely due to the decrease in parasympathetic activity and the remodeling of the maternal respiratory system which occurs during pregnancy. Thereafter, we perform a scoping review of the literature on maternal-fetal cardiac coupling. Our synthesis of the literature reveals

that this coupling relationship indeed exists and that it has potential for assessing perinatal health.

In conclusion, this thesis contains a comprehensive investigation into non-invasive measures of maternal autonomic regulation. We envision that this work will form the basis for using autonomic assessments for the early detection of pregnancy complications. Such early detection would not only reduce perinatal morbidity and mortality but, considering the life-long impact that these complications have on the mother and her offspring, would benefit the health of the society as a whole.

Table of contents

Section IV: Coupling between physiological systems during pregnancy

Chapter 1

Introduction

1. Pregnancy complications

The 40 weeks of pregnancy necessitates substantial changes to the physiology of the mother [1]–[3]. The most apparent change accompanying pregnancy is the growing maternal abdomen. However, this external change merely hints at the complex internal changes which occur to not only sustain the growing fetus but also to maintain maternal health throughout pregnancy and the postpartum period [1]–[3].

All maternal organ systems adapt during pregnancy [2], [3]. For example, by the end of pregnancy, the maternal blood volume has increased by up to 50%, promoting an increased heart rate (HR), vasodilation, and remodeling of the heart to accommodate this increase [3], [4]. Furthermore, to compensate for the strain placed on maternal respiration via the growing uterus pushing up against the thorax, the maternal intercostal muscles – i.e., the muscles between the ribs – relax to remodel the thoracic cavity [5]. This remodeling allows for sufficient lung expansion and maintains the maternal respiratory rate throughout pregnancy [3]–[5]. Even the maternal brain is affected by pregnancy. In evaluating scans of the brains of women who had been pregnant, researchers noticed reductions in the grey matter of these women for up to two years after they had given birth [6]. Additionally, a temporary organ system, namely, the placenta, develops throughout the pregnancy to permit the metabolic exchange between the maternal-fetal dyad [2].

Every year, 140 million babies are born [7], and each of the pregnancies leading up to these births undergoes these complex physiological changes. However, in 15 to 20% of these cases, the pregnancy does not progress as expected and pregnancy complications develop [8]–[10]. Prominent examples of prenancy complications are hypertensive disorders of pregnancy (HDP), gestational diabetes mellitus (GDM), and preterm delivery (PTD).

HDP, which occur in up to 10% of pregnancies [11], are characterized by new-onset hypertension after 20 weeks of gestation [12]. These conditions are the leading cause of maternal deaths [11]. Preeclampsia is a type of HDP that occurs in 3 to 8% of pregnancies [10]–[13]. This condition typically results in the immediate hospitalization of the pregnant woman and often results in the premature delivery of the fetus. Furthermore, preeclampsia is a leading cause of fetal growth restriction. As preeclampsia is thought to have its origins in the development of the placenta, removing this organ – which necessitates the often-premature delivery of the fetus – remains the only way to resolve this complication [13], [14].

Furthermore, 2 to 25% of women develop GDM [10], [15]–[17], depending on the population demographics. GDM, which is diabetes developed during pregnancy, is typically detected with a glucose test administered between the 24th and 28th week of pregnancy [15]. GDM can result in macrosomia, a condition where the fetal birthweight exceeds the 90th percentile (corrected for gestational age and fetal sex) [18]. Macrosomia leads to a riskier delivery, which can result in perinatal and infant morbidity and mortality [18]. Additionally, pregnancies with GDM more regularly result in unplanned cesarean sections [17].

In PTD, the fetus is delivered before 37 weeks of gestation, which is before fetal development is complete [19]. Approximately 11% of births are premature [19]. PTD can result in the newborn having developmental detriments, which may necessitate admission to the neonatal intensive care unit (ICU) if the birth occurs before 32 weeks of gestation, or to the medium care unit when the birth occurs thereafter. Moreover, about 1 million neonatal deaths and 125,000 deaths of children aged one to five are attributable to PTD, making it the leading cause of neonatal and childhood mortality [19].

It is evident that pregnancy complications negatively impact the health of the maternal-fetal pair during pregnancy. However, the danger of these complications is compounded by the long-term effects they can have on the mother and her offspring. The risk of cardiovascular disease is twice as high in women with a history of preeclampsia compared to those who were normotensive during pregnancy [20]. Furthermore, those women with a history of preeclampsia have a 60% increased risk of ischemic stroke later in life [14]. The offspring of women with HDP are also impacted by their mothers' condition, as they have a 23% increase in risk for early-onset cardiovascular disease [21]. Developing GDM during pregnancy results in an up to 50% chance of developing Type 2 diabetes within five years after birth [22], a condition that directly results in more than 1.5 million deaths yearly [23]. Moreover, the offspring of women who had GDM have an increased chance of developing childhood obesity and glucose intolerance [24]. Additionally, being born prematurely can have a detrimental effect on the mental and physiological development of offspring [19]. Finally, experiencing a pregnancy complication significantly increases a woman's risk for postpartum depression [25].

These complications not only place a burden on perinatal health but also on healthcare systems. In the United States (U.S.), the Commonwealth Fund investigated the cost of maternal morbidity, calculated from the year of the pregnancy until five years thereafter [26]. Yearly, HDP resulted in $5.97 billion in medical costs, while for GDM the medical cost was $3.94 billion. However, it is important to remember that pregnancy compli-

cations also result in nonmedical costs, such as lost productivity and the use of social services. For HDP and GDM, these costs add up to $1.57 billion and $0.90 billion [26].

Consequently, addressing the problem of pregnancy complications is important. Reducing the occurrence of these complications would not only reduce perinatal morbidity and mortality but would also improve the health of the general population and reduce financial strains on healthcare systems. The issue of reducing these complications is also pressing as the prevalence of pregnancy complications is increasing [10], and will likely continue to increase. Women are having children increasingly late in life and some researchers have shown that complication rates increase with maternal age [27], [28]. Furthermore, the prevalence of lifestyle diseases such as obesity and hypertension is also rising. In the U.S., between 2014 and 2018, hypertension and type II diabetes both increased by approximately 30% as a pre-existing condition in women who became pregnant, while diagnosed obesity increased by 100% in the same group [10]. As these diseases serve as risk factors for pregnancy complications, this trend will likely result in more women entering pregnancy with pre-existing conditions and consequently developing pregnancy complications [10], [29].

2. Advantages of the early detection of pregnancy complications

One of the main obstacles in reducing the impact of pregnancy complications on perinatal morbidity and mortality is the inability to detect these complications early enough to implement existing interventions [30]–[32]. Currently, complications are typically detected once their symptoms have already manifested, i.e., when the period for preventative care has passed. However, identifying high-risk pregnancies early in gestation could allow for implementing pharmaceutical or lifestyle interventions. These interventions may prevent complications or at least allow for improved management which reduces the impact of complications on perinatal morbidity and mortality [30], [33], [34], as well as on health care systems [35].

A prominent example of early pharmaceutical intervention is the impact of administering aspirin on the risk of developing HDP. Studies show that taking aspirin reduces the severity of preeclampsia, provided that treatment is started before 16 weeks of gestation [30], [32], [36]. However, a medical indication is necessary for such a phar-

maceutical intervention and preeclampsia can currently only be diagnosed after 20 weeks of gestation. Consequently, the accurate and earlier identification of pregnancies that are at risk for preeclampsia is crucial to reducing the impact of this condition. Identifying such high-risk pregnancies also allows for lifestyle interventions such as improvements in diet, a structured exercise plan, and better stress management. As an example, research has shown that lifestyle changes can reduce the risk of GDM, but these changes should ideally start before pregnancy, or at latest before 15 weeks of gestation [37]. However, appropriate allocation of such resources for maximum impact can only be done if high-risk pregnancies are accurately identified as early in pregnancy as possible.

The risk screening tools used in obstetrics – which focus on assessing obstetric history, pre-existing conditions, and intake measurements such as blood pressure (BP) and weight – need to be improved. In the U.S., 29% of pregnancies identified as low-risk encountered an unexpected complication requiring nonroutine obstetric or neonatal care [38]. While it is generally agreed upon that personalized prediction models would improve obstetric risk stratifications, such models are not available in practice [30]. Research on this topic is ongoing but many of the solutions suggested are computationally complex or require measurements that are invasive or which are not practical to acquire repeatedly, such as serum protein levels, for example placental growth factor, and fetal fibronectin [30], [39].

A logical approach for detecting a condition as early as possible is by focusing on the etiology of that condition, i.e., the factors which cause the condition to occur. In the case of pregnancy complications, however, the etiologies of these remain unknown [9], further impeding efforts in their early detection. However, studies have shown that women who develop pregnancy complications already show signs of dysfunctional autonomic regulation in the first trimester [15], [16]. Therefore, detecting abnormalities in autonomic activity may aid in improving obstetric risk screening [40], [41].

3. Pregnancy complications and the maternal autonomic nervous system

The autonomic nervous system (ANS) is the system in the human body responsible for regulating involuntary processes such as BP, respiration, and HR. The ANS comprises

two main branches: the parasympathetic nervous system (PNS) and the sympathetic nervous system (SNS). The PNS, of which the main component is the vagal nerve, is dominant during more restful conditions, such as relaxation and sleep. The SNS, which is often referred to as the 'fight-or-flight' system, controls the body's stress response and is dominant in situations such as exercise or where there is perceived danger. A healthy autonomic state comprises an interplay between these systems which appropriately regulates bodily homeostasis in reaction to internal and external stimuli [42], [43].

Considering the substantial maternal physiological changes necessary during pregnancy, it stands to reason that appropriate maternal autonomic regulation is essential in sustaining healthy gestation [1], [44]. This is further confirmend by the association of pregnancy complications with autonomic dysfunction [16], [40], [41], [45], [46]. The balance between the SNS and PNS, which is referred to as the sympathovagal balance, is altered in women with pregnancy complications [44]. Specifically, pregnancy complications are accompanied by sympathetic overactivity and vagal withdrawal [44]. Moreover, these changes can already be observed in the first trimester. Pal *et al.* investigated sympathovagal balance in women with at least one risk factor for developing HDP [40]. Already at 12 weeks of pregnancy, they found significantly stronger changes in sympathovagal balance in those who would eventually develop HDP. Furthermore, Qui *et al.* demonstrated that an elevated resting HR, which can also be linked to sympathetic overactivity and reduced activity of the PNS, was linked to a higher incidence of GDM in women who were considered low-risk [15].

4. Non-invasive, unobtrusive assessment of the autonomic nervous system

Not only are changes in autonomic activity present before the typical onset of the symptoms of pregnancy complications, but non-invasive, unobtrusive methods by which to assess the ANS exist. As the ANS is regulating the heartbeat, assessing heart rate variability (HRV) provides a window into autonomic regulation [42]. Assessing HRV requires continuous HR information. While several modalities exisit which can non-invasively acquired HR information, such as seismocardiography and phonocardiography, the most prominant two are electrocardiography (ECG) and photoplethysmography (PPG). ECG captures the electrophysiological activity of the heart as it

depolarizes and repolarizes with each beat, resulting in the bottom waveform seen in Figure 1. From the ECG, the times between the R-peaks (depicted as RR in Figure 1) are determined, which represent the time between heartbeats. ECG measurements serve as the gold standard when calculating HRV.

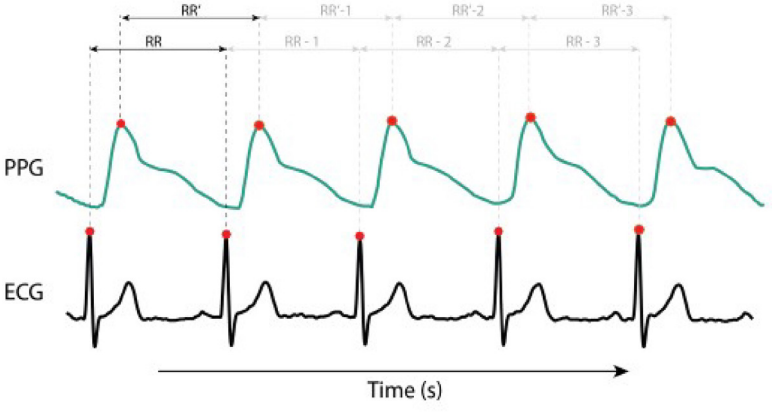

Figure 1: PPG (top) and ECG (bottom) waveforms, adapted from Vandenberk et al. [47]

However, an ECG measurement typically needs to be performed by a person trained to do so, either in a doctor's office or a clinical setting. Wearable ECG monitors do exist, referred to as Holter ECGs, but even these are cumbersome to wear and involve several wires, as can be seen in the left panel of Figure 2. An alternative non-invasive method for monitoring HRV is wrist-worn photoplethysmography (PPG) [48]. An example of this device can be seen in the right panel of Figure 2. PPG uses a light source and a photodetector at the surface of the skin to measure the volumetric variations of blood circulation, ultimately resulting in the top waveform in Figure 1, and can be used for unobtrusive, continuous monitoring. There are also peaks in the pulse waves detected with PPG, representing the heartbeats. Subsequently, the interval between these pulses (represented by RR' in Figure 1) can be determined and used to calculate HRV. Furthermore, the PPG waveform is a reflection of the compliance of the blood vessels, i.e., vascular tone, which is also autonomically regulated. Therefore, assessing the morphology of the pulse wave can offer additional insight into the ANS [48].

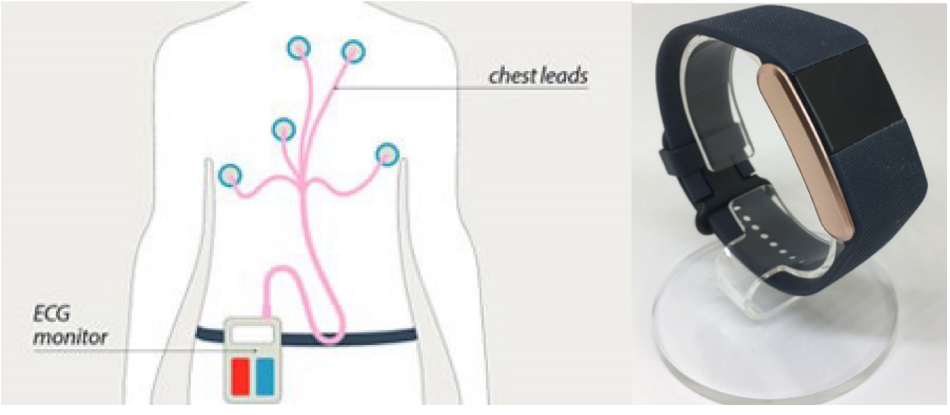

Figure 2: A diagram of a Holter ECG setup, from the British Heart Foundation, (left) and a wrist-worn PPG device (right), sourced from the Philips Asset Library.

While HRV is the most popular and pragmatic method, other methods are available by which to study autonomic activity. Specifically, the ANS facilitates fixed interactions between physiological systems and by assessing these interactions, further insight can be gained into autonomic functioning [49]. A prominent example of this is the interaction between the cardiac and respiratory systems, referred to as cardiorespiratory coupling (CRC), which varies in different autonomic states [49], [50]. As assessing physiological couplings typically requires multiple time-synchronized measurements over an extended period, this method is less pragmatic than HRV. However, assessing such couplings offer unique insights into physiology.

5. The goal of the thesis

Given the autonomic dysregulation present in high-risk pregnancies and the pragmatism of using HRV to assess autonomic regulation, monitoring maternal HRV during pregnancy may offer novel opportunities for assessing maternal health and in doing so, aid in the early detection of pregnancy complications. Enabling such a solution requires extensive knowledge of maternal autonomic regulation in a healthy pregnancy, particularly as assessed by non-invasive methods. However, this knowledge is currently lacking. The goal of this thesis, titled *Towards the early detection of pregnancy complications using non-invasive assessments of autonomic regulation*, is to develop the insights needed to enable the detection of pregnancy complications via assessments of autonomic activity.

We envisioned the ideal endpoint, one where a woman receives a PPG watch at their first antenatal appointment and wears it throughout their pregnancy. Her HRV, i.e., maternal HRV, is monitored throughout pregnancy and if abnormalities are detected, the risk profile of the pregnancy is re-examined, and extra monitoring or support is offered. Keeping in mind this endpoint, we attempted to gain the insights needed to reduce the obstacles hindering such a solution.

We approached this task from first principles and built up this thesis step by step. In clinically focused projects, collecting the physiological data necessary to investigate hypotheses is typically a major challenge. During this PhD study, we planned and executed a study in the obstetric high care unit of the Máxima Medical Center (Máxima MC), Veldhoven, the Netherlands, of which the results are reported in this thesis. However, considering how costly such data collection is in terms of labor, time, and finances – all further compounded by the onset of the Covid-19 pandemic a year into this PhD – we also investigated the possibilities of performing secondary analyses of data already available within our environment, which would help us move closer to the envisioned end goal. To this end, we acquired ethical approval from relevant institutions to reuse data from five different data collections. Additionally, we used data from Physionet, a public database of physiological signals. In total, seven datasets were analyzed.

As the starting point, we consider that HRV is an established research field and as such, the HRV of women of childbearing age has been extensively studied [51]–[53]. Subsequently, we first aim to understand the impact of pregnancy on autonomic regulation by comparing HRV and PPG pulse wave morphology between healthy pregnant and non-pregnant women. This enables us to understand whether assumptions of autonomic functioning based on non-pregnant women can be translated to the pregnant population, or, alternatively, what to expect concerning healthy maternal autonomic activity. However, identifying high-risk pregnancies based on abnormalities in maternal autonomic regulation necessitates identifying which other factors may also influence maternal HRV. To this end, we investigate the effect of the progression of pregnancy as well as the characteristics of the mother such as age or parity on maternal autonomic regulation. Furthermore, we also investigate how the administration of routine obstetric medications might affect autonomic regulation in women with complicated pregnancies. Once many of the obstacles hampering the use of maternal HRV and PPG in detecting autonomic abnormalities have been addressed, we shift our focus. We investigate coupling relationships between physiological systems in

pregnancy to gain deeper insight into the physiology of pregnancy and potentially open new avenues by which to assess maternal and fetal health.

6. Outline of the thesis

This thesis consists of nine first-authored articles written for publication in international journals. These works are divided into four sections, namely I) Maternal autonomic regulation during healthy pregnancy, II) Factors influencing maternal autonomic regulation during healthy pregnancy, III) The effect of corticosteroids on maternal autonomic regulation in complicated pregnancies, and IV) Coupling between physiological systems during pregnancy. The work was done in a collaboration between Eindhoven University of Technology, Philips Research, and Máxima MC.

Section I: Maternal autonomic regulation during healthy pregnancy

Considerable research has been performed to characterize HRV in healthy women, including women of childbearing age [51]–[53]. Consequently, if pregnant women do not differ remarkably from their non-pregnant counterparts in terms of autonomic activity, findings from these investigations can be translated to the pregnant population. Therefore, in **Chapter 2**, we perform the largest and most comprehensive comparison of HRV between pregnant and non-pregnant women available in the literature. We use ECG measurements in this study, which serve as the gold standard for HRV analyses, and focus on the effect sizes of the differences between the groups to understand the magnitude of the impact of pregnancy on HRV, as well as which features are most altered by gestation. Additionally, we repeat our analysis to compare differences between men and women, thereby further contextualizing our results with regard to effect sizes.

However, while it is important to use gold standard measurements to establish initial insights on maternal HRV in **Chapter 2**, wrist-worn PPG measurements would most likely be used in real-life applications of tracking maternal health as such devices are less obtrusive and more practical to wear during daily life. Furthermore, owing to the predisposition of PPG measurements to motion artifacts, measurements used towards this goal would likely occur during the night, when motion is more limited. Subsequently, in **Chapter 3**, we again compare HRV between pregnant and non-pregnant women, now based on wrist-worn PPG measurements. Additionally, we compare differences in the PPG pulse wave morphology between the two groups. Little is cur-

rently known about how pulse wave morphology is impacted by healthy pregnancy [54]–[58], but as vascular tone in autonomically regulated [48], features describing this morphology may be valuable in assessing maternal health. Furthermore, we aim to establish which HRV and morphological features are most impacted by healthy pregnancy, as these potentially reflect changes in the physiology characteristic of a healthy pregnancy and would likely be valuable in assessing maternal health. To this end, we employ a binary classification model as a tool to identify which features contribute the most to discriminating between these two groups. Furthermore, we stratify our analyses by sleep stages, each of which represents a different autonomic state [59], allowing us to investigate whether differences between pregnant and non-pregnant women are amplified under different autonomic environments.

Section II: Factors influencing maternal autonomic regulation during healthy pregnancy

From Section I, we gain an in-depth understanding of how non-invasive features of autonomic regulation are altered in a healthy pregnancy. However, facilitating the detection of pregnancy complications via the identification of abnormalities in maternal HRV requires not only an understanding of how pregnancy complications affect maternal HRV but also how other confounding factors may alter maternal HRV. One such factor is gestational age. Pregnancy is not a finite state but rather a period of continuous change. Consequently, in **Chapter 4**, we track how maternal HRV changes with progressing pregnancy.

Furthermore, HRV is known to be affected by an individual's characteristics. For example, HRV changes with age [52]. Still, the effects of individuals' characteristics on maternal HRV remain largely unexplored. In **Chapter 5**, we study the effects of maternal characteristics on their HRV by performing two analyses. First, we develop a multiple linear regression model based on a large dataset of single measurements to characterize the effects of maternal demographics and cardiorespiratory factors on maternal HRV. Second, we analyze a dataset of repeated measurements (median of eight per woman) to develop a linear mixed-effects model, which allows us to discern the impact of inter-subject variability.

Section III: The effect of corticosteroids on maternal autonomic regulation in complicated pregnancies

In addition to having a comprehensive understanding of autonomic activity in a healthy pregnancy, using non-invasive indices of autonomic activity to assess mater-

nal health also requires a clear understanding of how such indices are altered during pregnancy complications. However, women are directly hospitalized once pregnancy complications such as preeclampsia are detected and administered routine obstetric medications upon admission. As such, investigations into maternal HRV in complicated pregnancies often occur once participants have already received these medications, of which the potentially confounding effects are unknown [45], [60]. The most prominent of these medications are corticosteroids, which are administered to accelerate fetal maturation in anticipation of preterm birth [61]. As corticosteroids are known to affect fetal HRV [62]–[64], it stands to reason that maternal HRV might be likewise affected. In **Chapter 6**, we perform a secondary analysis of abdominal measurements – from which both fetal and maternal HR data can be extracted – which were initially acquired to study the effect of corticosteroids on fetal HRV. From these data, we track changes in maternal HRV in the five days following corticosteroid administration.

The group of women who receive corticosteroids is heterogeneous in terms of their pregnancy complications, age, etc. Furthermore, corticosteroids may be administered at any time of the day. Therefore, a within-subject comparison would be preferred to minimize the effect of maternal characteristics and circadian rhythm on the results, which the data analyzed in **Chapter 6** do not allow for. Therefore, to confirm the findings in **Chapter 6**, a prospective study is needed that is dedicated to assessing the effects of these medications on the mother using a within-subject analysis. Additionally, considering again that a wrist-worn PPG device would likely be used to track maternal autonomic regulation in practice, the effect of corticosteroids on the PPG pulse wave is also relevant. To this end, we designed and executed a prospective study in which PPG data were collected in hospitalized pregnant women with an indication for corticosteroids. The published protocol of this study is found in **Chapter 7**, while the results are presented in **Chapter 8**.

Section IV: Coupling between physiological systems during pregnancy

Finally, we investigate physiological coupling relationships between organ systems in pregnancy. Assessing such coupling relationships may in the future offer additional avenues for assessing perinatal health. Furthermore, studying such relationships deepens our understanding of the physiology of pregnancy. In **Chapter 9**, we assess the impact of pregnancy on CRC by comparing for the first time the difference in CRC between healthy pregnant and non-pregnant women. Following the same strategy employed in **Chapter 3**, we again stratify this analysis by sleep stages. As autonomic activity differs per sleep stage [50], this stratification offers a type of autonomic filter

that allows us to further delve into the physiological drivers underpinning potential differences in CRC.

Finally, we investigate a coupling that is unique to pregnancy. Gestation is a physiological period wherein the physiology of the mother and fetus are interconnected. Some researchers suggest that assessing the potential coupling between the cardiac systems of the mother and fetus may be beneficial to the field of obstetrics [65]–[67]. However, maternal-fetal cardiac coupling (MFCC) is still a new research domain, and it is not yet clear whether MFCC indeed exists and if so, how it may be utilized in assessing perinatal health. In **Chapter 10**, we aim to ascertain the current state of research on MFCC with a scoping review and, in doing so, form a foundation for future clinically oriented research on this topic. To this end, we perform a search of all available research in this field. Thereafter, we synthesize the evolution of the methodologies employed to capture coupling. Next, we summarize the results to determine whether MFCC indeed exists and if so, which physiological pathways have been proposed to possibly explain this coupling. Finally, we discuss the potential clinical implications of MFCC.

The conclusions of this work are presented in **Chapter 11**. Here, we synthesize the findings of **Chapters 2** to **10**. Furthermore, we reflect on the potential and possible pitfalls of maternal HRV as an obstetric screening tool and how such a solution may complement current antenatal care systems. To conclude, future work is proposed which needs to be undertaken to make the use of non-invasive assessments of maternal autonomic regulations for the early detection of pregnancy complications a reality. In summary, Figure 3 offers an overview of the different sections and chapters presented in this thesis.

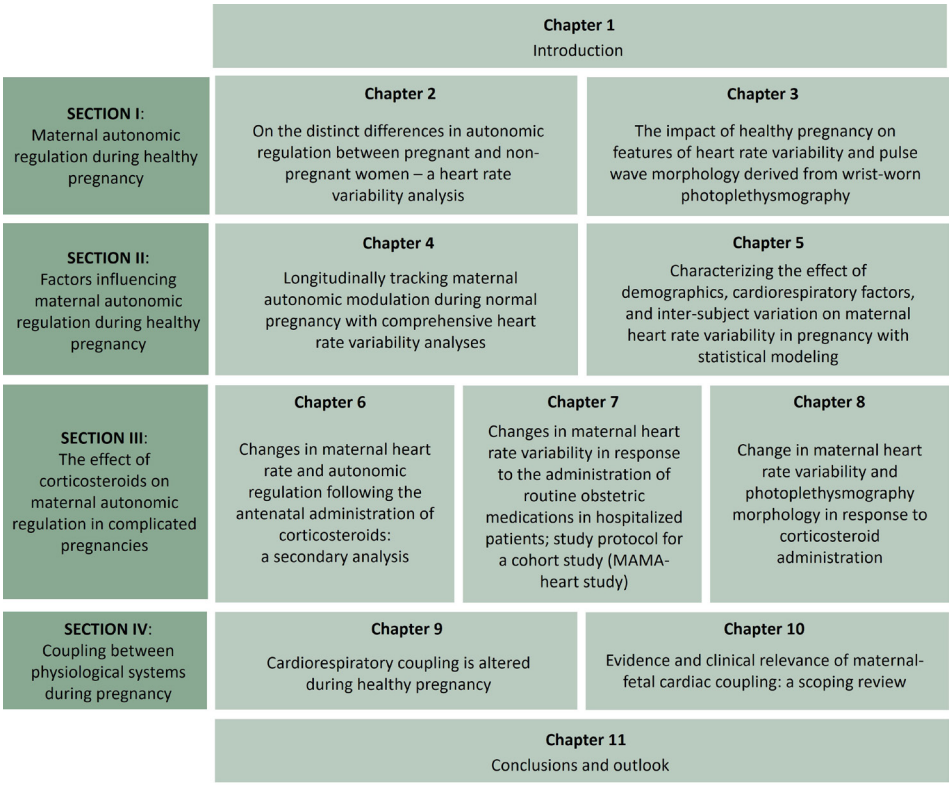

Figure 3: Overview of the different sections and chapters presented in this thesis.

References

[1] Q. Fu, "Hemodynamic and Electrocardiographic Aspects of Uncomplicated Singleton Pregnancy.," *Advances in experimental medicine and biology*, vol. 1065, pp. 413–431, 2018, doi: 10.1007/978-3-319-77932-4_26.

[2] J. M. Kazma, J. van den Anker, K. Allegaert, A. Dallmann, and H. K. Ahmadzia, "Anatomical and physiological alterations of pregnancy," *J Pharmacokinet Pharmacodyn*, Feb. 2020, doi: 10.1007/s10928-020-09677-1.

[3] P. Soma-Pillay, C. Nelson-Piercy, H. Tolppanen, and A. Mebazaa, "Physiological changes in pregnancy.," *Cardiovascular journal of Africa*, vol. 27, no. 2, pp. 89–94, 2016, doi: 10.5830/CVJA-2016-021.

[4] L. J. Green *et al.*, "Gestation-Specific Vital Sign Reference Ranges in Pregnancy," *Obstetrics & Gynecology*, vol. 135, no. 3, pp. 653–664, Mar. 2020, doi: 10.1097/AOG.0000000000003721.

[5] A. LoMauro and A. Aliverti, "Respiratory physiology of pregnancy: Physiology masterclass," *Breathe*, vol. 11, no. 4, pp. 297–301, Dec. 2015, doi: 10.1183/20734735.008615.

[6] E. Hoekzema *et al.*, "Pregnancy leads to long-lasting changes in human brain structure," *Nat Neurosci*, vol. 20, no. 2, pp. 287–296, Feb. 2017, doi: 10.1038/nn.4458.

[7] "Number of births per year," *The world counts*, Feb. 2023. https://www.theworldcounts.com/populations/world/births

[8] World Health Organization, United Nations Population Fund, Mailman School of Public Health. Averting Maternal Death and Disability, and United Nations Children's Fund (UNICEF), "Monitoring emergency obstetric care : a handbook," *Surveillance des soins obstétricaux d'urgence : manuel d'utilisation*, p. 152, 2009, Accessed: Jan. 18, 2023. [Online]. Available: https://apps.who.int/iris/handle/10665/44121

[9] Y. A. Barbitoff *et al.*, "A Data-Driven Review of the Genetic Factors of Pregnancy Complications," *IJMS*, vol. 21, no. 9, p. 3384, May 2020, doi: 10.3390/ijms21093384.

[10] "Trends in pregnancy and childbirth complications in the U.S.," Blue Cross Blue Shield Association, Jun. 2020. [Online]. Available: https://www.bcbs.com/sites/default/files/file-attachments/health-of-america-report/HoA_Maternal_Health.pdf

[11] M. Forrest *et al.*, "Arterial stiffness measurements in pregnancy as a predictive tool for hypertensive disorders of pregnancy and preeclampsia: Protocol for a systematic review and meta-analysis," *European Journal of Obstetrics & Gynecology and Reproductive Biology: X*, vol. 13, p. 100141, Jan. 2022, doi: 10.1016/j.eurox.2022.100141.

[12] J. O. Lo, J. F. Mission, and A. B. Caughey, "Hypertensive disease of pregnancy and maternal mortality," *Current Opinion in Obstetrics & Gynecology*, vol. 25, no. 2, pp. 124–132, Apr. 2013, doi: 10.1097/GCO.0b013e32835e0ef5.

[13] B. W. J. Mol, C. T. Roberts, S. Thangaratinam, L. A. Magee, C. J. M. de Groot, and G. J. Hofmeyr, "Pre-eclampsia," *The Lancet*, vol. 387, no. 10022, pp. 999–1011, Mar. 2016, doi: 10.1016/S0140-6736(15)00070-7.

[14] H. R. Turbeville and J. M. Sasser, "Preeclampsia beyond pregnancy: long-term consequences for mother and child," *American Journal of Physiology-Renal Physiology*, vol. 318, no. 6, pp. F1315–F1326, Jun. 2020, doi: 10.1152/ajprenal.00071.2020.

[15] J. Qiu, L. Chen, X. Wang, and W. Zhu, "Early-pregnancy maternal heart rate is related to gestational diabetes mellitus (GDM)," *European Journal of Obstetrics & Gynecology and Reproductive Biology*, vol. 268, pp. 31–36, Jan. 2022, doi: 10.1016/j.ejogrb.2021.11.007.

[16] L. M. Reyes *et al.*, "Sympathetic nervous system activity and reactivity in women with gestational diabetes mellitus," *Physiol Rep*, vol. 8, no. 13, Jul. 2020, doi: 10.14814/phy2.14504.

[17] C. Phaloprakarn and S. Tangjitgamol, "Risk score for predicting primary cesarean delivery in women with gestational diabetes mellitus," *BMC Pregnancy Childbirth*, vol. 20, no. 1, p. 607, Dec. 2020, doi: 10.1186/s12884-020-03306-y.

[18] X. Zhang, A. Decker, R. W. Platt, and M. S. Kramer, "How big is too big? The perinatal consequences of fetal macrosomia," *American Journal of Obstetrics and Gynecology*, vol. 198, no. 5, p. 517.e1-517.e6, May 2008, doi: 10.1016/j.ajog.2007.12.005.

[19] M. S. Harrison and R. L. Goldenberg, "Global burden of prematurity," *Seminars in Fetal and Neonatal Medicine*, vol. 21, no. 2, pp. 74–79, Apr. 2016, doi: 10.1016/j.siny.2015.12.007.

[20] W. Ying, J. M. Catov, and P. Ouyang, "Hypertensive Disorders of Pregnancy and Future Maternal Cardiovascular Risk," *JAHA*, vol. 7, no. 17, p. e009382, Sep. 2018, doi: 10.1161/JAHA.118.009382.

[21] C. Huang *et al.*, "Maternal hypertensive disorder of pregnancy and offspring early-onset cardiovascular disease in childhood, adolescence, and young adulthood: A national population-based cohort study," *PLoS Med*, vol. 18, no. 9, p. e1003805, Sep. 2021, doi: 10.1371/journal.pmed.1003805.

[22] "Diabetes in pregnancy: management from preconception to the postnatal period," National Institue for Health and Care Excellence, Feb. 2015. [Online]. Available: https://www.nice.org.uk/guidance/ng3/chapter/Recommendations-for-research#postnatal-treatment-for-women-diagnosed-with-gestational-diabetes

[23] Institute for Health Metrics and Evaluation, "Global Burden of Disease Collaborative Network. Global Burden of Disease Study 2019. Results.," 2020.

[24] E. Sheiner, "Gestational Diabetes Mellitus: Long-Term Consequences for the Mother and Child Grand Challenge: How to Move on Towards Secondary Prevention?," vol. 1, 2020.

[25] B. Mbarak, C. Kilewo, S. Kuganda, and B. F. Sunguya, "Postpartum depression among women with pre-eclampsia and eclampsia in Tanzania; a call for integrative intervention," *BMC Pregnancy Childbirth*, vol. 19, no. 1, p. 270, Dec. 2019, doi: 10.1186/s12884-019-2395-3.

[26] S. O'Neil *et al.*, "The High Costs of Maternal Morbidity Show Why We Need Greater Investment in Maternal Health," Commonwealth Fund, Nov. 2021. [Online]. Available: https://doi.org/10.26099/nz8s-4708

[27] S. C. Lean, H. Derricott, R. L. Jones, and A. E. P. Heazell, "Advanced maternal age and adverse pregnancy outcomes: A systematic review and meta-analysis," *PLoS ONE*, vol. 12, no. 10, p. e0186287, Oct. 2017, doi: 10.1371/journal.pone.0186287.

[28] A. Bouzaglou *et al.*, "Pregnancy at 40 years Old and Above: Obstetrical, Fetal, and Neonatal Outcomes. Is Age an Independent Risk Factor for Those Complications?," *Front. Med.*, vol. 7, p. 208, May 2020, doi: 10.3389/fmed.2020.00208.

[29] S. E. Geller, S. M. Cox, W. M. Callaghan, and C. J. Berg, "Morbidity and mortality in

pregnancy," *Women's Health Issues*, vol. 16, no. 4, pp. 176–188, Jul. 2006, doi: 10.1016/j.whi.2006.06.003.

[30] A. C. De Kat, J. Hirst, M. Woodward, S. Kennedy, and S. A. Peters, "Prediction models for preeclampsia: A systematic review," *Pregnancy Hypertension*, vol. 16, pp. 48–66, Apr. 2019, doi: 10.1016/j.preghy.2019.03.005.

[31] A. Mate, C. Reyes-Goya, Á. Santana-Garrido, and C. M. Vázquez, "Lifestyle, Maternal Nutrition and Healthy Pregnancy," *Current Vascular Pharmacology*, vol. 19, no. 2, pp. 132–140, Mar. 2021, doi: 10.2174/1570161118666200401112955.

[32] Y. Cui, B. Zhu, and F. Zheng, "Low-dose aspirin at ≤16 weeks of gestation for preventing preeclampsia and its maternal and neonatal adverse outcomes: A systematic review and meta-analysis," *Exp Ther Med*, vol. 15, no. 5, pp. 4361–4369, May 2018, doi: 10.3892/etm.2018.5972.

[33] US Preventive Services Task Force *et al.*, "Screening for Preeclampsia: US Preventive Services Task Force Recommendation Statement," *JAMA*, vol. 317, no. 16, p. 1661, Apr. 2017, doi: 10.1001/jama.2017.3439.

[34] M. Murphy, S. McHugh, L. M. O'Keeffe, R. A. Greene, P. Corcoran, and P. M. Kearney, "Preventive health counselling during antenatal care using the pregnancy risk assessment monitoring system (PRAMS) in Ireland," *BMC Pregnancy Childbirth*, vol. 20, no. 1, p. 98, Dec. 2020, doi: 10.1186/s12884-020-2756-y.

[35] L. Huynh *et al.*, "Systematic Literature Review of the Costs of Pregnancy in the US," *PharmacoEconomics*, vol. 31, no. 11, pp. 1005–1030, Nov. 2013, doi: 10.1007/s40273-013-0096-8.

[36] E. Bujold *et al.*, "Prevention of Preeclampsia and Intrauterine Growth Restriction With Aspirin Started in Early Pregnancy: A Meta-Analysis," *Obstetrics & Gynecology*, vol. 116, no. 2, pp. 402–414, Aug. 2010, doi: 10.1097/AOG.0b013e3181e9322a.

[37] C. Song, J. Li, J. Leng, R. C. Ma, and X. Yang, "Lifestyle intervention can reduce the risk of gestational diabetes: a meta-analysis of randomized controlled trials: Lifestyle Intervention and GDM," *Obesity Reviews*, vol. 17, no. 10, pp. 960–969, Oct. 2016, doi: 10.1111/obr.12442.

[38] V. A. Danilack, A. P. Nunes, and M. G. Phipps, "Unexpected complications of low-risk pregnancies in the United States," *American Journal of Obstetrics and Gynecology*, vol. 212, no. 6, p. 809.e1-809.e6, Jun. 2015, doi: 10.1016/j.ajog.2015.03.038.

[39] C. E. Kleinrouweler *et al.*, "Prognostic models in obstetrics: available, but far from applicable.," *American journal of obstetrics and gynecology*, vol. 214, no. 1, pp. 79-90.e36, Jan. 2016, doi: 10.1016/j.ajog.2015.06.013.

[40] G. K. Pal, P. Shyma, S. Habeebullah, P. Shyjus, and P. Pal, "Spectral Analysis of Heart Rate Variability for Early Prediction of Pregnancy-Induced Hypertension," *Clinical and Experimental Hypertension*, vol. 31, no. 4, pp. 330–341, Jan. 2009, doi: 10.1080/10641960802621333.

[41] S. Rang, H. Wolf, G. A. Montfrans, and J. M. Karemaker, "Non–invasive assessment of autonomic cardiovascular control in normal human pregnancy and pregnancy- associated hypertensive disorders: a review," *Journal of Hypertension*, vol. 20, no. 11, pp. 2111–2119, 2002.

[42] F. Shaffer and J. P. Ginsberg, "An Overview of Heart Rate Variability Metrics and Norms," *Front. Public Health*, vol. 5, p. 258, Sep. 2017, doi: 10.3389/fpubh.2017.00258.

[43] W. Jänig, *The Integrative Action of the Autonomic Nervous System: Neurobiology of Homeostasis*, 2nd ed. Cambridge University Press, 2022. doi: 10.1017/9781108778411.

[44] V. L. Brooks, Q. Fu, Z. Shi, and C. M. Heesch, "Adaptations in autonomic nervous system regulation in normal and hypertensive pregnancy," in *Handbook of Clinical Neurology*, Elsevier, 2020, pp. 57–84. doi: 10.1016/B978-0-444-64239-4.00003-5.

[45] S. Moors *et al.*, "Heart rate variability in hypertensive pregnancy disorders: a systematic review," *Pregnancy Hypertension*, Mar. 2020, doi: 10.1016/j.preghy.2020.03.003.

[46] L. M. Reyes, C. W. Usselman, M. H. Davenport, and C. D. Steinback, "Sympathetic Nervous System Regulation in Human Normotensive and Hypertensive Pregnancies.," *Hypertension (Dallas, Tex. : 1979)*, vol. 71, no. 5, pp. 793–803, May 2018, doi: 10.1161/HYPERTENSIONAHA.117.10766.

[47] T. Vandenberk *et al.*, "Clinical Validation of Heart Rate Apps: Mixed-Methods Evaluation Study," *JMIR Mhealth Uhealth*, vol. 5, no. 8, p. e129, Aug. 2017, doi: 10.2196/mhealth.7254.

[48] J. Allen, "Photoplethysmography and its application in clinical physiological measurement," *Physiol. Meas.*, vol. 28, no. 3, pp. R1–R39, Mar. 2007, doi: 10.1088/0967-3334/28/3/R01.

[49] T. E. Dick *et al.*, "Cardiorespiratory Coupling," in *Progress in Brain Research*, Elsevier, 2014, pp. 191–205. doi: 10.1016/B978-0-444-63274-6.00010-2.

[50] R. P. Bartsch, A. Y. Schumann, J. W. Kantelhardt, T. Penzel, and P. Ch. Ivanov, "Phase transitions in physiologic coupling," *Proc. Natl. Acad. Sci. U.S.A.*, vol. 109, no. 26, pp. 10181–10186, Jun. 2012, doi: 10.1073/pnas.1204568109.

[51] J. Koenig and J. F. Thayer, "Sex differences in healthy human heart rate variability: A meta-analysis," *Neuroscience & Biobehavioral Reviews*, vol. 64, pp. 288–310, May 2016, doi: 10.1016/j.neubiorev.2016.03.007.

[52] J. Zhang, "Effect of Age and Sex on Heart Rate Variability in Healthy Subjects," *Journal of Manipulative and Physiological Therapeutics*, vol. 30, no. 5, pp. 374–379, Jun. 2007, doi: 10.1016/j.jmpt.2007.04.001.

[53] A. Dart, "Gender, sex hormones and autonomic nervous control of the cardiovascular system," *Cardiovascular Research*, vol. 53, no. 3, pp. 678–687, Feb. 2002, doi: 10.1016/S0008-6363(01)00508-9.

[54] M. Balajewicz-Nowak, A. Furgala, K. Pitynski, P. Thor, H. Huras, and K. Rytlewski, "The dynamics of autonomic nervous system activity and hemodynamic changes in pregnant women," *Neuro Endocrinol Lett*, vol. 37, no. 1, pp. 70–77, 2016.

[55] C. D. Kuo, "Biphasic changes in autonomic nervous activity during pregnancy," p. 7.

[56] D. Chamchad, J. C. Horrow, L. Nakhamchik, and V. A. Arkoosh, "Heart rate variability changes during pregnancy: an observational study," *International Journal of Obstetric Anesthesia*, vol. 16, no. 2, pp. 106–109, Apr. 2007, doi: 10.1016/j.ijoa.2006.08.008.

[57] K. Li *et al.*, "Changes of Arterial Pulse Waveform Characteristics with Gestational Age during Normal Pregnancy," *Sci Rep*, vol. 8, no. 1, p. 15571, Dec. 2018, doi: 10.1038/s41598-018-33890-1.

[58] S. Fangming, L. Zhaoxi, S. Xiurong, H. Nan, W. Lei, and L. Xiaomin, "The Pulse Wave Analysis of Normal Pregnancy: Investigating the Gestational Effects on Photoplethys-

mographic Signals," *Bio-Medical Materials and Engineering*, no. 1, pp. 209–219, 2014, doi: 10.3233/BME-130801.

[59] M. G. Miglis, "Sleep and the Autonomic Nervous System," in *Sleep and Neurologic Disease*, Elsevier, 2017, pp. 227–244. doi: 10.1016/B978-0-12-804074-4.00018-2.

[60] S. Hantoushzadeh, M. Saleh, and A. Maleki, "Effects of antenatal corticosteroids on maternal cardiovascular system, an underestimated notion in pregnant women," *BJOG*, vol. 129, no. 5, pp. 834–835, Apr. 2022, doi: 10.1111/1471-0528.16995.

[61] R. L. Goldenberg, J. F. Culhane, J. D. Iams, and R. Romero, "Epidemiology and causes of preterm birth.," *Lancet (London, England)*, vol. 371, no. 9606, pp. 75–84, Jan. 2008, doi: 10.1016/S0140-6736(08)60074-4.

[62] K. M. Verdurmen, J. Renckens, J. O. van Laar, and S. G. Oei, "The influence of corticosteroids on fetal heart rate variability: a systematic review of the literature," *Obstetrical & gynecological survey*, vol. 68, no. 12, pp. 811–824, Dec. 2013, doi: 10.1097/OGX.0000000000000009 [doi].

[63] K. M. J. Verdurmen *et al.*, "The influence of betamethasone on fetal heart rate variability, obtained by non-invasive fetal electrocardiogram recordings," *Early Human Development*, vol. 119, pp. 8–14, Apr. 2018, doi: 10.1016/j.earlhumdev.2018.02.011.

[64] L. Noben, K. M. J. Verdurmen, G. J. J. Warmerdam, R. Vullings, S. G. Oei, and J. O. E. H. van Laar, "The fetal electrocardiogram to detect the effects of betamethasone on fetal heart rate variability," *Early Human Development*, vol. 130, pp. 57–64, 2019, doi: 10.1016/j.earlhumdev.2019.01.011.

[65] M. Alkhodari *et al.*, "Deep learning identifies cardiac coupling between mother and fetus during gestation," *Front. Cardiovasc. Med.*, vol. 9, p. 926965, Jul. 2022, doi: 10.3389/fcvm.2022.926965.

[66] A. H. Khandoker *et al.*, "Quantification of maternal-fetal cardiac couplings in normal and abnormal pregnancies applying high resolution joint symbolic dynamics," *Mathematical Biosciences and Engineering*, vol. 17, no. 1, pp. 802–813, 2020, doi: 10.3934/mbe.2020042.

[67] P. V. Leeuwen, D. Geue, S. Lange, D. Cysarz, H. Bettermann, and D. H. Grönemeyer, "Is there evidence of fetal-maternal heart rate synchronization?," *BMC Physiology*, p. 11, 2003.

Section I

Maternal autonomic regulation during healthy pregnancy

Chapter 2

On the distinct differences in autonomic regulation between pregnant and non-pregnant women – a heart rate variability analysis

Reproduced after: M Bester, R Joshi, M Mischi, JOEH van Laar, R Vullings. On the distinct differences in autonomic regulation between pregnant and non-pregnant women – a heart rate variability analysis. *Physiological Measurement.* 2023.

Abstract

Objective: Appropriate adaptation of the maternal autonomic nervous system to progressing gestation is essential to a healthy pregnancy. This is partly evidenced by the association between pregnancy complications and autonomic dysfunction. Therefore, assessing maternal heart rate variability (HRV) – a proxy measure for autonomic activity – may offer insights into maternal health, potentially enabling the early detection of complications. However, identifying abnormal maternal HRV requires a thorough understanding of normal maternal HRV. While HRV in women of childbearing age has been extensively investigated, less is known concerning HRV during pregnancy. Subsequently, we investigate the differences in HRV between healthy pregnant women and their non-pregnant counterparts.

Approach: We use a comprehensive suite of HRV features (assessing sympathetic and parasympathetic activity, heart rate (HR) complexity, HR fragmentation, and autonomic responsiveness) to quantify HRV in large groups of healthy pregnant (n=258) and non-pregnant women (n=252). We compare the statistical significance and effect size of the potential differences between the groups.

Main results: We find significantly increased sympathetic and decreased parasympathetic activity during healthy pregnancy, along with significantly attenuated autonomic responsiveness, which we hypothesize serves as a protective mechanism against sympathetic overactivity. HRV differences between these groups typically had a large effect size (Cohen's $d > 0.8$), with the largest effect accompanying the significantly reduced HR complexity and altered sympathovagal balance observed in pregnancy (Cohen's $d > 1.2$).

Significance: Healthy pregnant women are autonomically distinct from their non-pregnant counterparts. Subsequently, assumptions based on HRV research in non-pregnant women cannot be readily translated to pregnant women.

1. Introduction

The autonomic nervous system (ANS) regulates involuntary physiological processes in the human body and therefore plays a crucial role in maintaining and modulating heart rate (HR), blood pressure (BP), and respiration [1]. During pregnancy, all these involuntary processes need to adapt to the continuously evolving demands of the maternal-fetal pair, necessitating changes in maternal autonomic regulation [2]. Insufficient adaptation of the maternal ANS to pregnancy is associated with pregnancy complications, such as hypertensive disorders of pregnancy and gestational diabetes, which affect over 10% of pregnancies [3], [4]. Consequently, assessing maternal autonomic activity during pregnancy may offer insights into gestational health which are otherwise subclinical [5], [6]. However, to enable the identification of abnormal maternal autonomic regulation, an in-depth understanding is first needed of the normal activity of the ANS during a healthy pregnancy.

Our current understanding of healthy maternal autonomic regulation is based on conclusions drawn from studies using a variety of methods. Researchers who tested maternal cardiovascular reflexes concluded that activity from the parasympathetic branch of the ANS is reduced [7]. Concerning the sympathetic branch, results from studies that directly measured electrical activity in sympathetic nerves in the skeletal muscles indicated an increased sympathetic state [8]. Additionally, results from assessments of baroreflex sensitivity showed decreased autonomic regulation of BP toward the end of pregnancy [9].

Still, while these methods offer valuable insights, they require controlled test setups and would be impractical to use as part of standard perinatal care. A better-suited, unobtrusive method would consist of assessing heart rate variability (HRV) since this can be monitored longitudinally with wearable devices such as ECG-Holter monitors or wrist-worn photoplethysmography (PPG) [1]. Given that the ANS is responsible for regulating HR, assessing the variation in HR offers insight into autonomic regulation [1]. Standard time- and frequency-domain HRV features inform on the interplay of the sympathetic and parasympathetic systems, while more recently developed features describe further aspects of autonomic regulation such as HR complexity, HR responsiveness, and HR fragmentation [1], [10], [11]. HRV assessment is already used in the early detection of sepsis, assessment of fetal health, and risk stratification of cardiac disease [12]–[15], to name but a few. Similarly, assessing when maternal HRV (mHRV) deviates from the expected norm during pregnancy may aid in the stratification of high-risk pregnancies.

However, while HRV in healthy women has been extensively studied [16], less is known about how pregnancy affects HRV. Additionally, published studies are limited both in sample size (typically n < 30 per group, with the largest study still involving less than 100 participants per group [17]) as well as in the type of HRV features investigated [18]–[22]. Results from these studies – typically using only standard time and frequency domain HRV features – are at times conflicting and often fail to demonstrate clear findings [23], likely in part due to small sample sizes. A recent review on the potential of mHRV for assessing maternal health confirmed that an understanding of what constitutes healthy mHRV remains lacking [23]. Furthermore, these researchers advocate for mHRV investigations using HRV features outside of the standard time and frequency domain features, since features such as those capturing HR complexity may be better suited to reflecting the intricate physiological changes which occur during pregnancy [23].

Subsequently, to understand the potential of mHRV in detecting deteriorations in maternal health, a definitive understanding is needed of how mHRV changes during a healthy pregnancy. To this end, we employ a comprehensive set of HRV analyses to quantify the potential differences in autonomic regulation between healthy, non-pregnant women and healthy women at mid-pregnancy (n > 250 per group). By analyzing the largest dataset reported thus far in the literature, we aim to clarify how healthy pregnancy impacts standard time and frequency domain features. Furthermore, we investigate HRV features that capture HR complexity, HR responsiveness, and HR fragmentation, some of which are being compared between pregnant and non-pregnant women for the first time. Additionally, we determine the effect size of the differences in HRV features between these two groups to understand the magnitude of the impact of pregnancy on HRV as well as which features are most altered during gestation. Finally, we discuss our results in the context of findings on maternal autonomic regulation based on alternative methods of autonomic assessment. The work outlined in this paper represents the most comprehensive assessment of mHRV in healthy pregnancies to date and forms the basis for the potential use of mHRV in assessing maternal health.

2. Methods

2.1 Datasets

We retrospectively analyzed two datasets. The pregnant group is comprised of abdominal ECG measurements (NEMO Healthcare BV, the Netherlands) of approximately 30 minutes collected from 492 women with singleton pregnancies between 18 and 24 weeks of gestation [24]. Recordings (500 Hz) were taken while women were lying in a semi-recumbent position. The institutional review board at the Máxima Medical Center, Veldhoven, the Netherlands, approved the original study (NL48535.015.14) and all participants provided written informed consent. A waiver was granted for this secondary analysis by the same review board per the Dutch law on medical research with humans (reference number N21.008). The study protocol for the original study, which ran from 2014 to 2017, is described elsewhere [24].

Women with a body mass index (BMI) over 30 kg/m^2 were excluded (n = 67), as well as those who were recorded outside of the gestational age of 18 to 24 weeks of pregnancy (n = 53), as specified in the original protocol [24]. Furthermore, maternal HRV is known to vary across pregnancy [19], [25], [26], hence the gestational age is limited to within this range. Thereafter, those with pre-existing health conditions such as diabetes, maternal pregnancy complications such as hypertensive disorders of pregnancy, or those who were taking medications other than vitamins (n = 106), were also excluded from our analysis. A further two women are excluded owing to known atrial fibrillation. Furthermore, eight were excluded during data preprocessing (see next section). In total, we included 252 participants. Of these, 68 had fetuses with fetal congenital heart disease (CHD). However, it has been demonstrated that fetal CHD does not affect mHRV [27] and, therefore, they are not excluded here. Patient characteristics are presented in Table 1. For a few patients information on age (n = 17) or BMI (n = 5) is missing; these women are assigned the mean age and BMI.

The non-pregnant control group consists of participants from the Autonomic Aging dataset which is openly available from Physionet [28], [29]. ECG data were collected from 1121 participants in a resting, supine position. Participants were screened for any medical condition, use of illegal drugs or any medications potentially influencing cardiovascular function. All participants were at least 18 years old. Recordings were done at a sampling frequency of 1000 Hz using either a MP150 (ECG100C, BIOPAC systems inc., Golata, CA, USA) or a Task Force Monitor system (CNSystems Medizintechnik GmbH, Graz, AUT). These recordings varied considerably in length; subsequently,

recordings of lengths between 20 – 40 minutes were included (n = 468). We excluded all men (n = 165) and women 45 years old or older (n = 27). Furthermore, we excluded women with a BMI over 30 kg/m^2 (n = 15). Ten women were excluded during data preprocessing (see next section), finally resulting in the inclusion of 252 non-pregnant women. Participant characteristics are outlined in Table 1. The ages of the non-pregnant group are only available as grouped data, e.g., participant 1 is between 20 – 24 years old, participant 2 is between 40 – 44 years old, etc. For seven participants, no age data was available. While precise values are not available, we can estimate the mean and standard deviation of such grouped data. Subsequently, all data in Table 1 are reported as mean and standard deviation, where applicable.

Table 1: Characteristics of the datasets. Data on age, BMI, and measurement length are presented as mean and standard deviation.

Characteristic	Pregnant group	Non-pregnant group
Number of included participants	258	252
Age	30.8 (4.1) years	24.6 (4.8) years
BMI (before pregnancy)	23.9 (4.3) kg/m^2	21.9 (2.3) kg/m^2
GA at measurement	20 weeks 4 days (9 days)	
Nulliparous	53.1 %	
Fetal CHD	68 cases (26.4 %)	
Measurement length	29.9 (5.0) minutes	22.4 (4.2) minutes

2.2 Preprocessing

While abdominal ECG measurements are typically acquired to obtain fetal ECG information, the amplitude of the maternal ECG signal far exceeds that of the fetal ECG. In fact, extracting fetal information from abdominal ECG measurements is a persistent challenge [30], [31]. While preprocessing of these abdominal ECG measurements is done to improve the quality of the measurement, as detailed below, it is important to note that the fetal information does not pose an obstacle in detecting maternal R-peaks, as can be seen in Figure 1. Figure 1A is a representation of a typical abdominal ECG measurement; the fetal information is not visible. Figure 1B is a rarer example, where fetal peaks are visible. Still, the amplitude of the maternal R-peak dwarfs that of the fetal peak.

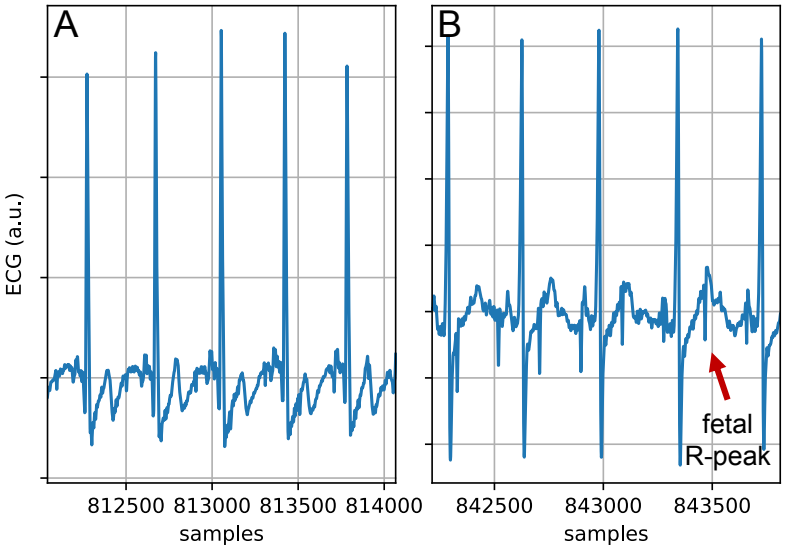

Figure 1: Examples of filtered abdominal ECG measurements. In panel A, no fetal information is visible, as is typically the case. In panel B, fetal R-peaks can be observed but with a substantially lower amplitude than that of the maternal R-peaks.

The multichannel abdominal ECG measurements from the pregnant group are filtered by applying a 4th order Butterworth bandpass filter of 1 to 70 Hz to suppress out-of-band noise and artifacts. Next, a notch filter is applied at 50 Hz to suppress powerline interference and a fixed linear combination of the various abdominal channels is applied to enhance maternal QRS peaks [32]. The processing of maternal RR intervals from fetal ECG measurements was done in MATLAB (MathWorks, USA). All further processing, analyses, and generating of figures were done in Python (PSF, USA).

For both datasets, a previously published peak detector is used to detect the R-peaks [25], [33] and generate the corresponding tachograms. RR-intervals that are physiologically improbable (shorter than 0.4 seconds or longer than 2 seconds) or that differ from the preceding interval by more than 20% are rejected [34]–[36]. Furthermore, missing RR-values are interpolated using cubic spline in cases where the HRV features require a continual time series (specifically, frequency domain and complexity HRV features). Since interpolation is known to influence HRV results, signals which required more than 1% interpolation across the entire recording are excluded when calculating these HRV features. This results in a comparison between 163 non-pregnant and 182 pregnant participants. For the remaining HRV features, all signals for which less than 15% of RR-intervals needed to be removed are included in the analysis. Subsequently, data from 258 pregnant and 252 non-pregnant women are used.

2.3 HRV features

2.3.1 Standard time- and frequency-domain features

The mean HR is calculated in beats per minute along with the standard deviation of the RR-intervals (SDNN) to represent overall variability. The root mean square of the successive differences of the RR-intervals (RMSSD) and the percentage of consecutive RR-intervals that differ by more than 50 ms (pNN50) are calculated as a measure of parasympathetic activity since such short-term variations are mediated by the vagus nerve. To study the spectral activity linked to the parasympathetic system, the power in the high frequency (HF) band of 0.15–0.40 Hz is calculated. Furthermore, the power in the low frequency (LF) band of 0.04–0.15 Hz (influenced by both branches of the ANS), as well as the LF/HF ratio, are calculated [1], [37].

For calculating these spectral features, Welch's method is used. Recordings are divided into five-minute segments with 50% overlap; the features are calculated for each five-minute segment and subsequently, the mean of all segments is presented as the final feature value for each recording. For the time-domain features as well as all the following HRV features, the feature is calculated across the entire recording.

2.3.2 Non-linear and complexity features

We use a Poincaré plot – a popular geometrical method to evaluate HRV dynamics – in which each RR-interval is plotted against its predecessor to form a scatter plot that is fitted with an elliptical shape. From this ellipse, three parameters are calculated: the short- and long-term RR variability (SD1 and SD2), as well as the ratio between them (SD1/SD2) [38]. Furthermore, we assess complexity in the tachograms with two features: Sample entropy (SampEn) and detrended fluctuation analysis (DFA) [39], [40]. SampEn quantifies the conditional probability that two epochs which are similar within a tolerance r for a window length m will remain similar when including the next data point (i.e. the next RR interval) [40], [41]. The parameters m and r are set to 2 and 0.2 times the standard deviation of the RR-intervals [40]. Lower SampEn indicates a more regular and predictable time series [1]. Additionally, DFA is used to quantify the fractal scaling properties of the time series to give an estimation of its long-range correlations. We calculate the short-term fractal scaling exponent α_1, which represents the correlation over 4–16 heartbeats [39]. A result of $\alpha = 0.5$ and $\alpha = 1.5$ represent no correlation (i.e., white noise) or a random walk process (i.e., Brownian noise), respectively. Positive correlations exist when $0.5 < \alpha < 1.5$, with $\alpha \approx 1$ suggesting a high level of complexity. Values above 1 suggest that the system becomes increasingly regular [39], [42].

2.3.3 Heart rate fragmentation

Overall, the presence of variability in the tachogram suggests healthy autonomic control. However, situations in which there is a breakdown in the controlled physiological variation of the HR (such as aging) may also result in higher levels of short-term variability [11]. Heart rate fragmentation (HRF) features capture this jagged type of variability which is likely a result of inadequate autonomic control, but rather of a breakdown in the neuroautonomic-electrophysiological control systems that regulate HR [11].

Four indices were developed by Costa et al. to capture this fragmentation in the HR [11]: PIP (percentage inflection points), IALS (inverse of accelerating or decelerating long segments); PSS (percentage short segments); and PAS (percentage alternating segments). PIP captures how often the acceleration sign of the HR is changing. IALS represents the inverse of the average length of sustained accelerating or decelerating RR-intervals. PSS is the complement of the percentage of RR-intervals with a sustained acceleration or deceleration in HR for at least three intervals. Finally, PAS is the percentage of the RR-intervals which are continuously alternating between accelerations and decelerations (starting from a minimum of four intervals). Note that increases in these indices reflect increased HR fragmentation.

2.3.4 Phase rectified signal averaging

Phase rectified signal averaging (PRSA) is a method that quantifies how the tachogram responds to accelerations and deceleration in the HR as a proxy measure for autonomic responsiveness. We briefly describe the method here; for a more detailed description and visualization of this technique, please refer to the original publication [10]. This method allows us to capture the quasi-periodicities in the tachogram, which can often be obscured by noise and non-stationarities. This is done by identifying a phase of interest, placing anchor points (APs) everywhere this phase occurs, isolating a signal segment of length $2L$ around each AP, aligning segments by their phase, and finally averaging these segments. We specify two sets of APs, namely each HR deceleration and HR acceleration. Furthermore, we define L as 50 RR values, as is also done in the literature [43].

The resulting PRSA waveform visualizes the behavior of HR in response to accelerations and decelerations. The magnitude and speed of the response observed in the waveform give an estimate of the robustness of the autonomic response [10]. (Note that the PRSA waveform's relationship to the time domain is units of RR values (spec-

ified here as RRi) and not in seconds.) Features are calculated to quantify the PRSA waveform (). The most established feature, deceleration capacity (DC), is calculated as follows:

$$DC = [X(0) + X(-1) - X(-2)]/4, \qquad (1)$$

with $X(0)$ representing the AP, $X(1)$ is the value following the AP, while $X(-1)$ and $X(-2)$ precede the AP [10]. The acceleration capacity (AC) is similarly calculated. Additionally, the difference between the maximum and minimum RRi within the neighborhood of five RRi preceding the AP and five after, including the AP, is calculated to determine the immediate deceleration response (IDR) and immediate acceleration response (IAR). The rates corresponding to these responses are also calculated with the slope of the deceleration and acceleration responses (SDR and SAR) [43].

2.5 Statistical analysis and data representation

The normality of data was tested with D'Agostino's K^2 test. Only mean HR was normally distributed for both groups; subsequently, a Student t-test was used to test for significance ($p < 0.05$) of the difference in HR, while a non-parametric test (the Mann-Whitney U test) was performed for all other features. Corresponding effect sizes were calculated with Cohen's d, where 0.2 amounts to a small effect, 0.5 to a medium effect, and 0.8 to a large effect. However, since Cohen's d assumes a normal distribution for the data, we perform a bootstrapping procedure (10,000 iterations) and report the subsequent mean d-value along with the 95% confidence intervals (CI), as is appropriate in non-parametric analyses [44]. Note that d-values may also be negative and that the magnitude of the change is inferred from the absolute d-value. To further contextualize the effect sizes of the differences between our two groups, we additionally calculated to effect sizes of the differences in HRV between women (i.e., our non-pregnant control group) and men. These two groups are known to have differences in their autonomic regulation [16]. The details and results of this analysis can be found in the Appendix.

3. Results

We graphically present our results along with the appropriate statistics. For the mean HR (the only feature with a normal distribution), we plot the distribution of each group; all other features are presented as boxplots. Figure 2 shows the distribution

of the mean HR for each group, clearly demonstrating a significantly increased HR in pregnant women (d = 1.27 (1.09 – 1.47). Additionally, features of HRV (Figure 3) that are linked to short-term variation (RMSSD and pNN50) are significantly reduced (d = -1.1 (-1.28 – -0.93) and -1.15 (-1.34 – -0.98), respectively). SDNN shows a statistically significant yet small change between groups (d = -0.35 (-0.55 – -0.16)).

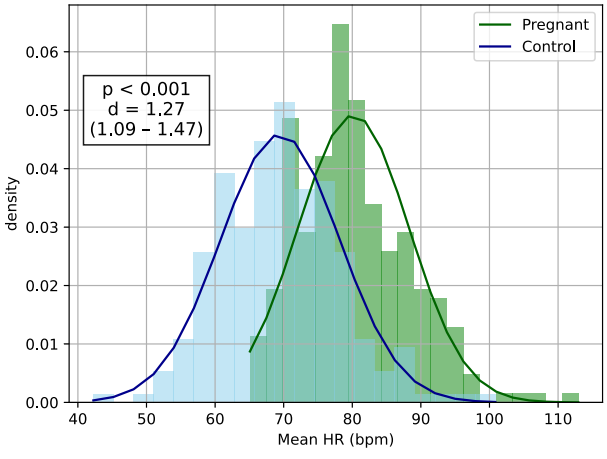

Figure 2: Distribution of the mean HR values of pregnant and control groups, with peaks at approximately 70 bpm and 80 bpm for pregnant and non-pregnant women, respectively

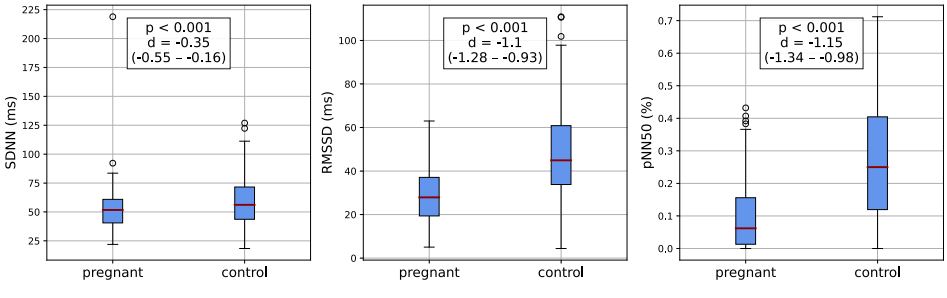

Figure 3: Boxplots of time-domain HRV features with corresponding statistical significance (p-value) and effect sizes (d-value) reported with 95% confidence intervals

In the frequency domain (Figure 4) we see a similar statistically significant reduction in HF, the feature linked to vagal activity (d = -1.03 (-1.23 – -0.83)). Low frequency (LF) is significantly elevated, while LF/HF increases significantly with a large effect size (d = 1.2 (0.96 – 1.44)).

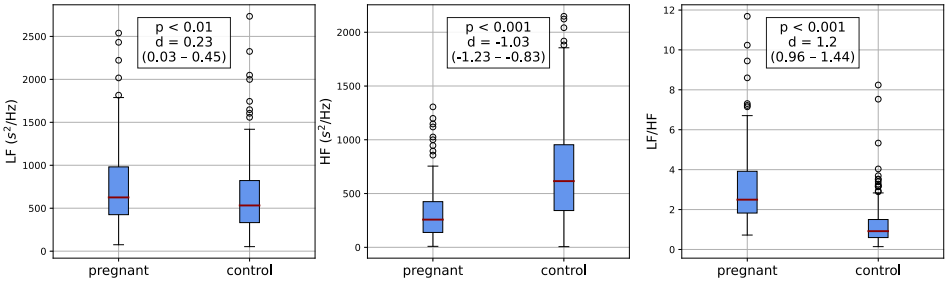

Figure 4: Boxplots of frequency-domain HRV features with corresponding statistical significance (p-value) and effect sizes (d-value) reported with 95% confidence intervals

Most non-linear features (Figure 5) show large changes. SD1/SD2 is significantly decreased (d = -1.39 (-1.58 – -1.21) during pregnancy, which is driven by a large change in SD1 (d = -1.1 (-1.27 – -0.93)). The latter is also linked to vagal activity. DFA (α_1) is increased in pregnancy with a remarkably large effect size (d = 1.74 (1.47 – 2.03)), a change that signals a decrease in the complexity of the HR. Additionally, the statistically significant and large decrease in SampEn (d = -0.89 (-1.11 – -0.68)) suggests the same.

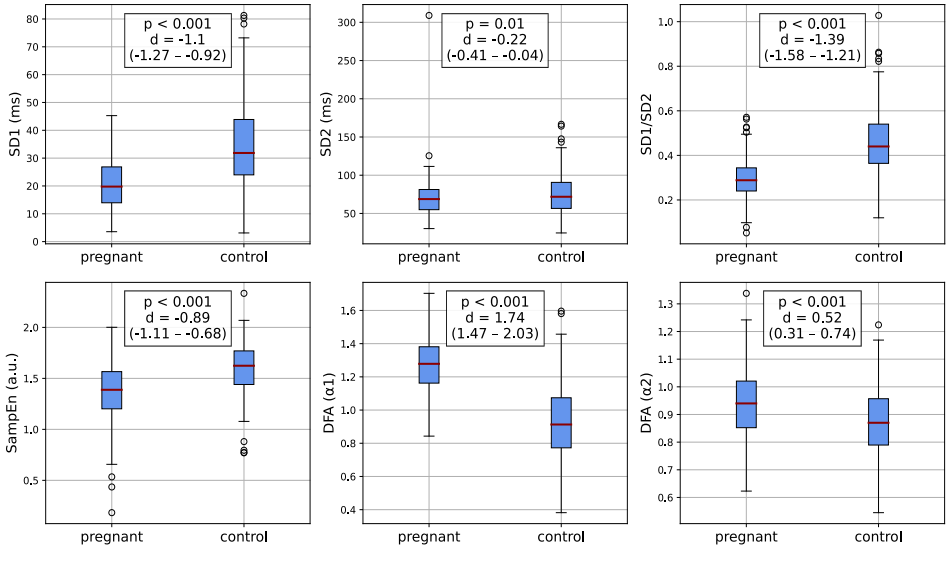

Figure 5: Boxplots of non-linear HRV features with corresponding statistical significance (p-value) and effect sizes (d-value) reported with 95% confidence intervals

One of the HRF features in Figure 6 (IALS and PSS) similarly has a large effect size between the two groups (d = -0.87 (-1.07 – -0.67)). This feature represents the absence of sustained HR accelerations and decelerations and is significantly decreased in pregnancy. Furthermore, PIP and IALS are also significantly decreased during pregnancy with small effect sizes, while PAS is significantly increased, also with a small effect size.

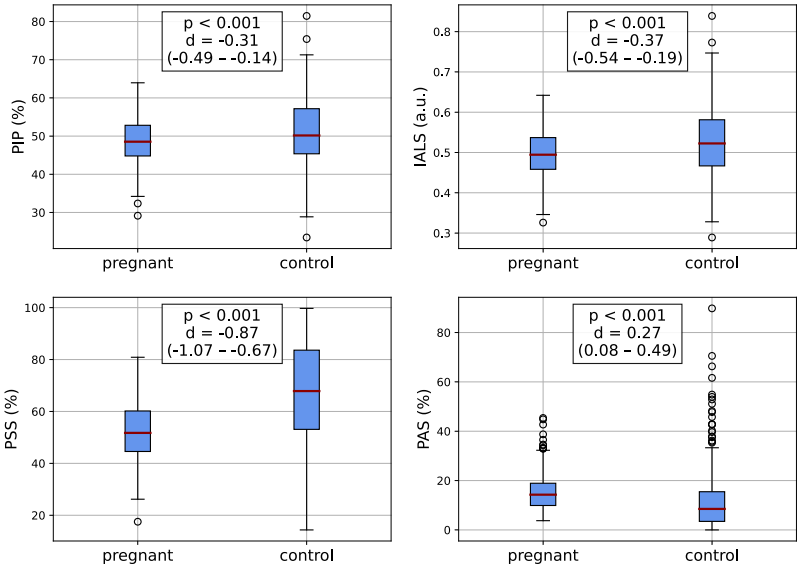

Figure 6: Boxplots of HRF features with corresponding statistical significance (p-value) and effect sizes (d-value) reported with 95% confidence intervals

For the PRSA analysis, the average PRSA waveform for each group is plotted (Figure 7) in addition to the boxplots representing the feature values (Figure 8). From Figure 7, we can see that the autonomic response of pregnant women is attenuated when compared to non-pregnant controls. This can be seen by noting the smaller amplitude of the blue waveform. This is further confirmed by the statistically significant decreases in features capturing the PRSA response for pregnant women in Figure 8, overall, with medium to large effect sizes. Furthermore, a smoother response is observed in the PRSA waveform of pregnant women (Figure 7). This prompted a visualization of the frequency domain of these waveforms using power spectral density (PSD). From the PSDs, we can approximately observe the spectral activity in the areas associated with the traditional LF and HF areas of HRV. Increased activity in the LF region and decreased activity in the HF region is observed for pregnant women, again suggesting increased sympathetic and decreased parasympathetic (or vagal) activity.

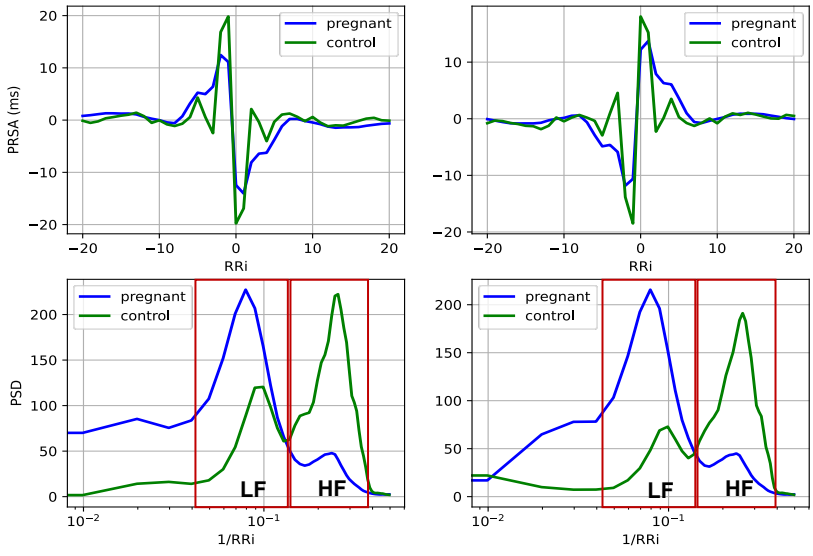

Figure 7: Top: PRSA waveforms with HR accelerations as anchor points (left) and HR decelerations as anchor points (right). Bottom: PSD plots corresponding to the PRSA waveforms directly above

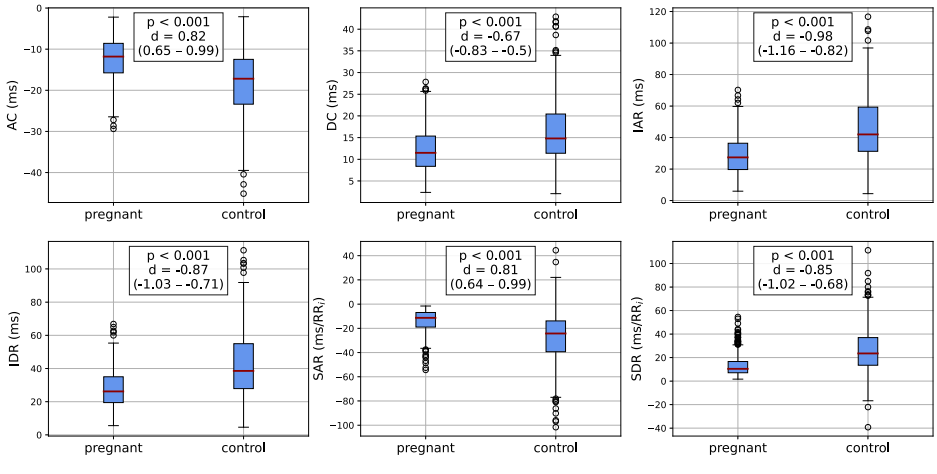

Figure 8: Boxplots of PRSA features with corresponding statistical significance (p-value) and effect sizes (d-value) reported with 95% confidence intervals

Finally, Figure 9 presents the effect sizes with 95% CI for all features in descending absolute magnitude. Most features show changes between pregnant and non-pregnant women with large effect sizes ($d > 0.8$). DFA (α_1) – linked to HR complexity – has

the largest effect size. SD1/SD2 and LF/HF also have similarly large effect sizes; both these features relate to the balance between the sympathetic and parasympathetic systems. All the features closely linked to vagal activity (pNN50, SD1, RMSSD, and HF) show similar effect sizes around d = 1.1.

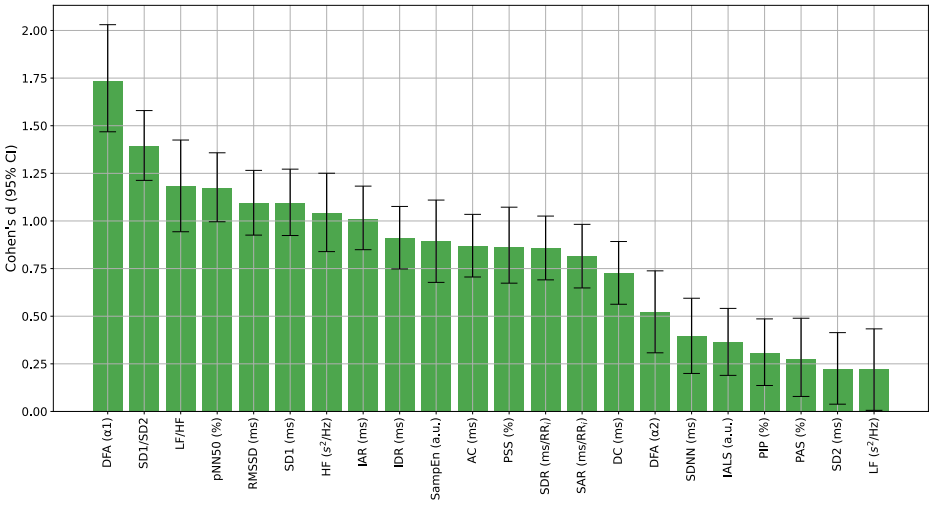

Figure 9: Cohen's d effect sizes with 95% CI, plotted in order of descending absolute magnitude

In the Appendix, a similar graph (Figure A1) can be found which presents the effect sizes of the differences in HRV between women (i.e., the non-pregnant control group) and men. When comparing Figure 9 to Figure A1, it appears that there are larger changes in autonomic regulation between non-pregnant women and pregnant women than there are between non-pregnant women and men.

4. Discussion

Dramatic changes occur in maternal physiology during pregnancy. Not only are there substantial adaptations in most organ systems, but large shifts also occur in autonomic regulation. In this paper, we outline the differences in autonomic regulation as assessed with a comprehensive set of HRV between pregnant and non-pregnant women in large cohorts. We compare features such as SampEn and those related to HRF for the first time between pregnant and non-pregnant women, finding that lower HR complexity and HRF are present during pregnancy. Furthermore, we demonstrate that pregnant women have significantly reduced autonomic responsiveness, building

on preliminary work by our group (based on only nine participants per group) which indicated that only some PRSA features were affected by pregnancy [45]. Additionally, based on the large groups assessed in this work, we find that mHRV in pregnancy reflects reduced parasympathetic and increased sympathetic activity, resolving the often conflicting findings of smaller studies [23]. Moreover, we investigated the effect sizes of differences between these groups; overall, we find that healthy women at mid-pregnancy are autonomically distinct from their non-pregnant counterparts.

We find that HR complexity is remarkably reduced during pregnancy; the significantly lower SampEn in the pregnant group suggests a large drop in complexity at mid-pregnancy (Figure 5, d = -0.89 (-1.11 – -0.68)). Furthermore, the feature α_1 from DFA, which captures short-term changes in HR over multiple timescales, shows a large, significantly increased in the pregnant group as compared to the non-pregnant group (d = 1.74 (1.47 – 2.03)), which signals reduced self-similarity in the HR signal. The latter result confirms that of a smaller study, which found significantly elevated α_1 in late pregnancy compared to non-pregnant controls (n = 16) [42]. HR complexity and self-similarity have rarely been explored in pregnancy and, as such, there is no known physiological explanation for this change.

However, recent studies have shown that α_1 is well-suited for capturing the fatigue of ultramarathon runners [46], [47], even in cases where HR remains steady [47] or when standard features such as SDNN and RMSSD show little relation to fatigue [46]. The researchers who performed this work suggest that during a fatigued state, the integration between the physiological subsystems of the human body over different timescales starts to break down, manifesting as the decoupling between systems (e.g., the cardiac and respiratory systems). This may act as a protective mechanism, ensuring that interactions between systems fail before whole systems do [47]. We hypothesize a similar mechanism to be in place during pregnancy. The increased physiological stress of pregnancy, along with the added burden of the placental-fetal unit on the maternal cardiovascular system, likely results in systems functioning more independently, leading to a decrease in HR complexity. These results support previously published work, which found that these non-linear features are more sensitive to GA than standard HRV features when tracked from 15 to 41 weeks of gestation [25]. Furthermore, these researchers found that SampEn has a statistically significant relationship with GA even across the narrow range of 18 to 24 weeks of gestation, while SDNN and RMSSD showed no relationship [27].

Additionally, we investigated the effect of pregnancy on HRF for the first time. Three HRF features are significantly reduced in pregnant women (Figure 6), with PSS showing a large change (d = -0.87 (-1.07 – -0.67)). This finding is somewhat surprising as it suggests that pregnancy reduces HR fragmentation. Alternatively, an increase in HR fragmentation would suggest a breakdown in the hierarchy of the physiological systems regulating HR, as is the case in older populations and those with coronary artery disease [11], [48]. Since participants in the pregnant group are healthy, we would not expect increased fragmentation. However, we should note here that HRF is not yet as well established as the other HRV features assessed in this study and that the basic mechanisms underlying fragmentation still need to be fully explored [49]. Still, the large decrease in PSS in pregnant women suggests an increase in sustained accelerations and decelerations of the heart rhythm (or conversely, a decrease in RR-intervals quickly alternating between acceleration and deceleration).

This may be at least partially ascribed to a state of decreased vagal activity, which regulates beat-to-beat HR variation, in conjunction with the increased sympathetic activity, which is responsible for changing the HR over longer time scales. The mHRV study with the largest sample size in the literature (99 pregnant women and 63 controls) found this autonomic state to be present in the first trimester [17], however, other researchers found increased vagal activity [50] and decreased sympathetic activity in early pregnancy [50], [51]. Considering analyses done on women in mid-pregnancy, as is also the case for our study group, Ekholm et al. found in 1992 that pregnant women have decreased parasympathetic activity and increased sympathetic activity at mid-pregnancy [52]. These findings are also supported by further investigations [19], [26]. However, other studies have found sympathetic activity, as assessed with LF, to be decreased [20], [21] or not significantly altered during pregnancy [53], rather than increased. However, these studies were performed using small sample sizes ($n < 30$). Furthermore, LF is known to be a sensitive metric that should be interpreted with caution [54]. Still, the results of our standard HRV features reaffirm those of [19], [26], [52] in that vagal activity (as assessed by RMSSD, pNN50, and HF, Figures 3 and 4) is reduced in pregnant women, while sympathetic activity – in so far as we can infer sympathetic activity from changes in LF and LF/HF (Figure 4) – is increased. The increased HR (Figure 2), which we expect based on the literature [55], [56], as well as the decreased SD1/SD2, further suggest increased sympathetic and decreased parasympathetic activity. Furthermore, the overall findings on vagal and sympathetic activity also align with the conclusions drawn from investigations using microneurography (i.e., direct measurement of sympathetic activity in the skeletal muscles) and cardiovascular reflex tests to assess maternal autonomic tone [6], [8].

Results from the PRSA analysis also suggest reduced vagal activity (AC and DC are significantly reduced in pregnancy; Figure 8). This is further confirmed by the clear reduction in HF activity observed in the corresponding PSDs in Figure 7. Looking at the magnitude and rate of the responses (IAR, IDR, SAR, and SDR), we can further conclude that autonomic responsiveness is diminished in pregnant women. This is another notable result since reduced responsiveness is typically associated with states such as cardiac disease and fetal distress [10], [57]. Yet, from visual inspection of the PRSA waveforms, it appears that the dampening seen in a healthy pregnancy is smaller than that seen in cases of cardiac disease [58]. However, since effect sizes are not reported for the latter, it is not possible to make a definitive comparison. Still, this dampened autonomic responsiveness during healthy gestation is echoed in other areas of research. Investigators have found attenuated baroreflex sensitivity [9], reduced physiological responsiveness to stimuli such as pain and relaxation tests [59], and – interestingly – reduced neurocardiovascular transduction. The latter refers to a state where the amount of sympathetic activity in the body has a lower than expected effect on cardiovascular end-points, such as HR [8]. The only prior work comparing PRSA between pregnant (n = 9) and non-pregnant (n = 9) women is a preliminary analysis performed by our group [45]; here, AC, IAR, SAR, and SDR were significantly reduced in pregnant women, while DC, IDR, ADR, and AAR showed no significant changes, potentially due to the small sample sizes.

Overall, we can infer from our results that healthy pregnancy is indeed a state of reduced vagal activity and overactive sympathetic activity compared to non-pregnant controls. Such an autonomic state is likely necessary to maintain a healthy pregnancy, for example, to ensure proper perfusion of the placenta. However, this altered autonomic regulation is possibly dangerous, as it is similar to that found in cases of cardiac disease. To this end, we hypothesize that the reduced autonomic responsiveness (which is reflected in our PRSA analyses as well as the known reduced neurocardiovascular transduction in pregnancy) is a mechanism by which the mother is protected against her autonomic state. This theory is further reflected in findings from Casati et al. [60], who observed increased autonomic responsiveness in women with pregnancy complications (such as hypertensive disorders of pregnancy) when compared to healthy pregnant controls. Subsequently, we believe PRSA analysis may be particularly useful in assessing maternal health via mHRV.

It should be noted that our study is limited in terms of measurement length (≈ 25 minutes). Future studies should aim at incorporating 24-hour measurements, which may offer additional information on the underlying slower processes influencing HRV. Additionally, as the mean age of the pregnant women is approximately five years greater than that of the non-pregnant women, the results observed in this paper are potentially exaggerated. However, based on reference ranges for HRV in the non-pregnant population as well as prior work from our group on the impact of age on mHRV [27], [61], it is unlikely that the differences observed between the groups are predominantly a result of their age difference. Furthermore, recordings were acquired in different positions for the respective groups. While the supine position is typical for resting HRV assessments in non-pregnant women, a semi-recumbent position is preferred in the case of pregnant women since aortocaval compression can occur in the supine position which is known to affect autonomic regulation [62]. While the impact of this difference in positions on the results is not known, both groups are in the preferred position for HRV measurements. Additionally, we could not account for the potential impact of the different stages of the menstrual cycle which the non-pregnant women may be in. However, the impact of these stages on HRV is small compared to the changes observed in this study [63], [64].

Furthermore, this work is a secondary analysis of data collected to define normative fetal ECG ranges between 18 and 24 weeks of gestation; as such, only data from mid-pregnancy are analyzed for the pregnant group. Previous work has shown that HRV also changes significantly with progressing pregnancy [25]. Therefore, further studies are needed to definitively conclude how mHRV differs between non-pregnant women and those in early- and late pregnancy, respectively. However, the work presented here has several advantages over the current state of the art in the literature, chiefly the variety of HRV features investigated (instead of only the standard time- and frequency-domain features) as well as the large sample groups, which allow us to confidently draw conclusions concerning mHRV at mid-pregnancy.

Finally, to contextualize the magnitude of the changes we observe between pregnant and non-pregnant women, we repeated our analysis to compare the group of non-pregnant women against men (see Appendix). We found that the effect sizes of the differences between pregnant and non-pregnant women (Figure 9) are overall larger than those of non-pregnant women compared to men (Appendix, Figure A1). While autonomic regulation is known to differ between the sexes [16], from our analysis it appears that women are more autonomically different from their pregnant counterparts than they are from men.

5. Conclusion

Subsequently, we conclude that healthy mid-pregnant and non-pregnant women are two autonomically distinct groups, and findings of HRV in non-pregnant women cannot be translated to pregnant women. Furthermore, our findings on mHRV not only align with results from other areas of autonomic investigation but also provide additional information on the maternal autonomic state. These changes often have large effect sizes, the most remarkable of which are for DFA (α_1), SD1/SD2, and LF/HF, suggesting that these may be particularly useful in assessing maternal health.

Appendix

We repeated the analysis detailed in this paper to compare HRV between women and men. The women in this comparison are the same as in the non-pregnant control group. Therefore, 252 women were included when comparing HRV features that do not require interpolation of the RR-intervals, and 166 women were included in comparisons that necessitate interpolation. These women were included from the Autonomic Aging dataset (available at Physionet) which also contained ECG recordings of men. Subsequently, we also obtained our male group from this Autonomic Aging dataset by applying similar inclusion and exclusion criteria. Subsequently, 131 men were included in the analyses which did not require interpolation, and 78 were included in the analyses which did. Figure A1 represents the effect sizes of the differences between each feature listed on the x-axis. Effect sizes were calculated with Cohen's *d*, where 0.2 amounts to a small effect, 0.5 to a medium effect, and 0.8 to a large effect.

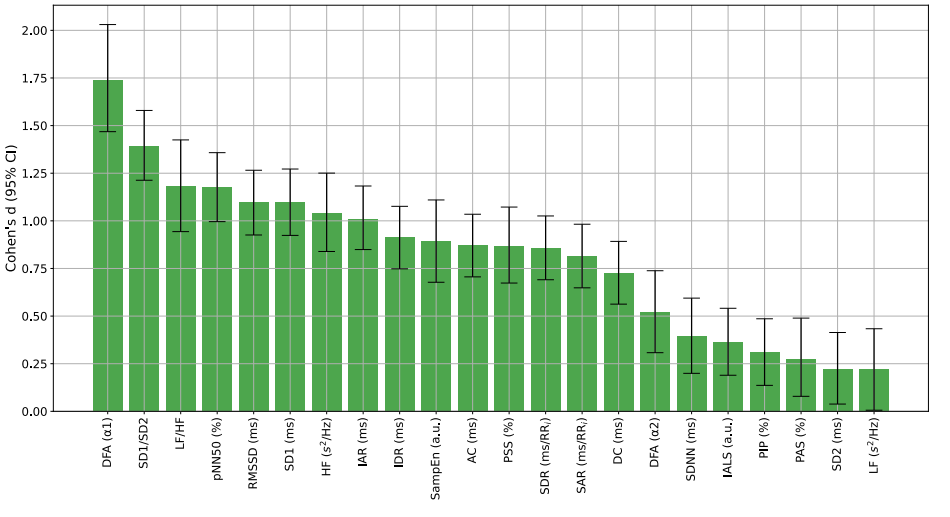

Figure A1 Cohen's *d* effect sizes with 95% CI, plotted in order of descending absolute magnitude, for the HRV comparison between women and men

References

[1] F. Shaffer and J. P. Ginsberg, "An Overview of Heart Rate Variability Metrics and Norms," *Front. Public Health*, vol. 5, p. 258, Sep. 2017, doi: 10.3389/fpubh.2017.00258.

[2] Q. Fu, "Hemodynamic and Electrocardiographic Aspects of Uncomplicated Singleton Pregnancy.," *Advances in experimental medicine and biology*, vol. 1065, pp. 413–431, 2018, doi: 10.1007/978-3-319-77932-4_26.

[3] S. Moors *et al.*, "Heart rate variability in hypertensive pregnancy disorders: a systematic review," *Pregnancy Hypertension*, Mar. 2020, doi: 10.1016/j.preghy.2020.03.003.

[4] L. M. Reyes *et al.*, "Sympathetic nervous system activity and reactivity in women with gestational diabetes mellitus," *Physiol Rep*, vol. 8, no. 13, Jul. 2020, doi: 10.14814/phy2.14504.

[5] G. K. Pal, P. Shyma, S. Habeebullah, P. Shyjus, and P. Pal, "Spectral Analysis of Heart Rate Variability for Early Prediction of Pregnancy-Induced Hypertension," *Clinical and Experimental Hypertension*, vol. 31, no. 4, pp. 330–341, Jan. 2009, doi: 10.1080/10641960802621333.

[6] S. Rang, H. Wolf, G. A. Montfrans, and J. M. Karemaker, "Non–invasive assessment of autonomic cardiovascular control in normal human pregnancy and pregnancy- associated hypertensive disorders: a review," *Journal of Hypertension*, vol. 20, no. 11, pp. 2111–2119, 2002.

[7] E. M. K. Ekholm, S. J. Piha, R. U. Erkkola, and K. J. Antila, "Autonomic cardiovascular reflexes in pregnancy. A longitudinal study," *Clinical Autonomic Research*, vol. 4, no. 4, pp. 161–165, Aug. 1994, doi: 10.1007/BF01826181.

[8] L. M. Reyes, C. W. Usselman, M. H. Davenport, and C. D. Steinback, "Sympathetic Nervous System Regulation in Human Normotensive and Hypertensive Pregnancies.," *Hypertension (Dallas, Tex. : 1979)*, vol. 71, no. 5, pp. 793–803, May 2018, doi: 10.1161/HYPERTENSIONAHA.117.10766.

[9] V. L. Brooks, Q. Fu, Z. Shi, and C. M. Heesch, "Adaptations in autonomic nervous system regulation in normal and hypertensive pregnancy," in *Handbook of Clinical Neurology*, Elsevier, 2020, pp. 57–84. doi: 10.1016/B978-0-444-64239-4.00003-5.

[10] A. Bauer *et al.*, "Phase-rectified signal averaging detects quasi-periodicities in non-stationary data," *Physica A: Statistical Mechanics and its Applications*, vol. 364, pp. 423–434, May 2006, doi: 10.1016/j.physa.2005.08.080.

[11] M. D. Costa, R. B. Davis, and A. L. Goldberger, "Heart Rate Fragmentation: A New Approach to the Analysis of Cardiac Interbeat Interval Dynamics," *Front. Physiol.*, vol. 8, p. 255, May 2017, doi: 10.3389/fphys.2017.00255.

[12] C. Eick *et al.*, "Autonomic Nervous System Activity as Risk Predictor in the Medical Emergency Department: A Prospective Cohort Study," *Critical Care Medicine*, vol. 43, no. 5, pp. 1079–1086, May 2015, doi: 10.1097/CCM.0000000000000922.

[13] A. M. Ponsiglione, C. Cosentino, G. Cesarelli, F. Amato, and M. Romano, "A Comprehensive Review of Techniques for Processing and Analyzing Fetal Heart Rate Signals," *Sensors*, vol. 21, no. 18, p. 6136, Sep. 2021, doi: 10.3390/s21186136.

[14] S. Ahmad *et al.*, "Continuous Multi-Parameter Heart Rate Variability Analysis Heralds

Onset of Sepsis in Adults," *PLoS ONE*, vol. 4, no. 8, p. e6642, Aug. 2009, doi: 10.1371/journal.pone.0006642.

[15] U. Rajendra Acharya, K. Paul Joseph, N. Kannathal, C. M. Lim, and J. S. Suri, "Heart rate variability: a review," *Med Bio Eng Comput*, vol. 44, no. 12, pp. 1031–1051, Dec. 2006, doi: 10.1007/s11517-006-0119-0.

[16] J. Koenig and J. F. Thayer, "Sex differences in healthy human heart rate variability: A meta-analysis," *Neuroscience & Biobehavioral Reviews*, vol. 64, pp. 288–310, May 2016, doi: 10.1016/j.neubiorev.2016.03.007.

[17] R. E. Carpenter, L. A. D'Silva, S. J. Emery, O. Uzun, D. Rassi, and M. J. Lewis, "Changes in heart rate variability and QT variability during the first trimester of pregnancy," *Physiol. Meas.*, vol. 36, no. 3, pp. 531–545, Mar. 2015, doi: 10.1088/0967-3334/36/3/531.

[18] G. Speranza, G. Verlato, and A. Albiero, "Autonomic changes during pregnancy: Assessment by spectral heart rate variability analysis," *Journal of Electrocardiology*, vol. 31, no. 2, pp. 101–109, Apr. 1998, doi: 10.1016/S0022-0736(98)90040-1.

[19] M. Balajewicz-Nowak, A. Furgala, K. Pitynski, P. Thor, H. Huras, and K. Rytlewski, "The dynamics of autonomic nervous system activity and hemodynamic changes in pregnant women," *Neuro Endocrinol Lett*, vol. 37, no. 1, pp. 70–77, 2016.

[20] E. M. K. Ekholm, J. Hartiala, and H. V. Huikuri, "Circadian rhythm of frequency-domain measures of heart rate variability in pregnancy," *BJOG:An international journal of O&G*, vol. 104, no. 7, pp. 825–828, Jul. 1997, doi: 10.1111/j.1471-0528.1997.tb12027.x.

[21] A. Voss *et al.*, "Baroreflex sensitivity, heart rate, and blood pressure variability in normal pregnancy," *American Journal of Hypertension*, vol. 13, no. 11, pp. 1218–1225, Nov. 2000, doi: 10.1016/S0895-7061(00)01199-7.

[22] C. D. Kuo, G. Y. Chen, M. J. Yang, H. M. Lo, and Y. S. Tsai, "Biphasic changes in autonomic nervous activity during pregnancy," *British Journal of Anaesthesia*, vol. 84, no. 0, pp. 323–329, 2000, doi: 10.1093/oxfordjournals.bja.a013433.

[23] Z. Sharifiheris, A. Rahmani, J. Onwuka, and M. Bender, "The Utilization of Heart Rate Variability for Autonomic Nervous System Assessment in Healthy Pregnant Women: Systematic Review," *JMIR Bioinform Biotech*, vol. 3, no. 1, p. e36791, Nov. 2022, doi: 10.2196/36791.

[24] K. M. J. Verdurmen *et al.*, "Normal ranges for fetal electrocardiogram values for the healthy fetus of 18–24 weeks of gestation: a prospective cohort study," *BMC Pregnancy and Childbirth*, p. 7, 2016.

[25] M. Bester, R. Joshi, M. Mischi, J. O. E. H. van Laar, and R. Vullings, "Longitudinally Tracking Maternal Autonomic Modulation During Normal Pregnancy With Comprehensive Heart Rate Variability Analyses," *Front. Physiol.*, vol. 13, p. 874684, May 2022, doi: 10.3389/fphys.2022.874684.

[26] P. Garg, K. Yadav, A. K. Jaryal, G. Kachhawa, A. Kriplani, and K. K. Deepak, "Sequential analysis of heart rate variability, blood pressure variability and baroreflex sensitivity in healthy pregnancy," *Clin Auton Res*, Jan. 2020, doi: 10.1007/s10286-020-00667-4.

[27] M. Bester, R. Joshi, A. Linders, M. Mischi, J. O. E. H. van Laar, and R. Vullings, "Characterizing the effect of demographics, cardiorespiratory factors, and inter-subject variation on maternal heart rate variability in pregnancy with statistical modeling: a retrospective observational analysis," *Sci Rep*, vol. 12, no. 1, p. 19305, Nov. 2022, doi: 10.1038/s41598-022-21792-2.

[28] A. Schumann and K.-J. Bär, "Autonomic aging – A dataset to quantify changes of cardiovascular autonomic function during healthy aging," *Sci Data*, vol. 9, no. 1, p. 95, Dec. 2022, doi: 10.1038/s41597-022-01202-y.

[29] A. L. Goldberger *et al.*, "PhysioBank, PhysioToolkit, and PhysioNet: Components of a New Research Resource for Complex Physiologic Signals," *Circulation*, vol. 101, no. 23, Jun. 2000, doi: 10.1161/01.CIR.101.23.e215.

[30] R. Jaros, R. Martinek, and R. Kahankova, "Non-Adaptive Methods for Fetal ECG Signal Processing: A Review and Appraisal," *Sensors*, vol. 18, no. 11, p. 3648, Oct. 2018, doi: 10.3390/s18113648.

[31] E. Fotiadou, R. J. G. van Sloun, J. O. E. H. van Laar, and R. Vullings, "A dilated inception CNN-LSTM network for fetal heart rate estimation," *Physiol. Meas.*, vol. 42, no. 4, p. 045007, Apr. 2021, doi: 10.1088/1361-6579/abf7db.

[32] M. J. Rooijakkers *et al.*, "Influence of Electrode Placement on Signal Quality for Ambulatory Pregnancy Monitoring," *Computational and Mathematical Methods in Medicine*, vol. 2014, pp. 1–12, 2014, doi: 10.1155/2014/960980.

[33] M. J. Rooijakkers, C. Rabotti, S. G. Oei, and M. Mischi, "Low-complexity R-peak detection for ambulatory fetal monitoring," *Physiol. Meas.*, vol. 33, no. 7, pp. 1135–1150, Jul. 2012, doi: 10.1088/0967-3334/33/7/1135.

[34] C. Peters, R. Vullings, J. Bergmans, G. Oei, and P. Wijn, "The effect of artifact correction on spectral estimates of heart rate variability," in *2008 30th Annual International Conference of the IEEE Engineering in Medicine and Biology Society*, Vancouver, BC: IEEE, Aug. 2008, pp. 2669–2672. doi: 10.1109/IEMBS.2008.4649751.

[35] C. H. L. Peters, R. Vullings, M. J. Rooijakkers, J. W. M. Bergmans, S. G. Oei, and P. F. F. Wijn, "A continuous wavelet transform-based method for time-frequency analysis of artefact-corrected heart rate variability data," *Physiol. Meas.*, vol. 32, no. 10, pp. 1517–1527, Oct. 2011, doi: 10.1088/0967-3334/32/10/001.

[36] L. M. Campana, R. L. Owens, G. D. Clifford, S. D. Pittman, and A. Malhotra, "Phase-rectified signal averaging as a sensitive index of autonomic changes with aging," *Journal of Applied Physiology*, vol. 108, no. 6, pp. 1668–1673, Jun. 2010, doi: 10.1152/japplphysiol.00013.2010.

[37] Task Force of The European Society of Cardiology and The North American Society of Pacing and Electrophysiology, "Heart rate variability. Standards of measurement, physiological interpretation, and clinical use.," *European heart journal*, vol. 17, no. 3, pp. 354–381, Mar. 1996.

[38] A. H. Khandoker, C. Karmakar, M. Brennan, M. Palaniswami, and A. Voss, *Poincaré Plot Methods for Heart Rate Variability Analysis*. Boston, MA: Springer US, 2013. doi: 10.1007/978-1-4614-7375-6.

[39] C. -K. Peng, S. Havlin, H. E. Stanley, and A. L. Goldberger, "Quantification of scaling exponents and crossover phenomena in nonstationary heartbeat time series," *Chaos*, vol. 5, no. 1, pp. 82–87, Mar. 1995, doi: 10.1063/1.166141.

[40] J. S. Richman and J. R. Moorman, "Physiological time-series analysis using approximate entropy and sample entropy," *American Journal of Physiology-Heart and Circulatory Physiology*, vol. 278, no. 6, pp. H2039–H2049, Jun. 2000, doi: 10.1152/ajpheart.2000.278.6.H2039.

[41] A. Bakhchina, K. Arutyunova, A. Sozinov, A. Demidovsky, and Y. Alexandrov, "Sample Entropy of the Heart Rate Reflects Properties of the System Organization of Behaviour," *Entropy*, vol. 20, no. 6, p. 449, Jun. 2018, doi: 10.3390/e20060449.

[42] R.-G. Yeh, J.-S. Shieh, G.-Y. Chen, and C.-D. Kuo, "Detrended fluctuation analysis of short-term heart rate variability in late pregnant women," *Autonomic Neuroscience*, vol. 150, no. 1–2, pp. 122–126, Oct. 2009, doi: 10.1016/j.autneu.2009.05.241.

[43] R. Joshi, D. Kommers, X. Long, L. Feijs, and S. V. Huffel, "Cardiorespiratory coupling in preterm infants," *J Appl Physiol*, vol. 126, pp. 202–213, doi: 10.1152/japplphysiol.00722.2018.

[44] K. Kelley, "The Effects of Nonnormal Distributions on Confidence Intervals Around the Standardized Mean Difference: Bootstrap and Parametric Confidence Intervals," *Educational and Psychological Measurement*, vol. 65, no. 1, pp. 51–69, Feb. 2005, doi: 10.1177/0013164404264850.

[45] M. Bester, R. Rizea, R. Joshi, M. Mischi, J. Van Laar, and R. Vullings, "Maternal autonomic responsiveness is attenuated in healthy pregnancy: a phase rectified signal averaging analysis," in *2022 44th Annual International Conference of the IEEE Engineering in Medicine & Biology Society (EMBC)*, Glasgow, Scotland, United Kingdom: IEEE, Jul. 2022, pp. 4982–4986. doi: 10.1109/EMBC48229.2022.9870894.

[46] T. Gronwald, B. Rogers, L. Hottenrott, O. Hoos, and K. Hottenrott, "Correlation Properties of Heart Rate Variability during a Marathon Race in Recreational Runners: Potential Biomarker of Complex Regulation during Endurance Exercise," *jsportscimed*, pp. 557–563, Jul. 2021, doi: 10.52082/jssm.2021.557.

[47] B. Rogers, L. Mourot, G. Doucende, and T. Gronwald, "Fractal correlation properties of heart rate variability as a biomarker of endurance exercise fatigue in ultramarathon runners," *Physiol Rep*, vol. 9, no. 14, Jul. 2021, doi: 10.14814/phy2.14956.

[48] M. D. Costa, R. B. Davis, and A. L. Goldberger, "Heart Rate Fragmentation: A Symbolic Dynamical Approach," *Front. Physiol.*, vol. 8, p. 827, Nov. 2017, doi: 10.3389/fphys.2017.00827.

[49] M. D. Costa, S. Redline, R. B. Davis, S. R. Heckbert, E. Z. Soliman, and A. L. Goldberger, "Heart Rate Fragmentation as a Novel Biomarker of Adverse Cardiovascular Events: The Multi-Ethnic Study of Atherosclerosis," *Front. Physiol.*, vol. 9, p. 1117, Sep. 2018, doi: 10.3389/fphys.2018.01117.

[50] T. Alam, A. Choudhary, and S. D, "Maternal heart rate variability during different trimesters of pregnancy," *Natl J Physiol Pharm Pharmacol*, vol. 8, no. 9, p. 1475, 2018, doi: 10.5455/njppp.2018.8.0723327072018.

[51] P. K. Stein, M. T. Hagley, P. L. Cole, P. P. Domitrovich, R. E. Kleiger, and J. N. Rottman, "Changes in 24-hour heart rate variability during normal pregnancy," *American Journal of Obstetrics and Gynecology*, vol. 180, no. 4, pp. 978–985, Apr. 1999, doi: 10.1016/S0002-9378(99)70670-8.

[52] E. M. K. Ekholm, R. U. Erkkola, S. J. Piha, J. O. Jalonen, T. H. Metsälä, and K. J. Antila, "Changes in autonomic cardiovascular control in mid-pregnancy," *Clin Physiol*, vol. 12, no. 5, pp. 527–536, Sep. 1992, doi: 10.1111/j.1475-097X.1992.tb00356.x.

[53] E. Eneroth-Grimfors, M. Westgren, M. Ericson, C. Ihrman-Sandahl, and L. E. Lindblad, "Autonomic cardiovascular control in normal and pre-eclamptic pregnancy," *Acta Obstet Gynecol Scand*, vol. 73, no. 9, pp. 680–684, Jan. 1994, doi: 10.3109/00016349409029402.

[54] J. A. J. Heathers, "Everything Hertz: methodological issues in short-term frequency-do-

main HRV," *Front. Physiol.*, vol. 5, May 2014, doi: 10.3389/fphys.2014.00177.

[55] L. Loerup *et al.*, "Trends of blood pressure and heart rate in normal pregnancies: a systematic review and meta-analysis," *BMC Med*, vol. 17, no. 1, p. 167, Dec. 2019, doi: 10.1186/s12916-019-1399-1.

[56] L. J. Green *et al.*, "Gestation-Specific Vital Sign Reference Ranges in Pregnancy," *Obstetrics & Gynecology*, vol. 135, no. 3, pp. 653–664, Mar. 2020, doi: 10.1097/AOG.0000000000003721.

[57] J. Weyrich *et al.*, "Intrapartum PRSA: a new method to predict fetal acidosis?—a case-control study," *Arch Gynecol Obstet*, vol. 301, no. 1, pp. 137–142, Jan. 2020, doi: 10.1007/s00404-019-05419-y.

[58] A. Bauer *et al.*, "Deceleration capacity of heart rate as a predictor of mortality after myocardial infarction: cohort study," *The Lancet*, vol. 367, no. 9523, pp. 1674–1681, May 2006, doi: 10.1016/S0140-6736(06)68735-7.

[59] J. A. DiPietro, T. Mendelson, E. L. Williams, and K. A. Costigan, "Physiological blunting during pregnancy extends to induced relaxation," *Biological Psychology*, vol. 89, no. 1, pp. 14–20, Jan. 2012, doi: 10.1016/j.biopsycho.2011.07.005.

[60] D. Casati *et al.*, "Maternal cardiac deceleration capacity: a novel insight into maternal autonomic function in pregnancies complicated by hypertensive disorders and intrauterine growth restriction," *European Journal of Obstetrics & Gynecology and Reproductive Biology*, vol. 206, pp. 6–11, Nov. 2016, doi: 10.1016/j.ejogrb.2016.08.007.

[61] S. Sammito and I. Böckelmann, "Reference values for time- and frequency-domain heart rate variability measures," *Heart Rhythm*, vol. 13, no. 6, pp. 1309–1316, Jun. 2016, doi: 10.1016/j.hrthm.2016.02.006.

[62] G.-Y. Chen, C.-D. Kuo, M.-J. Yang, H.-M. Lo, and Y.-S. Tsai, "Comparison of supine and upright positions on autonomic nervous activity in late pregnancy: the role of aortocaval compression: Autonomic nervous activity in late pregnancy," *Anaesthesia*, vol. 54, no. 3, pp. 215–219, Mar. 1999, doi: 10.1046/j.1365-2044.1999.00648.x.

[63] M. Vallejo, M. F. Márquez, V. H. Borja-Aburto, M. Cárdenas, and A. G. Hermosillo, "Age, body mass index, and menstrual cycle influence young women's heart rate variability: A multivariable analysis," *Clin Auton Res*, vol. 15, no. 4, pp. 292–298, Aug. 2005, doi: 10.1007/s10286-005-0272-9.

[64] M. S. Tenan, R. M. Brothers, A. J. Tweedell, A. C. Hackney, and L. Griffin, "Changes in resting heart rate variability across the menstrual cycle: Heart rate variability and the menstrual cycle," *Psychophysiol*, vol. 51, no. 10, pp. 996–1004, Oct. 2014, doi: 10.1111/psyp.12250.

Chapter 3

The impact of healthy pregnancy on features of heart rate variability and pulse wave morphology derived from wrist-worn photoplethysmography

Reproduced after: The impact of healthy pregnancy on features of heart rate variability and pulse wave morphology derived from wrist-worn photoplethysmography. M Bester, MJ Almario Escorcia, P Fonseca, M Mollura, MM van Gilst, R Barbieri, M Mischi, JOEH van Laar, R Vullings, R Joshi. *Under review*. 2023.

Abstract

Owing to the importance of appropriate maternal autonomic regulation in maintaining gestational health, there is growing interest in tracking autonomic activity to identify early deteriorations in maternal health. The prime candidates for non-invasively tracking autonomic activity are smartwatches that collect photoplethysmography (PPG) measurements. Features of heart rate variability (HRV) and features describing the PPG pulse wave morphology (morphological features) can be extracted for the PPG and offer valuable insights into autonomic activity. However, even though a plethora of HRV and morphological features exist in the literature, it is unclear which of these measures may be valuable for tracking maternal health. A reasonable first step is to identify the features which best differentiate healthy pregnancy from non-pregnant women, as these features potentially capture the physiological adaptations necessary for sustaining healthy pregnancy. In this work, we compute sets of HRV and morphological features from nighttime PPG measurements and compare them between healthy pregnant and non-pregnant women. Using logistic regression and stepwise forward feature elimination, we find that the systolic pulse duration of the PPG pulse wave discriminates best between these groups, followed by mean heart rate (HR). Overall, morphological features were more valuable for discriminating between pregnant and non-pregnant women than HRV features (area under the receiver operating characteristics curve (AUROC) of 0.825 and 0.74, respectively). This is likely because morphological features capture both the autonomic and cardiovascular differences between these groups, while HRV are mainly associated with autonomic changes. As a sub-analysis, we stratified our analysis by sleep stages and found that using features calculated only from deep sleep enhanced the differences between the two groups. In conclusion, we postulate that in addition to HRV features, morphological features may also be useful in tracking maternal health. Furthermore, propose a list of potentially relevant HRV and morphological features to be included in future research concerning maternal health.

1. Introduction

During pregnancy, continuous and finely tuned changes occur in the maternal physiology to maintain maternal health while supporting the growing fetus [1]. Adaptations in the maternal autonomic nervous system (ANS) are particularly important given that the ANS regulates involuntary physiological processes such as respiration, blood pressure, and heart rate (HR) and is consequently essential to maintaining homeostasis throughout this physiologically dynamic period [2]. In comparison to healthy pregnancies, altered maternal autonomic regulation has been found in women who develop pregnancy complications such as hypertensive disorders of pregnancy (HDP) or gestational diabetes mellitus (GDM), even as early as in the first trimester [3], [4]. While pregnancy complications are typically detected after the time window for clinical intervention has passed, earlier detection can improve maternal and perinatal outcome by allowing for adequate management and treatment [5]–[7].

Since dysfunctional maternal autonomic regulation has been found in women with pregnancy complications [3], [4], [8]–[11], there is ongoing research into the potential of tracking maternal autonomic regulation to detect early deteriorations in maternal health [12]–[14]. Autonomic regulation can be longitudinally assessed by tracking heart rate variability (HRV) via wearable heart rate (HR) monitors. Longitudinal HRV tracking might be measured by photoplethysmography (PPG) recorded from wearable HR monitors such as smartwatches. PPG is an optical measure that captures blood-volume changes in the vasculature from which HR and HRV can be derived [15]. Additionally, features describing PPG pulse wave morphology can also be determined [16], [17], here forth referred to as morphological features. While the exact physiological interpretation of morphological features is not as well-established as that of HRV, these features reflect changes in vascular tone [18] – which is autonomically regulated – and may offer additional, complementary information. Furthermore, as pregnancy necessitates vasodilation of the systematic vasculature to prevent hypertension from developing during gestation, these features might be particularly useful in capturing changes in the maternal physiology essential to a healthy pregnancy.

A plethora of HRV and morphological features have been considered in the literature, and it is unclear which of these would be valuable for assessing maternal health. Research into the characteristics of the autonomic dysfunction that precedes the onset of different types of pregnancy complications is ongoing [2], [9], [10], [19], and consequently, it is uncertain which of these non-invasive features would be best suited

to identifying these impending complications. However, a reasonable starting point would be to identify the features which differ the most between healthy pregnant and healthy non-pregnant women, as these potentially reflect changes in the physiology characteristic of a healthy pregnancy and are likely to be altered in complicated pregnancies.

In this work, we compare a comprehensive set of HRV and morphological features between healthy pregnant and non-pregnant women. Comparisons of HRV between these groups have been performed by our group and others based on ECG recordings [20], [21], but none have done so using PPG measurements with relatively low sampling rates. The latter would likely be the modality used if regular tracking of autonomic activity were to be implemented as part of antenatal care [22]. Furthermore, research on the PPG waveform in pregnancy is very limited; to our knowledge, only one study has compared a limited number of morphological features between pregnant and non-pregnant women [23].

To establish which features from the feature sets of HRV and morphological features are most impacted by pregnancy, we employ a binary classification model as a tool to identify which features contribute the most to discriminating between these two groups. Furthermore, as we use nighttime recordings in this work, we perform a sub-analysis to explore the impact of stratifying the analysis per sleep stage. Sleep stages approximate a pseudo-controlled environment that both groups share, reducing potential environmental influences on the HRV and morphological features. Furthermore, each sleep stage is governed by a different autonomic state [24], which could potentially enhance or elucidate differences in features between the groups that are less apparent when using data from the entire night.

2. Methods

In this section, we detail the datasets used (Section 2.1), the preprocessing of the PPG recordings (Section 2.2.), and the extraction of the HRV and morphological features (Section 2.3). Next, we describe the analyses. First, we detail the binary classification model and the corresponding feature selection in Section 2.4.1. This is followed by the sleep scoring of the PPG measurements and the subsequent stratification of the classification analysis by sleep stage (Section 2.4.2). Finally, we describe an investigation into the effect of gestational age on the HRV and morphological features (Section 2.4.3).

2.1 Datasets

Two datasets were analyzed during this study, one containing data from healthy pregnant women and the other with data from healthy, non-pregnant women of childbearing age [25]. PPG and accelerometry measurements for both groups were acquired using the Elan sensor (Philips Electronics Nederland B.V.), a wristband that contains the Cardio and Motion Monitoring Module (CM3 Generation-3), which includes a PPG sensor and a triaxial accelerometer data [26], [27]. Data for the non-pregnant group were acquired at 32 Hz, while data for the pregnant group was acquired at 128 Hz and subsequently downsampled to 32 Hz. For both groups, accelerometry data were collected at 128 Hz.

For the pregnant group, as part of a volunteer study, forty-five women with healthy, singleton pregnancies were recruited during their second or third trimester of pregnancy. These participants were at least 18 years old and nulliparous and had a body mass index (BMI) of between 18 and 30 kg/m^2. Participants had no pregnancy complications or history of cardiovascular or psychiatric disease. Furthermore, participants did not use any blood pressure or sleep medication. During the study, participants were asked to wear the wristband at home for two nighttime measurement sessions approximately eight weeks apart, attaching the wristband when going to bed and removing it upon waking. PPG measurements of sufficient quality and duration to be used for sleep scoring (further described in Section 2.4.2) were included in the analysis; subsequently, 36 recordings are included from the first night and 30 are included from the second night. This volunteer study, which was carried out in the Netherlands in 2015, was approved by the Internal Committee of Biomedical Experiments of Philips Research, Eindhoven, the Netherlands; all participants provided written consent to participate in the study. Participant characteristics are found in Table 1. Note that recordings from the first night are used for the comparison against non-pregnant women (Section 2.4.1), while recordings from both nights are used to assess the impact of gestational age on HRV and morphological features (Section 2.4.3).

Data for the non-pregnant group were selected from a larger dataset of healthy volunteers recruited for a sleep study (2017 and 2018) [25]. One night of measurements was acquired per participant at a sleep clinic (Kempenhaeghe, Heeze, the Netherlands). Exclusion criteria for the data collection were indications of depression, anxiety, neurologic or psychiatric disorders, and the use of any medications apart from birth control. Importantly, pregnancy served as an exclusion criterion. Data from all women in this group who were between the ages of 18 and 45 were available for

analysis. Of these women, 36 had measurements of sufficient quality for sleep stage classification and were subsequently included. Participant characteristics are found in Table 1. The use of the data for the investigation presented in this paper was approved by the medical ethics committee of Sleep Medicine Center Kempenhaeghe, the Netherlands (CSG_2022_007).

Table 1: Demographic information of the groups, presented as median and interquartile range. BMI = body mass index.

	Pregnant group	**Non-pregnant group**
Number of participants	36 (first night)	36
	30 (second night)	
Age	31 (28 – 33) years	24 (21– 28) years
BMI (pre-pregnancy)	23.0 (20.7 – 25.5) kg/m^2	23.1 (22.1 – 24.6) kg/m^2
Gestational age (first night)	21 (18 – 23) weeks	
Gestational age (second night)	29 (26 – 32) weeks	

2.2 Pre-processing of the PPG data

Preprocessing of the raw PPG data from the wristband was needed to facilitate feature extraction. Data were first filtered to remove information that was not physiologically relevant. Segments with motion artifacts (which often plague recordings from wrist-worn devices such as the ones used in this study) were removed. Finally, the processed PPG data were further segmented to identify fiducial points and isolate each pulse wave for feature calculation.

2.2.1 Filtering

A third-order Butterworth band-pass filter with a high-pass cutoff frequency of 0.007 Hz and a low-pass cutoff frequency of 10 Hz was applied to suppress noise. These cutoff frequencies were chosen based on examples from the literature [26], [28], [29], as well as evaluating the power spectral density (PSD) estimate of the raw PPG signals from the datasets (obtained with Welch's method).

2.2.2 Removal of motion artifacts

A signal instability index (SII) was calculated based on the PPG data to detect signal segments with motion artifacts. The SII is a non-parametric measure based on the

probability density function of a physiological signal, calculated using kernels density estimation (KDE) employing Gaussian kernels [30]. KDE is calculated as follows:

$$\widehat{f_h}(x) = \frac{1}{nh}\sum_{i=1}^{n} K\left(\frac{x-x_i}{h}\right), \qquad (1)$$

where n is the number of equally distributed points that divide the length of the signal x, K is the Gaussian kernel centered at the point i, and h is the bandwidth of the Gaussian kernels. The bandwidth of the KDE is the SII, which was calculated based on 15 seconds epochs with a one-second sliding window [30]. Periods in the PPG signal where the SII exceeds an empirically chosen threshold of 0.8* σ +μ (i.e., mean of the SII plus 0.8 times the standard deviation) were noted as motion artefacts and excluded from the analysis.

2.2.3 Segmentation of PPG waveforms

Hereafter, the PPG signal was segmented using the pulse segmentation method developed by Elgendi et al. [17], as implemented in the NeuroKit2 package in Python [31]. Thereafter, a further refinement step was performed. To ensure the systolic peak (SP) was not misdetected (see Figure 1, Section 2.3.2), the detected peak was checked against point e2 on the second derivative of the PPG pulse wave (Figure 1), which corresponds to the notch between the SP and diastolic peak (DP). If the detected peak occurred after this reference point, the SP was redefined as the peak between the initial trough (IT in Figure 1) and point *e*.

2.3 Feature extraction

Features based on the variability between heartbeats (HRV features) and the morphology of the pulse wave (morphological features) were calculated. These features are calculated based on five-minute measurement segments, as is further elaborated upon in Section 2.4. Considering the large number of features calculated (n = 67), these are briefly described or illustrated in the following sections. In all cases, references are added which provide more detailed information.

2.3.1 Heart rate variability

HRV is the fluctuation in the duration of the interbeat intervals (IBIs) along time, resulting from the complex and non-linear oscillations of the heart. This fluctuation is regulated by the dynamic relationship between the two ANS branches, namely the parasympathetic and sympathetic nervous systems [32], [33]. Specific selections of HRV features were calculated with time-domain, frequency-domain, non-linear, phase

rectified signal averaging (PRSA), and heart rate fragmentation (HRF) analyses [33]–[36]. For all the methods, the IBIs were calculated based on the distance between two consecutive pulse wave troughs. To further eliminate erratic or incorrectly detected IBIs, those that varied more than 20% from the preceding IBI or were not between 0.3 and 2.4 seconds in duration were removed. For methods requiring a continuous signal, i.e., frequency-domain features and some non-linear features such as sample entropy, the IBIs were interpolated using an on-time approach detailed elsewhere [37], in which the timestamps of the missing heartbeats are found with quadratic interpolation.

Time domain features [33], [38]–[40]

- Mean HR: The mean IBI per segment, converted to beats per minute (bpm).
- SDNN: Standard deviation of normal-to-normal (NN) IBIs. SDNN is related to the total variability of the HR and is impacted by both the sympathetic and parasympathetic nervous system.
- RMSSD: Root mean square of the time differences between successive normal heartbeats. RMSSD estimates the beat-to-beat variance of HR mediated by the vagus nerve, which is the main component of the PNS.
- pNN50: Percentage of contiguous IBIs which differ with more than 50ms. This feature measures the parasympathetic modulation of IBIs [39].
- Kurtosis: the kurtosis of the spread of the IBIs.
- Skewness: the skewness of the spread of the IBIs.

Frequency-domain features

The power spectral density and the subsequent features estimations were performed with the Fast Fourier Transform (FFT) algorithm based on the Welch method using pyHRV, a reliable open-source Python toolbox for the computation of HRV parameters [36], [41]. IBI series are divided into shorter, overlapping segments (5 minutes in length, 50% overlap) during computation, and the mean of the values computed per segment is taken as the result for the corresponding IBI series. The following features were calculated [33], [38], [39]:

- Very-low-frequency (VLF) power: Absolute power of frequency band between 0Hz and 0.04Hz. Information about the physiological mechanisms of which the activity is reflected in this band is uncertain, but it has been linked mainly to PNS activity.

- Low-frequency (LF) power: Absolute power of frequency band between 0.04Hz and 0.15Hz, mainly reflecting baroreceptor activity.
- High-frequency (HF) power: Absolute power of frequency band between 0.04Hz and 0.15Hz. HF power reflects parasympathetic activity, with respiration having a major contribution.
- Normalized LF: LF power normalized by the sum of LF and HF powers.
- Normalized HF: HF power normalized by the sum of LF and HF powers.
- LF/HF: This ratio is considered a measure of sympathovagal balance.

Non-linear features

Non-linear features aim to capture the regularity or complexity of the IBIs [33], [39]. For this analysis, the pyHRV toolbox was also used. The Poincaré plot was first determined, in which a scatter plot is obtained by plotting the IBIs against their precursor to then fit an ellipse. From this ellipse, the width (SD1) and length (SD2) are determined, which capture short-term and long-term variability, respectively [42]. Furthermore, the SD1/SD2 is calculated, which represents the relationship between short- and long-term variability and is correlated with the LF/HF ratio [33], [43]. Finally, the area of the ellipse (S) is determined, giving a measure of total HRV.

Additionally, the self-similarity of the IBIs over time was analyzed using detrended fluctuation analysis (DFA). Rather than being fully predictable or completely random, patterns within the HR signal are expected to repeat over different timescales. To capture these correlations, the short-term (4 to 16 beats) fractal scaling exponent from DFA is calculated, namely, α_1[44]. Additionally, sample entropy (SampEn) is calculated to assess the complexity of the IBIs. SampEn determines the conditional probability that two epochs that are similar within a tolerance r for a window length m will remain similar when including the next data point (i.e., the next IBI) [45], [46]. The parameters m and r were set to 2 and 0.2 times the standard deviation of the IBIs [45]. Lower SampEn indicates a more regular and predictable time series.

PRSA features

Quasi-periodicities may exist within the HR which are obscured by noise. PRSA is a signal analysis method that can detect such quasi-periodicities in physiological signals to assess system dynamics, regardless of the noise that is typically present. Briefly, this method compresses the signal into a shorter, averaged waveform that captures the relevant quasi-periodicities while discarding non-stationarities, artifacts, and noise by synchronizing the phase of the periodic components [34], [47].

The method comprises three steps. First, the phases of interest are identified, referred to as the anchor points (APs). Here, there are two sets, HR accelerations, and HR decelerations. Thereafter, a signal segment is identified around each AP. Next, these segments are aligned by their AP and averaged, resulting in a waveform that captures the behavior of the signal relative to the AP. If there is no periodicity linked to the AP, this averaging would result in a flatline. However, if such a periodicity exists, the averaging should result in a waveform with oscillations.

This waveform is described with several features. Consider the case where HR decelerations are the APs. Deceleration capacity (DC) is calculated to capture the magnitude of the response in the waveform to the AP by summing the value of the two points preceding the AP, the value at the AP, before diving this sum by four. Furthermore, the immediate deceleration response (IDR) is computed as the difference between maximum and minimum values of the waveform in the five data points preceding the AP and the five thereafter, including the AP. Correspondingly, the slope of this deceleration response (SDR) is determined. Finally, the average deceleration response (ADR) is estimated as the differences between the mean of the 50 values preceding the APs and the mean of the 50 values thereafter, including the AP. Similarly, these features are also calculated for the case where HR accelerations are the APs: acceleration capacity (DC), immediate acceleration response (IDR), acceleration response (SDR), and average acceleration response (ADR) [34], [48].

HRF features

This method is used to discern whether the short-term dynamics of the HRV are being vagally or non-vagally mediated. If the short-term variation is smooth, it is likely vagally mediated. Conversely, if this variation is jagged, or fragmented, it likely results from a breakdown in physiological control over HR rather than healthy autonomic modulation. The features which were developed to capture this HRF are the following: PIP (percentage inflection points); PAS (percentage alternating segments); PSS (percentage short segments); and IALS (inverse of accelerating or decelerating long segments). Increases in these features indicate increased fragmentation in HR [35].

2.3.2 Morphological features

The PPG pulse wave mainly reflects blood flow dynamics through the vascular bed [16]. The rising edge of the pulse reflects the systolic phase of the heartbeat (i.e., between IT and SP in Figure 1), and the diastolic phase is reflected in the falling edge (i.e., between SP and the final trough (FT) in Figure 1). Morphological features were

calculated from the literature [28], [49], [50]. In addition, features describing angles, slopes, and velocity were added. Only the fully segmented pulses were considered for feature extraction, i.e., pulses for which the IT, the SP, and the FT were all detected, as shown in Figure 1. The PPG waveform as well as the waveforms resulting from its first and second derivatives were used to compute several features; these waveforms and their relative characteristics are detailed in Figure 1. Note that the first and second derivatives reflect the velocity and acceleration of the PPG waveform, respectively [51]. The morphological features, which are found in Table 2, are clustered by amplitudes, time differences, areas under the curve (AUCs), velocity and acceleration, ratios, slopes, and angles. It should be noted that most of these features do not yet have a clear physiological interpretation but rather attempt to capture the characteristics of the pulse as fully as possible.

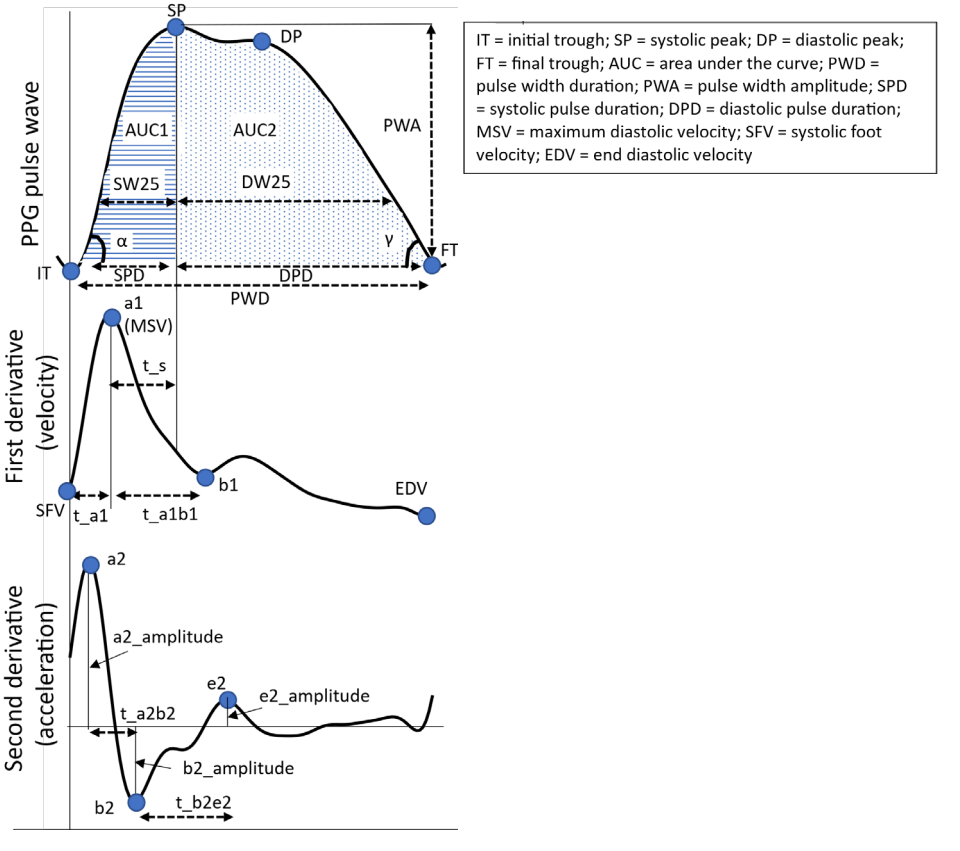

Figure 1: The top waveform represents the PPG pulse wave, followed by the first and second derivatives of the waveform. Aspects of these waveforms relevant to the morphological features listed in Table 2 are indicated in the figures.

Table 2: Description of the morphological features. The fiducial points on the PPG pulse wave discussed in the table can be found in Figure 1. Note that in Figure 1, DW25 and SW25 can be found, which represent the diastolic and systolic widths at 25% of the amplitude. Where features such as DW are mentioned in the table, these are similar to DW25, but at 10% instead of 25%.

Features		Explanation
Amplitude	PWA	Pulse width amplitude, i.e., the difference between SP and IT.
	b2_ amplitude	The absolute value of the amplitude of the deepest trough of the second derivative signal (b2)
Time differences	PWD	Pulse width duration; time interval between IT and FT.
	SPD	Systolic phase duration; time interval between IT and SP
	DPD	Diastolic phase duration; time interval between SP and FT
	t_a1	Time interval between IT and a1 on the first derivative signal
	t_a1b1	Time interval between the a1 and the first valley of the first derivative signal (b1)
	t_a2b2	Time interval between points a2 and b2 on the second derivative signal
	t_b2e2	Time interval between points b2 and e2 on the second derivative signal
AUC	AUC_total	AUC of the full pulse wave, i.e., between IT and FT
	AUC1	AUC of systolic phase, i.e., between IT and SP
	AUC2	AUC of diastolic phase, i.e., between SP and FT
Velocity and acceleration	mean(V)	Mean velocity, i.e., mean of the first derivative signal
	IDR(V)	Interdecile range of velocity, i.e., interdecile range of the first derivative signal
	Mean (Acc)	Mean of the second derivative signal
	MSV	Max systolic velocity; a1 on the first derivative
	SFV	Systolic foot velocity, i.e., value of the point on the first derivative signal corresponding to IT of the pulse wave

Ratio	DW10/SW10	The ratio of systolic width to diastolic width at 10% of the pulse wave amplitude; similar features are calculated at 25%, 50%, and 60%.
	t_s/PWD	The ratio between the time interval between a1 and SP (i.e., t_s), and the pulse width duration (PWD), which is the time interval between IT and FT.
	t_a1/PWD	The ratio of the time interval between the IT and a1 (i.e., t_a1) to PWD
	t_a1b1/PWD	The ratio of t_a1b1 to PWD
	t_a2b2/PWD	The ratio of t_a2b2 to PWD
	t_b2e2/PWD	The ratio of t_b2e2 to PWD
	b2/a2	The ratio of b2_amplitude to a2_amplitude, found on the second derivative signal
	e2/a2	The ratio of e2_amplitude to a2_amplitude, found on the second derivative signal
	SPD/PWD	The ratio of SPD to PWD
	SP/SPD	The ratio of the value of SP to SPD
	Pulsatility index	(Max systolic velocity (i.e., a1 on the first derivative) – end diastolic velocity (i.e., EDV on the first derivative) / (mean of the first derivative)
Slope	slope_IT_SP	The slope of line that connects IT and SP
	slope_SP_FT	The slope of line that connects SP and FT
Angle	α	The angle of the slope between IT and SP
	γ	The angle of the slope between SP and FT

2.4 Data analysis and statistics

The features described in Section 2.3 are calculated based on 5-minute segments of non-overlapping PPG data. Morphological features are obtained for every pulse and then averaged over the full segment. Segments are discarded if 20% of the data in the segment was removed during motion artifact correction (Section 2.2.2), or if 20% of the IBIs are deemed unreliable as defined in Section 2.3.1. Once all the features are calculated, these are used for the classification model discussed in Section 2.4.1 below. Furthermore, we compare these features between the pregnant and non-pregnant groups using the Mann-Whitney-U test for statistical significance, along with Cohen's d for effect size, reported with 95% confidence interval [52].

2.4.1 Logistic regression model and feature selection

We use a logistic regression model to classify women as either pregnant or non-pregnant, using data extracted from wrist-worn PPG measurements. We develop three sets of models, the first using only HRV features, the second only morphological features, and the third using a combination of HRV and morphological features. Note that we do not consider PWD (pulse width duration) for the morphological feature set, as PWD is analogous to mean HR, which forms part of the HRV features. A sevenfold cross-validation was performed. Feature importance was estimated based on a stepwise forward elimination process, which was performed for each of the seven runs. Features were ranked according to their importance for each iteration and ultimately the ten most popular features across all iterations were selected to be used for the logistic regression models.

Using these identified features, women are classified as either pregnant or non-pregnant. The classification is first performed using only the most important feature identified for each feature set. Thereafter, the second most important feature for each set is incorporated and the classification is again performed. The rest of the ten features for each feature set are likewise introduced into the model one by one. The predictive strength of the classifier was evaluated by calculating the area under the receiver operating characteristic curve (AUROC) from the left-out folds of a sevenfold cross-validation, repeated seven times to provide an average estimate of the AUROC along with its standard deviation to provide a measure of dispersion. Furthermore, considering that multiple measurements are available per participant, the classification was also repeated with measurements stratified per participant. Note that the data for the pregnant group comprises recordings from the first night of the pregnancy dataset.

2.4.2 Stratification by sleep stages

As a sub-analysis, we repeat the analysis detailed in Section 2.4.1 using features calculated only from data from a specified sleep stage. Sleep stages are determined for both datasets using a published, automated algorithm that scores sleep based on PPG and accompanying accelerometer data [53]. Sleep scoring is done per 30-second epoch, classifying data as light sleep (N1/N2), deep sleep (N3), rapid eye movement (REM), and Wake [53]. Not that only the data from the identified sleep stages are used and Wake data are discarded for this sub-analysis. Again, the segments used are non-overlapping PPG segments of five minutes, as described in Section 2.4, each of which now have to contain data from only one sleep stage.

2.4.3 Comparison between different gestational ages

Finally, as a further sub-analysis, we compare the features identified in Section 2.4.1 between the first and second night of recordings of the pregnant group to assess whether the features capture the changes of progressing gestation.

3. Results

3.1 Descriptive statistics of HRV and morphological features

Differences in the HRV and morphological features, as calculated based on five-minute segments from the full recordings, are tabulated in Appendix A in Tables A1 and A2, respectively. The vast majority of features differed significantly between the groups, with the largest effect sizes found for the following features, reported with 95% confidence interval: SPD (d = 1.03 (0.98 - 1.09)), mean HR (0.93 (0.86 - 1.01)), t_a1 (d = 0.82 (0.74 - 0.89)), DW10/SW10 (d = 0.72 (0.66 – 0.78)), SPD/PWD (d = 0.66 (0.60 – 0.72)), RMSSD (d = 0.65 (0.59 - 0.72)) and SD1 (d = 0.65 (0.59 - 0.73)). The latter two features relate to parasympathetic modulation, while those before all relate to the cardiac cycle to some extent.

3.2 Feature importance

In Table 3, the features which were identified to be most valuable in discriminating between pregnant and non-pregnant women are listed for each feature set. Note that for HRV, mean HR and PSS were consistently the most and second most important features in each iteration; the same is true for SPD and t_ab for both the morphological feature set as well as the combined feature set. Additionally, IALS was the third most important feature for the combination of features in each iteration.

Table 3: The most important features for discriminating between pregnant and non-pregnant women, as chosen by stepwise forward elimination, for each of the feature sets as well as the combination of the two feature sets.

Importance	HRV	Morphology	HRV+ Morphology
1	Mean HR	SPD	SPD
2	PSS	t_a2b2	t_a2b2
3	SAR	IDR(V)	IALS
4	SDR	FSV	FSV

5	S (Poincaré)	AUC2	b2_amplitude
6	PIP	b2_amplitude	slope_IT_SP
7	AC	SP/SPD	PWA
8	IAR	t_s/PWD	S (Poincaré)
9	IDR	PWA	SP/SPD
10	SD2	slope_IT_SP	AUC1

3.3 Logistic regression model

The number of five-minute data segments available for the classification model is listed in Table 4, both considering the entire recording as well as per sleep stage. Furthermore, the number of participants for which data were available in each stratified analysis is also listed. Note that these numbers are lower than the total number of participants as in some cases participants did not have five-minute measurements available which were continuously in the relevant sleep stage and of sufficient quality, as defined in Section 2.4.Considering the sleep stages, the highest number of segments are available for light sleep (N1/N2), substantially less for deep sleep (N3), and the least for REM sleep.

Table 4: Number of measurements available for the classification model based on the entire night's recording, as well as only N1/N2, N3, or REM, respectively.

	Pregnant group		**Non-pregnant group**	
	No. of segments	**No. of participants**	**No. of segments**	**No. of participants**
Full night	1629	36	1407	36
N1/N2 (light sleep)	903	33	788	32
N3 (deep sleep)	200	29	288	30
REM	152	23	172	27

Figure 2 shows the AUROC scores (with standard deviation), for the classification based on only HRV features, only morphological features, and a combination of the two feature sets. The classification is first performed using one feature, thereafter two features, etc., until ten features are reached. The features used are the ones detailed in Table 3. To illustrate, consider the HRV features: first, only mean HR is used for the classification; next, mean HR and PSS are both used; thereafter, mean HR, PSS, and SAR are used; etc.

The results in the left panel (A) reflect the model when all measurement segments are treated as unique, while in the right panel (B), the classification was repeated, now with measurement segments stratified per participant. The performance of the models, as measured with the AUROC, remains comparable between panels A and B. However, when stratifying per participant the performance variance increases substantially. In both cases, notice that the classifiers using only PPG or a combination of PPG and HRV perform comparably well while using only HRV results in the poorer performance. Comparable variance in the performance is seen for each feature set. Furthermore, for the HRV feature set, the addition of HRV to mean HR offers only slight improvements to the performance (Figure 2A) or none at all (Figure 2B), at least not within the first ten features. For the morphological feature set or the combination feature set, incremental improvements are seen in performance when adding additional features to SPD.

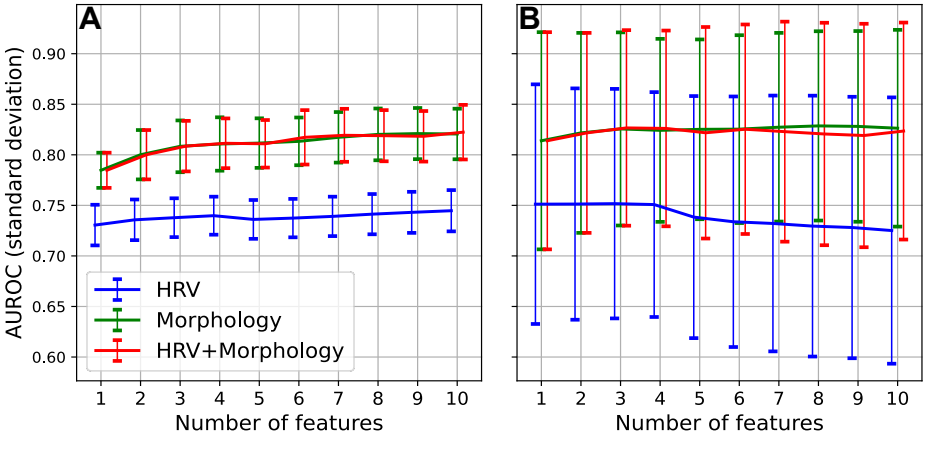

Figure 2: A) The AUROC scores, with standard deviation, for the models based on HRV features only (blue), morphological features only (green), and a combination of the two sets (red), plotted against the number of features used. B) AUROC scores, with standard deviation, for classification based on HRV features only (blue), morphological features only (green), and a combination of the two sets (blue), stratified by participant level, plotted against the number of features used. The features correspond to those listed in Table 3. For example, when three features are used, the first three features listed in Table 3 have been used.

3.4 Sleep stage stratification

The classification process in the previous section is repeated, now based only on data from each scored sleep stage (Figure 3), namely N1/N2, N3, and REM. Considering the performance of the models at ten features, the model performs best when data

from N3 are used (Figure 3B), although the improvement compared to that of N1/N2 is small (Figure 3A). The performance of the latter closely resembles the performance based on data from the entire night (Figure 2A), likely in part due to N1/N2 being the most prevalent sleep stage. The classifier performs worst when data from the REM stage is used (Figure 3C).

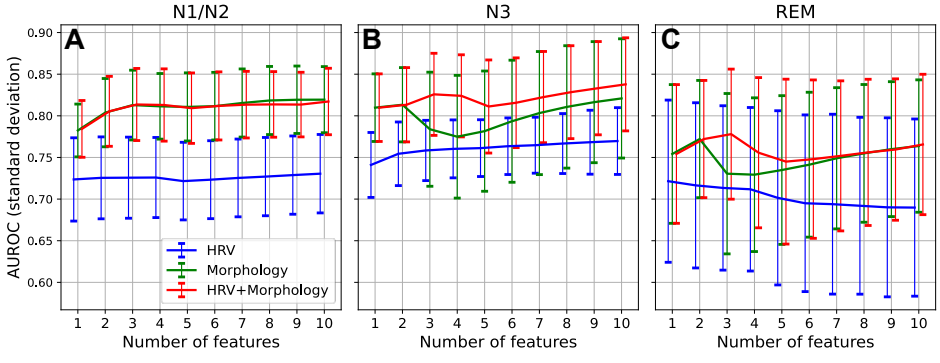

Figure 3: A) AUROC scores, with standard deviation, for the models using only data from the REM, N1/N2 (light sleep), or N3 (deep sleep). For each, the results of three models are presented, based on HRV features only (blue), morphological features only (green), and a combination of the two sets (red), respectively. B) Again, the AUROC scores, with standard deviation, are presented. In this case, the classification was stratified on the participant level.

Furthermore, notice the classification based on only HRV features for the N3 stage; even at only one feature, the classifier outperforms the ones based on data from N1/N2 or REM. Moreover, in N3 we observe that incorporating further HRV features systematically improves the model's performance.

3.5 The impact of gestational age on HRV and morphological features

The features which were identified as important were further compared between the recordings of the first and second nights of the pregnant group. Differences in these HRV and morphological features are tabulated in Table A3 in Appendix A. Concerning the HRV features, there were significant differences between the groups for all features. Mean HR further increased in later pregnancy, while most features that were reduced compared to non-pregnant women, such as RMSSD and IALS, decreased further. For the morphological features, fewer features significantly differed between the gestational age groups, although the area under the PPG curve (as assessed with AUC1 and AUC2), as well as the PWA (pulse wave amplitude), continued to decrease. Notice-

ably, SPD, which is the most important feature for discriminating between pregnant and non-pregnant women (Table 3) does not change with progressing pregnancy, at least not within the eight weeks between the first and second night of measurements.

4. Discussion

A plethora of wearable monitors is available to track cardiac activity, of which the most popular are wrist-worn PPG monitors. As a healthy pregnancy necessitates continuous changes in maternal autonomic regulation, tracking HRV is considered to be a potential tool for assessing maternal health [12], [13], [54]–[56]. In addition to HRV features, morphological features – which describe the autonomically regulated morphology of the pulse wave – can also be extracted from PPG measurements [16]. While many HRV and morphological features exist in the literature, typically used in other application areas, it is unclear which of these would be valuable in assessing maternal health. As a foundational step towards identifying potentially useful features, we investigated which of these are most important in discriminating between healthy pregnant and non-pregnant women.

Based on a stepwise forward elimination process, we find that SPD (systolic phase duration) and mean HR are, individually, the most important features for discriminating between these two groups (Table 3), with an AUROC of 0.73 and 0.78, respectively (Figure 2A). It stands to reason that the difference in SPD between pregnant and non-pregnant women is largely driven by the increased mean HR observed in the pregnant group. However, if we consider the differences in the DPD (diastolic phase duration) and SPD/PWD, i.e., the ratio of the SPD to the pulse wave duration (in Table A2), we can observe that the relative decrease in SPD during pregnancy is larger than the decrease in DPD. Therefore, SPD likely outperforms mean HR because it reflects not only the autonomic changes that accompany gestation but also, to some extent, the cardiovascular adaptions which occur during pregnancy. The overall performance of the models (Figures 2 and 3) further supports this. In all cases, using only morphological features results in an improved performance when compared to using only HRV features. Furthermore, if we consider the performance of the combination of HRV and morphological features, we see that this improves considerably on the performance of only HRV but is generally comparable to using only morphological features.

Consequently, we suggest that the longitudinal tracking of maternal HRV with wearable PPG monitors would benefit from also incorporating morphological features.

Specifically, SPD, t_a2b2, IDR(V) (i.e., the interdecile range of the first derivative), the FSV (foot systolic velocity), and b2_amplitude appear to be particularly valuable. However, it is important to note that while HRV features are reasonably explainable [33], substantial future work is needed to determine the physiology underpinning morphological features, especially during pregnancy. Yet, considering our results, along with the fact that the data for determining these features can be easily acquired, we believe that morphological features are of additional value and should be included in the assessment of the maternal condition. Moreover, morphological features may in the future be particularly useful in identifying pregnancy complications such as HDP, since these are associated with cardiovascular dysfunction as well as autonomic dysfunction. Furthermore, preeclampsia (a type of HDP) is characterized by endothelial damage to the systematic vasculature, which may be detectable with morphological features [55], [57], [58].

Considering the HRV features, we notice that for the model based only on these features, the addition of further HRV features to the mean HR does not seem to improve the model performance (Figures 2A, 3A, and 3C). Yet, research indicates that healthy pregnant women have increased sympathetic and decreased parasympathetic activity compared to healthy controls [2], [21], [59], [60]. While this autonomic imbalance does contribute to the increased HR that we see in pregnant women [61], [62], it is doubtful that HRV features offer no additional physiological information. Potentially, it is the low sampling rate (32 Hz) of PPG that offers inadequate precision to fully capture differences in HRV.

Half of the HRV features identified as important (Table 3) for discriminating between pregnant and non-pregnant women are those of the PRSA analysis, suggesting that this category of features should be incorporated in future assessments of maternal health. These features are linked to autonomic responsiveness, and potentially reflect the damped physiological responsiveness which is observed during pregnancy [63], [64]. Moreover, PRSA features are particularly robust against noise [34], [47], which is advantageous when assessing PPG data collected in free-living conditions. Additionally, HRF features also play an important role, with PSS and IALS being the second most important feature in the HRV feature set and the third most important feature in the combined feature set, respectively (Table 3). The purpose of HRF features is to capture variability in the IBIs which is not vagally regulated [35]; therefore, these may add unique value since they capture information that is not reflected in the majority of HRV features, which capture some aspect of vagal or sympathetic activity [33]. Subsequently, in addition to PRSA features, HRF features may also be valuable in tracking maternal health.

Furthermore, the results for the classification using HRV features calculated from deep sleep data (N3) are interesting (Figure 3B). Here the classification performance is comparable to the other sleep stages when using mean HR only, but thereafter it increases incrementally to the best performance at ten features. During deep sleep, movements are minimal; therefore, measurements from this sleep stage may be of higher quality than other stages, allowing for more accurate HRV analysis. Additionally, considering that pregnant women have reduced parasympathetic activity compared to non-pregnant women and that deep sleep is a state of parasympathetic dominance [24], the autonomic differences between these two groups may be heightened during N3 sleep, making HRV more impactful in discriminating between the two groups. The latter hypothesis is further strengthened when noting the performance of the classifier using only features calculated from REM data (Figure 3C). During REM sleep, sympathetic influence is increased [24]. While healthy pregnant women also have increased sympathetic activity compared to non-pregnant women, REM is characterized by regular shifts in autonomic balance [24], potentially obscuring physiological differences between the groups which are more prominent during deep sleep.

Consequently, we postulate that when tracking non-invasive indices of maternal autonomic regulation to assess maternal health, it would be beneficial to focus on data from the N3 sleep stage. Doing so might elucidate differences in these features which are not apparent when performing assessments based on the entire night's recording or based on a specific timepoint, e.g., using data recorded daily at 05:00 hours. This sleep stage can act as a pseudo-controlled environment in free-living conditions that repeats nightly, with minimum motion artifacts. This would allow for tracking the progression of these features over time with reduced influence from environmental factors. Additionally, considering again that the ultimate goal would be to detect pregnancy complications early in pregnancy, using N3 data would exploit prior knowledge of differences between healthy and complicated pregnancies, namely that complicated pregnancies have reduced parasympathetic activity compared to healthy pregnancies [10], [11].

The study presented here has some limitations, primarily the relatively low sampling rate of the PPG measurements (32 Hz). The necessary sampling rate to determine HRV from PPG measurements is widely debated; however, feature accuracy is improved when measurements have been collected at rest, as is the case in this work [65]. When we compare our HRV results (Table A1, Appendix A) to prior work based on ECG measurements [20], we observe similar trends, i.e., features linked to para-

sympathetic activity (e.g., RMSDD and HF), PRSA features, and HRF features are generally lower in the pregnant group, while mean HR is increased. Still, in future work, PPG measurements of a higher sampling rate should be used; alternatively, features that are the most susceptible to errors due to low sampling rates, such as frequency domain features, should be excluded. Furthermore, while we find in this work that HRV features perform poorer than morphological features in discriminating between pregnant and non-pregnant women, HRV features may perform better at higher sampling frequencies. However, performance may also similarly improve in this case for the morphology features.

The reliability of morphological features at different sampling rates has been less extensively researched, although one study has shown that several features are reliable even at a sampling rate of 30 Hz [66]. Still, despite the low sampling rate, we observe robust differences between our groups (Appendix A). Furthermore, there is a median age difference of six years between our groups. While age does impact HRV, the impact of this small age difference is unlikely to be larger than the impact of pregnancy itself [67].

Finally, an algorithm that scores sleep stages based on PPG data was used for sleep scoring in this analysis rather than sleep scoring performed by a technician based on polysomnography data. Using this automated sleep scorer, which has been shown to have reasonable accuracy [53], allows for comparable sleep scoring in both datasets. Furthermore, using an algorithm that scores sleep stages based only on PPG and accelerometer data would allow for sleep staging information to be incorporated in longitudinal assessments of maternal health in free-living conditions, as suggested earlier in this discussion.

To conclude, we have demonstrated that in addition to differences in HRV, there are also significant differences in morphological features between healthy pregnant and non-pregnant women. SPD (systolic pulse duration) and mean HR are the most important features for discriminating between these two groups, based on PPG measurements at a relatively low sampling rate (32 Hz). Moreover, morphological features were overall more valuable for discriminating between the groups than HRV features. We suggest that morphological features may in the future be valuable for tracking maternal health. Furthermore, when using HRV to assess maternal health, PRSA and HRF should be included in the analyses.

Appendix A

Table A1: HRV features, presented as median and interquartile range, along with significance and effect size of differences between pregnant and non-pregnant women (p-value and d-value)

Features		Pregnant group	Non-pregnant group	*p*-value	*d*-value (95% confidence interval)
Time domain	Mean HR	65.43 (60.91 - 69.43)	59.19 (54.13 - 63.84)	< **0.0001**	0.93 (0.86 - 1.01)
	SDNN	57.92 (43.67 - 76.75)	71.08 (50.8 - 92.5)	< **0.0001**	0.28 (0.21 - 0.38)
	RMSSD	51.87 (40.57 - 62.96)	66.83 (46.09 - 88.22)	< **0.0001**	0.65 (0.59 - 0.72)
	pNN50	34.97 (22.12 - 44.92)	45.66 (28.65 - 59.03)	< **0.0001**	0.56 (0.49 - 0.64)
Frequency domain	VLF	740.06 (346.13 - 1536.69)	955.4 (449.91 - 2038.09)	< **0.0001**	0.24 (0.18 - 0.3)
	LF	900.79 (400.04 - 2049.59)	1350.22 (587.1 - 2656.8)	< **0.0001**	0.28 (0.21 - 0.34)
	HF	1167.39 (591.57 - 2237.11)	1970.65 (808.53 - 3947.78)	< **0.0001**	0.42 (0.35 - 0.48)
	Normalized LF	0.43 (0.29 - 0.58)	0.4 (0.29 - 0.54)	**0.0022**	0.13 (0.06 - 0.2)
	Normalized HF	0.57 (0.42 - 0.71)	0.6 (0.46 - 0.71)	**0.0022**	0.13 (0.06 - 0.2)
	LF/HF	0.76 (0.41 - 1.38)	0.68 (0.4 - 1.18)	**0.0022**	0.19 (0.13 - 0.26)
Non-linear	SD1	36.68 (28.69 - 44.49)	47.19 (32.59 - 62.11)	< **0.0001**	0.65 (0.59 - 0.73)
	SD2	67.68 (49.62 - 90.77)	82.44 (58.12 - 107.18)	< **0.0001**	0.39 (0.32 - 0.46)
	SD1/SD2	0.55 (0.43 - 0.68)	0.6 (0.47 - 0.74)	< **0.0001**	0.25 (0.18 - 0.32)
	S	7741.15 (4820.81 - 12246.44)	12057.77 (6467.05 - 20484.69)	< **0.0001**	0.57 (0.51 - 0.64)
	α_1	0.86 (0.7 - 1.04)	0.83 (0.68 - 0.97)	< **0.0001**	0.18 (0.11 - 0.25)
	SampEn	1.49 (1.26 - 1.68)	1.65 (1.37 - 1.95)	< **0.0001**	0.54 (0.46 - 0.61)

PRSA	DC	21.06 (15.62 - 27.55)	24.0 (17.89 - 32.23)	< **0.0001**	0.29 (0.21 - 0.36)
	AC	-21.57 (-28.71 - -16.33)	-25.61 (-36.01 - -19.33)	< **0.0001**	0.41 (0.33 - 0.48)
	IDR	53.43 (44.41 - 65.35)	65.84 (46.88 - 87.01)	< **0.0001**	0.49 (0.42 - 0.56)
	IAR	55.21 (44.2 - 68.29)	66.4 (49.91 - 88.87)	< **0.0001**	0.48 (0.41 - 0.55)
	SDR	40.24 (27.14 - 51.68)	42.2 (21.05 - 59.85)	0.081	0.05 (-0.02 - 0.12)
	SAR	-40.86 (-53.58 - -29.35)	-46.88 (-68.24 - -33.98)	< **0.0001**	0.32 (0.25 - 0.4)
	ADR	1.37 (-2.02 - 5.41)	1.27 (-2.83 - 6.08)	0.2638	0.08 (0.01 - 0.15)
	AAR	-2.05 (-5.89 - 1.49)	-2.36 (-6.98 - 1.74)	0.0849	0.07 (-0.0 - 0.14)
HRF	PIP	74.79 (66.55 - 82.51)	71.02 (62.35 - 78.8)	< **0.0001**	0.28 (0.21 - 0.35)
	PAS	0.38 (0.34 - 0.41)	0.41 (0.37 - 0.45)	< **0.0001**	0.62 (0.55 - 0.7)
	PSS	54.68 (47.1 - 67.8)	63.97 (54.35 - 79.9)	< **0.0001**	0.64 (0.57 - 0.71)
	IALS	50.59 (46.45 - 54.81)	51.52 (47.42 - 55.86)	< **0.0001**	0.22 (0.15 - 0.29)
Spread	Kurtosis	0.54 (-0.14 - 2.19)	0.21 (-0.33 - 1.49)	< **0.0001**	0.06 (-0.01 - 0.13)
	Skewness	-0.08 (-0.68 - 0.48)	-0.11 (-0.67 - 0.27)	0.1183	0.09 (-0.04 - 0.2)
Rejected IBIs (%)		2 (0 - 4)	2 (0 - 6)	**0.0001**	0.22 (0.15 - 0.29)

Table A2: Morphological features, presented as median and interquartile range, along with significance and effect size of differences between pregnant and non-pregnant women (p-value and d-value). The last metric, i.e., Missing data, refers to the percentage of the PPG segment which was disregarded due to motion artifacts (Section 2.2.2).

Features		**Pregnant group**	**Non-pregnant group**	***p*-value**	***d*-value (95% confidence interval)**
Amplitude	PWA	292.67 (208.0 - 413.53)	329.43 (196.81 - 524.88)	< **0.0001**	0.2 (-0.13 - 0.27)
	b_amplitude	15.97 (10.3 - 25.14)	12.89 (7.21 - 20.43)	< **0.0001**	0.39 (0.32 - 0.45)
Time differences	SPD	0.26 (0.25 - 0.28)	0.3 (0.28 - 0.33)	< **0.0001**	1.03 (0.98 - 1.09)
	DPD	0.66 (0.61 - 0.72)	0.69 (0.64 - 0.76)	< **0.0001**	0.41 (0.34 - 0.48)
	t_a1	0.08 (0.07 - 0.09)	0.09 (0.08 - 0.09)	< **0.0001**	0.82 (0.74 - 0.89)
	t_a1b1	0.25 (0.24 - 0.27)	0.27 (0.25 - 0.31)	< **0.0001**	0.65 (0.59 - 0.71)
	t_a2b2	0.34 (0.32 - 0.36)	0.36 (0.34 - 0.39)	< **0.0001**	0.51 (0.44 - 0.59)
	t_b2e2	0.24 (0.22 - 0.25)	0.23 (0.2 - 0.25)	< **0.0001**	0.18 (0.11 - 0.24)
AUC	AUC Tot	72.52 (48.27 - 100.98)	88.2 (55.24 - 140.78)	< **0.0001**	0.39 (0.33 - 0.46)
	AUC1	21.7 (14.46 - 30.18)	28.74 (17.78 - 42.56)	< **0.0001**	0.47 (0.4 - 0.54)
	AUC2	46.74 (30.34 - 66.46)	55.34 (34.81 - 89.9)	< **0.0001**	0.37 (0.31 - 0.44)
Velocity/ acceleration	mean(V)	0.02 (-0.02 - 0.13)	-0.0 (-0.08 - 0.04)	< **0.0001**	0.2 (0.13 - 0.33)
	IDR(V)	2.2 (1.47 - 3.3)	2.82 (1.79 - 4.13)	< **0.0001**	0.14 (0.02 - 0.3)
	mean(Acc)	-0.02 (-0.05 - 0.0)	-0.01 (-0.04 - 0.0)	0.9334	0.0 (-0.07 - 0.07)
	MSV	63.5 (43.56 - 93.11)	59.79 (34.74 - 95.22)	**0.001**	0.12 (0.06 - 0.19)
	SFV	14.45 (9.51 - 21.53)	13.43 (7.54 - 21.1)	< **0.0001**	0.17 (0.11 - 0.24)

Ratio	DW10/SW10	2.77 (2.53 - 3.13)	2.56 (2.29 - 2.84)	**< 0.0001**	0.72 (0.66 - 0.78)
	DW25/SW25	2.86 (2.62 - 3.22)	2.64 (2.37 - 2.93)	**< 0.0001**	0.7 (0.64 - 0.76)
	DW50/ SW50	2.77 (2.55 - 3.13)	2.64 (2.4 - 2.91)	**< 0.0001**	0.54 (0.48 - 0.61)
	DW66/ SW66	2.62 (2.4 - 2.92)	2.56 (2.34 - 2.84)	**< 0.0001**	0.22 (0.15 - 0.29)
	t_s/PWD	0.01 (0.01 - 0.01)	0.01 (0.01 - 0.01)	**< 0.0001**	0.63 (0.57 - 0.69)
	t_a1/PWD	0.08 (0.07 - 0.09)	0.09 (0.08 - 0.09)	**< 0.0001**	0.31 (0.24 - 0.39)
	t_a1b1/PWD	0.27 (0.25 - 0.28)	0.28 (0.25 - 0.3)	**< 0.0001**	0.5 (0.44 - 0.56)
	t_a2b2/PWD	0.35 (0.33 - 0.38)	0.36 (0.33 - 0.39)	0.0038	0.01 (-0.06 - 0.08)
	t_b2e2/PWD	0.24 (0.22 - 0.26)	0.23 (0.2 - 0.25)	**< 0.0001**	0.14 (0.07 - 0.22)
	b2/a2	7.68 (-5.55 - 22.72)	6.28 (-2.98 - 18.22)	0.2547	0.04 (-0.02 - 0.08)
	e2/a2	1.62 (-1.18 - 4.83)	1.23 (-0.54 - 3.76)	0.1158	0.03 (-0.04 - 0.08)
	SPD/PWD	0.29 (0.27 - 0.31)	0.3 (0.28 - 0.33)	**< 0.0001**	0.66 (0.6 - 0.72)
	SP/SPD	34.57 (24.47 - 49.53)	34.32 (18.89 - 54.36)	0.0738	0.03 (-0.04 - 0.1)
	Pulsatility index	10.84 (-65.42 - 90.45)	3.03 (-59.8 - 73.06)	0.063	0.06 (-0.01 - 0.11)
Slope	slope_IT_SP	1106.12 (783.0 - 1584.88)	1098.29 (604.48 - 1739.57)	0.0738	0.03 (-0.04 - 0.1)
	slope_SP_FT	-434.82 (-629.44 - -309.37)	-495.13 (-761.95 - -286.64)	**0.0022**	0.1 (0.03 - 0.18)
Angle	α	1.57 (1.57 - 1.57)	1.57 (1.57 - 1.57)	0.0821	0.27 (0.15 - 0.39)
	α	1.57 (1.57 - 1.57)	1.57 (1.57 - 1.57)	0.1855	0.07 (-0.05 - 0.19)
Missing data (%)		7 (2 - 13)	6 (2 - 12)	**0.0001**	0.13 (0.06 - 0.2)

Table A3: Statistical significance and effect sizes (p-value and d-value) of differences in selected HRV and morphological features (Table 3) between N1 and N2 measurements for the pregnant group. Results are presented as median with interquartile range.

Features		Pregnant group (night 1)	Pregnant group (night 2)	*p*-value	*d*-value (95% confidence interval)
HRV features	Mean HR	65.43 (60.91 - 69.43)	67.77 (63.34 - 72.64)	< **0.0001**	0.39 (0.3 - 0.47)
	PSS	54.68 (47.1 - 67.8)	51.51 (45.23 - 60.63)	< **0.0001**	0.3 (0.22 - 0.38)
	SAR	-40.86 (-53.58 - -29.35)	-39.29 (-47.55 - -27.47)	< **0.0001**	0.15 (0.07 - 0.23)
	SDR	40.24 (27.14 - 51.68)	38.63 (25.33 - 47.07)	< **0.0001**	0.14 (0.06 - 0.22)
	S (Poincaré)	7741.15 (4820.81 - 12246.44)	6469.14 (4280.16 - 9796.16)	< **0.0001**	0.34 (0.26 - 0.42)
	PIP	74.79 (66.55 - 82.51)	75.85 (67.78 - 83.5)	**0.045**	0.11 (0.02 - 0.19)
	AC	-21.57 (-28.71 - -16.33)	-20.71 (-27.35 - -15.68)	**0.0224**	0.16 (0.08 - 0.24)
	IAR	55.21 (44.2 - 68.29)	50.55 (42.46 - 62.94)	< **0.0001**	0.29 (0.21 - 0.36)
	IDR	53.43 (44.41 - 65.35)	49.37 (42.44 - 60.59)	< **0.0001**	0.26 (0.18 - 0.34)
	SD2	67.68 (49.62 - 90.77)	61.48 (48.03 - 80.38)	< **0.0001**	0.22 (0.14 - 0.3)
	IALS	0.38 (0.34 - 0.41)	0.37 (0.33 - 0.39)	< **0.0001**	0.22 (0.14 - 0.3)
Morphological features	SPD	0.26 (0.25 - 0.28)	0.26 (0.24 - 0.28)	0.1962	0.09 (0.01 - 0.18)
	t_a2b2	0.34 (0.32 - 0.36)	0.34 (0.31 - 0.36)	**0.0174**	0.12 (0.04 - 0.21)
	IDR(V)	2.2 (1.47 - 3.3)	2.09 (1.42 - 3.07)	0.0571	0.1 (0.04 - 0.17)
	FSV	14.45 (9.51 - 21.53)	12.89 (8.59 - 19.34)	**0.0002**	0.18 (0.11 - 0.26)
	AUC2	46.74 (30.34 - 66.46)	39.81 (28.84 - 55.57)	< **0.0001**	0.24 (0.15 - 0.32)
	b_amplitude	15.97 (10.3 - 25.14)	15.84 (10.11 - 23.48)	0.1504	0.1 (0.02 - 0.17)
	SP/SPD	34.57 (24.47 - 49.53)	34.34 (23.66 - 47.71)	0.2834	0.09 (0.01 - 0.17)
	t_s/PWD	0.01 (0.01 - 0.01)	0.01 (0.01 - 0.01)	0.938	0.06 (0.03 - 0.14)
	PWA	292.67 (208.0 - 413.53)	278.1 (199.45 - 388.11)	**0.025**	0.15 (0.07 - 0.23)
	slope_IT_SP	1106.12 (783.0 - 1584.88)	1098.8 (757.23 - 1526.8)	0.2834	0.09 (0.01 - 0.17)
	AUC1	21.7 (14.46 - 30.18)	19.59 (14.27 - 27.06)	**0.0009**	0.2 (0.12 - 0.27)

References

[1] P. Soma-Pillay, C. Nelson-Piercy, H. Tolppanen, and A. Mebazaa, "Physiological changes in pregnancy.," *Cardiovascular journal of Africa*, vol. 27, no. 2, pp. 89–94, 2016, doi: 10.5830/CVJA-2016-021.

[2] V. L. Brooks, Q. Fu, Z. Shi, and C. M. Heesch, "Adaptations in autonomic nervous system regulation in normal and hypertensive pregnancy," in *Handbook of Clinical Neurology*, Elsevier, 2020, pp. 57–84. doi: 10.1016/B978-0-444-64239-4.00003-5.

[3] G. K. Pal, P. Shyma, S. Habeebullah, P. Shyjus, and P. Pal, "Spectral Analysis of Heart Rate Variability for Early Prediction of Pregnancy-Induced Hypertension," *Clinical and Experimental Hypertension*, vol. 31, no. 4, pp. 330–341, Jan. 2009, doi: 10.1080/10641960802621333.

[4] J. Qiu, L. Chen, X. Wang, and W. Zhu, "Early-pregnancy maternal heart rate is related to gestational diabetes mellitus (GDM)," *European Journal of Obstetrics & Gynecology and Reproductive Biology*, vol. 268, pp. 31–36, Jan. 2022, doi: 10.1016/j.ejogrb.2021.11.007.

[5] A. C. De Kat, J. Hirst, M. Woodward, S. Kennedy, and S. A. Peters, "Prediction models for preeclampsia: A systematic review," *Pregnancy Hypertension*, vol. 16, pp. 48–66, Apr. 2019, doi: 10.1016/j.preghy.2019.03.005.

[6] M. Murphy, S. McHugh, L. M. O'Keeffe, R. A. Greene, P. Corcoran, and P. M. Kearney, "Preventive health counselling during antenatal care using the pregnancy risk assessment monitoring system (PRAMS) in Ireland," *BMC Pregnancy Childbirth*, vol. 20, no. 1, p. 98, Dec. 2020, doi: 10.1186/s12884-020-2756-y.

[7] US Preventive Services Task Force *et al.*, "Screening for Preeclampsia: US Preventive Services Task Force Recommendation Statement," *JAMA*, vol. 317, no. 16, p. 1661, Apr. 2017, doi: 10.1001/jama.2017.3439.

[8] L. M. Reyes, C. W. Usselman, M. H. Davenport, and C. D. Steinback, "Sympathetic Nervous System Regulation in Human Normotensive and Hypertensive Pregnancies.," *Hypertension (Dallas, Tex. : 1979)*, vol. 71, no. 5, pp. 793–803, May 2018, doi: 10.1161/HYPERTENSIONAHA.117.10766.

[9] L. M. Reyes *et al.*, "Sympathetic nervous system activity and reactivity in women with gestational diabetes mellitus," *Physiol Rep*, vol. 8, no. 13, Jul. 2020, doi: 10.14814/phy2.14504.

[10] S. Moors *et al.*, "Heart rate variability in hypertensive pregnancy disorders: a systematic review," *Pregnancy Hypertension*, Mar. 2020, doi: 10.1016/j.preghy.2020.03.003.

[11] S. V. Khlybova, V. I. Tsirkin, S. A. Dvoryanskii, I. A. Makarova, and A. N. Trukhin, "Heart rate variability in normal and complicated pregnancies," *Hum Physiol*, vol. 34, no. 5, pp. 625–632, Sep. 2008, doi: 10.1134/S0362119708050113.

[12] F. Sarhaddi, I. Azimi, A. Axelin, H. Niela-Vilen, P. Liljeberg, and A. M. Rahmani, "Trends in Heart Rate and Heart Rate Variability During Pregnancy and the 3-Month Postpartum Period: Continuous Monitoring in a Free-living Context," *JMIR Mhealth Uhealth*, vol. 10, no. 6, p. e33458, Jun. 2022, doi: 10.2196/33458.

[13] S. P. Rowan, C. L. Lilly, E. A. Claydon, J. Wallace, and K. Merryman, "Monitoring one heart to help two: heart rate variability and resting heart rate using wearable technology in

active women across the perinatal period," *BMC Pregnancy Childbirth*, vol. 22, no. 1, p. 887, Nov. 2022, doi: 10.1186/s12884-022-05183-z.

[14] A. Maugeri, M. Barchitta, and A. Agodi, "How Wearable Sensors Can Support the Research on Foetal and Pregnancy Outcomes: A Scoping Review," *JPM*, vol. 13, no. 2, p. 218, Jan. 2023, doi: 10.3390/jpm13020218.

[15] A. Galli, R. J. H. Montree, S. Que, E. Peri, and R. Vullings, "An Overview of the Sensors for Heart Rate Monitoring Used in Extramural Applications," *Sensors*, vol. 22, no. 11, p. 4035, May 2022, doi: 10.3390/s22114035.

[16] J. Allen, "Photoplethysmography and its application in clinical physiological measurement," *Physiol. Meas.*, vol. 28, no. 3, pp. R1–R39, Mar. 2007, doi: 10.1088/0967-3334/28/3/R01.

[17] M. Elgendi, I. Norton, M. Brearley, D. Abbott, and D. Schuurmans, "Systolic Peak Detection in Acceleration Photoplethysmograms Measured from Emergency Responders in Tropical Conditions," *PLoS ONE*, vol. 8, no. 10, p. e76585, Oct. 2013, doi: 10.1371/journal.pone.0076585.

[18] Y. Sheng and L. Zhu, "The crosstalk between autonomic nervous system and blood vessels," *Int J Physiol Pathophysiol Pharmacol*, vol. 10, no. 1, pp. 17–28, 2018.

[19] D. Yousif *et al.*, "Autonomic Dysfunction in Preeclampsia: A Systematic Review," *Front. Neurol.*, vol. 10, Aug. 2019, doi: 10.3389/fneur.2019.00816.

[20] M. Bester, R. Joshi, M. Mischi, J. O. E. H. Van Laar, and R. Vullings, "On the distinct differences in autonomic regulation between healthy pregnant and non-prengnant women - a HRV analysis," *Submitted*, 2023.

[21] Z. Sharifiheris, A. Rahmani, J. Onwuka, and M. Bender, "The Utilization of Heart Rate Variability for Autonomic Nervous System Assessment in Healthy Pregnant Women: Systematic Review," *JMIR Bioinform Biotech*, vol. 3, no. 1, p. e36791, Nov. 2022, doi: 10.2196/36791.

[22] K. Grym *et al.*, "Feasibility of smart wristbands for continuous monitoring during pregnancy and one month after birth," *BMC Pregnancy Childbirth*, vol. 19, no. 1, p. 34, Dec. 2019, doi: 10.1186/s12884-019-2187-9.

[23] S. Fangming, L. Zhaoxi, S. Xiurong, H. Nan, W. Lei, and L. Xiaomin, "The Pulse Wave Analysis of Normal Pregnancy: Investigating the Gestational Effects on Photoplethysmographic Signals," *Bio-Medical Materials and Engineering*, no. 1, pp. 209–219, 2014, doi: 10.3233/BME-130801.

[24] M. G. Miglis, "Sleep and the Autonomic Nervous System," in *Sleep and Neurologic Disease*, Elsevier, 2017, pp. 227–244. doi: 10.1016/B978-0-12-804074-4.00018-2.

[25] F. B. van Meulen *et al.*, "Contactless Camera-Based Sleep Staging: The HealthBed Study," *Bioengineering*, vol. 10, no. 1, p. 109, Jan. 2023, doi: 10.3390/bioengineering10010109.

[26] L. M. Eerikäinen *et al.*, "Comparison between electrocardiogram- and photoplethysmogram-derived features for atrial fibrillation detection in free-living conditions," *Physiol Meas*, vol. 39, no. 8, p. 084001, 08 2018, doi: 10.1088/1361-6579/aad2c0.

[27] A. G. Bonomi *et al.*, "Atrial Fibrillation Detection Using a Novel Cardiac Ambulatory Monitor Based on Photo-Plethysmography at the Wrist," *JAHA*, vol. 7, no. 15, p. e009351, Aug. 2018, doi: 10.1161/JAHA.118.009351.

[28] C. Fischer, B. Domer, T. Wibmer, and T. Penzel, "An Algorithm for Real-Time Pulse Waveform Segmentation and Artifact Detection in Photoplethysmograms," *IEEE J. Biomed. Health Inform.*, vol. 21, no. 2, pp. 372–381, Mar. 2017, doi: 10.1109/JBHI.2016.2518202.

[29] J. Park, H. S. Seok, S.-S. Kim, and H. Shin, "Photoplethysmogram Analysis and Applications: An Integrative Review," *Front. Physiol.*, vol. 12, p. 808451, Mar. 2022, doi: 10.3389/fphys.2021.808451.

[30] R. Joshi *et al.*, "A Ballistographic Approach for Continuous and Non-Obtrusive Monitoring of Movement in Neonates," *IEEE J. Transl. Eng. Health Med.*, vol. 6, pp. 1–10, 2018, doi: 10.1109/JTEHM.2018.2875703.

[31] D. Makowski *et al.*, "NeuroKit2: A Python toolbox for neurophysiological signal processing," *Behav Res*, vol. 53, no. 4, pp. 1689–1696, Aug. 2021, doi: 10.3758/s13428-020-01516-y.

[32] W. Jänig, *The Integrative Action of the Autonomic Nervous System: Neurobiology of Homeostasis*, 2nd ed. Cambridge University Press, 2022. doi: 10.1017/9781108778411.

[33] F. Shaffer and J. P. Ginsberg, "An Overview of Heart Rate Variability Metrics and Norms," *Front. Public Health*, vol. 5, p. 258, Sep. 2017, doi: 10.3389/fpubh.2017.00258.

[34] A. Bauer *et al.*, "Deceleration capacity of heart rate as a predictor of mortality after myocardial infarction: cohort study," *The Lancet*, vol. 367, no. 9523, pp. 1674–1681, May 2006, doi: 10.1016/S0140-6736(06)68735-7.

[35] M. D. Costa, R. B. Davis, and A. L. Goldberger, "Heart Rate Fragmentation: A New Approach to the Analysis of Cardiac Interbeat Interval Dynamics," *Front. Physiol.*, vol. 8, p. 255, May 2017, doi: 10.3389/fphys.2017.00255.

[36] P. Gomes, P. Margaritoff, and H. Silva, "pyHRV: Development and Evaluation of an Open-Source Python Toolbox for Heart Rate Variability (HRV)," presented at the IcETRAN, 2019, pp. 882–887.

[37] D. Morelli, A. Rossi, M. Cairo, and D. A. Clifton, "Analysis of the Impact of Interpolation Methods of Missing RR-intervals Caused by Motion Artifacts on HRV Features Estimations," *Sensors*, vol. 19, no. 14, p. 3163, Jul. 2019, doi: 10.3390/s19143163.

[38] Task Force of The European Society of Cardiology and The North American Society of Pacing and Electrophysiology, "Heart rate variability. Standards of measurement, physiological interpretation, and clinical use.," *European heart journal*, vol. 17, no. 3, pp. 354–381, Mar. 1996.

[39] R. E. Kleiger, P. K. Stein, and J. T. Bigger, "Heart Rate Variability: Measurement and Clinical Utility," *Annals of Noninvasive Electrocardiology*, vol. 10, no. 1, pp. 88–101, Jan. 2005, doi: 10.1111/j.1542-474X.2005.10101.x.

[40] G. Ernst, "Heart-Rate Variability—More than Heart Beats?," *Front. Public Health*, vol. 5, p. 240, Sep. 2017, doi: 10.3389/fpubh.2017.00240.

[41] E. Shaqiri and M. Gusev, "A Programmatic Approach for Development of the ViewHRV Service Platform with Accurate and Reliable Results," in *2020 43rd International Convention on Information, Communication and Electronic Technology (MIPRO)*, Opatija, Croatia: IEEE, Sep. 2020, pp. 343–348. doi: 10.23919/MIPRO48935.2020.9245419.

[42] A. H. Khandoker, C. Karmakar, M. Brennan, M. Palaniswami, and A. Voss, *Poincaré Plot Methods for Heart Rate Variability Analysis*. Boston, MA: Springer US, 2013. doi: 10.1007/978-1-4614-7375-6.

[43] F. J. Bohanon *et al.*, "Heart rate variability analysis is more sensitive at identifying neonatal sepsis than conventional vital signs," *The American Journal of Surgery*, vol. 210, no. 4, pp. 661–667, Oct. 2015, doi: 10.1016/j.amjsurg.2015.06.002.

[44] M. V. Kamath, M. A. Watanabe, and A. R. M. Upton, *Heart rate variability (HRV) signal analysis: clinical applications*. Boca Raton: Taylor & Francis, 2013.

[45] J. S. Richman and J. R. Moorman, "Physiological time-series analysis using approximate entropy and sample entropy," *American Journal of Physiology-Heart and Circulatory Physiology*, vol. 278, no. 6, pp. H2039–H2049, Jun. 2000, doi: 10.1152/ajpheart.2000.278.6.H2039.

[46] A. Bakhchina, K. Arutyunova, A. Sozinov, A. Demidovsky, and Y. Alexandrov, "Sample Entropy of the Heart Rate Reflects Properties of the System Organization of Behaviour," *Entropy*, vol. 20, no. 6, p. 449, Jun. 2018, doi: 10.3390/e20060449.

[47] A. Bauer *et al.*, "Phase-rectified signal averaging detects quasi-periodicities in non-stationary data," *Physica A: Statistical Mechanics and its Applications*, vol. 364, pp. 423–434, May 2006, doi: 10.1016/j.physa.2005.08.080.

[48] R. Joshi, D. Kommers, X. Long, L. Feijs, and S. V. Huffel, "Cardiorespiratory coupling in preterm infants," *J Appl Physiol*, vol. 126, pp. 202–213, doi: 10.1152/japplphysiol.00722.2018.

[49] F. Li, L. Yang, H. Shi, and C. Liu, "Differences in photoplethysmography morphological features and feature time series between two opposite emotions: Happiness and sadness," *ARTRES*, vol. 18, no. C, p. 7, 2017, doi: 10.1016/j.artres.2017.02.003.

[50] C. El Hajj and P. A. Kyriacou, "Recurrent Neural Network Models for Blood Pressure Monitoring Using PPG Morphological Features," in *2021 43rd Annual International Conference of the IEEE Engineering in Medicine & Biology Society (EMBC)*, Mexico: IEEE, Nov. 2021, pp. 1865–1868. doi: 10.1109/EMBC46164.2021.9630319.

[51] M. Elgendi, Y. Liang, and R. Ward, "Toward Generating More Diagnostic Features from Photoplethysmogram Waveforms," *Diseases*, vol. 6, no. 1, p. 20, Mar. 2018, doi: 10.3390/diseases6010020.

[52] K. Kelley, "The Effects of Nonnormal Distributions on Confidence Intervals Around the Standardized Mean Difference: Bootstrap and Parametric Confidence Intervals," *Educational and Psychological Measurement*, vol. 65, no. 1, pp. 51–69, Feb. 2005, doi: 10.1177/0013164404264850.

[53] B. M. Wulterkens *et al.*, "It is All in the Wrist: Wearable Sleep Staging in a Clinical Population versus Reference Polysomnography," *NSS*, vol. Volume 13, pp. 885–897, Jun. 2021, doi: 10.2147/NSS.S306808.

[54] M. Bester, R. Joshi, M. Mischi, J. O. E. H. van Laar, and R. Vullings, "Longitudinally Tracking Maternal Autonomic Modulation During Normal Pregnancy With Comprehensive Heart Rate Variability Analyses," *Front. Physiol.*, vol. 13, p. 874684, May 2022, doi: 10.3389/fphys.2022.874684.

[55] P. H. Charlton, P. A. Kyriacou, J. Mant, V. Marozas, P. Chowienczyk, and J. Alastruey, "Wearable Photoplethysmography for Cardiovascular Monitoring," *Proc. IEEE*, vol. 110, no. 3, pp. 355–381, Mar. 2022, doi: 10.1109/JPROC.2022.3149785.

[56] A. Alim and M. H. Imtiaz, "Wearable Sensors for the Monitoring of Maternal Health—A Systematic Review," *Sensors*, vol. 23, no. 5, p. 2411, Feb. 2023, doi: 10.3390/s23052411.

[57] A. Khalil, D. Cooper, and K. Harrington, "Pulse wave analysis: a preliminary study of a novel technique for the prediction of pre-eclampsia," *BJOG: An International Journal of Obstetrics & Gynaecology*, vol. 116, no. 2, pp. 268–277, Jan. 2009, doi: 10.1111/j.1471-0528.2008.01906.x.

[58] T. Y. Euliano *et al.*, "Photoplethysmography and Heart Rate Variability for the Diagnosis of Preeclampsia:," *Anesthesia & Analgesia*, vol. 126, no. 3, pp. 913–919, Mar. 2018, doi: 10.1213/ANE.0000000000002532.

[59] V. L. Brooks, "Autonomic control during pregnancy," in *Primer on the Autonomic Nervous System*, Elsevier, 2023, pp. 273–277. doi: 10.1016/B978-0-323-85492-4.00084-3.

[60] S. Rang, H. Wolf, G. A. Montfrans, and J. M. Karemaker, "Non–invasive assessment of autonomic cardiovascular control in normal human pregnancy and pregnancy- associated hypertensive disorders: a review," *Journal of Hypertension*, vol. 20, no. 11, pp. 2111–2119, 2002.

[61] L. J. Green *et al.*, "Gestation-Specific Vital Sign Reference Ranges in Pregnancy," *Obstetrics & Gynecology*, vol. 135, no. 3, pp. 653–664, Mar. 2020, doi: 10.1097/AOG.0000000000003721.

[62] L. Loerup *et al.*, "Trends of blood pressure and heart rate in normal pregnancies: a systematic review and meta-analysis," *BMC Med*, vol. 17, no. 1, p. 167, Dec. 2019, doi: 10.1186/s12916-019-1399-1.

[63] J. A. DiPietro, T. Mendelson, E. L. Williams, and K. A. Costigan, "Physiological blunting during pregnancy extends to induced relaxation," *Biological Psychology*, vol. 89, no. 1, pp. 14–20, Jan. 2012, doi: 10.1016/j.biopsycho.2011.07.005.

[64] M. Bester, R. Rizea, R. Joshi, M. Mischi, J. Van Laar, and R. Vullings, "Maternal autonomic responsiveness is attenuated in healthy pregnancy: a phase rectified signal averaging analysis," in *2022 44th Annual International Conference of the IEEE Engineering in Medicine & Biology Society (EMBC)*, Glasgow, Scotland, United Kingdom: IEEE, Jul. 2022, pp. 4982–4986. doi: 10.1109/EMBC48229.2022.9870894.

[65] A. Choi and H. Shin, "Photoplethysmography sampling frequency: pilot assessment of how low can we go to analyze pulse rate variability with reliability?," *Physiol. Meas.*, vol. 38, no. 3, pp. 586–600, Mar. 2017, doi: 10.1088/1361-6579/aa5efa.

[66] D. Fujita and A. Suzuki, "Evaluation of the Possible Use of PPG Waveform Features Measured at Low Sampling Rate," *IEEE Access*, vol. 7, pp. 58361–58367, 2019, doi: 10.1109/ACCESS.2019.2914498.

[67] M. Bester, R. Joshi, A. Linders, M. Mischi, J. O. E. H. van Laar, and R. Vullings, "Characterizing the effect of demographics, cardiorespiratory factors, and inter-subject variation on maternal heart rate variability in pregnancy with statistical modeling: a retrospective observational analysis," *Sci Rep*, vol. 12, no. 1, p. 19305, Nov. 2022, doi: 10.1038/s41598-022-21792-2.

Section II

Factors influencing maternal autonomic regulation during healthy pregnancy

Chapter 4

Longitudinally tracking maternal autonomic modulation during normal pregnancy with comprehensive heart rate variability analyses

Reproduced after: M Bester, R Joshi, M Mischi, JOEH van Laar, R Vullings. Longitudinally Tracking Maternal Autonomic Modulation During Normal Pregnancy with Comprehensive Heart Rate Variability Analyses. *Frontiers in Physiology*. 2022.

Abstract

Changes in the maternal autonomic nervous system are essential in facilitating the physiological adaptations that pregnancy necessitates. Insufficient autonomic adaptation is linked to complications such as hypertensive disorders of pregnancy. Consequently, tracking autonomic modulation during progressing pregnancy could allow for the early detection of emerging deteriorations in maternal health. Autonomic modulation can be longitudinally and unobtrusively monitored by assessing heart rate variability (HRV). Yet, changes in maternal HRV (mHRV) throughout pregnancy remain poorly understood. In previous studies, mHRV is typically assessed only once per trimester with standard HRV features. However, since gestational changes are complex and dynamic, assessing mHRV comprehensively and more frequently may better showcase the changing autonomic modulation over pregnancy. Subsequently, we longitudinally (median sessions = 8) assess mHRV in 29 healthy pregnancies with features that assess sympathetic and parasympathetic activity, as well as heart rate (HR) complexity, HR responsiveness, and HR fragmentation. We find that vagal activity, HR complexity, HR responsiveness, and HR fragmentation significantly decrease. Their associated effect sizes are small, suggesting that the increasing demands of advancing gestation are well tolerated. Furthermore, we find a notable change in autonomic activity during the transition from the second to third trimester, highlighting the dynamic nature of changes in pregnancy. Lastly, while we saw the expected rise in mean HR with gestational age, we also observed increased autonomic deceleration activity, seemingly to counter this rising mean HR. These results are an important step towards gaining insights into gestational physiology as well as tracking maternal health via mHRV.

1. Introduction

The period of pregnancy necessitates major physiological changes to sustain the growing fetus while maintaining maternal health [1], [2]. Some changes are apparent and can be readily monitored, such as the mother's growing abdomen. Abdominal measurements (i.e. symphysial fundal height) are typically taken at prenatal check-ups to track the progressing pregnancy and the growing fetus [3]. Other changes are internal, such as the substantial adaptations in the maternal cardiovascular system, which are largely regulated by the autonomic nervous system (ANS) [1], [4], [5]. Similar to tracking the symphysial fundal height, longitudinal assessment of autonomic modulation throughout pregnancy may offer insights into gestational health [6].

In fact, several pregnancy complications are linked to the insufficient adaptation of the ANS to advancing gestation. Complications such as preeclampsia (a hypertensive disorder of pregnancy) and preterm birth have been associated with dysfunctional maternal autonomic regulation [1]–[3]. These complications are challenging to detect in early gestation when available interventional options (such as aspirin for mitigating preeclampsia) would be most effective [4], [5]. As a result, such pregnancy complications remain major causes of perinatal morbidity and mortality [6]–[9].

Alleviating the burden of pregnancy complications partly depends on developing screening methods for their early detection [10], [11]. Owing to the association between pregnancy complications and autonomic dysfunction, tracking autonomic changes throughout pregnancy may allow for detecting deteriorations in maternal health [12], [13]. However, the normative values of autonomic activity and the trajectory thereof during pregnancy remain insufficiently explored [14], [15].

Autonomic activity can be assessed by tracking heart rate variability (HRV) since autonomic regulation modulates the time-intervals between heartbeats [16], [17]. Tracking HRV is attractive due to the pervasiveness of unobtrusive, wearable technologies that can monitor heart rate (HR) [18]. However, limited research has longitudinally assessed maternal HRV (mHRV) in healthy pregnancy [19]. Moreover, existing research has offered conflicting results [2], [3], [15]. On the one hand, some researchers have found that mHRV – and by proxy, autonomic activity – is unaffected by gestational age (GA) [20], [21]. On the other hand, the findings of other researchers suggest increased activity of the parasympathetic branch of the ANS in early gestation with a shift towards sympathetic dominance by the end of pregnancy [15], [22], [23].

Changes in maternal physiology during pregnancy are complex and dynamic [14]. Consequently, regular prenatal checkups, initially monthly and culminating in weekly appointments, are necessary to capture possible changes [24]. Although measuring the abdomen's symphysial fundal height during these checkups provides valuable information on the health of the pregnancy, it is not the only information considered. Maternal blood pressure, fetal HR, and fetal growth are also assessed to generate a more comprehensive overview of gestational health [25].

Similarly, assessing mHRV with more regularity by employing multiple measures of HRV may better showcase the progression of autonomic modulation in normal pregnancy. In literature, mHRV is typically assessed only three times (i.e. once per trimester) with a methodological focus on standard time and frequency domain features [19]. These features inform on the relative activity of the sympathetic and parasympathetic branches of the ANS, which has been the focus of mHRV research in pregnancy. However, further information can be obtained from HRV. The variability observed in HR results from the interaction of a network of non-linear physiological systems over different time scales [26], [27]. Calculating HRV features that exploit characteristics of these interactions – such as complexity, responsiveness, and fragmentation – may allow for a more comprehensive overview of maternal autonomic modulation during pregnancy [28].

While features that capture these characteristics have rarely been employed in assessing mHRV, they have been used elsewhere. For instance, sample entropy and detrended fluctuation analysis, which assess the complexity in the HR time series, have been used in research on sepsis, heart failure, sleep staging, and stress [26], [29]–[31]. Diseased states and stress typically result in reduced HR complexity. Pregnancy is often described as a stress-test for the mother owing to the increasing physiological strain accompanying advancing gestation [32]–[34]. Consequently, measures of HR complexity may be particularly sensitive to progressing pregnancy.

Furthermore, the increased stress of pregnancy might affect the responsiveness of the ANS. Autonomic responsivity can be probed with phase rectified signal averaging (PRSA) [35], a method that quantifies how the tachogram responds to accelerations and deceleration in HR as a proxy measure for autonomic responsiveness. PRSA-based features not only independently predict mortality in cardiac disease [36], [37] but are also sensitive to aging and fitness levels [38]. This method is increasingly being employed to assess fetal health [39], [40] but has rarely been used to assess maternal autonomic modulation [41], [42].

Lastly, physiologically stressful conditions (such as aging or cardiovascular disease) are associated with a breakdown in the neuroautonomic-electrophysiological control systems that regulate HR, resulting in increased short-term HRV [43]. This high short-term variability can be misleading since it indicates healthy autonomic modulation, which is not typically present in aging populations or those with cardiac disease. However, in cases of such breakdown, the variation is fragmented – i.e. with HR quickly alternating between acceleration and deceleration – rather than gradual, as is inherent to vagally regulated variation. A recent class of HRV features, namely heart rate fragmentation (HRF), exploits this phenomenon to probe the integrity of the physiological systems controlling the heartbeats. HRF features outperform traditional HRV features in capturing the degenerative impact of conditions such as aging and heart disease [43]. Assessing these features in pregnancy for the first time could indicate whether advancing gestation affects the physiological systems that control the heartbeat.

Subsequently, in this study, we will implement a variety of HRV methods and apply these repeatedly in a healthy pregnant population to investigate the progression of maternal autonomic modulation under the stress-test of advancing gestation. This investigation will not only strengthen our understanding of gestational physiology but also serve towards providing evidence for the trajectory of mHRV during healthy pregnancy that may, in turn, be used as a guideline for obstetric screening.

2. Methods

This research is a secondary analysis of a prospective observational study carried out from 2007 to 2009. Healthy women (18 years and older) with uneventful, singleton pregnancies were recruited before 12 weeks of gestation for participation (n=40). Pregnancy duration was determined from the last menstrual period and then confirmed at 10 – 12 weeks of gestation by the crown-rump length. Participants took no medication apart from iron supplements or vitamins [44]. Women who developed pregnancy complications during the study were excluded from the final analysis (hypertension, n=4; preterm birth, n=3). Four participants were further excluded due to drop out from the study of datafiles that were missing. The data from the remaining 29 participants were included. These participants had a mean age of 31 (± 4) years and a mean pre-pregnancy body mass index of 23.9 (± 4) kg/m², as seen in Table 1.

Table 1: Patient characteristics

Characteristics	% or mean (standard deviation)
Maternal body mass index before pregnancy	23.9 (4) kg/m^2
Nulliparous	66 %
Maternal age at birth	31 (4) years
Gestational age at birth	40 weeks (10 days)

All participants provided written informed consent. The institutional review board at the Máxima Medical Center, Veldhoven, the Netherlands, approved the study (reference number 0650) and granted a waiver for this secondary analysis in 2021 (reference number N21.008). The study design and original analyses are detailed in a previous article [44].

2.1 Data acquisition

Fetal ECG measurements – which also capture maternal ECG – were acquired at 1000 Hz from the maternal abdomen with a non-invasive electrophysiologic monitor (the NEMO device, Maastricht Instruments, the Netherlands) [44]. Repeated measurements were performed at approximately 14, 18, 22, 24, 26, 30, 34, 36, 38, and 40 weeks of gestation while the participant was lying in a semi-recumbent position. 45-minute long measurements were performed between 08:00 and 18:00 hours. Included participants had a median of eight measurement sessions (IQR: 7 – 9). Relevant patient metadata was also collected [44].

2.2 Preprocessing

A 4th-order Butterworth bandpass filter (1 to 70 Hz) and a notch filter (50 Hz) were applied to the ECG recordings, as proposed in a previous publication [45]. Next, maternal ECG data were isolated from fetal recordings by applying a fixed linear combination to enhance the maternal QRS complexes [45]. Thereafter, a peak detection algorithm was employed as detailed by Rooijakkers et al. [46] to determine the RR series, or tachogram. As this algorithm was originally designed for fetal ECG, relevant parameters were adapted as appropriate for maternal ECG by the original authors of the algorithm: the relative characteristic frequency of the wavelet was set to 19 and the HR limits to 30 and 210 beats per minute. Processing of maternal RR intervals from fetal ECG measurements was done in MATLAB (MathWorks, USA), with all further processing done in Python (PSF, USA). To further eliminate possible ectopic beats or motion

artifacts and improve the accuracy of HRV features, RR intervals that fell outside a specified range (0.4 to 2 seconds) or differed from the preceding interval by 20% were removed [38], [47], [48]. RR intervals for which both preceding and following values were excluded based on the above criteria, were also excluded. In cases where more than 25% of RR intervals needed to be removed, the measurement was excluded from the analysis. For HRV features where beat-to-beat changes were highly important (i.e., time-domain features, PRSA, HRF, and Poincaré analysis), beats were replaced with NaN values. Where signal continuity was of higher importance (i.e., sample entropy, detrended fluctuation analysis, and frequency-domain analyses), missing values were linearly interpolated.

2.3 Heart rate variability

A range of HRV features was calculated on the entire RR series for each measurement session: standard time and frequency domain features [16], [17], non-linear (i.e. geometrical and complexity) features [17], [30], [49], [50], phase rectified signal averaging (PRSA) [35], and heart rate fragmentation (HRF) [43]. The standard features and complexity features were calculated using pyHRV [51], a Python signal processing toolbox shown to be reliable [52]. For the frequency domain analysis, each RR series was divided into shorter, overlapping segments (5 minutes in length, 50% overlap) during computation, where it was assumed that during these shorter segments, the RR series is stationary. The mean of the values computed per segment was taken as the result for the corresponding RR series. All HRV features, further detailed in the following sections, were calculated for each measurement session.

2.3.1 Standard time and frequency domain features

- SDNN: standard deviation of all RR intervals
- RMSSD: root mean squared successive differences of RR intervals
- pNN50: percentage of pairs of consecutive RR intervals differing by more than 50 ms
- LF: the power in the low frequency band (0.04–0.15 Hz)
- HF: the power in the high frequency band (0.15–0.40 Hz)
- TP: the total power in the frequency bands
- LF/HF: the ratio between low and high frequency power

While SDNN represents overall variability, other features inform on the relative contributions of the sympathetic and parasympathetic branches of the ANS. RMSSD, pNN50, and HF reflect the vagal modulation of HR. Both sympathetic and parasympa-

thetic activity contribute to LF while LF/HF is typically attributed to sympathovagal balance [16], [17].

2.3.2 Non-linear features

In addition to standard time- and frequency-domain features, we evaluated methods designed to better capture the non-stationary and non-linear characteristics of the HR time series. We employed a Poincaré plot analysis, which is a popular geometrical method to evaluate HRV dynamics. Each NN interval is plotted against its predecessor, resulting in a scatter plot. SD1 denotes the standard deviation of the short-term NN interval variability. Similarly, SD2 represents the standard deviation of the long-term NN interval variability. The ratio between these two features is noted as SD1/SD2 [49].

Furthermore, we employ two measures that address the complexity within the HR time series: sample entropy (SampEn) and detrended fluctuation analysis (DFA) [30], [50]. The first, SampEn, calculates the conditional probability that two epochs which are similar within a tolerance r for a window length m, will remain similar if the next data point (i.e. the next NN value) is included [26], [50]. It can be defined as follows:

$$SampEn = -log\frac{A}{B}, \qquad (1)$$

A is defined as the number of pairs of vector (x) for m points which satisfy the condition $d[xm(i), xm(j)] \leq r$, while B is the number of pairs of vectors for (m+1) points that satisfy the same condition [26]. The values for m and r were set to 2 and 0.2 times the standard deviation of the RR intervals, as is typically reported in the literature [50]. Smaller values of SampEn indicate a more regular and predictable time series [17].

The second method, DFA, also gives an estimate of the long-range correlations of the time series by quantifying its fractal scaling properties follows [30]. In short, the total time series is integrated (X_t) and then divided into segments of length n. Each segment is then detrended by subtracting the best linear fit (X_y). The fluctuation function is calculated as shown in Equation 2.

$$F(n) = \sqrt{\frac{1}{N}\sum_{t=1}^{N}(X_t - Y_t)^2}, \qquad (2)$$

Thereafter, the scaling exponent α (which represents the correlation properties of the time series) is estimated from the log-log plot of $F(n)$ vs n. Typically, both α_1, and α_2 are determined, which represent short-term and long-term fractal scaling exponents.

In our case, only α_1 (which calculates correlation over n = 4–16 beats) is calculated, as α_2 requires several hours of data to achieve sufficient accuracy. When there is no correlation present (i.e. white noise) or the signal resembles a random walk process (i.e. Brownian noise), $\alpha = 0.5$ and $\alpha = 1.5$, respectively. Positive correlations exist when $0.5 < \alpha < 1.5$, with $\alpha \approx 1$ suggesting a high level of complexity. When values start exceeding 1, it suggests that the system becomes increasingly regular [30], [53].

2.3.3 Phase rectified signal averaging (PRSA)

PRSA is a technique that can identify and elucidate quasi-periodicities in time-series data that are often obscured by noise and non-stationarities, as is typical for physiological signals [35]. In PRSA, signal segments are aligned corresponding to a predetermined shared phase and then averaged, canceling out the noise and isolating the underlying composite trend. These isolated quasi-periodicities are representative of the underlying physiological processes that regulate HR.

Isolating these quasi-periodicities is achieved in a few steps. Firstly, anchor points (APs) are defined on the RR series in relation to the phases that are of interest. Here, two sets of APs are identified, namely HR accelerations and decelerations. If the PRSA parameter of T is set to one, each acceleration and deceleration are marked as an AP. A higher value of T evokes a low pass filtering effect since then an AP would be identified as an acceleration or deceleration averaged over T points.

After the APs have been identified, a signal segment is defined around each AP with a length of L both preceding and following the AP (resulting in a total segment length of $2L + 1$). This signal segment should be sufficiently long to capture the slowest anticipated oscillation of relevance in the time-series. We define L as 50 RR values, as is also done in the literature [54]. All signal segments are then aligned corresponding to their APs and averaged across segments, resulting in the PRSA waveform. This waveform (also of length $2L + 1$ and consisting of averaged RR values) visualizes the behavior of HR in response to accelerations and decelerations, which is associated with sympathetic and vagal activity, respectively [36]. In essence, the magnitude and speed of this response in HR gives an estimate of the robustness of the autonomic response [35].

To quantify this response, several features are calculated from the PRSA waveform, represented as X. Note that the PRSA waveform's relationship to the time domain is units of RR values (specified here as RRi) and not in seconds. Firstly, deceleration

capacity (DC) and acceleration (AC) are calculated to capture the magnitude of the response. The calculation of DC is shown in Equation 3. AC is similarly calculated.

$$DC = [X(0) + X(1) - X(-1) - X(-2)]/4, \quad (3)$$

Here *X(0)* represents the AP, *X(1)* is value following the AP, and *X(-1)* and *X(-2)* precede the AP [35]. AC is similarly calculated. Furthermore, the immediate deceleration response (IDR) and immediate acceleration response (IAR) are calculated as the difference between the maximum and minimum RRi within the neighborhood of five RRi preceding the AP and five after, including the AP. This captures the maximum response in HR in the immediate neighborhood of the AP. The rate of this maximum response is captured in the slope of the deceleration and acceleration responses (SDR and SAR), which notes the slope of the line joining the maximum and minimum RRi corresponding to IDR and IAR. Lastly, the average HR response to accelerations (AAR) and deceleration (ADR) is calculated by taking the difference between the mean of the 50 RRi following the AP, which is included, and the mean of the 50 preceding RRi [54].

Lastly, the PRSA waveform is also studied in the frequency domain. The power spectral density (PSD) plots are calculated for all PRSA waveforms, with the frequency content measured in time units of 1/RRi. Calculating the PSD of these rectified waveforms has been shown to perform better than traditional spectral analysis [35], [36], [54]. PRSA allows for separating the acceleration and deceleration responses; subsequently, we calculate features to capture the ratio between the two responses to better understand autonomic control of the maternal HR. To this end, we first determine the power and peaks in the LF and HF frequency bands in the PSDs, as well as the TP for both the acceleration and deceleration response. Thereafter, we determine the ratio between the features (for example, HFacc:HFdec).

2.3.4 Heart rate fragmentation (HRF)

HRF aims to capture variability resulting from a breakdown in physiological control over HR rather than healthy autonomic modulation. Costa et al. [43] first developed these indices to address the phenomenon of increased HR variability in older populations and populations with heart disease where vagal modulation is known to be decreased. Closer investigation revealed the variability to be jagged rather than smooth as would be expected from vagal control. Subsequently, a set of indices were developed to capture this jagged variation, referred to as fragmentation. These indices are: PIP (percentage inflection points); PAS (percentage alternating segments); PSS

(percentage short segments); and IALS (inverse of accelerating or decelerating long segments). Increases in these indices indicate increased fragmentation in HR [43].

2.4 Data analysis

Data were analyzed with two aims in mind. Firstly, we aimed to explore the possibly dynamic relationship between the HRV features and GA. To this end, we grouped HRV features into bins of four weeks. The mean and standard error of the mean of the HRV features for all participants per bin is plotted against GA to show the evolution of the features over time. The mean and standard error of the mean are preferred over the median and interquartile range since we are interested in the trajectory of the features and the support in each bin (i.e. the number of measurements) varies. However, due to the possibly non-normal distribution of the data, we also plot the median and interquartile range to confirm the trends observed. The data are grouped into the following GA bins, with the lower limit excluded and upper limit included: 12 to 16 weeks (19 measurements); 16 to 20 weeks (24 measurements); 20 to 24 weeks (31 measurements); 24 to 28 weeks (46 measurements); 28 to 32 weeks (28 measurements); 32 to 36 weeks (30 measurements); and above 36 weeks (52 measurements).

Secondly, we aimed to capture the significance and magnitude of changes observed. To this end, the data were divided into three groups based to facilitate comparison: less than 23 weeks (GA_1), between 23 and 32 weeks (GA_2), and over 32 weeks of gestation (GA_3). The groups span a comparative number of weeks and allow most participants to have at least one measurement per group. The upper limit is included and the lower is excluded in each group. Participants typically had multiple measurements in each group; subsequently, the mean of these values was taken per participant per gestational group. One participant did not have a measurement in each of the three gestational groups and was subsequently excluded from this second part of the analysis, resulting in a total of 28 participants.

2.5 Statistical analysis

Physiological data is typically not normally distributed and therefore non-parametric analyses were done. We also confirmed the nature of the distribution by using a Kolmogorov-Smirnov test (only three out of 28 features were normally distributed). Subsequently, a Friedman's test with a Dunn's post hoc test was applied to determine whether statistically significant differences occurred across the three GA groups (i.e., GA_1, GA_2, and GA_3) as well as between individual groups (e.g., GA_1 vs GA_2,), with Bonferroni correction to control for family-wise error. This analysis tests whether A value of $p < 0.05$ was considered statistically significant.

Corresponding effect sizes were calculated with Cohen's U_1, which provides a measure of the overlap between the distributions of two groups. A Cohen's U_1 of 1 indicates two entirely separate groups, while complete overlap results in a U_1 of 0. While the standards for what constitutes a large effect are more clearly defined for Cohen's d (used in parametric data), this is not the case for Cohen's U_1. A Cohen's d of 0.2 (small effect) is similar to U_1 = 0.15, while a d = 0.5 (medium effect) corresponds to U_1 = 0.33 [55].

3. Results

3.1 Time and frequency domain features

4

Similar trends can be observed (Figure 1) across the temporal evolution of all standard time and frequency domain features. Mean HR and LF/HF increased significantly over pregnancy, RMSSD, pNN50, TP, LF, and HF showed significant decreases with GA (Figure 1, Table 2). The change in pNN50 from GA_1 and GA_3 had the largest effect size (U_1 = 0.196, Table 2), although this remains a small effect. The trend in overall variability (SDNN) was less distinct, showing first a decrease and thereafter an increase in values (Figure 1b, Table 2). Interestingly, the most notable changes in most features occur approximately between 24 and 32 weeks of gestation (Figure 1). All features except SDNN show sharp increases or decreases during this period.

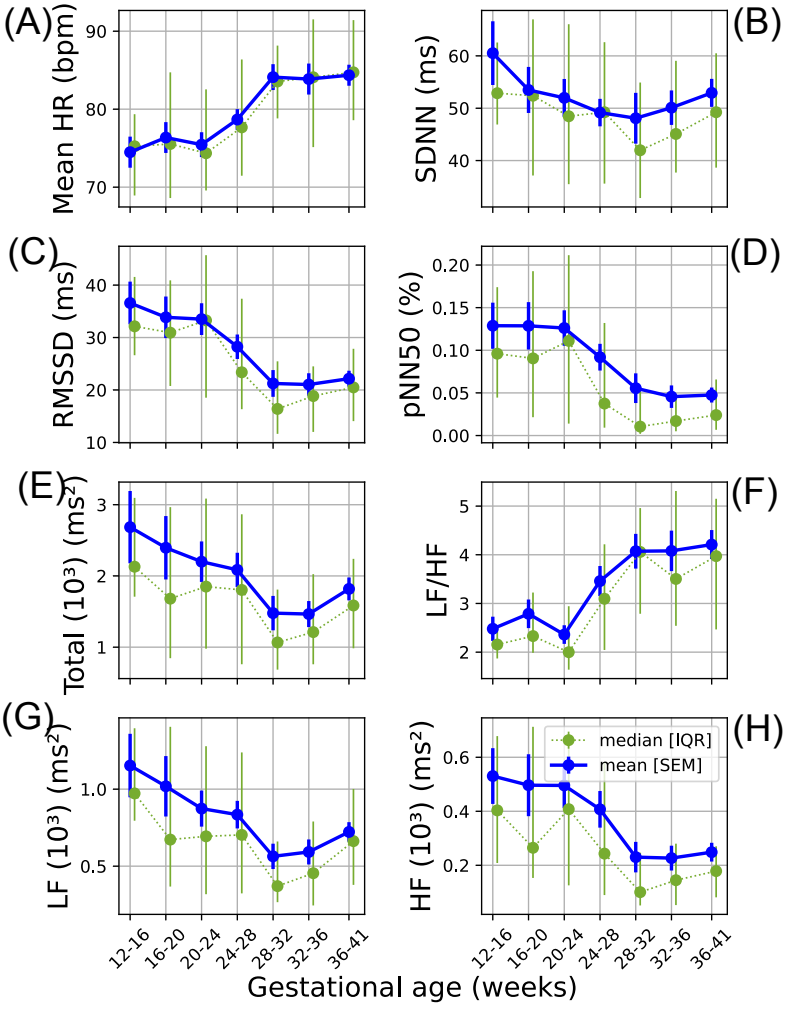

Figure 1: Temporal evolution of standard time and frequency domain measures over GA bins. HRV features for all participants were grouped into bins of four weeks. The mean and standard error of the mean (full line) as well as the median and interquartile range (dotted line) of the HRV features per bin is plotted against GA. (A) Mean HR; (B) SDNN; (C) RMSSD; (D) pNN50; (E) Total power; (F) LF/HF; (G) LF power; and (H) HF power.

Table 2: Results from the grouped analysis for standard time- and frequency-domain features. All continuous data are presented as median (IQR). First, the Friedman's p-value is calculated to determine whether significant changes occur over all groups. Thereafter, the Dunn's post-hoc test with Bonferroni correction is applied to determine the p-value between groups. Cohen's U_1 is calculated to determine effect size. Values of approximately 0.15 and 0.33 represent small and medium effects, respectively.

Features	**GA_1 median (IQR)**	**GA_2 median (IQR)**	**GA_3 median (IQR)**	**Friedman *p*-value**	**$GA_1 \rightarrow GA_2$**		**$GA_2 \rightarrow GA_3$**		**$GA_1 \rightarrow GA_3$**	
					p	U_1	*p*	U_1	*p*	U_1
GA (weeks)	18.4 (18.2 – 20.3)	27.1 (26.7 – 27.7)	36.8 (36.1 – 37.4)							
HR (beats per minute)	74.6 (68.2 – 81.7)	79.8 (76.1 – 87.1)	85.5 (77.8 – 90.8)	**<0.0001**	0.056	0.161	0.577	0.036	**<0.001**	0.196
SDNN (ms)	53.2 (39.3 – 65.7)	47.0 (34.6 – 62.0)	48.6 (40.4 – 60.8)	**0.039**	0.750	0.054	1	0	1	0.054
RMSSD (ms)	32.9 (21.7 – 44.8)	25.4 (15.7 – 33.1)	20.7 (15.4 – 26.2)	**<0.0001**	0.103	0.125	1	0	**0.006**	0.125
pNN50 (%)	0.12 (0.03 – 0.20)	0.05 (0.01 – 0.12)	0.03 (0.01 – 0.06)	**<0.0001**	0.110	0.161	0.834	0	**0.004**	0.196
Total power (ms^2)	2080 (1302 – 3220)	1632 (732 – 2484)	1557 (876 – 2188)	**<0.001**	0.533	0.054	1	0.034	0.322	0.072
LF (ms^2)	738 (568 – 1376)	650 (304 – 1119)	635 (349 – 920)	**<0.001**	0.417	0.034	1	0.018	0.253	0.071
HF (ms^2)	398 (193 – 757)	195 (98 – 433)	168 (83 – 289)	**<0.0001**	0.128	0.089	1	0.018	**0.019**	0.125
LF/HF	2.29 (1.77 – 2.89)	3.32 (2.30 – 3.91)	4.05 (2.7 – 5.38)	**<0.0001**	0.064	0.071	0.566	0.018	**<0.001**	0.107

3.2 Non-linear features

From Figures 2a and 2c, a gradual decrease can be seen in both SD1 and SD1/SD2 (calculated from the Poincaré analysis) over GA. Similar to the standard features discussed in the previous section, the sharpest change is seen around 24 to 32 weeks of gestation. A decrease in this ratio indicates a reduction in short-term variability (typically associated with vagal activity). This is confirmed by the significant changes reported in Table 3.

Table 3: results from the grouped analysis for non-linear HRV features. All continuous data are presented as median (IQR). First, the Friedman's p-value is calculated to determine whether significant changes occur over all groups. Thereafter, the Dunn's post-hoc test with Bonferroni correction is applied to determine the p-value between groups. Cohen's U_1 is calculated to determine effect size. Values of approximately 0.15 and 0.33 represent small and medium effects, respectively.

Features	GA_1 median (IQR)	GA_2 median (IQR)	GA_3 median (IQR)	Friedman *p*-value	$GA_1 \rightarrow GA_2$		$GA_2 \rightarrow GA_3$		$GA_1 \rightarrow GA_3$	
					p	U_1	*p*	U_1	*p*	U_1
SD1 (ms)	23.2 (15.4 – 31.6)	18.0 (11.1 – 23.4)	14.7 (10.9 – 18.5)	**<0.0001**	0.101	0.125	1	0	**0.006**	0.125
SD2 (ms)	68.0 (52.9 – 85.9)	61.6 (46.2 – 82.9)	65.8 (55.4 – 81.4)	0.131	1	0.054	1	0.054	1	0.036
SD1/SD2	0.34 (0.27 – 0.38)	0.26 (0.22 – 0.35)	0.21 (0.17 – 0.26)	**<0.0001**	0.093	0.107	0.051	0.089	**<0.0001**	0.196
SampEn (a.u.)	1.40 (1.27 – 1.53)	1.19 (1.01 – 1.38)	0.94 (0.83 – 1.24)	**<0.0001**	**0.050**	0.071	0.061	0.071	**<0.0001**	0.214
DFA α_1 (a.u.)	1.19 (1.07 – 1.27)	1.29 (1.19 – 1.44)	1.41 (1.29 – 1.50)	**<0.0001**	**0.042**	0.107	0.177	0.071	**<0.0001**	0.125

A decrease and increase are seen in SampEn and α_1, respectively (Figure 2b and 2c, Table 3). The decrease in SampEn points to a time series that becomes more regular and predictable. Changes in SampEn are accompanied by an effect size of $U_1 = 0.214$ between GA_1 and GA_3, which is the largest effect observed across all HRV features. Increases in α_1 ranging across 1 and 1.5 indicate stronger correlations within the time series, pointing to a less complex signal. Again, both features display sharp

changes over 24 to 32 weeks of gestation (Figures 2b and 2c). Note that the changes for all non-linear features are highly significant ($p < 0.0001$, Table 3). Furthermore, the changes from $GA_1 \rightarrow GA_3$ are all highly significant ($p < 0.0001$), while this is not the case for the standard features (Table 2).

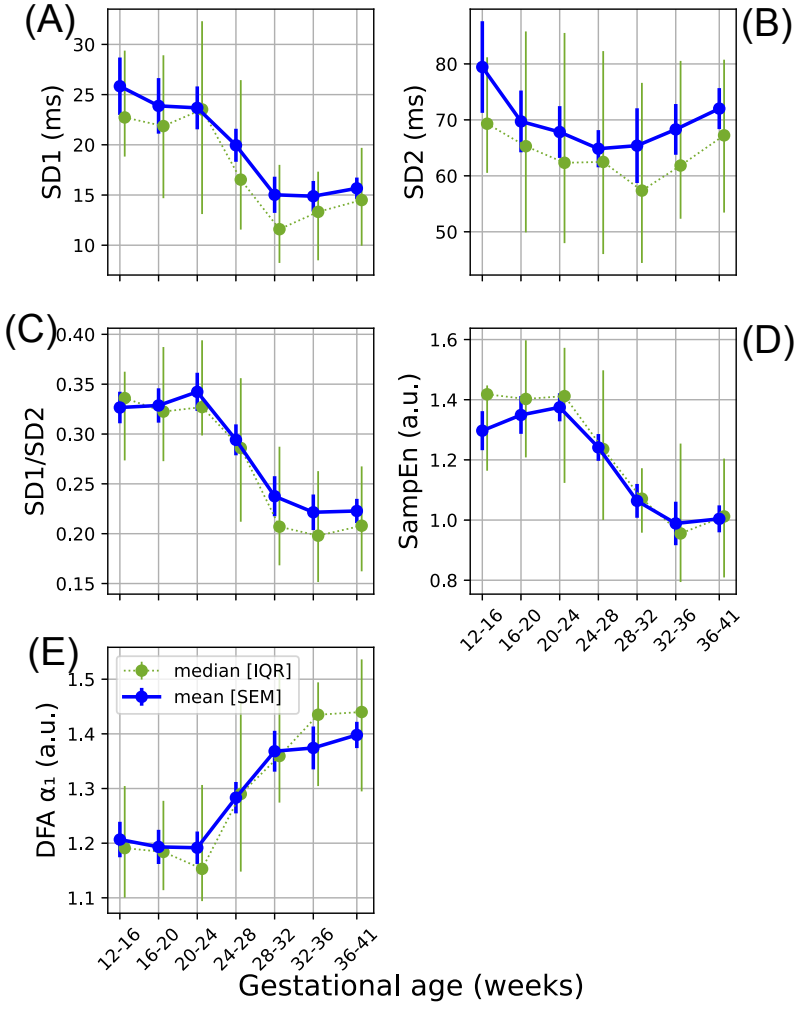

Figure 2: Temporal evolution of non-linear features over GA bins. HRV features for all participants were grouped into bins of four weeks. The mean and standard error of the mean (full line) as well as the median and interquartile range (dotted line) of the HRV features per bin is plotted against GA for (A) SD1; (B); SD2; (C) SD1/SD2; (D) SampEn; and (E) DFA α_1.

3.3 HRF

Most HRF (IALS, PSS, and PAS) showed a downward trend with progressing GA (Figures 3b - d), with IALS, PSS, and PAS decreasing significantly (Table 4). Although not significant, PIP does decrease steadily from 20 weeks onward (Figure 3a). All features decrease noticeably between 24 and 32 weeks of GA, although this is particularly evident for IALS and PSS.

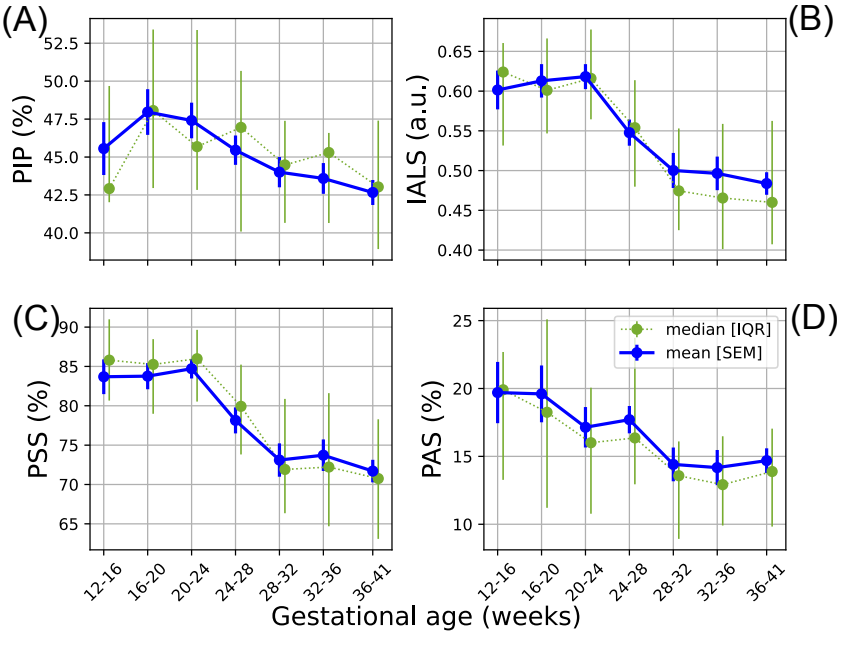

Figure 3: Temporal evolution of HRF features over GA bins. HRV features for all participants were grouped into bins of four weeks. The mean and standard error of the mean (full line) as well as the median and interquartile range (dotted line) of the HRV features per bin is plotted against GA: (A) PIP; (B) IALS; (C) PSS; and (D) PAS.

The largest effect size between GA_1 and GA_3 for a significant change occurred for IALS (U_1 = 0.179, from Table 4), yet this is still a small effect. While an increase in HRF would have suggested a breakdown in the physiological systems regulating HR, these findings instead suggest that there is a decrease in fragmentation with the increasing demands of pregnancy.

Table 4: Results from the grouped analysis for HRF features. All continuous data are presented as median (IQR). First, the Friedman's p-value is calculated to determine whether significant changes occur over all groups. Thereafter, the Dunn's post-hoc test with Bonferroni correction is applied to determine the p-value between groups. Cohen's U_1 is calculated to determine effect size. Values of approximately 0.15 and 0.33 represent small and medium effects, respectively.

Features	GA_1 median (IQR)	GA_2 median (IQR)	GA_3 median (IQR)	Friedman *p*-value	$GA_1 \rightarrow GA_2$		$GA_2 \rightarrow GA_3$		$GA_1 \rightarrow GA_3$	
					p	U_1	*p*	U_1	*p*	U_1
PIP (%)	47.5 (42.3 – 52.5)	45.7 (40.4 – 48.9)	45.4 (40.3 – 46.5)	0.074	1	0.018	0.909	0.036	0.144	0.196
IALS (a.u.)	0.62 (0.55 – 0.66)	0.54 (0.48 – 0.59)	0.49 (0.42 – 0.55)	**<0.0001**	**0.014**	0.107	0.291	0.054	**<0.0001**	0.179
PSS (%)	86.6 (80.1 – 88.7)	77.4 (71.8 – 83.8)	73.4 (65.9 – 77.8)	**<0.0001**	**0.011**	0.054	0.409	0.018	**<0.0001**	0.089
PAS (%)	17.5 (12.7 – 20.0)	16.8 (11.8 – 18.8)	13.9 (11.2 – 16.2)	**0.031**	1	0.054	0.653	0	0.146	0.071

3.4 PRSA

The temporal evolution of the PRSA features (Figure 4) shows a downward trend across features, with an uptick at the end of pregnancy. Note that SAR is inherently negative but is also decreasing in absolute terms. Also note that AC (4a), IAR (4b), IDR (4e), SAR (4c), and SDR (4f) already start decreasing before 20 weeks GA. (The average responses, i.e., AAR and ADR, displayed no discernable trends and are not shown here.)

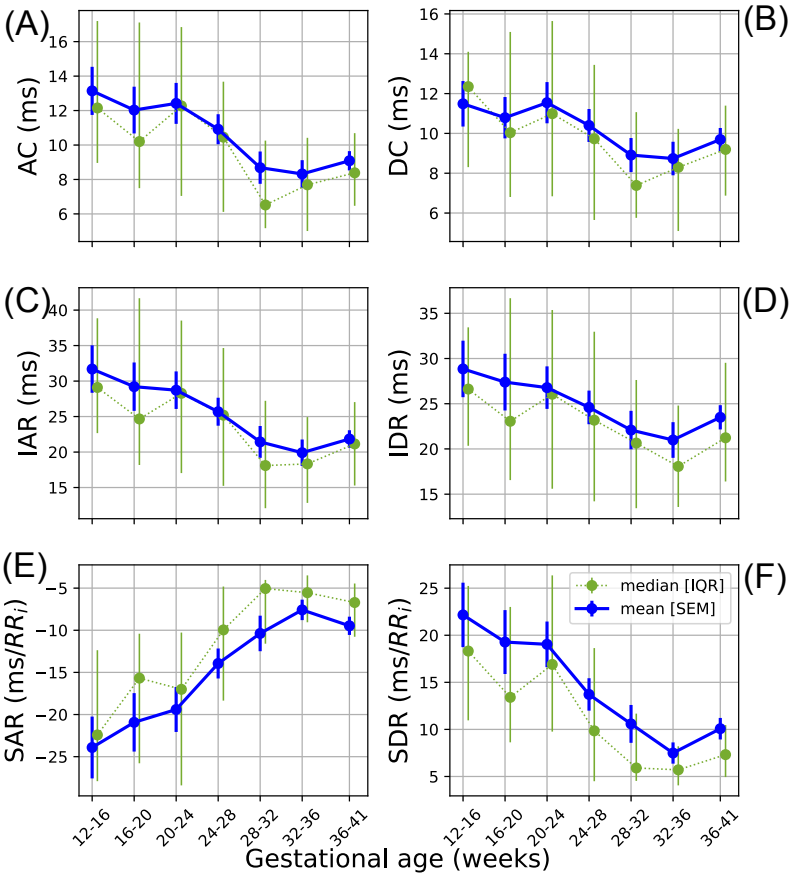

Figure 4: Temporal evolution of PRSA features over GA bins. HRV features for all participants were grouped into bins of four weeks. The mean and standard error of the mean (full line) as well as the median and interquartile range (dotted line) of the HRV features per bin is plotted against GA. (A) AC; (B) DC; (C) IAR; (D) IDR; (E) SAR; and (F) SDR.

This dampened response in later gestation, which is also reflected in the PRSA waveforms (Figure 5) and the decreased PRSA features (Table 5), indicates reduced responsiveness in HR. All features except AAR and ADR (the average responses) show significant reductions across GA groups (Table 5). The largest changes are seen in the slopes of the instant responses (SAR and SDR, both with U_1 = 0.125 between GA_1 and GA_3) and the IAR (U_1 = 0.143), although their effect sizes are still small.

Table 5: Results from the grouped analysis for PRSA features. All continuous data are presented as median (IQR). First, the Friedman's p-value is calculated to determine whether significant changes occur over all groups. Thereafter, the Dunn's post-hoc test with Bonferroni correction is applied to determine the p-value between groups. Cohen's U_1 is calculated to determine effect size. Values of approximately 0.15 and 0.33 represent small and medium effects, respectively.

Features	GA_1 median (IQR)	GA_2 median (IQR)	GA_3 median (IQR)	Friedman *p*-value	$GA_1 \rightarrow GA_2$		$GA_2 \rightarrow GA_3$		$GA_1 \rightarrow GA_3$	
					p	U_1	*p*	U_1	*p*	U_1
AC (ms)	12.5 (8.3 – 17.3)	9.7 (5.9 – 13.0)	8.2 (6.1 – 11.2)	**<0.0001**	0.245	0.054	1	0.036	**0.033**	0.107
IAR (ms)	28.9 (19.7 – 43.2)	24.0 (15.8 – 30.3)	19.6 (16.5 – 26.7)	**<0.0001**	0.329	0.089	0.989	0.071	**0.030**	0.143
SAR (ms/RRi)	-17.3 (-27.1 – -12.3)	-11.7 (-16.0 – -6.8)	-7.2 (-10.1 – -4.4)	**<0.0001**	**0.032**	0.054	0.348	0.018	**0.0001**	0.125
AAR (ms/RRi)	-1.3 (-3.3 – 0.1)	-2.1 (-2.8 – -1.5)	-2.1 (-3.5 – -1.4)	0.174	0.207	0.018	1	0.018	0.324	0.036
DC (ms)	11.7 (8.3 – 14.9)	9.5 (5.8 – 12.8)	8.4 (6.2 – 11.7)	**0.001**	0.553	0.054	1	0.018	0.217	0.036
IDR (ms)	27.1 (18.6 – 39.7)	23.3 (16.2 – 30.5)	20.8 (16.0 – 27.9)	**<0.001**	0.678	0.054	1	0.018	0.228	0.071
SDR (ms/RRi)	15.8 (11.6 – 29.3)	11.9 (7.1 – 16.0)	7.2 (5.6 – 11.5)	**<0.0001**	**0.047**	0.089	0.444	0.018	**<0.001**	0.125
ADR (ms/RRi)	2.6 (1.5 – 3.6)	2.0 (1.4 – 2.9)	3.2 (2.2 – 4.8)	0.091	1	0.018	**0.034**	0.018	0.058	0.089

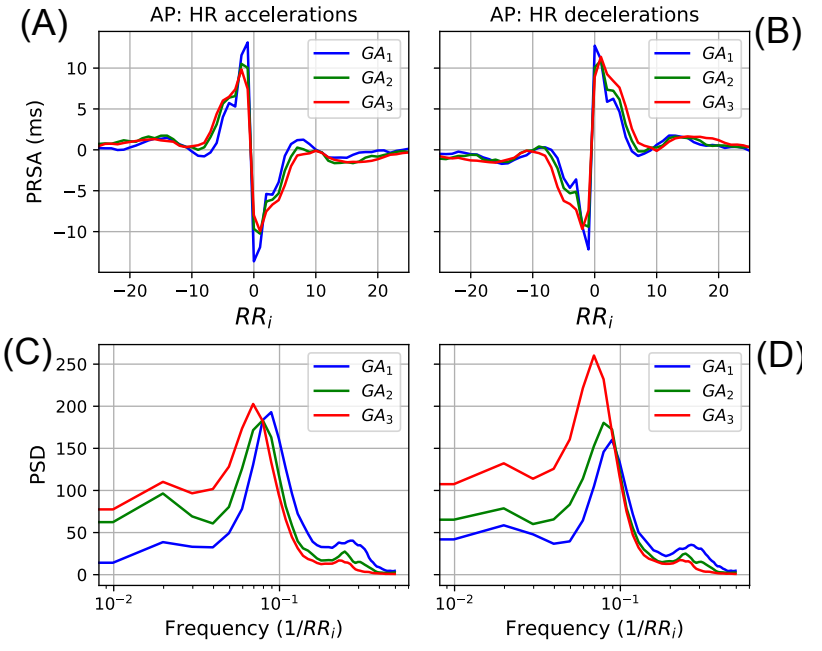

Figure 5: PRSA curves for each GA group with (A) accelerations as AP and (B) decelerations as AP, and T = 1. In all cases, the mean values have been subtracted from the graphs to enable comparison. Furthermore, (C) and (D) show the power spectral densities (PSD) of the PRSA graphs with accelerations and decelerations as AP, respectively.

Moving to the frequency domain, in the PSDs in Figure 6 a similar response is observed for both accelerations and decelerations (T = 5). However, for the LF band in Figure 5 (0.035/RRi Hz to 0.15/RRi Hz, translating to approximately 0.04 to 0.2 Hz) the behavior is markedly different. For accelerations (Figure 5c), activity in the LF band remains similar throughout. However, when decelerations serve as APs, the LF activity increases substantially with progressing pregnancy. (Note that the shifting peaks that can be observed are a result of an increase in mean HR since the frequency is a function of the RR intervals.)

The observation that the LF power in the deceleration response increases relative to that of the acceleration response is also confirmed in Table 6, which reports the ratio between frequency domain values in the acceleration and deceleration response. In fact, although it may not be visually evident from Figure 5, we see that the deceleration values significantly increase relative to the acceleration values for all features. Overall, we also see the largest effect sizes of our analysis. LFacc:LFdec and HFpeakacc:HFpeakdec both have $U_1 > 0.3$, while TPacc:TPdec has an effect size of 0.607 between GA_1

and GA_3. These changes suggest that increasing activity goes into decelerating the HR towards the end of pregnancy.

Table 6: Results from the grouped analysis for the ratio between PRSA frequency features with accelerations and decelerations as APs, respectively (T = 1). All continuous data are presented as median (IQR). First, the Friedman's p-value is calculated to determine whether significant changes occur over all groups. Thereafter, the Dunn's post-hoc test with Bonferroni correction is applied to determine the p-value between groups. Cohen's U_1 is calculated to determine effect size. Values of approximately 0.15 and 0.33 represent small and medium effects, respectively.

Features	**GA_1 median (IQR)**	**GA_2 median (IQR)**	**GA_3 median (IQR)**	**Friedman *p*-value**	**$GA_1 \rightarrow GA_2$**		**$GA_2 \rightarrow GA_3$**		**$GA_1 \rightarrow GA_3$**	
					p	U_1	*p*	U_1	*p*	U_1
LFacc: LFdec	1.17 (1.05 – 1.38)	0.98 (0.88 – 1.09)	0.93 (0.76 – 0.97)	**<0.0001**	**0.004**	0.089	0.220	0.143	**<0.0001**	0.329
HFacc: HFdec	1.08 (0.99 – 1.27)	0.99 (0.89 – 1.10)	0.93 (0.80 – 1.02)	**<0.0001**	**0.040**	0.125	0.507	0.018	**<0.001**	0.179
TPacc: TPdec	1.17 (0.99 – 1.26)	0.96 (0.86 – 1.09)	0.83 (0.70 – 0.94)	**<0.0001**	**0.018**	0.089	**0.015**	0.161	**<0.0001**	0.607
LF peakacc:LF peakdec	1.16 (0.99 – 1.42)	0.95 (0.88 – 1.09)	0.89 (0.70 – 0.94)	**<0.0001**	**0.024**	0.036	0.142	0.107	**<0.0001**	0.196
HF peakacc: HF peakdec	1.18 (0.99 – 1.42)	0.93 (0.86 – 1.14)	0.82 (0.62 – 0.94)	**<0.001**	0.071	0.071	**0.039**	0.125	**<0.0001**	0.375

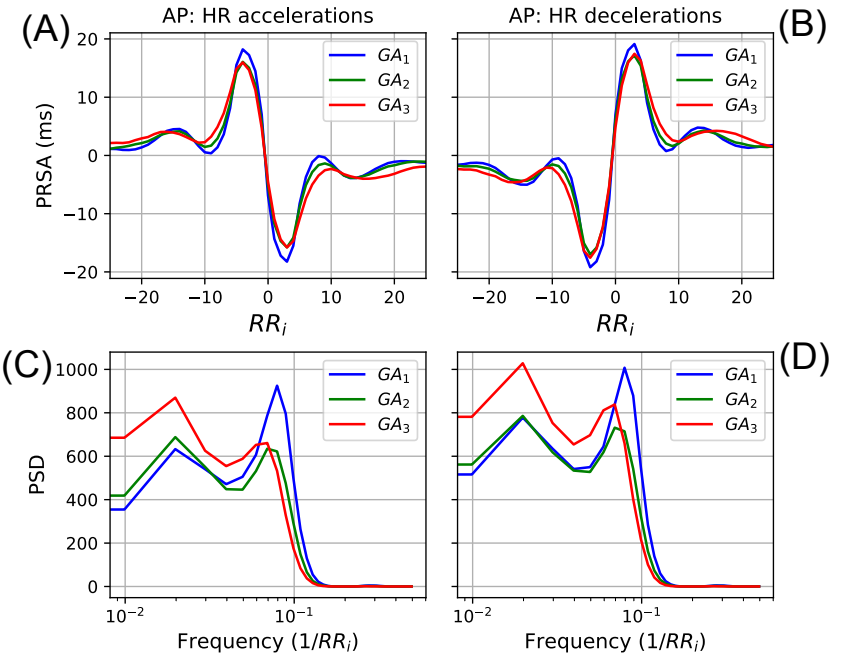

Figure 6: PRSA curves for each GA group with (A) accelerations as AP and (B) decelerations as AP, and $T = 5$. In all cases, the mean values have been subtracted from the graphs to enable comparison. Furthermore, (C) and (D) show the power spectral densities (PSD) of the PRSA graphs with accelerations and decelerations as AP, respectively.

Lastly, Table 7 lists the number of accelerations, decelerations, and constant points (i.e. with no change from one RR to the next) that were detected for $T = 1$ and $T = 5$, respectively. In both cases the number of constant points remains relatively stable, while decelerations decrease relative to accelerations. This shift is more pronounced for $T = 1$.

Table 7: The number of accelerations, decelerations, and constant points (i.e. no change from one RR to the next) for $T = 1$ and $T = 5$, respectively. Ratio refers to the ratio of accelerations, decelerations, and constants.

	$T = 1$				**$T = 5$**			
	Accelerations	**Decelerations**	**Constants**	**Ratio**	**Accelerations**	**Decelerations**	**Constants**	**Ratio**
GA_1	102829	105248	19734	1:1.02:0.19	113144	108705	5402	1:0.96:0.05
GA_2	127584	123119	21074	1:0.97:0.17	136696	128779	5678	1:0.94:0.04
GA_3	138837	127466	21029	1:0.92:0.15	147070	134498	5108	1:0.91:0.03

4. Discussion

In this paper, we comprehensively analyzed HRV at a high temporal granularity to track the dynamic progression of maternal autonomic modulation over normal pregnancy. We generate a holistic overview of autonomic changes by incorporating non-linear, HRF, and PRSA features in addition to the standard time and frequency domain analysis. These features have rarely or, in the case of HRF, never been assessed in a pregnant population. We find that some of these features are more sensitive to GA than standard time and frequency features. Furthermore, contrary to previous research in this field, we also calculated the effect sizes of the changes in mHRV. Overall, our findings indicate that decreased vagal modulation, dampened autonomic response, reduced complexity, and decreased HR fragmentation accompany advancing gestation. Our results show that even though changes in HRV features are often statistically significant, their effect sizes are small – indicating that the increasing physiological demands of progressing pregnancy are well tolerated by the maternal ANS. Interestingly, while overall autonomic activity remained fairly stable, we found a burst of autonomic activity occurring between approximately 24 and 32 weeks of gestation.

This burst of autonomic activity, which coincides approximately with the transition from the second to the third trimester, is reflected in the temporal analyses of almost all HRV features (Figures 1 to 4). To our knowledge, this change has not been reported in literature and demonstrates the value of assessing autonomic modulation at regular intervals throughout pregnancy. Physiological changes during gestation are non-linear for both mother and fetus [56], [57]. Therefore, it seems unlikely that changes in autonomic modulation would be linear. We speculate that this burst in maternal autonomic activity could be attributed to fetal autonomic modulation. The transition from late-second to early- third trimester is associated with an acceleration in fetal autonomic maturation [58]. Since autonomic modulation is mirrored in cardiovascular regulation and there is evidence for maternal-fetal cardiac coupling [59], [60], it may be that the maternal autonomic activity is reflecting that of the fetus.

Current literature on maternal autonomic modulation typically investigates the interplay of the autonomic branches by assessing standard HRV features from both time and frequency domains. Concurrent with most research, we find that vagal modulation reduces as reflected in pNN50, RMSSD, and HF (Table 2 and Figure 1). An upward trend was also noted in LF/HF, indicating a shift in sympathovagal ratio, aligning with this decrease in vagal activity. Additionally, even though mean HR increased

over pregnancy as expected [61], SDNN – a measure of overall variability – decreased until about 32 weeks of gestation before increasing again. This may suggest that while vagal activity decreases, compensatory processes stabilize the overall variation in HR in the third trimester.

Our findings that parasympathetic activity reduces towards the end of gestation, are in agreement with the results of some investigators [15], [22], [23], but contrast the work of others who found that no significant autonomic changes occur across gestation [20], [21]. It should be noted that in the studies contrasting ours, one only compares between two GA groups [20] and the other focused on early pregnancy [21]. Concerning sympathetic activity, we found a decrease in LF (Table 2 and Figure 1). This contradicts the findings of most researchers that there is an increase [15], [22] or no significant changes in LF during pregnancy [20], [23]. It should be noted that the validity of LF as a measure of sympathetic activity is often disputed [62]. However, findings from microneurography studies – which more directly assess sympathetic activity – indicate that there is increased sympathetic activity in pregnancy accompanied by decreased sympathetic signaling to end-organs, such as the heart [63], [64]. Subsequently, the decrease in LF may be a result of reduced sympathetic influence on HR and decreased parasympathetic activity, which overlaps with the sympathetic activity in the LF band.

Poincaré plots and associated features are commonly used in HRV analyses [49], yet (to our knowledge) this method has not been calculated longitudinally over normal pregnancy. We find that the ratio obtained from this plot (SD1/SD2) is sensitive to progressing pregnancy (Table 3 and Figures 2a). The decrease is mainly driven by a decrease in SD1 which signals reduced vagal activity, which aligns with the results of pNN50, RMSSD, and HF (Figure 1).

Furthermore, our research indicates that HR complexity decreases throughout normal pregnancy as confirmed by both SampEn and α_1 (Table 3 and Figures 2b and c). While one study found increasing complexity with progressing pregnancy [65], others confirm our results that complexity decreases towards the end of gestation [66]. Furthermore, complexity was found reduced in pregnant women compared to non-pregnant controls [53], likely due to the increased demands on the maternal cardiac system during pregnancy. It is also noticeable that changes in complexity measures seemed more sensitive to advancing gestation than most standard HRV features, with SampEn having a larger effect size than standard features (U_1=0.214, Table 3).

Since pregnancy is essentially an alteration in a normal physiological system, complexity measures may indicate how well the body is responding to this change. Subsequently, reducing complexity could indicate that it becomes increasingly difficult for the maternal ANS to quickly respond under the increasing demands of gestation. Indeed, this hypothesis is also supported by other findings. Note that for most features – pNN50 and RMSSD in Figure 1 are good examples – which decrease with advancing gestation, its standard error of the mean also becomes narrower (Figure 1d), indicating that large variations in beat-to-beat HR are uncommon for most participants by the end of pregnancy. Additionally, the PRSA analysis (Figures 4 to 6) showed a dampened response towards the end of gestation. This is further echoed in the significant reduction in almost all PRSA features (Table 5). However, the accompanying effect sizes are small and the dampening in HR responsiveness is not comparable to that seen in diseased states [36]. Furthermore, the two other studies that have calculated PRSA to study maternal HRV found no significant correlations with GA [41], [67], although only DC was studied and assessing its correlation with GA was not the primary aim of these studies.

This dampened autonomic response does not necessarily indicate a deterioration in autonomic function. On the contrary, in our participant group, HRF indices decrease during healthy pregnancy (Table 4 and Figure 3). While an increase in HRF would suggest a breakdown in the hierarchy of physiological systems controlling HR, these findings suggest that the integration of systems controlling HR does not fragment with the increasing physiological demands of pregnancy. Rather, it seems that a smoother control of HR is exhibited in later pregnancy. This could suggest that the dampened autonomic response is not a sign of strain, but rather indicative of a more stable autonomic system that is tightly regulated to balance the complex demands of pregnancy. However, the trade-off for this stability might be that the mother is unable to optimally respond to environmental perturbations such as stress in late pregnancy.

The exact mechanisms that promote stable ANS activity in this situation are not known. However, the PSD of the PRSA graphs (Figures 5c, 5d, 6c, and 6d) offer some insight into how processes mediating HR accelerations and decelerations change with progressing gestation. In the low frequency range (0.035/RRi Hz to 0.15/RRi Hz, i.e. approximately 0.04 to 0.2 Hz), similar behavior is seen when $T = 5$ (Figure 6). However, for $T = 1$, while the frequency response for accelerations (Figure 5c) is stable across GA groups, there is a remarkable increase with gestation for decelerations. This is also reflected in the significant decrease in the ratio (acceleration: deceleration) of all PRSA frequency parameters (Table 6), in particular for TP which has an accompanying

effect size of U_1>0.6, by far the largest of our analysis. Since pregnancy results in an increase in basal HR [61], we hypothesize that there is an increase in activity in this LF frequency region (which is associated with both branches of the ANS) of decelerations to ensure that the increasing mean HR stays within a healthy range. This would align with what is seen in Figure 1a, where the increase in mean HR starts to plateau after 32 weeks GA. Additionally, when studying the normal ranges for mean HR throughout the pregnancies of over 1000 women, Green et al. found not only a similar plateau but also a slight decrease in mean HR during the final weeks of pregnancy [61].

Furthermore, Figures 5c and d show the diminishing effect of respiratory modulation in the HF band over time. As the abdomen grows with advancing gestation, the depth of breathing reduces. Subsequently, as can be explained through the Frank-Starling, and lower HR modulation ensues. This is reflected in the decreases in pNN50 and RMSSD (Figures 1c and d), which have also been observed by others [15], [23].

Overall, while the changes in mHRV are significant, the effect sizes of these changes are typically small. This stable autonomic modulation offers good news for obstetric screening opportunities as it suggests that there is a stable autonomic baseline to track gestational changes against. As pregnancy complications such as preeclampsia are associated with insufficient autonomic regulation, detecting changes in HRV features with larger effects than we observed in this study may facilitate better screening for such complications. Furthermore, PRSA features such as AC, IDR, IAR, SDR, and SAR show decreasing trends earlier than all other features and, importantly, before 20 weeks of gestation. Currently, hypertensive disorders of pregnancy can only be diagnosed after 20 weeks of gestation. Subsequently, investigating these features in populations who develop pregnancy complications may contribute to the eventual early detection of such complications. Additionally, an uptick can be seen in PRSA features (Figure 4) just before the end of pregnancy. If this sudden change is associated with the body preparing for delivery, it could be of value to investigate whether such findings are also observed in cases of preterm delivery.

It should be noted that autonomic activity is not the only driving force behind the physiological changes in pregnancy. Major hormonal changes occur throughout pregnancy. Yet, their link to autonomic activity (as assessed by HRV) remains unclear [68], likely in part due to the difficulty of isolating the effect of a hormone in an already complex physiological system. Some researchers conclude that estrogen is linked to increased parasympathetic activity [69], [70], while others found a negative relation-

ship between progesterone and vagal activity [68], [71]. A combination of estrogen and progesterone (as is the case in pregnancy) seemed to not affect HRV [70], [72], though it should be noted that these studies were not performed in pregnant populations.

Finally, we note that while this study offers novel information on gestational autonomic modulation, the results are limited by the modest sample size. Similar assessments are necessary in larger populations to confidently draw conclusions about pregnant populations. Although our dataset does have a uniquely high median number of measurements per participant, some participants naturally have less than eight. Moreover, the timings of participants' measurements relative to their GA do vary when compared to the protocol. Subsequently, it was necessary to divide the data into three GA groups to facilitate appropriate statistical testing, taking the average per participant if they have multiple measurements in a group. Additionally, the dataset is further limited regarding participant information for the mother, in part because the focus of the original analysis was on fetal HRV. Subsequently, information on factors that may influence mHRV during recording sessions (e.g., fasting, coffee consumption, and smoking habits) are unavailable and cannot be accounted for in our analysis.

Furthermore, during the preprocessing for the frequency domain and some complexity features, unreliable RR intervals were interpolated. This interpolation is necessary for determining these HRV features but may affect their results and subsequent interpretation, particularly regarding HF [47]. However, since the changes in HF in our analysis reflect those of pNN50 and RMSSD as is expected from literature [17], we believe the trend observed in HF is reliable. Still, frequency domain features should be interpreted with caution, since their calculation relies on an assumption of stationarity which is not guaranteed and involves averaging multiple segments which may represent different physiological states. Lastly, our measurements start at 14 weeks of gestation, while major cardiovascular and autonomic changes are also known to occur within the first few weeks of pregnancy. Ideally, future work would incorporate measurements from as early in gestation as possible.

In conclusion, this work offers a comprehensive look at autonomic modulation in normally progressing pregnancy. By assessing HRV at a high temporal granularity with a variety of features, we find that although significant reductions in vagal activity, complexity, HR responsiveness, and HRF do occur, these changes are of small effect and weakly correlated to GA. Therefore, in a healthy pregnancy, the increasing stress of advancing gestation is tolerated well.

References

[1] S. V. Khlybova, V. I. Tsirkin, S. A. Dvoryanskii, I. A. Makarova, and A. N. Trukhin, "Heart rate variability in normal and complicated pregnancies," *Hum Physiol*, vol. 34, no. 5, pp. 625–632, Sep. 2008, doi: 10.1134/S0362119708050113.

[2] S. Moors *et al.*, "Heart rate variability in hypertensive pregnancy disorders: a systematic review," *Pregnancy Hypertension*, Mar. 2020, doi: 10.1016/j.preghy.2020.03.003.

[3] D. Yousif *et al.*, "Autonomic Dysfunction in Preeclampsia: A Systematic Review," *Front. Neurol.*, vol. 10, Aug. 2019, doi: 10.3389/fneur.2019.00816.

[4] Y. Cui, B. Zhu, and F. Zheng, "Low-dose aspirin at ≤16 weeks of gestation for preventing preeclampsia and its maternal and neonatal adverse outcomes: A systematic review and meta-analysis," *Exp Ther Med*, vol. 15, no. 5, pp. 4361–4369, May 2018, doi: 10.3892/etm.2018.5972.

[5] R. Shanmugalingam, A. Hennessy, and A. Makris, "Aspirin in the prevention of preeclampsia: the conundrum of how, who and when," *J Hum Hypertens*, vol. 33, no. 1, pp. 1–9, Jan. 2019, doi: 10.1038/s41371-018-0113-7.

[6] K. S. Khan, D. Wojdyla, L. Say, A. M. Gulmezoglu, and P. F. V. Look, "WHO analysis of causes of maternal death: a systematic review," *Lancet (London, England)*, vol. 367, no. 9516, pp. 1066–1074, Apr. 2006.

[7] M. Umesawa and G. Kobashi, "Epidemiology of hypertensive disorders in pregnancy: prevalence, risk factors, predictors and prognosis," *Hypertension research : official journal of the Japanese Society of Hypertension*, vol. 40, no. 3, pp. 213–220, 2017, doi: 10.1038/hr.2016.126.

[8] H. A. Frey and M. A. Klebanoff, "The epidemiology, etiology, and costs of preterm birth," *Seminars in Fetal and Neonatal Medicine*, vol. 21, no. 2, pp. 68–73, Apr. 2016, doi: 10.1016/j.siny.2015.12.011.

[9] S. Saleem *et al.*, "A prospective study of maternal, fetal and neonatal deaths in low- and middle-income countries," *Bull. World Health Organ.*, vol. 92, no. 8, pp. 605–612, Aug. 2014, doi: 10.2471/BLT.13.127464.

[10] C. E. Kleinrouweler *et al.*, "Prognostic models in obstetrics: available, but far from applicable.," *American journal of obstetrics and gynecology*, vol. 214, no. 1, pp. 79-90.e36, Jan. 2016, doi: 10.1016/j.ajog.2015.06.013.

[11] A. C. De Kat, J. Hirst, M. Woodward, S. Kennedy, and S. A. Peters, "Prediction models for preeclampsia: A systematic review," *Pregnancy Hypertension*, vol. 16, pp. 48–66, Apr. 2019, doi: 10.1016/j.preghy.2019.03.005.

[12] P. Antonazzo, I. Cetin, D. Tarricone, F. Lombardi, and G. Pardi, "Cardiac autonomic modulation in normal, high-risk, and in vitro fertilization pregnancies during the first trimester," *American Journal of Obstetrics and Gynecology*, vol. 190, no. 1, pp. 199–205, Jan. 2004, doi: 10.1016/S0002-9378(03)00896-2.

[13] G. K. Pal, P. Shyma, S. Habeebullah, P. Shyjus, and P. Pal, "Spectral Analysis of Heart Rate Variability for Early Prediction of Pregnancy-Induced Hypertension," *Clinical and Experimental Hypertension*, vol. 31, no. 4, pp. 330–341, Jan. 2009, doi: 10.1080/10641960802621333.

[14] V. L. Brooks, Q. Fu, Z. Shi, and C. M. Heesch, "Adaptations in autonomic nervous system regulation in normal and hypertensive pregnancy," in *Handbook of Clinical Neurology*, Elsevier, 2020, pp. 57–84. doi: 10.1016/B978-0-444-64239-4.00003-5.

[15] P. Garg, K. Yadav, A. K. Jaryal, G. Kachhawa, A. Kriplani, and K. K. Deepak, "Sequential analysis of heart rate variability, blood pressure variability and baroreflex sensitivity in healthy pregnancy," *Clin Auton Res*, Jan. 2020, doi: 10.1007/s10286-020-00667-4.

[16] Task Force of The European Society of Cardiology and The North American Society of Pacing and Electrophysiology, "Heart rate variability. Standards of measurement, physiological interpretation, and clinical use.," *European heart journal*, vol. 17, no. 3, pp. 354–381, Mar. 1996.

[17] F. Shaffer and J. P. Ginsberg, "An Overview of Heart Rate Variability Metrics and Norms," *Front. Public Health*, vol. 5, p. 258, Sep. 2017, doi: 10.3389/fpubh.2017.00258.

[18] K. Grym *et al.*, "Feasibility of smart wristbands for continuous monitoring during pregnancy and one month after birth," *BMC Pregnancy Childbirth*, vol. 19, no. 1, p. 34, Dec. 2019, doi: 10.1186/s12884-019-2187-9.

[19] D. Schlembach and M. G. Moertl, "Heart Rate Variability and Blood Pressure Variability in Obstetrics and Gynecology," in *Heart rate variability (HRV) signal analysis: Clinical applications*, M. V. Kamath, M. A. Watanabe, and A. Upton, Eds., 1st ed.CRC Press, 2012.

[20] A. Voss *et al.*, "Baroreflex sensitivity, heart rate, and blood pressure variability in normal pregnancy," *American Journal of Hypertension*, vol. 13, no. 11, pp. 1218–1225, Nov. 2000, doi: 10.1016/S0895-7061(00)01199-7.

[21] M. G. Moertl *et al.*, "Changes in haemodynamic and autonomous nervous system parameters measured non-invasively throughout normal pregnancy," *European Journal of Obstetrics & Gynecology and Reproductive Biology*, vol. 144, pp. S179–S183, May 2009, doi: 10.1016/j.ejogrb.2009.02.037.

[22] V. Kolovetsiou-Kreiner *et al.*, "Maternal cardiovascular and endothelial function from first trimester to postpartum," *PLoS ONE*, vol. 13, no. 5, p. e0197748, May 2018, doi: 10.1371/journal.pone.0197748.

[23] M. Balajewicz-Nowak, A. Furgala, K. Pitynski, P. Thor, H. Huras, and K. Rytlewski, "The dynamics of autonomic nervous system activity and hemodynamic changes in pregnant women," *Neuro Endocrinol Lett*, vol. 37, no. 1, pp. 70–77, 2016.

[24] American Academy of Pediatrics and American College of Obstetricians and Gynecologists, Eds., *Guidelines for perinatal care*, Eighth edition. Elk Grove Village, IL : Washington, DC: American Academy of Pediatrics ; The American College of Obstetricians and Gynecologists, 2017.

[25] NVOG, "Basis Prenatale Zorg: opsporing van de belangrijkste zwangerschapscomplicaties bij laag risico zwangeren (in de 2 de en 3 de lijn)," NVOG, Richtlijn 1.0, 2015.

[26] A. Bakhchina, K. Arutyunova, A. Sozinov, A. Demidovsky, and Y. Alexandrov, "Sample Entropy of the Heart Rate Reflects Properties of the System Organization of Behaviour," *Entropy*, vol. 20, no. 6, p. 449, Jun. 2018, doi: 10.3390/e20060449.

[27] F. Shaffer, R. McCraty, and C. L. Zerr, "A healthy heart is not a metronome: an integrative review of the heart's anatomy and heart rate variability," *Front. Psychol.*, vol. 5, Sep. 2014, doi: 10.3389/fpsyg.2014.01040.

[28] L. E. V. Silva, C. A. A. Silva, H. C. Salgado, and R. Fazan, "The role of sympathetic and vagal cardiac control on complexity of heart rate dynamics," *American Journal of Physiology-Heart and Circulatory Physiology*, vol. 312, no. 3, pp. H469–H477, Mar. 2017, doi: 10.1152/ajpheart.00507.2016.

[29] S. Ahmad *et al.*, "Continuous Multi-Parameter Heart Rate Variability Analysis Heralds Onset of Sepsis in Adults," *PLoS ONE*, vol. 4, no. 8, p. e6642, Aug. 2009, doi: 10.1371/journal.pone.0006642.

[30] C. -K. Peng, S. Havlin, H. E. Stanley, and A. L. Goldberger, "Quantification of scaling exponents and crossover phenomena in nonstationary heartbeat time series," *Chaos*, vol. 5, no. 1, pp. 82–87, Mar. 1995, doi: 10.1063/1.166141.

[31] D. E. Vigo *et al.*, "Nonlinear analysis of heart rate variability within independent frequency components during the sleep–wake cycle," *Autonomic Neuroscience*, vol. 154, no. 1–2, pp. 84–88, Apr. 2010, doi: 10.1016/j.autneu.2009.10.007.

[32] T. D. Bilhartz, P. A. Bilhartz, T. N. Bilhartz, and R. D. Bilhartz, "Making Use of a Natural Stress Test: Pregnancy and Cardiovascular Risk," *Journal of Women's Health*, vol. 20, no. 5, p. 8, 2011, doi: 10.1089/jwh.2010.2291.

[33] L. Chasan-Taber, "It Is Time to View Pregnancy as a Stress Test," *JOURNAL OF WOMEN'S HEALTH*, vol. 25, no. 1, p. 2, 2016, doi: 10.1089/jwh.2015.5653.

[34] D. Williams, "Pregnancy: a stress test for life:," *Current Opinion in Obstetrics and Gynecology*, vol. 15, no. 6, pp. 465–471, Dec. 2003, doi: 10.1097/00001703-200312000-00002.

[35] A. Bauer *et al.*, "Phase-rectified signal averaging detects quasi-periodicities in non-stationary data," *Physica A: Statistical Mechanics and its Applications*, vol. 364, pp. 423–434, May 2006, doi: 10.1016/j.physa.2005.08.080.

[36] A. Bauer *et al.*, "Deceleration capacity of heart rate as a predictor of mortality after myocardial infarction: cohort study," *The Lancet*, vol. 367, no. 9523, pp. 1674–1681, May 2006, doi: 10.1016/S0140-6736(06)68735-7.

[37] C. Eick *et al.*, "Autonomic Nervous System Activity as Risk Predictor in the Medical Emergency Department: A Prospective Cohort Study," *Critical Care Medicine*, vol. 43, no. 5, pp. 1079–1086, May 2015, doi: 10.1097/CCM.0000000000000922.

[38] L. M. Campana, R. L. Owens, G. D. Clifford, S. D. Pittman, and A. Malhotra, "Phase-rectified signal averaging as a sensitive index of autonomic changes with aging," *Journal of Applied Physiology*, vol. 108, no. 6, pp. 1668–1673, Jun. 2010, doi: 10.1152/japplphysiol.00013.2010.

[39] E. M. Graatsma *et al.*, "Average acceleration and deceleration capacity of fetal heart rate in normal pregnancy and in pregnancies complicated by fetal growth restriction," *The Journal of Maternal-Fetal & Neonatal Medicine*, vol. 25, no. 12, pp. 2517–2522, Dec. 2012, doi: 10.3109/14767058.2012.704446.

[40] A. Georgieva, A. Papageorghiou, S. Payne, M. Moulden, and C. Redman, "Phase-rectified signal averaging for intrapartum electronic fetal heart rate monitoring is related to acidaemia at birth," *BJOG: Int J Obstet Gy*, vol. 121, no. 7, pp. 889–894, Jun. 2014, doi: 10.1111/1471-0528.12568.

[41] D. Casati *et al.*, "Maternal cardiac deceleration capacity: a novel insight into maternal autonomic function in pregnancies complicated by hypertensive disorders and intrauterine growth restriction," *European Journal of Obstetrics & Gynecology and Reproduc-*

tive Biology, vol. 206, pp. 6–11, Nov. 2016, doi: 10.1016/j.ejogrb.2016.08.007.

[42] E. Tejera, M. J. Areias, A. I. Rodrigues, J. M. Nieto-Villar, and I. Rebelo, "Blood Pressure and Heart Rate Variability Complexity Analysis in Pregnant Women with Hypertension," *Hypertension in Pregnancy*, vol. 31, no. 1, pp. 91–106, Feb. 2012, doi: 10.3109/10641955.2010.544801.

[43] M. D. Costa, R. B. Davis, and A. L. Goldberger, "Heart Rate Fragmentation: A New Approach to the Analysis of Cardiac Interbeat Interval Dynamics," *Front. Physiol.*, vol. 8, p. 255, May 2017, doi: 10.3389/fphys.2017.00255.

[44] J. O. E. H. van Laar *et al.*, "Fetal heart rate variability during pregnancy, obtained from non-invasive electrocardiogram recordings," *Acta Obstet Gynecol Scand*, vol. 93, no. 1, pp. 93–101, Jan. 2014, doi: 10.1111/aogs.12286.

[45] M. J. Rooijakkers *et al.*, "Influence of Electrode Placement on Signal Quality for Ambulatory Pregnancy Monitoring," *Computational and Mathematical Methods in Medicine*, vol. 2014, pp. 1–12, 2014, doi: 10.1155/2014/960980.

[46] M. J. Rooijakkers, C. Rabotti, M. Bennebroek, J. van Meerbergen, and M. Mischi, "Low-complexity R-peak detection in ECG signals: A preliminary step towards ambulatory fetal monitoring," in *2011 Annual International Conference of the IEEE Engineering in Medicine and Biology Society*, Boston, MA: IEEE, Aug. 2011, pp. 1761–1764. doi: 10.1109/IEMBS.2011.6090503.

[47] C. Peters, R. Vullings, J. Bergmans, G. Oei, and P. Wijn, "The effect of artifact correction on spectral estimates of heart rate variability," in *2008 30th Annual International Conference of the IEEE Engineering in Medicine and Biology Society*, Vancouver, BC: IEEE, Aug. 2008, pp. 2669–2672. doi: 10.1109/IEMBS.2008.4649751.

[48] C. H. L. Peters, R. Vullings, M. J. Rooijakkers, J. W. M. Bergmans, S. G. Oei, and P. F. F. Wijn, "A continuous wavelet transform-based method for time-frequency analysis of artefact-corrected heart rate variability data," *Physiol. Meas.*, vol. 32, no. 10, pp. 1517–1527, Oct. 2011, doi: 10.1088/0967-3334/32/10/001.

[49] A. H. Khandoker, C. Karmakar, M. Brennan, M. Palaniswami, and A. Voss, *Poincaré Plot Methods for Heart Rate Variability Analysis*. Boston, MA: Springer US, 2013. doi: 10.1007/978-1-4614-7375-6.

[50] J. S. Richman and J. R. Moorman, "Physiological time-series analysis using approximate entropy and sample entropy," *American Journal of Physiology-Heart and Circulatory Physiology*, vol. 278, no. 6, pp. H2039–H2049, Jun. 2000, doi: 10.1152/ajpheart.2000.278.6.H2039.

[51] P. Gomes, P. Margaritoff, and H. Silva, "pyHRV: Development and Evaluation of an Open-Source Python Toolbox for Heart Rate Variability (HRV)," presented at the IcETRAN, 2019, pp. 882–887.

[52] E. Shaqiri and M. Gusev, "A Programmatic Approach for Development of the ViewHRV Service Platform with Accurate and Reliable Results," in *2020 43rd International Convention on Information, Communication and Electronic Technology (MIPRO)*, Opatija, Croatia: IEEE, Sep. 2020, pp. 343–348. doi: 10.23919/MIPRO48935.2020.9245419.

[53] R.-G. Yeh, J.-S. Shieh, G.-Y. Chen, and C.-D. Kuo, "Detrended fluctuation analysis of short-term heart rate variability in late pregnant women," *Autonomic Neuroscience*, vol. 150, no. 1–2, pp. 122–126, Oct. 2009, doi: 10.1016/j.autneu.2009.05.241.

[54] R. Joshi, D. Kommers, X. Long, L. Feijs, and S. V. Huffel, "Cardiorespiratory coupling in preterm infants," *J Appl Physiol*, vol. 126, pp. 202–213, doi: 10.1152/japplphysiol.00722.2018.

[55] C. O. Fritz, P. E. Morris, and J. J. Richler, "Effect size estimates: Current use, calculations, and interpretation.," *Journal of Experimental Psychology: General*, vol. 141, no. 1, pp. 2–18, 2012, doi: 10.1037/a0024338.

[56] E. K. Tan and E. L. Tan, "Alterations in physiology and anatomy during pregnancy," *Best Practice and Research: Clinical Obstetrics and Gynaecology*, vol. 27, no. 6, pp. 791–802, Dec. 2013, doi: 10.1016/j.bpobgyn.2013.08.001.

[57] C. M. J. Tan and A. J. Lewandowski, "The Transitional Heart: From Early Embryonic and Fetal Development to Neonatal Life," *Fetal Diagn Ther*, vol. 47, no. Suppl. 5, pp. 373–386, 2020, doi: 10.1159/000501906.

[58] U. Schneider *et al.*, "Developmental milestones of the autonomic nervous system revealed via longitudinal monitoring of fetal heart rate variability," *PLoS ONE*, vol. 13, no. 7, p. e0200799, Jul. 2018, doi: 10.1371/journal.pone.0200799.

[59] R. Avci, D. Escalona-Vargas, E. R. Siegel, C. L. Lowery, and H. Eswaran, "Coupling Analysis of Fetal and Maternal Heart Rates via Transfer Entropy Using Magnetocardiography," in *2018 40th Annual International Conference of the IEEE Engineering in Medicine and Biology Society (EMBC)*, Honolulu, HI: IEEE, Jul. 2018, pp. 1–4. doi: 10.1109/EMBC.2018.8513053.

[60] A. H. Khandoker *et al.*, "Analysis of maternal–fetal heart rate coupling directions with partial directed coherence," *Biomedical Signal Processing and Control*, vol. 30, pp. 25–30, Sep. 2016, doi: 10.1016/j.bspc.2016.06.010.

[61] L. J. Green *et al.*, "Gestation-Specific Vital Sign Reference Ranges in Pregnancy," *Obstetrics & Gynecology*, vol. 135, no. 3, pp. 653–664, Mar. 2020, doi: 10.1097/AOG.0000000000003721.

[62] J. A. J. Heathers, "Everything Hertz: methodological issues in short-term frequency-domain HRV," *Front. Physiol.*, vol. 5, May 2014, doi: 10.3389/fphys.2014.00177.

[63] C. W. Usselman *et al.*, "Regulation of Sympathetic Nerve Activity During the Cold Pressor Test in Normotensive Pregnant and Nonpregnant Women," *Hypertension*, vol. 66, no. 4, pp. 858–864, Oct. 2015, doi: 10.1161/HYPERTENSIONAHA.115.05964.

[64] C. D. Steinback *et al.*, "Blunted sympathetic neurovascular transduction during normotensive pregnancy," *J Physiol*, vol. 597, no. 14, pp. 3687–3696, Jul. 2019, doi: 10.1113/JP277714.

[65] M. A. Peña *et al.*, "Short-term heart rate dynamics of pregnant women," *Autonomic Neuroscience*, vol. 159, no. 1–2, pp. 117–122, Jan. 2011, doi: 10.1016/j.autneu.2010.09.006.

[66] M. Baumert, M. Javorka, A. Seeck, R. Faber, P. Sanders, and A. Voss, "Multiscale entropy and detrended fluctuation analysis of QT interval and heart rate variability during normal pregnancy," *Computers in Biology and Medicine*, vol. 42, no. 3, pp. 347–352, Mar. 2012, doi: 10.1016/j.compbiomed.2011.03.019.

[67] Carpenter, "Influence of a supervised antenatal exercise program on estimates of heart rate responsiveness," *Edorium J Matern Child Health.*

[68] J. J. von Holzen, G. Capaldo, M. Wilhelm, and P. Stute, "Impact of endo- and exogenous estrogens on heart rate variability in women: a review," *Climacteric*, vol. 19, no. 3, pp. 222–228, May 2016, doi: 10.3109/13697137.2016.1145206.

[69] A. Dart, "Gender, sex hormones and autonomic nervous control of the cardiovascular system," *Cardiovascular Research*, vol. 53, no. 3, pp. 678–687, Feb. 2002, doi: 10.1016/S0008-6363(01)00508-9.

[70] M. Gökçe, B. Karahan, R. Yilmaz, C. Örem, C. Erdöl, and Ş. Özdemir, "Long term effects of hormone replacement therapy on heart rate variability, QT interval, QT dispersion and frequencies of arrhytmia," *International Journal of Cardiology*, vol. 99, no. 3, pp. 373–379, Mar. 2005, doi: 10.1016/j.ijcard.2003.03.030.

[71] K. M. Schmalenberger *et al.*, "Menstrual Cycle Changes in Vagally-Mediated Heart Rate Variability Are Associated with Progesterone: Evidence from Two Within-Person Studies," *JCM*, vol. 9, no. 3, p. 617, Feb. 2020, doi: 10.3390/jcm9030617.

[72] E. O. Fernandes, R. S. Moraes, E. L. Ferlin, M. C. O. Wender, and J. P. Ribeiro, "Hormone Replacement Therapy Does Not Affect the 24-Hour Heart Rate Variability in Postmenopausal Women:. Results of a Randomized, Placebo-Controlled Trial with Two Regimens," *Pacing Clin Electro*, vol. 28, no. s1, pp. S172–S177, Jan. 2005, doi: 10.1111/j.1540-8159.2005.00041.x.

Chapter 5

Characterizing the effect of demographics, cardiorespiratory factors, and inter-subject variation on maternal heart rate variability in pregnancy with statistical modeling

Reproduced after: M Bester, R Joshi, A Linders, M Mischi, JOEH van Laar, R Vullings. Characterizing the effect of demographics, cardiorespiratory factors, and inter-subject variation on maternal heart rate variability in pregnancy with statistical modeling: a retrospective observational analysis. *Scientific Reports*. 2022.

Abstract

Pregnancy complications are associated with insufficient adaptation of the maternal autonomic nervous system to the physiological demands of pregnancy. Consequently, assessing maternal heart rate variability (mHRV) – which reflects autonomic regulation – is a promising tool for detecting early deterioration in maternal health. However, before mHRV can be used to screen for complications, an understanding of the factors influencing mHRV during healthy pregnancy is needed. In this retrospective observational study, we develop regression models to unravel the effects of maternal demographics (age, body mass index (BMI), gestational age (GA), and parity), cardiorespiratory factors (heart rate and breathing rate), and inter-subject variation on mHRV. We develop these models using two datasets which are comprised of, respectively, single measurements in 290 healthy pregnant women and repeated measurements (median = 8) in 29 women with healthy pregnancies. Our most consequential finding is that between one-third and two-thirds of the variation in mHRV can be attributed to inter-subject variability. Additionally, median heart rate dominantly affects mHRV ($p<0.001$), while BMI and parity have no effect. Moreover, we found that median breathing rate, age, and GA all impact mHRV ($p<0.05$). These results suggest that personalized, long-term monitoring would be necessary for using mHRV for obstetric screening.

1. Introduction

Assessing heart rate variability (HRV) offers a non-invasive opportunity for monitoring autonomic activity [1]. HRV has been used to assess cardiac health, predict short-term mortality in emergency-room patients, investigate fetal well-being [2], and – through longitudinal and continuous monitoring – detect conditions such as sepsis and Covid-19 infection before the onset of observable symptoms [1], [3]–[5]. More recently, investigations have focused on the association between the HRV of the mother during pregnancy – henceforth referred to as maternal HRV (mHRV) – and maternal health, in large part driven by the need for tools for the early detection of pregnancy complications [6], [7]. The inability to detect these complications early enough to implement risk-mitigating interventions remains a barrier to reducing perinatal mortality and morbidity [8]. For example, the increase in blood pressure symptomatic of pregnancy-induced hypertension only arises after 20 weeks of gestation pregnancy, which is beyond the window in which the clinically available suite of interventions has an optimal impact [8], [9].

Motivated by the suspected autonomic dysfunction associated with preeclampsia (a type of hypertensive disorder in pregnancy), Eneroth et al. were amongst the first to investigate mHRV in complicated pregnancies [10]. Further investigations not only confirmed their initial result that preeclamptic women had altered mHRV in comparison to healthy pregnancies [9] but also demonstrated similar findings in other pregnancy complications [11], [12]. Consequently, assessing mHRV may offer a tool for identifying pregnancy complications before the onset of the typical symptoms associated with the complication [13], [14].

Despite the potential of HRV as an obstetric screening method, interpreting HRV is challenging due to the sensitivity of the metric to a multitude of factors [1], [15]. For instance, HRV features have a well-documented relationship with cardiorespiratory factors [16], [17] and have also been shown to be influenced by demographics such as age and body mass index (BMI) [18]–[20]. However, apart from a single study analyzing only frequency domain features of HRV [21], these associations have not been investigated in a pregnant population. Notably, pregnancy alters autonomic regulation, and these regulatory effects change through the course of advancing gestation [6], [22]. Therefore, it is imperative to establish an understanding of how maternal demographics influence mHRV in a healthy pregnancy to, in turn, be able to identify abnormal values of mHRV.

In this paper, we describe the effects of maternal characteristics on selected mHRV features using regression modeling. In all cases, the null hypothesis being tested is that the maternal characteristic does not affect mHRV. We analyze two datasets to test this hypothesis. First, we develop a multiple linear regression model based on a dataset of single measurements in 290 healthy pregnant women to characterize the effects of maternal demographics and cardiorespiratory factors on mHRV. Second, we analyze a dataset of repeated measurements (median of eight per participant) taken over the course of 29 healthy pregnancies to develop a linear mixed-effects model. This model allows for discerning the inter-subject variability by making use of these repeated measurements. Finally, considering the results from both models, we discuss their implications for using mHRV as an obstetric screening tool.

2. Methods

2.1 Datasets

This study is a retrospective observational analysis of two existing datasets of abdominal ECG measurements (from which maternal R-peaks can be extracted). The first dataset, referred to as *Dataset 1*, contains abdominal ECG recordings (NEMO Healthcare BV, the Netherlands) from 494 women with singleton pregnancies between 18 and 24 weeks of gestation [23]. Measurements of approximately 30-minute duration were acquired at 500 Hz while women were lying in a semi-recumbent position. The study was conducted between May 2014 and February 2017. The study protocol for the original study has been previously described [23]. For our analysis, women with missing information on BMI, age, and gestational age (GA)were excluded (n = 79). Furthermore, women with maternal pregnancy complications such as preeclampsia or gestational diabetes, health conditions such as asthma, hyperthyroidism, or heart disease, or who were taking any medications (e.g., anti-coagulants, anti-hypertensives, psychotropics) except vitamins were excluded (n = 121). Finally, women with more than 25% unreliable data in their recordings (as defined in the *Preprocessing section*) were excluded (n = 4), resulting in a total of 290 participants. Of the participants included in the analysis, 74 were diagnosed with fetal congenital heart disease (CHD). These participants were not excluded, since there is no evidence that fetal CHD would affect mHRV. However, this assumption is assessed during the model development (see section: *Statistical modeling*). Patient characteristics are presented in Table 1.

Table 1: Characteristics of *Dataset 1*. Where applicable, values are presented as median and interquartile range.

Characteristic	**Dataset 1**
Number of included participants	290
Number of measurements	290
Age	30 (28 – 34) years
BMI before pregnancy	22.7 (20.7 – 25.9) kg/m^2
Gestational age at measurement	20 weeks 3 days (19 weeks 4 days – 21 weeks 3 days)
Nulliparous	54.5 %
Fetal CHD	78 cases (26.9 %)
Measurement length	30.8 (29.1 – 32.3) minutes

The second dataset, *Dataset 2*, was collected between 2008 to 2009. Healthy women (18 years and older) with uneventful, singleton pregnancies were recruited before 12 weeks of gestation for participation (n = 40) [24]. Abdominal ECG measurements (the NEMO device, Maastricht Instruments, the Netherlands) of approximately 45 minutes were obtained at a sampling rate of 1000 Hz. Recordings were done between 08:00 and 18:00 while women were lying comfortably in a semi-recumbent position. Repeated measurements were performed at approximately 14, 18, 22, 24, 26, 30, 34, 36, 38, and 40 weeks of gestation. The seven women who developed complications and the four for whom all ECG data were missing were subsequently excluded, resulting in a cohort of 29 women with a total of 248 ECG recordings. ECG recordings with more than 25% unreliable data (see: *Preprocessing*) were also removed from the analysis, resulting in a total of 230 measurements and a median of eight measurements per participant (interquartile range: 7 – 9). Participants took no medication apart from iron supplements or vitamins. Table 2 outlines the characteristics of the included participants. The original study has been described previously[24].

Table 2: Characteristics of *Dataset 2*. Where applicable, values are represented as median and interquartile ranges.

Characteristic	**Dataset 2**
Number of included participants	29
Number of measurements	230

Age	31 (28 – 34) years
BMI	22.9 (20.9 – 26.1) kg/ m2
Gestational age at birth	39 weeks 6 days (38 weeks 6 days – 41 weeks 3 days)
Nulliparous	65.5 %
Fetal CHD	0 %
Measurement length	44.8 (40.9 – 46.1) minutes

All participants provided written informed consent. The institutional review board at the Máxima Medical Center, Veldhoven, the Netherlands, approved the original studies (DS1: NL48535.015.14; DS2: reference number 0650), which were performed in accordance with the Declaration of Helsinki. The same review board granted a waiver for this secondary analysis in 2021 (reference number N21.008) in accordance with the Dutch law on medical research with humans.

2.2 Signal processing and calculating HRV features

2.2.1 Preprocessing

Multichannel abdominal ECG measurements were filtered by applying a 4th order Butterworth bandpass filter of 1 to 70 Hz to suppress out-of-band noise and artifacts and a notch filter at 50 Hz to suppress powerline interference. Thereafter, a fixed linear combination of the various abdominal channels was applied to enhance maternal QRS peaks [25] and R-peaks were detected with a previously reported algorithm [22], [26]. These R-peaks were used to determine the corresponding tachograms (i.e., the sequence of durations of the RR intervals). RR intervals that were outside of a realistic physiological range (0.4 to 2 seconds) or differed from preceding RR intervals by more than 20% were rejected [27]–[29]. Furthermore, RR intervals for which both the preceding and following values were excluded based on the above criteria, were also excluded. For HRV features that require a continual time series, the missing values were linearly interpolated.

2.2.2 Cardiorespiratory factors

In our analysis, we aim to determine the effect of cardiorespiratory factors on mHRV. To this end, the median heart rate (HR) was calculated for each ECG measurement in beats per minute (bpm). Furthermore, the BR was estimated from the tachogram by applying empirical mode decomposition (EMD) [30], [31]. EMD performs a time adaptive decomposition of a complex signal into elementary components that do not overlap in frequency. These extracted components have well-behaved Hilbert transforms from which the instantaneous frequencies can subsequently be deter-

mined. As respiration is the highest frequency oscillation contributing to HRV, the first decomposition is taken as the respiratory modulation[31]. The BR was calculated based on 2-minute segments, moved along the total signal with a 50% overlap between segments. If more than 5% of the RR intervals in a segment were unreliable (as defined in the *Preprocessing* section), the entire segment was disregarded from the BR analysis. Information above 0.5 Hz and below 0.1 Hz was filtered out and the dominant remaining frequency was taken as the estimated BR per segment. The median of all the BRs calculated per measurement segment was taken as the median BR of the total measurement. The BR is presented in breaths per minute (brpm). For *Dataset 2*, which has multiple measurements per participant, no BR could be calculated for five measurements owing to a high occurrence of unreliable RR intervals. In these cases, the average median BR for that participant was used as a replacement. The median HR and BR per dataset are reported in Table 3.

2.2.3 HRV features

Three HRV features were used for the analysis: SDNN (standard deviation of all NN intervals), RMSSD (root mean squared successive differences of NN intervals), and SampEn (sample entropy of HR) [15], [32]. SDNN and RMSSD are the most widely used time-domain features for HRV[1]. SDNN reflects overall variability and is influenced by both sympathetic and vagal activity. RMSSD captures immediate beat-to-beat variability. Consequently, this feature mainly indexes vagal activity, which can influence immediate subsequent heartbeats [15], [33]. Lastly, SampEn characterizes the complexity of the HR time series, with lower SampEn indicating a more regular signal [15]. In previous work, we found that SampEn is particularly sensitive to healthily progressing gestation [22]. The medians of the HRV features per dataset are reported in Table 3.

Table 3: Cardiorespiratory and heart rate variability parameters, reported as median with interquartile range

Variable	Dataset 1	Dataset 2
SDNN (ms)	54.0 (42.2 – 66.8)	47.2 (36.6 – 59.9)
RMSSD (ms)	29.6 (21.2 – 42.9)	22.5 (14.9 – 33.3)
SampEn (a.u.)	1.4 (1.2 – 1.6)	1.2 (0.9 – 1.4)
HR (bpm)	78.1 (71.5 – 84.0)	79.9 (72.6 – 87.3)
BR (brpm)	14.1 (13.2 – 15.2)	13.8 (12.8 – 15.1)

ms = milliseconds; a.u. = arbitrary units ; bpm = beats per minute; brpm = breaths per minute

The processing of maternal RR intervals from fetal ECG measurements, as well as the development of statistical models described in the next section, was done in MATLAB (MathWorks, USA). All other processing was done in Python (PSF, USA).

2.3 Statistical modeling and testing

Multiple linear regression models (MLRs) enable the quantification of the influence of multiple independent variables (IVs) – in our case, participant demographics and cardiorespiratory factors – on each of the three dependent variables (DVs), i.e., the HRV features. These models only incorporate fixed effects (FEs), which represent the effects of the IVs, i.e., age, BMI, GA, parity, median HR, and median BR. We developed MLRs for both datasets. Parity is considered a categorical variable, with participants being labeled either nulliparous or parous. Fetal CHD was also added as a categorical IV to test the assumption that this fetal condition does not affect mHRV. In all cases, the null hypothesis is that the maternal characteristics being investigated do not affect mHRV.

We assessed the fit of our models by performing the *F*-test. If the *F*-test of overall significance is statistically significant ($p < 0.05$), it indicates that the fit of the model with the FEs is significantly better than that of an intercept-only model (i.e., a model with only a constant term and no IVs). We also quantified the goodness-of-fit of our models by calculating the adjusted R^2, i.e., the coefficient of determination. The adjusted R^2 specifies what percentage of the variation observed in the DV can be explained by the model. For example, an adjusted R^2 of 0.70 means that 70% of the variation in the DV can be attributed to the IVs in the model. The remaining 30% would then be a result of variables that were not incorporated into the model.

Another likely source of variances in the DVs is the possible inherent differences between subjects' baseline mHRV. When multiple measurements are available per participant (as is the case in *Dataset 2*, where repeated measurements were recorded at different GAs throughout pregnancy), a linear mixed-effects model (LMM) can be developed to quantify this inter-subject variability. LMMs capture the influence of both FEs and random effects (REs). In our case, the REs correspond to an individual intercept which is estimated for each participant (as opposed to the single intercept estimated in the MLRs). Subsequently, we developed an LMM for *Dataset 2*. We compared the LMM against an FE-only model with the log-likelihood ratio test to test whether adding the REs significantly improves the fit. Finally, the intra-class correlation (ICC), which is the ratio of the variance of the random intercept to the

total variance, was calculated to determine how much of the overall variance in DVs can be explained by inter-subject variability [33].

2.4 Model development and diagnostics

Before developing the model, multicollinearity between the IVs was assessed by calculating their variable inflation factors (VIF). A VIF of between one and five is acceptably low. All VIFs were between one and two; subsequently, all IVs were included in the model. Furthermore, the distributions of the DVs were checked, since LMMs are typically more appropriate for normally distributed DVs. SDNN and RMSSD were right-skewed and subsequently log-transformed to yield a more normal distribution. SampEn, which was originally left-skewed, was more normally distributed once the values were squared. Hereafter, MLRs were developed for both datasets and LMMs were developed for *Dataset 2* (which included repeated measurements per participant). The models were developed for each of the three DVs in the datasets.

Several checks were implemented after the models had been developed to assess their validity and to check whether the appropriate statistical assumptions were satisfactorily met. The following plots were generated to check these assumptions [33]:

1. Normal probability plots of the residuals of the models (i.e., the error between the predicted value and the observed value) to visually assess whether the residuals were normally distributed.
2. Plots of fitted values versus the residuals to identify heteroscedasticity.
3. Plots of IVs and residuals to determine whether there are trends in the data that suggest that it would be appropriate to transform IVs before modeling them.
4. Plots of residuals versus leverage with overlaid contour plots of Cook's distance to identify and characterize the effect of any outliers. Leverage measures the distance between an observation and the mean value of the remaining observations; in essence, it measures the unusualness of the observation. Cook's distance is a measure of the influence of an observation in changing the slope of the regression line.
5. The histogram of the random effect to identify whether the random intercept was roughly normally distributed and that no individual subject exhibits patterns distinctly different from the rest.

2.5 Model interpretation

The *F*-statistic and its corresponding *p*, along with the adjusted R^2 are reported for each model. Furthermore, the ICC is reported for the LMMs. Since all the DVs were transformed before modeling, the MLRs and LMMs, in effect, modeled DVs that have non-linear relationships with the IVs. Therefore, instead of reporting the regression table, we plot the effects of all IVs (with 95% confidence intervals, CI) against the suitably transformed DVs for ease of interpretation. Where the effect of an IV is significant, the corresponding *p* is reported on the plot. For these plots, the IVs were varied between the 5th to 95th percentile ranges of values, as estimated from the corresponding dataset, while all other independent variables were held constant at their corresponding median levels.

3. Results

Statistical models were independently developed on both datasets to explain the variation observed in three mHRV features: SDNN, RMSSD, and SampEn. All models developed were significantly better ($p < 0.001$) at explaining this variation than a model consisting of only a constant term. Concerning *Dataset 1*, fetal CHD was initially added as a categorical IV but had no significant or discernable effect on the DVs. Subsequently, fetal CHD was removed as an IV and no further distinction was made between participants with fetal CHD and those without. For the models based on *Dataset 2*, adding REs to the FEs significantly improved the model for all DVs ($p < 0.001$). Table 4 details the *F*-statistic and adjusted R^2 for models based on both datasets, as well as the ICC for models based on *Dataset 2*. Graphs showing that the models comply with the appropriate statistical assumptions required for regression modeling can be found in Appendix A. For the MLR developed for SDNN, based on *Dataset 1*, two observations were found to have an undue level of influence in changing the slope of the regression line (as assessed with Cook's distance). These two observations were removed for the development of this specific model, resulting in a total of 288 observations being included.

Table 4: The statistics for both the MLR and LLM models, which incorporate FEs and FEs + REs, respectively. The *F*-statistic, R^2(adjusted), and, where applicable, ICC are reported for each DV in both datasets.

	DV	MLRs: Fes		LMMs: FEs + REs		ICC
		F-statistic	R^2(adjusted)	*F*-statistic	R^2(adjusted)	
Dataset 1	SDNN	39.1 ($p < 0.001$)	0.44			
	RMSSD	58.8 ($p < 0.001$)	0.55			
	SampEn	29.2 ($p < 0.001$)	0.37			
Dataset 2	SDNN	20.1 ($p < 0.001$)	0.33	8.6	0.65	0.48
	RMSSD	53.5 ($p < 0.001$)	0.58	75.1	0.87	0.68
	SampEn	28.3 ($p < 0.001$)	0.42	30.2	0.59	0.28

DV = dependent variable; MLR = multiple linear regression model; LMM = linear mixed-effects model; FE = fixed effect; RE = random effect; ICC = intra-class correlation

In both datasets, RMSSD is the HRV feature for which the variance is best explained by the IVs. It is also the DV most affected by inter-subject variability as assessed by the ratio of the variance of the random intercept to the total variance (ICC = 0.68). In the models for SDNN and SampEn, about 50% and 30% of the total variance is attributable to the variance of the random intercepts, respectively. When comparing the models with only FEs for both datasets, one noticeable difference is a higher adjusted R^2 and *F*-statistic for the SDNN in *Dataset 1* compared to *Dataset 2*. The remaining statistics are comparable between datasets.

The individual effects of all IVs are characterized in Figures 1 and 2 for *Dataset 1* and *Dataset 2*, respectively. For *Dataset 2*, the results of the LMM are plotted as this is the more appropriate model for the dataset. (The results of the MLR for *Dataset 2* are visualized in Figure S6 in Appendix B). Notice that for both datasets, SDNN and RMSSD are dominantly influenced by median HR, with a decrease in HR corresponding to increased variability. In both figures, a significant negative relationship between SDNN and the median BR can also be seen. RMSSD is also further negatively influenced by age in *Dataset 1* (Figure 1), while Figure 2 shows that RMSSD also decreases with advancing GA.

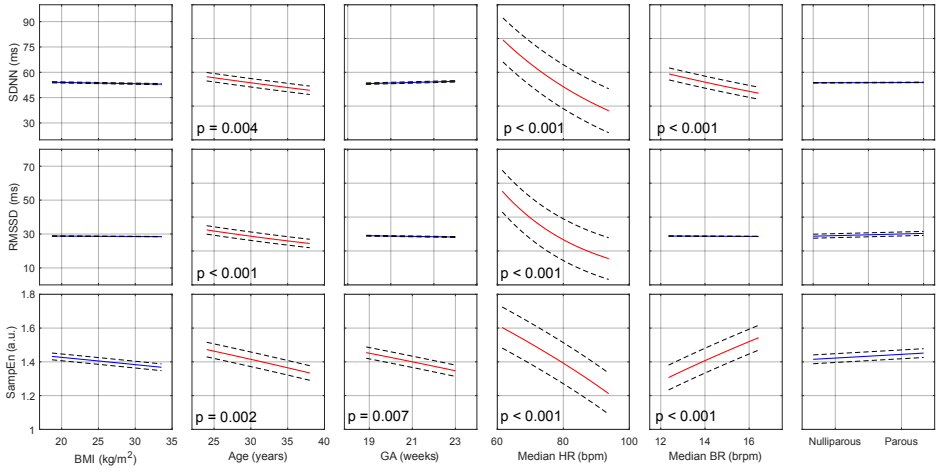

Figure 1: Individual regression plots showing the relationship between individual IVs (from left to right: BMI, Age, GA, Median HR, Median BR, and parity) and the three DVs (from top to bottom: SDNN, RMSSD, and SampEn) of the MLR developed for *Dataset 1*.

Concerning SampEn, in both cases, this feature is influenced by a multitude of factors. Similar to SDNN and RMSSD, it is affected by the median HR, although this effect is not as dominant as for the time-domain features. SampEn is also comparably influenced by median BR. Furthermore, SampEn decreases with GA. Interestingly, this is not only seen over the long-term progression of pregnancy (*Dataset 2*, Figure 2) but even within the 18 to 24-week window of *Dataset 1* (Figure 1). Lastly, BMI and parity have no significant effect on any of the DVs in either dataset.

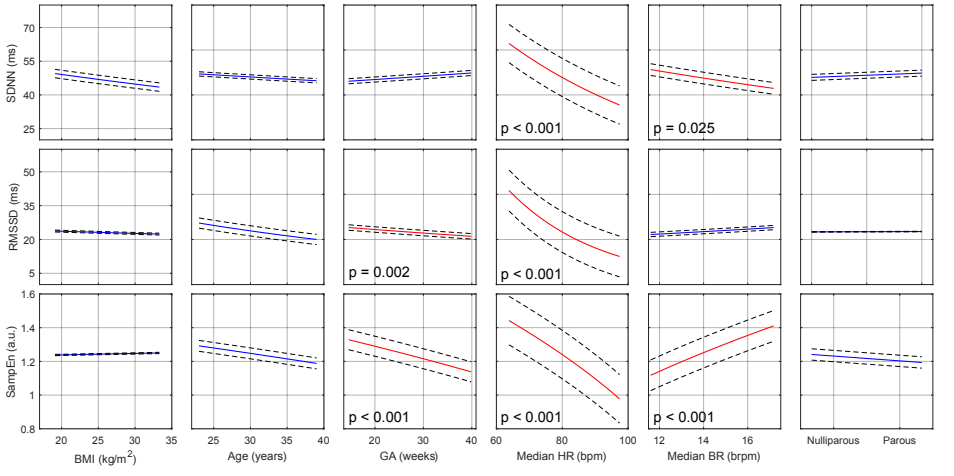

Figure 2: Individual regression plots showing the relationship between individual IVs (from left to right: BMI, Age, GA, Median HR, Median BR, and parity) and the three DVs (from top to bottom: SDNN, RMSSD, and SampEn) of the LMM developed for *Dataset 2*.

4. Discussion

In this study, we use statistical modeling to unravel the effects of maternal demographics and cardiorespiratory factors on mHRV. Owing to the association between pregnancy complications and maternal autonomic dysfunction, there is increasing interest in the possibility of using mHRV as a screening tool for maternal health [13], [14]. Therefore, it is important to establish the factors influencing mHRV in healthy pregnancies. Overall, our results suggest that we should reject the null hypothesis that median HR, median BR, age, and GA do not affect mHRV. At the same time, there is no evidence to support that BMI and parity affect mHRV.

We performed our analyses with two datasets. First, we developed an MLR using a relatively large dataset (n=290) with a single measurement per participant to characterize the effects of our host of DVs (age, BMI, GA, parity, median HR, and median BR) on selected mHRV features (SDNN, RMSSD, and SampEn). Thereafter, based on a dataset of 29 women with a median of eight measurements taken over pregnancy, we developed an LMM to further quantify the contribution of inter-subject variability on mHRV features. To our knowledge, this is the first analysis of this nature performed in a pregnant population.

The most consequential finding is the large contribution of inter-subject variability. Not only does incorporating REs significantly improve the models for *Dataset 2* compared to models with only FEs ($p < 0.001$), but also all models have large ICC values (Table 4). For SDNN and SampEn, about half and one-third of the overall explained variation is attributable to inter-subject variability, respectively; for RMSSD, this number is over two-thirds.

Further adding to the complexity of interpreting mHRV is that it changes significantly with GA. This is evident not only from our results for RMSSD and SampEn in Figure 2 but also from previous research reported in the literature [6], [34]. These results suggest that if mHRV is used for screening purposes, the focus should be on longitudinal trends rather than absolute comparisons, with each mother serving as her own baseline. It is already possible to implement such personalized monitoring since a plethora of wearable HR monitors is available that could longitudinally and unobtrusively track trends in mHRV throughout pregnancy. Furthermore, researchers have already shown high compliance with wrist-worn monitoring of maternal HR during pregnancy [35].

It is interesting to note the strong, negative relationship between SampEn and GA. This reduction in complexity with progressing pregnancy is seen both over the span of 16 to 41 weeks of gestation (*Dataset 2*, Figure 2) as well as over the narrower range of 18 to 24 weeks (*Dataset 1*, Figure 1). This downward trend in HR complexity has been previously reported as well [36]. In contrast, the effect of GA on RMSSD is less pronounced between 16 to 41 weeks of gestation (*Dataset 2*, Figure 2) and not present over the shorter range (*Dataset 1*, Figure 1), even though maternal parasympathetic activity is known to decrease during gestation [6], [34], [37]. These results suggest that complexity features such as SampEn may be more sensitive to the autonomic changes occurring within gestation than traditional time domain HRV features.

Furthermore, we also observe a significant decrease in all mHRV features with increasing age for *Dataset 1* (Figure 1). These relationships are not evident in Figure 2 (*Dataset 2*); however, for RMSSD the age-related effect is likely captured in the inter-subject variation. In the MLR for *Dataset 2* (Figure S6, Appendix B), a significant relationship between RMSSD and age can be observed. For SDNN and SampEn, the lack of evident relationship could be owing to the smaller sample size in *Dataset 2* (n=290 vs n=29). Researchers have previously found reduced SDNN in older populations[20]. Similarly, vagal activity is also known to decrease with age. Although this reduction is typically

more pronounced later in life, some studies have found a decrease within the age range of childbearing women [19], [20]. SampEn, on the other hand, has been less frequently studied in relation to age. A small study found that complexity indeed decreases with age, but offers no information on the possible physiological mechanisms responsible for this change [38]. Reduced SampEn may reflect a less adaptive autonomic system in older women. While it should be noted that women in this study are within a fairly narrow age range (18 to 45 years), significant decreases in other HRV features have been observed between these decades of age [19], [20].

The final two demographics (BMI and parity) did not have a significant effect on mHRV features in our study. Literature on whether HRV is linked to BMI is contradictory. While the majority of studies have found a higher BMI to be associated with reduced HRV in non-pregnant participants [18], [19], others observed the opposite [39]. Parity, which refers to the number of times a woman has previously given birth to a fetus with a gestational age of 24 weeks or more, has been shown to affect hemodynamic parameters [40]. Pregnancy necessitates unique maternal cardiovascular changes. Subsequently, researchers theorize that maternal physiology may adapt more quickly in a second pregnancy, given that gestational cardiovascular needs have previously been encountered. However, we found that parity does not affect mHRV. Parity was denoted as a binary categorical variable in our analysis (i.e., nulliparous or parous). Incorporating parity as a numerical variable in the models showed similar results, though it should be noted that the number of women with a parity over one was limited. In their assessment of mHRV in the frequency domain, Al-Shadei et al. also observed no changes in mHRV in relation to BMI and parity [21].

Finally, cardiorespiratory factors dominantly affect mHRV. SDNN and RMSSD seem to be the most strongly influenced by median HR (Figures 1 and 2), with a higher HR associated with lower variability. SampEn is affected by both median BR and median HR. The relationship between HRV features and HR is well-established in the literature [16], [41]. This relationship, along with the fact that baseline HR differs greatly between participants [39] and will increase with healthily progressing pregnancy[42], further supports the case for individualized, long-term mHRV analysis.

A major strength of our analysis is the size of the datasets used to develop the models. *Dataset 1*, which contains maternal ECG measurements for 290 women, is one of the largest maternal datasets in the obstetric literature. This dataset enabled us to establish the statistical significance of factors influencing mHRV. Moreover, to our

knowledge, *Dataset 2* contains the highest number of repeated maternal ECG measurements during pregnancy that has been reported in the literature. This allowed for a unique opportunity to establish the effect of inter-subject variability on mHRV.

Still, our study has some limitations. Even by accounting for inter-subject variability, 13% to 41% of the variation observed in the mHRV features could not be explained. Future studies should aim to incorporate further demographics and measurements, such as blood pressure and fitness level. Lastly, owing to a lack of standardized measures of respiration in our measurements, we estimated the median BR from participants' tachograms using EMD. Although this method gives an estimation of BR which aligns with the ranges expected in a healthy pregnant population [42], it remains an estimation. We recommend that future studies incorporate direct respiration measurements to verify our results.

In conclusion, if mHRV measurements were to be used as a screening tool for high-risk pregnancies, then age, median HR, median BR, and GA should be controlled for. Furthermore, owing to the large contribution of inter-subject variability to mHRV, assessments of mHRV should be personalized to each woman. Consequently, we would recommend the long-term tracking of trends in mHRV over periodic assessments that are compared against predefined, normative mHRV ranges.

Appendix A

In the following figures, we show exemplary examples of model diagnostics corresponding to the model of SDNN, based on *Dataset 1*, as well as the distribution of the REs of the model for SDNN, based on *Dataset 2*. Based on the initial diagnostics of the models for SDNN, two outlier values were identified and removed. The figures reported below are representative of the models after the removal of these outliers.

1. Normal probability plot

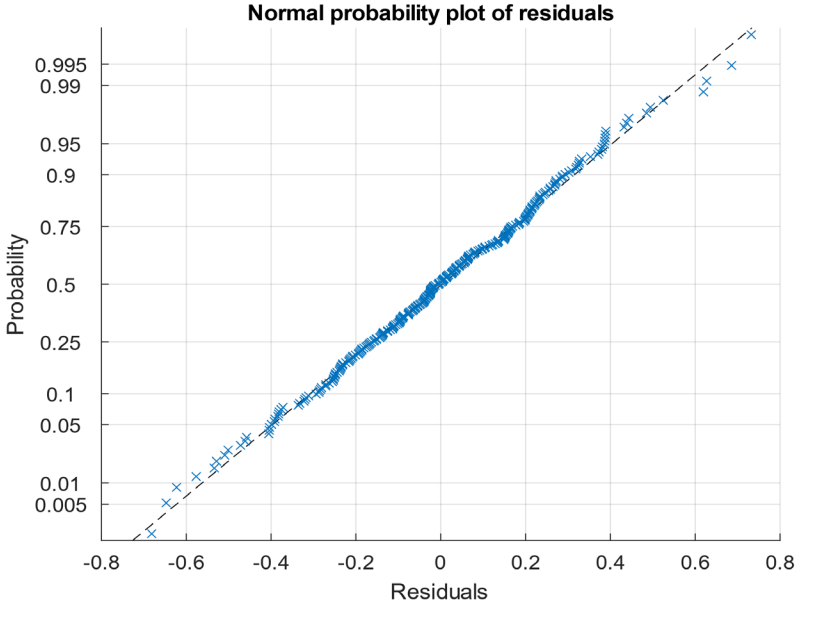

Figure 3: The normal probability plot of the residuals of the MLR model developed for SDNN, based on *Dataset 1*.

Other than the few outliers in the tails, the largely diagonal distribution of the residuals indicates that the distribution of residuals was overall normally distributed.

2. The fitted values versus the residuals

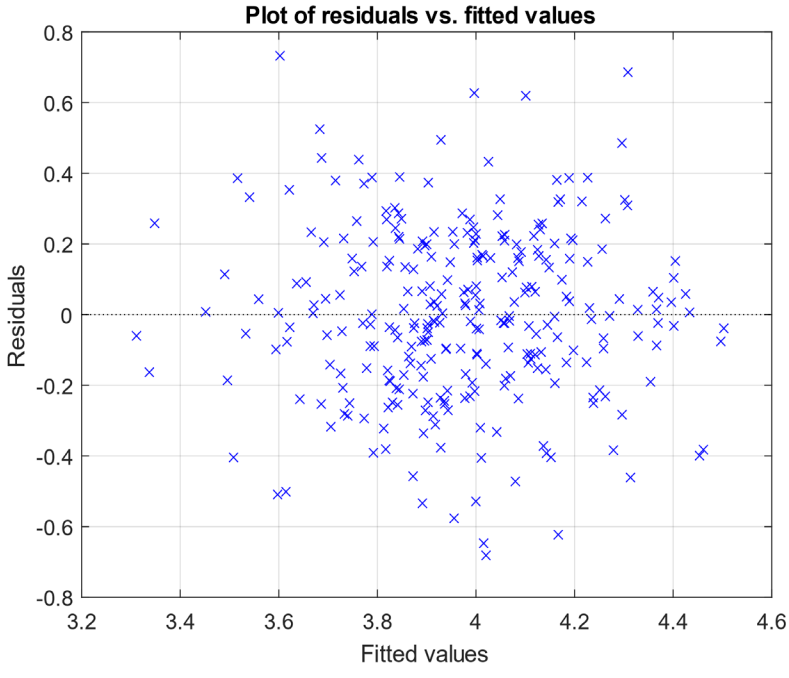

Figure 4: The residuals vs. the fitted values of the MLR model developed for SDNN, based on *Dataset 1*.

The residuals appear to be randomly distributed around the fitted values and have no predictive value, suggesting that the model is sufficiently homoscedastic.

3. The plot of BMI (an IV) versus the residuals.

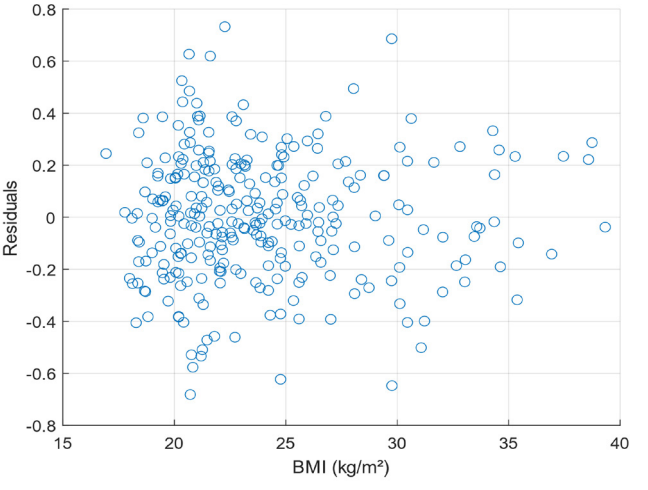

Figure 5: BMI (an IV) vs. the residuals of the MLR model developed for SDNN, based on *Dataset 1*.

There are no trends in the data, therefore there is no need to transform the IV prior to the model development.

4. A plot of the residuals versus the leverage with overlaid Cook's distance.

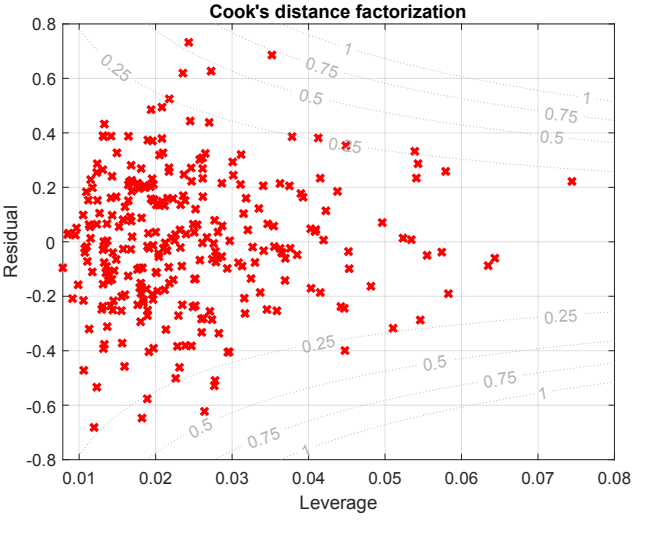

Figure 6: The leverage vs. the residuals of the MLR model developed for SDNN, based on *Dataset 1*, with overlaid contours of Cook's distance.

By assessing Cook's distance, we see that all observations fall within a Cook's distance of less than one (which serves as a rule of thumb). Furthermore, all observations have relatively low leverage values. Subsequently, there are no notable outliers.

5. Histogram of the REs

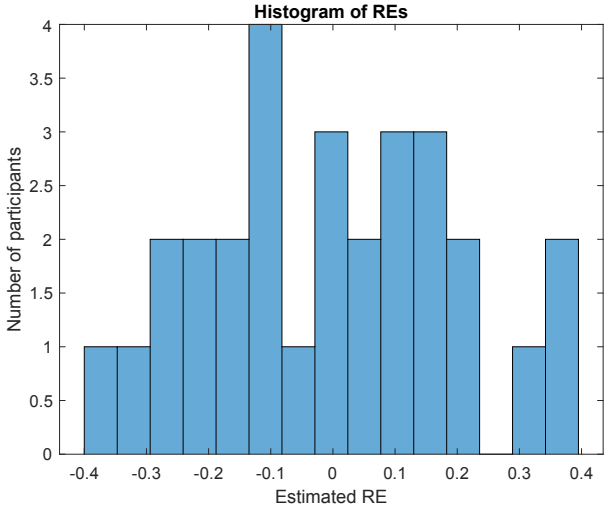

Figure 7: The distribution of the REs for the LMM model developed for SDNN, based on *Dataset 2*.

The REs appear to be approximately normally distributed.

Appendix B

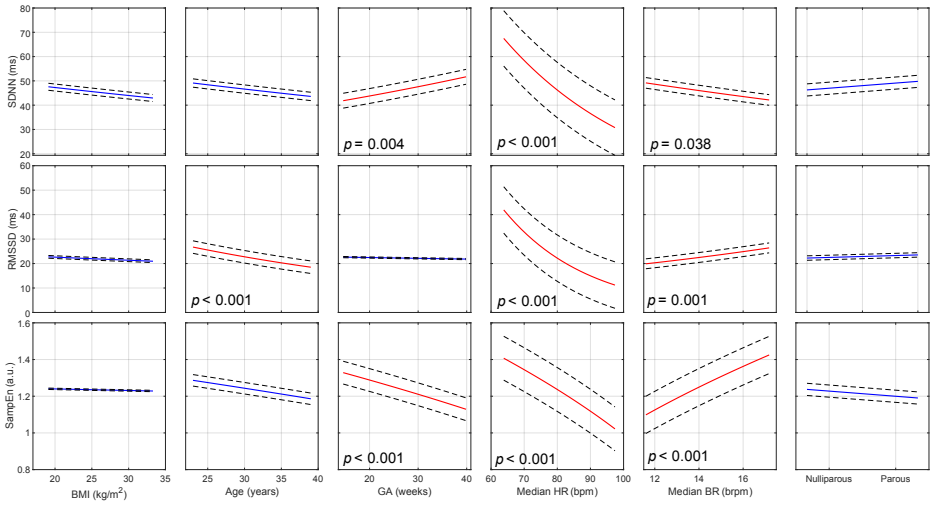

Figure 8: Individual regression plots showing the relationship between individual IVs (from left to right: BMI, Age, GA, Median HR, Median BR, and parity) and the three DVs (from top to bottom: SDNN, RMSSD, and SampEn) of the MLR for *Dataset 2*.

References

[1] U. Rajendra Acharya, K. Paul Joseph, N. Kannathal, C. M. Lim, and J. S. Suri, "Heart rate variability: a review," *Med Bio Eng Comput*, vol. 44, no. 12, pp. 1031–1051, Dec. 2006, doi: 10.1007/s11517-006-0119-0.

[2] A. M. Ponsiglione, C. Cosentino, G. Cesarelli, F. Amato, and M. Romano, "A Comprehensive Review of Techniques for Processing and Analyzing Fetal Heart Rate Signals," *Sensors*, vol. 21, no. 18, p. 6136, Sep. 2021, doi: 10.3390/s21186136.

[3] S. Ahmad *et al.*, "Continuous Multi-Parameter Heart Rate Variability Analysis Heralds Onset of Sepsis in Adults," *PLoS ONE*, vol. 4, no. 8, p. e6642, Aug. 2009, doi: 10.1371/journal.pone.0006642.

[4] T. Mishra *et al.*, "Pre-symptomatic detection of COVID-19 from smartwatch data," *Nat Biomed Eng*, vol. 4, no. 12, pp. 1208–1220, Dec. 2020, doi: 10.1038/s41551-020-00640-6.

[5] C. Eick *et al.*, "Autonomic Nervous System Activity as Risk Predictor in the Medical Emergency Department: A Prospective Cohort Study," *Critical Care Medicine*, vol. 43, no. 5, pp. 1079–1086, May 2015, doi: 10.1097/CCM.0000000000000922.

[6] P. Garg, K. Yadav, A. K. Jaryal, G. Kachhawa, A. Kriplani, and K. K. Deepak, "Sequential analysis of heart rate variability, blood pressure variability and baroreflex sensitivity in

healthy pregnancy," *Clin Auton Res*, Jan. 2020, doi: 10.1007/s10286-020-00667-4.

[7] S. Moors *et al.*, "Heart rate variability in hypertensive pregnancy disorders: a systematic review," *Pregnancy Hypertension*, Mar. 2020, doi: 10.1016/j.preghy.2020.03.003.

[8] A. C. De Kat, J. Hirst, M. Woodward, S. Kennedy, and S. A. Peters, "Prediction models for preeclampsia: A systematic review," *Pregnancy Hypertension*, vol. 16, pp. 48–66, Apr. 2019, doi: 10.1016/j.preghy.2019.03.005.

[9] D. Yousif *et al.*, "Autonomic Dysfunction in Preeclampsia: A Systematic Review," *Front. Neurol.*, vol. 10, Aug. 2019, doi: 10.3389/fneur.2019.00816.

[10] E. Eneroth-Grimfors, M. Westgren, M. Ericson, C. Ihrman-Sandahl, and L. E. Lindblad, "Autonomic cardiovascular control in normal and pre-eclamptic pregnancy," *Acta Obstet Gynecol Scand*, vol. 73, no. 9, pp. 680–684, Jan. 1994, doi: 10.3109/00016349409029402.

[11] S. V. Khlybova, V. I. Tsirkin, S. A. Dvoryanskii, I. A. Makarova, and A. N. Trukhin, "Heart rate variability in normal and complicated pregnancies," *Hum Physiol*, vol. 34, no. 5, pp. 625–632, Sep. 2008, doi: 10.1134/S0362119708050113.

[12] D. Casati *et al.*, "Maternal cardiac deceleration capacity: a novel insight into maternal autonomic function in pregnancies complicated by hypertensive disorders and intra-uterine growth restriction," *European Journal of Obstetrics & Gynecology and Reproductive Biology*, vol. 206, pp. 6–11, Nov. 2016, doi: 10.1016/j.ejogrb.2016.08.007.

[13] G. K. Pal, P. Shyma, S. Habeebullah, P. Shyjus, and P. Pal, "Spectral Analysis of Heart Rate Variability for Early Prediction of Pregnancy-Induced Hypertension," *Clinical and Experimental Hypertension*, vol. 31, no. 4, pp. 330–341, Jan. 2009, doi: 10.1080/10641960802621333.

[14] S. Rang, H. Wolf, G. A. Montfrans, and J. M. Karemaker, "Non–invasive assessment of autonomic cardiovascular control in normal human pregnancy and pregnancy- associated hypertensive disorders: a review," *Journal of Hypertension*, vol. 20, no. 11, pp. 2111–2119, 2002.

[15] F. Shaffer and J. P. Ginsberg, "An Overview of Heart Rate Variability Metrics and Norms," *Front. Public Health*, vol. 5, p. 258, Sep. 2017, doi: 10.3389/fpubh.2017.00258.

[16] E. J. C. de Geus, P. J. Gianaros, R. C. Brindle, J. R. Jennings, and G. G. Berntson, "Should heart rate variability be 'corrected' for heart rate? Biological, quantitative, and interpretive considerations: XXXX," *Psychophysiology*, vol. 56, no. 2, p. e13287, Feb. 2019, doi: 10.1111/psyp.13287.

[17] B. Aysin and E. Aysin, "Effect of Respiration in Heart Rate Variability (HRV) Analysis," in *2006 International Conference of the IEEE Engineering in Medicine and Biology Society*, New York, NY: IEEE, Aug. 2006, pp. 1776–1779. doi: 10.1109/IEMBS.2006.260773.

[18] A. Molfino, A. Fiorentini, L. Tubani, M. Martuscelli, F. R. Fanelli, and A. Laviano, "Body mass index is related to autonomic nervous system activity as measured by heart rate variability," *Eur J Clin Nutr*, vol. 63, no. 10, pp. 1263–1265, Oct. 2009, doi: 10.1038/ejcn.2009.35.

[19] M. Vallejo, M. F. Márquez, V. H. Borja-Aburto, M. Cárdenas, and A. G. Hermosillo, "Age, body mass index, and menstrual cycle influence young women's heart rate variability: A multivariable analysis," *Clin Auton Res*, vol. 15, no. 4, pp. 292–298, Aug. 2005, doi: 10.1007/s10286-005-0272-9.

[20] J. Zhang, "Effect of Age and Sex on Heart Rate Variability in Healthy Subjects," *Journal of Manipulative and Physiological Therapeutics*, vol. 30, no. 5, pp. 374–379, Jun. 2007, doi: 10.1016/j.jmpt.2007.04.001.

[21] A. I. Al-Shafei, S. M. Musa, D. A. Rayis, M. F. Lutfi, O. A. El-Gendy, and I. Adam, "Heart rate variability and hematological parameters in pregnant women," *J Clin Lab Anal*, vol. 34, no. 6, Jun. 2020, doi: 10.1002/jcla.23250.

[22] M. Bester, R. Joshi, M. Mischi, J. O. E. H. van Laar, and R. Vullings, "Longitudinally Tracking Maternal Autonomic Modulation During Normal Pregnancy With Comprehensive Heart Rate Variability Analyses," *Front. Physiol.*, vol. 13, p. 874684, May 2022, doi: 10.3389/fphys.2022.874684.

[23] K. M. J. Verdurmen *et al.*, "Normal ranges for fetal electrocardiogram values for the healthy fetus of 18–24 weeks of gestation: a prospective cohort study," *BMC Pregnancy and Childbirth*, p. 7, 2016.

[24] J. O. E. H. van Laar *et al.*, "Fetal heart rate variability during pregnancy, obtained from non-invasive electrocardiogram recordings," *Acta Obstet Gynecol Scand*, vol. 93, no. 1, pp. 93–101, Jan. 2014, doi: 10.1111/aogs.12286.

[25] M. J. Rooijakkers *et al.*, "Influence of Electrode Placement on Signal Quality for Ambulatory Pregnancy Monitoring," *Computational and Mathematical Methods in Medicine*, vol. 2014, pp. 1–12, 2014, doi: 10.1155/2014/960980.

[26] M. J. Rooijakkers, C. Rabotti, M. Bennebroek, J. van Meerbergen, and M. Mischi, "Low-complexity R-peak detection in ECG signals: A preliminary step towards ambulatory fetal monitoring," in *2011 Annual International Conference of the IEEE Engineering in Medicine and Biology Society*, Boston, MA: IEEE, Aug. 2011, pp. 1761–1764. doi: 10.1109/IEMBS.2011.6090503.

[27] C. Peters, R. Vullings, J. Bergmans, G. Oei, and P. Wijn, "The effect of artifact correction on spectral estimates of heart rate variability," in *2008 30th Annual International Conference of the IEEE Engineering in Medicine and Biology Society*, Vancouver, BC: IEEE, Aug. 2008, pp. 2669–2672. doi: 10.1109/IEMBS.2008.4649751.

[28] C. H. L. Peters, R. Vullings, M. J. Rooijakkers, J. W. M. Bergmans, S. G. Oei, and P. F. F. Wijn, "A continuous wavelet transform-based method for time-frequency analysis of artefact-corrected heart rate variability data," *Physiol. Meas.*, vol. 32, no. 10, pp. 1517–1527, Oct. 2011, doi: 10.1088/0967-3334/32/10/001.

[29] L. M. Campana, R. L. Owens, G. D. Clifford, S. D. Pittman, and A. Malhotra, "Phase-rectified signal averaging as a sensitive index of autonomic changes with aging," *Journal of Applied Physiology*, vol. 108, no. 6, pp. 1668–1673, Jun. 2010, doi: 10.1152/japplphysiol.00013.2010.

[30] A. Quinn, V. Lopes-dos-Santos, D. Dupret, A. Nobre, and M. Woolrich, "EMD: Empirical Mode Decomposition and Hilbert-Huang Spectral Analyses in Python," *JOSS*, vol. 6, no. 59, p. 2977, Mar. 2021, doi: 10.21105/joss.02977.

[31] R. Balocchi *et al.*, "Deriving the respiratory sinus arrhythmia from the heartbeat time series using empirical mode decomposition," *Chaos, Solitons & Fractals*, vol. 20, no. 1, pp. 171–177, Apr. 2004, doi: 10.1016/S0960-0779(03)00441-7.

[32] P. Gomes, P. Margaritoff, and H. Silva, "pyHRV: Development and Evaluation of an Open-Source Python Toolbox for Heart Rate Variability (HRV)," presented at the IcETRAN, 2019, pp. 882–887.

[33] R. Joshi *et al.*, "Statistical Modeling of Heart Rate Variability to Unravel the Factors Affecting Autonomic Regulation in Preterm Infants," *Sci Rep*, vol. 9, no. 1, p. 7691, Dec. 2019, doi: 10.1038/s41598-019-44209-z.

[34] M. Balajewicz-Nowak, A. Furgala, K. Pitynski, P. Thor, H. Huras, and K. Rytlewski, "The dynamics of autonomic nervous system activity and hemodynamic changes in pregnant women," *Neuro Endocrinol Lett*, vol. 37, no. 1, pp. 70–77, 2016.

[35] K. Grym *et al.*, "Feasibility of smart wristbands for continuous monitoring during pregnancy and one month after birth," *BMC Pregnancy Childbirth*, vol. 19, no. 1, p. 34, Dec. 2019, doi: 10.1186/s12884-019-2187-9.

[36] M. Baumert, M. Javorka, A. Seeck, R. Faber, P. Sanders, and A. Voss, "Multiscale entropy and detrended fluctuation analysis of QT interval and heart rate variability during normal pregnancy," *Computers in Biology and Medicine*, vol. 42, no. 3, pp. 347–352, Mar. 2012, doi: 10.1016/j.compbiomed.2011.03.019.

[37] V. L. Brooks, Q. Fu, Z. Shi, and C. M. Heesch, "Adaptations in autonomic nervous system regulation in normal and hypertensive pregnancy," in *Handbook of Clinical Neurology*, Elsevier, 2020, pp. 57–84. doi: 10.1016/B978-0-444-64239-4.00003-5.

[38] R. Goya-Esteban, J. P. Marques de Sa, J. L. Rojo-Alvarez, and O. Barquero-Perez, "Characterization of Heart Rate Variability loss with aging and heart failure using Sample Entropy," in *2008 Computers in Cardiology*, Bologna, Italy: IEEE, Sep. 2008, pp. 41–44. doi: 10.1109/CIC.2008.4748972.

[39] G. Quer, P. Gouda, M. Galarnyk, E. J. Topol, and S. R. Steinhubl, "Inter- and intraindividual variability in daily resting heart rate and its associations with age, sex, sleep, BMI, and time of year: Retrospective, longitudinal cohort study of 92,457 adults," *PLoS ONE*, vol. 15, no. 2, p. e0227709, Feb. 2020, doi: 10.1371/journal.pone.0227709.

[40] S. Turan *et al.*, "Computerized fetal heart rate analysis, Doppler ultrasound and biophysical profile score in the prediction of acid-base status of growth-restricted fetuses," *Ultrasound Obstet Gynecol*, vol. 30, no. 5, pp. 750–756, Aug. 2007, doi: 10.1002/uog.4101.

[41] J. Bolea, E. Pueyo, M. Orini, and R. Bailón, "Influence of Heart Rate in Non-linear HRV Indices as a Sampling Rate Effect Evaluated on Supine and Standing," *Front. Physiol.*, vol. 7, p. 501, Nov. 2016, doi: 10.3389/fphys.2016.00501.

[42] L. J. Green *et al.*, "Gestation-Specific Vital Sign Reference Ranges in Pregnancy," *Obstetrics & Gynecology*, vol. 135, no. 3, pp. 653–664, Mar. 2020, doi: 10.1097/AOG.0000000000003721.

Section III

The effect of corticosteroids on maternal autonomic regulation in complicated pregnancies

Chapter 6

Changes in maternal heart rate and autonomic regulation following the antenatal administration of corticosteroids: a secondary analysis

6

Reproduced after: M Bester, R Joshi, JHAM van Dooren, M Mischi, R Vullings, JOEH van Laar. Changes in Maternal Heart Rate and Autonomic Regulation following the Antenatal Administration of Corticosteroids: A Secondary Analysis. *Journal of Clinical Medicine*. 2023.

Abstract

While the effect of antenatally administered corticosteroids on fetal heart rate (HR) and heart rate variability (HRV) is well established, little information is available on how these drugs affect maternal physiology. In this secondary analysis of a prospective, observational study, we quantify how corticosteroids affect maternal HR and HRV, which serves as a proxy measure for autonomic regulation. Abdominal ECG measurements were recorded before and in the five days following the administration of betamethasone – a corticosteroid commonly used for fetal maturation – in 46 women with singleton pregnancies. Maternal HR and HRV were determined from these recordings and compared between these days. HRV was assessed with time- and frequency-domain features, as well as non-linear and complexity features. In the 24 hours after betamethasone administration, maternal HR was significantly increased ($p < 0.01$) by approximately 10 beats per minute while HRV features linked to parasympathetic activity and HR complexity were significantly decreased ($p < 0.01$ and $p < 0.001$, respectively). The effects of betamethasone typically diminished within four days after initial administration. We conclude that betamethasone administration results in changes in maternal HR and HRV despite the heterogeneity of the studied population. Therefore, its recent administration should be considered when evaluating these cardiovascular metrics.

1. Introduction

The use of antenatally administered corticosteroids has had a profound impact on the survival rates and outcomes of prematurely born neonates [1], [2]. Therefore, their administration in cases of anticipated preterm birth or cesarean section is standard clinical practice. Still, many uncertainties remain regarding the perinatal use of corticosteroids. These uncertainties have been widely investigated and debated in the literature, such as the prudence and timing of administering a second course, as well as the impact of in-utero exposure to synthetic corticosteroids on the child in the long term [3]. However, a potential effect that is rarely investigated or addressed is the influence of these maternally administered corticosteroids on the cardiac and autonomic nervous systems (ANS) of the mother [4], [5].

Research suggests that glucocorticoids, the class of steroids to which corticosteroids belong [6], may act as a sympathetic cardiovascular stimulus that influences heart rate (HR) [7]. Changes in maternal vital signs inform clinicians of the mother's well-being and consequently play a role in clinical decision-making [8], [9]. Therefore, quantifying the potential effect of corticosteroids on maternal HR is necessary.

Additionally, since pregnancy is accompanied by substantial changes in the maternal cardiovascular and ANS, drugs administered during pregnancy that might affect these systems need to be carefully studied [10]. Further compounding this need is the fact that many women who receive corticosteroids also have pregnancy complications such as hypertensive disorders of pregnancy. These complications not only alter maternal cardiac and autonomic function but also increase the long-term risk for cardiovascular diseases [11], [12]. Subsequently, it is important to investigate whether administering these synthetic corticosteroids – which incidentally also increases the risk of cardiovascular disease with long-term use [7] – further alters maternal autonomic regulation.

Understanding how administering corticosteroids alters maternal autonomic regulation is not only physiologically important but also clinically relevant. Owing to the association between maternal autonomic dysfunction and pregnancy complications [10], [13], there is increasing interest in using maternal heart rate variability (HRV) – a proxy measure for the ANS [14] – as an obstetric screening tool [15]–[17]. However, using HRV to track maternal health, as well as appropriately interpreting HRV in women who've received corticosteroids, requires quantifying the potential effect of this routinely administered medication on maternal HRV [11], [18].

Subsequently, in this study, we investigate the effects of betamethasone – the most used corticosteroid in the antenatal period – on the maternal system. The objectives of our analysis are twofold. First, we investigate whether antenatally administering betamethasone alters maternal HR in a clinically relevant manner. Second, we determine whether receiving this drug results in altered maternal autonomic regulation, as assessed via HRV.

2. Methods

We perform a secondary analysis of a dataset of abdominal ECG measurements collected during a longitudinal cohort study (March 2013 to July 2016) at the Máxima Medical Centre (Máxima MC), a tertiary care teaching hospital in Veldhoven, the Netherlands. The primary purpose of the data collection was to quantify the effect of betamethasone on fetal HRV; results from this analysis were previously published [19], [20]. The original study was approved by the institutional review board at Máxima MC in Veldhoven, the Netherlands (NL43294.015.13), which granted a waiver for this secondary analysis (N21.008).

2.1. Study population

Women with singleton pregnancies who were admitted to the Obstetric High Care unit at Máxima MC with a risk for preterm delivery were recruited for this study. The aim was to include at least 50 patients. Those who received betamethasone (Celestone Chrondose®, Schering AG, Berlin, Germany; 2 doses of 12 mg intramuscularly, 24 h apart) as part of their standard clinical care were eligible to participate in the study. Co-administration of medications was allowed since this was part of the standard treatment protocol. Nifedipine was administered as a tocolytic to attenuate contractions as needed in case of threatened preterm labor, at times in conjunction with indomethacin when contractions persisted while betamethasone treatment had not yet been completed. Antibiotics (erythromycin 250 mg, 4 times daily for 10 days) were administered to patients with preterm rupture of membranes to prevent infection. Furthermore, women with preeclampsia typically received antihypertensive drugs (specifically, methyldopa or labetalol). Patients under 18 years of age were not eligible for participation. Metadata collected from participants were indications for betamethasone administration, medications administered during the study period, parity, body mass index (BMI), gestational age at inclusion, and general and obstetric medical history [19].

2.2 Measurements

Repeated abdominal ECG measurements – from which maternal HR and HRV can be determined – were performed over several days. Measurements, which were approximately 30 minutes in duration, were recorded while the patient was lying in a semi-recumbent position. Ideally, the first measurement took place before betamethasone was administered; this timestamp was defined as *day 0*. Thereafter, measurements were taken over the next five days at approximately 24 hours intervals, i.e., at 24 hours after (*day 1*), 48 hours (*day 2*), 72 hours (*day 3*), 96 hours (*day 4*), and finally 120 hours (*day 5*) after the first betamethasone injection. Each measurement was performed between 20 to 28 hours after its preceding measurement to reduce the impact of diurnal rhythms. No measurements were performed between midnight and 07h00.

2.3 Analysis

As previously noted, this study is a secondary analysis of a dataset originally collected to assess the effect of betamethasone on fetal HRV. This dataset was originally collected to compare the progressing changes in fetal HRV after the administration of betamethasone against a reference measurement. Ideally, this reference measurement would occur before the administration of betamethasone. However, Máxima MC is a tertiary care hospital to which many patients are transferred after an initial assessment at their primary care hospital. Consequently, women often have already received their first injection of betamethasone before arriving at Máxima MC. Additionally, evidence from the literature indicates that the effect of betamethasone on fetal HRV wears off within four days of the first injection [21]. Therefore, theoretically, *day 4* or *day 5* could serve as the reference measurement in lieu of *day 0* (i.e., the measurement taken before betamethasone is administered) when investigating the effect of the drug on fetal HRV. Therefore, the original protocol stipulated that measurements would be collected for five days following the first betamethasone injection [19].

However, limited information is available on the expected effect of betamethasone on maternal HRV. Therefore, we make no assumption on the duration of the effect of this drug on the maternal HRV and define no reference measurement in addition to *day 0*. Rather, we track the potentially transient effect of betamethasone on maternal HRV over the six days of measurements. We assess the overall trend in maternal HR and HRV, as well as compare, individually, between all days. Owing to the explorative nature of the analysis, we include all participants, regardless of their number of measurements.

2.4 Outcome measures

The outcomes of interest are maternal HR and maternal HRV. The latter is quantified by HRV features from the time domain and frequency domain, as well as features describing the complexity or non-linearity in the HR signal. The features used to capture HRV are detailed in Section 2.6.

2.5 Data acquisition and signal pre-processing

The multichannel abdominal ECG recordings were acquired with one of two non-invasive electrophysiological monitoring devices, namely the Nemo (Nemo Healthcare BV, Eindhoven, the Netherlands) at a sampling rate of 500 Hz and the Porti system (Twente Medical Systems International B.V., Enschede, the Netherlands) at a sampling rate of 512 Hz. A 4th order Butterworth bandpass filter of 1 to 70 Hz was applied to the recordings to suppress artifacts and out-of-band noise, followed by a notch filter at 50 Hz which suppressed powerline interference. Next, a fixed linear combination of the various abdominal channels was applied to enhance maternal QRS peaks [22] and hereafter a previously detailed peak detector was used to detect the maternal R-peaks [23], [24]. Once these peaks were detected, signals representing the RR-intervals could be generated. These signals were further pre-processed to reduce the impact of potential noise and erroneous beats. Physiologically improbable RR-intervals (shorter than 0.4 seconds or longer than 2 seconds) or those with too large a change between consequent RR-intervals (i.e., a change of more than 20%) were rejected [25]–[27]. For the calculation of HRV features that relate to the frequency domain or complexity, a continual time series is needed, and subsequently, missing RR-intervals are replaced with cubic spline interpolation when calculating these features. Recordings were excluded from the analysis if more than 10% of RR-intervals were rejected.

2.6 HR and HRV analysis

First, the HR is determined by taking the average of the RR-intervals and converting this to beats per minute (bpm). Thereafter, HRV features are calculated. Each feature is calculated over the entire recording; for the HRV features in the frequency domain, the average is taken after the features are calculated on 5-minute segments from the recording with a 50% overlap between segments. The set of time domain features comprises the standard deviation of the RR intervals (SDNN), the root mean square of the successive differences of the RR intervals (RMSSD), and the percentage of consecutive RR intervals that differ by more than 50 ms (pNN50). The latter two capture parasympathetic activity (of which the vagus nerve is the main component influencing HR), since such short-term variations are mediated by the parasympathetic nervous system, while SDNN represents the overall HRV [14].

HRV can also be assessed in the frequency domain and subsequently, we determine the following features: the power in the high-frequency band of 0.15–0.40 Hz (HF), the power in the low-frequency band of 0.04–0.15 Hz, and the ratio between the two (LF/HF). HF captures mainly parasympathetic activity while LF is influenced by both branches of the ANS (i.e., both parasympathetic and sympathetic activity). LF/HF informs on the balance between the two branches by capturing what is referred to as the sympathovagal balance [14], [28].

Additionally, we also assess the non-linearity and aspects relating to the complexity of the signal representing the RR-intervals. We use a popular geometrical method to evaluate HRV dynamics, namely a Poincaré plot, in which each RR-interval is plotted against its predecessor to form a scatter plot. An ellipse is then fitted to the plot from which two standard descriptors (SD1 and SD2) are calculated to represent the short- and long-term HRV, respectively. These are presented as a ratio (SD1/SD2) which informs on the relationship between long- and short-term variability, which – similarly to LF/HF – offers a window into sympathovagal balance [14], [29]. Furthermore, we investigate the complexity of the signal representing the RR-intervals with two methods: Sample entropy (SampEn) and detrended fluctuation analysis (DFA) [30], [31]. SampEn quantifies the conditional probability that two epochs that are similar within a tolerance r for a window length m, will remain similar when including the next data point (i.e. the next RR-interval) [31], [32]. The parameters m and r were set to 2 and 0.2 times the standard deviation of the RR-intervals [31]. Lower SampEn indicates a more regular and predictable time series [14]. Concerning DFA, this method is used to quantify the self-similarity of RR-intervals over time. In a healthy HR pattern, we expect that certain trends will repeat over different timescales; subsequently, the signal which represents the RR-intervals should be neither fully predictable nor completely random, but rather somewhere in between. To capture this characteristic, we calculate the short-term fractal scaling exponent of the DFA, namely, α_1, which represents the correlation in the RR-signal over 4–16 heartbeats [30]. A result of $\alpha_1 = 1$ suggests a high level of correlation or self-similarity. As α_1 increases, the level of correlation decreases [30], [33].

2.7 Statistical analysis

Since the data are not normally distributed, non-parametric analyses are performed. We use a Kruskal-Wallis test to ascertain whether significant changes in maternal HR and HRV occur over the six days. Furthermore, we use Dunn's post hoc test with Bonferroni correction to test for differences between the days. A value of $p < 0.05$ is

seen as significant. Results are presented as boxplots with the appropriate statistics added to the plots.

3. Results

A total of 68 women were initially enrolled. Three participants withdrew from the study, while five had no measurements available. Seven participants ultimately did not receive betamethasone and were therefore excluded. Two more women were excluded due to known cardiac arrhythmias, and two more due to delivering and being discharged immediately after inclusion, respectively. Finally, the data from three women were excluded from analysis due to them having no measurements done at the correct times with regards to the betamethasone injection, resulting in 46 women being included. Of these inclusions, 31 had measurements from the Nemo device, 13 from the Porti system, and two had measurements from both monitoring systems. The characteristics of those included can be found in Table 1.

Table 1: Patient characteristics presented as occurrence or median and interquartile range, as appropriate.

Characteristic	
Indication for betamethasone (no. of participants)	
Threatened preterm labor	18
Vaginal bleeding	9
Preterm rupture of membranes	12
Preeclampsia	2
HELLP	2
Fetal intra-uterine growth restriction	3
Gestational age at inclusion (weeks + days)	29 weeks 2 days (26 weeks – 31 weeks 2 days)
BMI	24.4 (21.9 – 29.3) kg/m^2
Nulliparous	41.3 %

For these 46 women, a total of 219 recordings were available of which 21 were rejected for having more than 10% unreliable RR-intervals. A further 15 measurements were done outside of the timeframe specified by the study protocol (i.e., within 20 – 28

hours after the previous measurement) and were consequently excluded from the analysis. Subsequently, 183 recordings are included of which there are 13 on *day 0*, 59 on *day 1*, 39 on *day 2*, 31 on *day 3*, 24 on *day 4*, and 17 on *day 5*. In some cases, women had two recordings available per day; both recordings were then incorporated. Note that the recordings for *day 1* could be either before or after the second injection of betamethasone, which is given 24 hours after the first injection. We compared these two sets of recordings (i.e., recordings done shortly before and shortly after the second betamethasone injection) and found neither apparent nor statistically significant differences between the two sets; subsequently, all these recordings were included as *day 1*.

3.1 Maternal HR

Maternal HR changes significantly ($p < 0.01$) following the administration of betamethasone (Figure 1). Compared to the pre-betamethasone measurement (*day 0*), HR is significantly increased by about 10 bpm 24 hours after the first injection and reduces significantly again on *day 3* to a similar level as pre-betamethasone administration. No further significant differences are present after *day 3*.

To confirm the increase in HR observed from pre-betamethasone administration (*day 0*) to post-administration (*day 1*), we also considered a subanalysis with only participants who had measurements on both of these days (n = 12). Correspondingly, we observed a similar increase from a median of 81.7 bpm (interquartile range: 77.8–83.5 bpm) to a median of 88.4 bpm (interquartile range: 85.0–91.8 bpm).

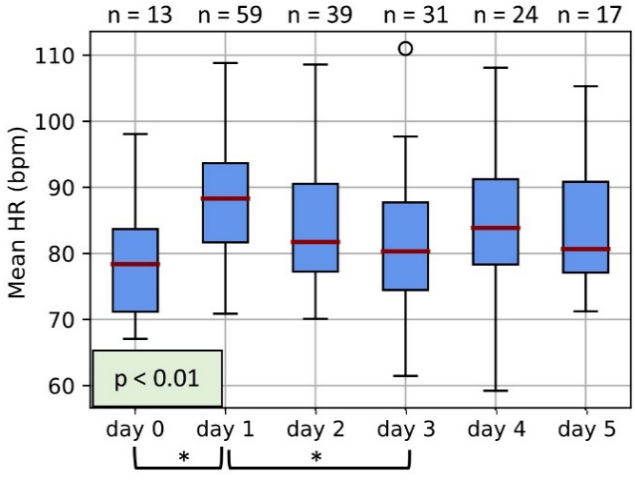

Figure 1. Boxplots of the HR of participants on *days 0* to *5*. Boxplots represent the median, interquartile range and interdecile range of the values. *Day 0* represents measurements taken before the first injection of Betamethasone, while *day 1* represents 24 hours after the first injection, *day 2* represents 48 hours after the first injection, etc. * represents a statistically significant finding with $p < 0.05$. The number of measurements incorporated in each day is displayed at the top of the graph.

3.2 Maternal HRV

Figure 2 details the changes in maternal HRV features spanning *day 0* to *day 5*. Overall, the most noticeable change in the HRV features can be observed on *day 1* in comparison to the preceding or following days. Note that all statistically significant relationships seen in Figure 2 are in comparison to *day 1*.

While no significant differences are seen in SDNN and LF, all features linked to parasympathetic activity (RMSSD, pNN50, and HF) are significantly altered ($p < 0.01$). Furthermore, all three features also show significant ($p < 0.05$) differences between both *day 0* and *day 1*, as well as between *day 1* and *day 3*.

LF/HF and SD1/SD2 (representing sympathovagal balance) change significantly over the five days ($p < 0.01$ and $p < 0.001$, respectively). Furthermore, LF/HF increases and SD1/SD2 decreases on day 1 (both signaling reduced vagal control) compared to day zero. Both thereafter revert to values similar to the pre-betamethasone period via significant changes between day 1 and days 2 and 3.

Likewise, both features that are linked to complexity (SampEn and α_1 from DFA) show significant changes ($p < 0.01$ and $p < 0.001$, respectively) over the study period. The drop in SampEn and the increase in α_1 on *day 1* indicate that there is a decrease in complexity and self-similarity following the first injection of betamethasone. SampEn increases and α_1 decreases again on *day 2* and *day 3*, with statistically significant relationships present between *day 1* and *day 2* as well as *day 1* and *day 3* ($p < 0.01$). In the case of α1, *day 4* is also significantly reduced compared to *day 1* ($p < 0.05$).

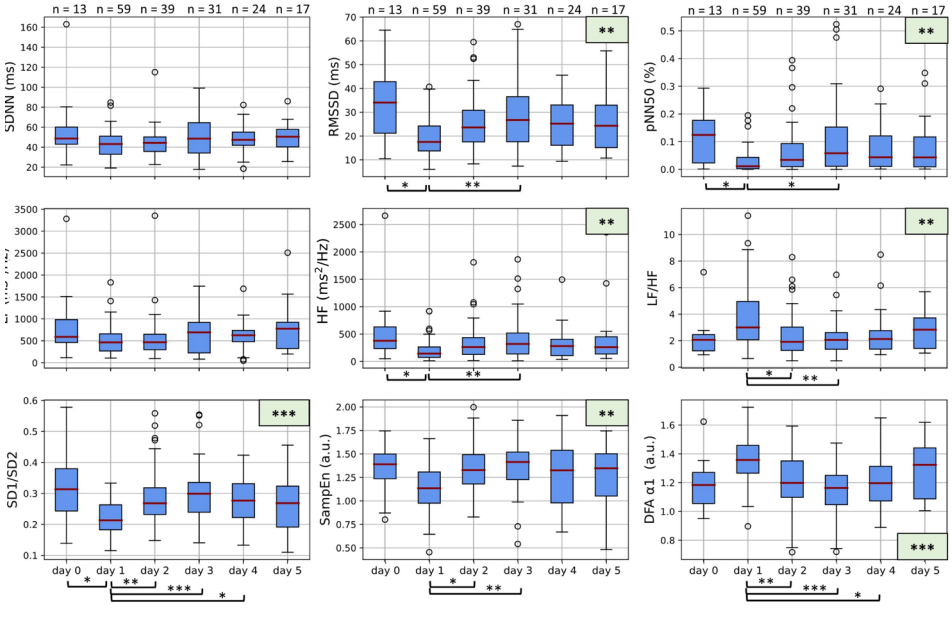

Figure 2: Boxplots of maternal HRV on *days 0* to *5*. Boxplots represent the median, interquartile range and interdecile range of the values. *Day 0* represents measurements taken before the first injection of Betamethasone, while *day 1* represents 24 hours after the first injection, *day 2* represents 48 hours after the first injection, etc. * represents a statistically significant finding with $p < 0.05$, while ** presents $p < 0.01$ and *** represents $p < 0.001$. The number of measurements incorporated in each *day* is displayed at the top of the graph.

4. Discussion

This study provides evidence that antenatally administered corticosteroids (specifically, betamethasone) significantly influence maternal physiology. Maternal HR (Figure 1) is increased by about 10 bpm within 24 hours after the first betamethasone injection before returning to levels similar to those pre-administration. Parasympa-

thetic activity (Figure 2) significantly decreases after betamethasone administration (*day 1*) before stabilizing (*day 2* or *day 3*). Features representing sympathovagal balance (i.e., LF/HF and SD1/SD2) also exhibit decreased vagal control on *day 1*, while HR complexity and self-similarity is also significantly decreased on *day 1* (Figure 2). Finally, for all features the most notable change is that on *day 1* compared to the pre-betamethasone period (*day 0*) and the two- or three-days following *day 1*. Consequently, any significant effects of betamethasone on maternal HR and HRV likely wear off by *day 3* or *day 4*.

This is the first study, to our knowledge, which addresses the effect of antenatally administered betamethasone on the maternal cardiac and ANS. A major strength is the longitudinal nature of the dataset analyzed. Assessing measurements ranging from pre-betamethasone administration to 120 hours thereafter allows for tracking the effect of corticosteroids over several days rather than merely assessing the immediate effect. This longitudinal analysis also allows us to observe when the effect of betamethasone appears to be mitigated.

Still, more nuanced effects of betamethasone are perhaps obscured by the unpaired nature of our analysis, the small number of participants, the largely unavoidable co-administration of other medications such as nifedipine, and the heterogeneity of our dataset in terms of complications, age, parity, etc. Yet, despite these limitations, we still observe large statistically significant changes in our outcome measures, increasing our confidence that betamethasone indeed affects maternal HR and HRV. Furthermore, the heterogeneity of our study group reflects the typical characteristics of the population that receives corticosteroids during pregnancy, thereby increasing the clinical relevance of these results.

Changes in the maternal heart rhythm are relevant for clinical decision-making [8], [9]. In a recent review on assessing and interpreting maternal bradycardia and tachycardia, the administration of medications such as beta-blockers is listed as a potential cause for bradycardia. However, for tachycardia (defined in the review as maternal HR > 100 bpm), no medications are considered to be potential triggers for an elevated maternal HR [8]. Yet, we find that approximately 24 hours after betamethasone administration maternal HR is elevated by about 10 bpm (Figure 1). Since this may result in perceived tachycardia in women with a high baseline HR (as is quite common during pregnancy [34]), we believe clinicians should consider whether corticosteroids had recently been administered when evaluating an elevated maternal HR.

Along with these changes to maternal HR, we observe significant changes in several HRV features (Figure 2). Significant changes in RMSSD, pNN50, and HF – as well as LF/HF and SD1/SD2 – suggest reduced parasympathetic activity after betamethasone administration (Figure 2), while the lack of change in LF suggests stable sympathetic activity (Figure 2). Furthermore, an increase in α1, as is also seen on *day 1*, is also linked to decreased parasympathetic activity [35], [36]. This decrease implies reduced vagal control of the heart, which is also reflected in the increased maternal HR (Figure 1). All significant changes in maternal HR and HRV seem to be mitigated by *day 3* or *day 4*; a similar timeline is seen in the case of fetal HRV [19]–[21]. Therefore, investigations into maternal HRV in complicated pregnancies should take care to perform measurements either preceding or at least four days following betamethasone administration.

Presumably, these changes in our outcome measures may also be a result of either the stress of hospitalization due to a complicated pregnancy or the consequence of other administered medications. However, the transient nature of the changes observed on *day 1*, along with the apparent return to normal on *day 3*, suggests that these effects result from betamethasone administration. Furthermore, the most commonly co-administered medication is nifedipine and researchers have found that while nifedipine provokes reflex tachycardia, HR returns to baseline within two hours [37]. Therefore, it is unlikely to be the main driver of the observed changes.

Still, the effect of nifedipine on maternal HR and HRV remains poorly explored. Subsequently, to ensure that nifedipine is not markedly affecting our results, we also performed a sub-analysis with participants who did not receive this drug (see Figures S1 and S2). The same trends in outcome measures were observed, albeit with fewer statistically significant changes, seeing as the sample size was more than halved. Additionally, we repeated this sub-analysis with participants who did not receive anti-hypertensive drugs (see Figures S3 and S4). While only five participants received these drugs, anti-hypertensives are known to affect HRV. Similarly, there was little noticeable change in the trends observed, increasing our confidence that the changes we observe are primarily due to betamethasone administration.

No work has been published on how betamethasone might influence maternal HR and HRV apart from a case report detailing maternal bradycardia after betamethasone administration (a rare but known side effect [38]) and a small animal study assessing maternal HR [39]. The latter compares the HR between four pregnant baboons who receive betamethasone and five controls; no significant changes were observed between these two groups during the 72-hour study period. Subsequently, little guidance

is available from the literature on the potential mechanism behind the changes we observe in maternal HR and HRV after betamethasone administration.

We hypothesize that these changes in maternal physiology relate to the effect of betamethasone on the hypothalamus-pituitary-adrenal axis (HPA-axis), a major neuroendocrine system that plays an important role in the long-term stress response via cortisol secretion [6]. Increased cortisol, which is an endogenous glucocorticoid, invokes the cardiovascular stress response leading to increased blood pressure (BP) and cardiac output [40]. When betamethasone – an exogenous glucocorticoid – enters the body, an increased level of cortisol is detected and the HPA-axis is suppressed via a negative feedback mechanism [41]–[43]. The biological half-life of betamethasone, i.e., the period during which the HPA-axis is suppressed and cortisol is correspondingly increased, is 36 to 59 hours [44], [45], suggesting that the effects of betamethasone should start to wane around *day 3* (i.e., approximately 48 hours after the second injection). Researchers have demonstrated a negative relationship between cortisol levels and vagal tone [46]–[48]; correspondingly, in Figure 2 features linked to vagal activity (RMSSD, pNN50, and HF) are decreased on *days 1* and *2* before normalizing around *day 3*. Furthermore, HR is increased in this period, likely due to the decreased vagal control (which acts as a 'brake' on the HR) and the increased cardiovascular stress response. However, it should be noted that the relationship between HPA-axis and the ANS is poorly understood, as are the pathways by which the cortisol invokes the cardiovascular stress reflex [49], [50].

Interestingly, the opposite response is observed in the fetus, where HR decreases and HRV increases in the first 24 hours [19]. Researchers hypothesize that it is due to the activation of the fetal baroreflex in response to the increase in the fetal BP which lowers HR and increases HRV [19]. It should also be noted that the half-life of betamethasone in the fetus is double that of the mother [51]. Subsequently, even if similar effects occur in both mother and fetus, these would likely be at different timescales. Further considering that we only have spot measurements every 24 hours, it is not possible to conclude why the response in the mother and fetus seems to differ.

However, regardless of the physiological mechanisms at play, we find that betamethasone influences autonomic activity in women with pregnancy complications. Future studies should further investigate the potential long-term impact of these effects, as women with complicated pregnancies already have abnormal autonomic regulation and an increased risk for cardiovascular disease later in life.

5. Conclusion

Antenatally administered betamethasone increases maternal HR and therefore its recent administration should be considered when evaluating maternal tachycardia. Furthermore, betamethasone alters autonomic regulation in these women, who already have dysfunctional autonomic regulation owing to their pregnancy complication. Further investigation is necessary to ascertain whether this has an impact on the future health of the mother.

Supplementary material

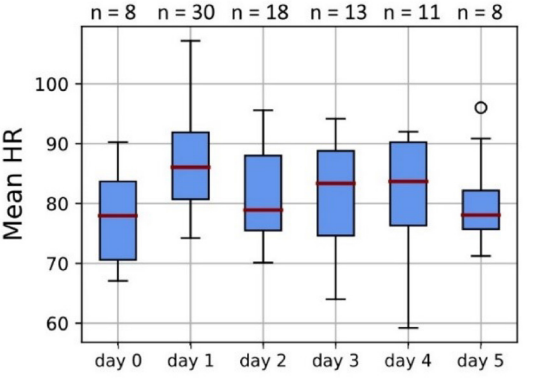

Figure S1: *Boxplots of the HR of participants on days 0 to 5, excluding all participants who were also administered nifedipine.* Boxplots represent the median, interquartile range and interdecile range of the values. *Day 0* represents measurements taken before the first injection of betamethasone, while *day 1* represents 24 hours after the first injection, *day 2* represents 48 hours after the first injection, etc. * represents a statistically significant finding with $p < 0.05$. The number of measurements incorporated in each day is displayed at the top of the graph.

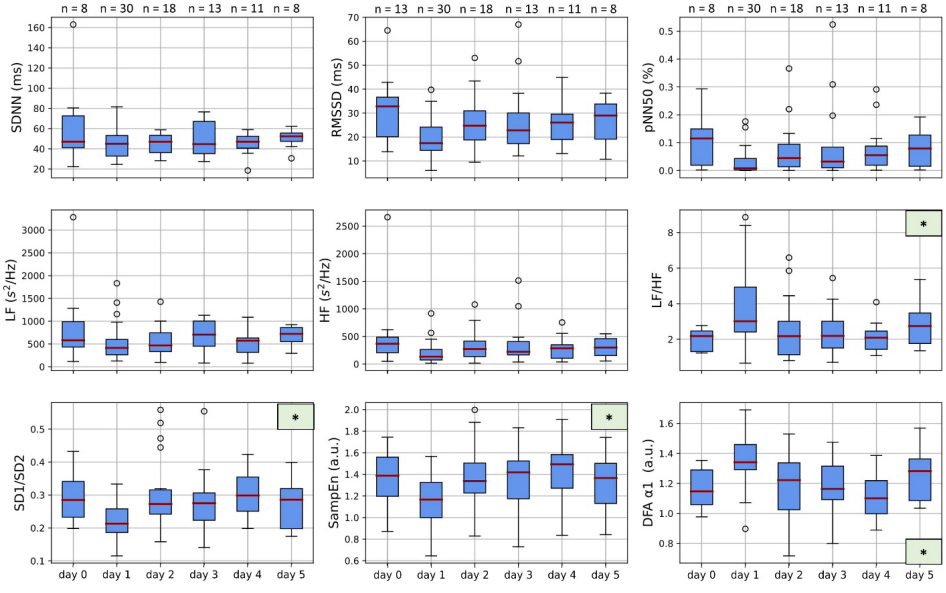

Figure S2: *Boxplots of maternal HRV on days 0 to 5, excluding all participants who were also administered nifedipine.* Boxplots represent the median, interquartile range and interdecile range of the values. *Day 0* represents measurements taken before the first injection of betamethasone, while *day 1* represents 24 hours after the first injection, *day 2* represents 48 hours after the first injection, etc. * represents a statistically significant finding with $p < 0.05$, while ** presents $p < 0.01$ and *** represents $p < 0.001$. The number of measurements incorporated in each day is displayed at the top of the graph.

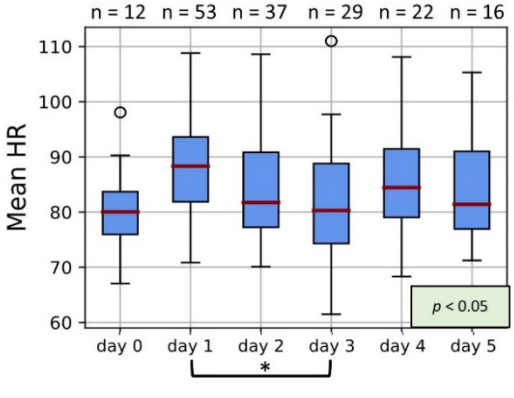

Figure S3: *Boxplots of the HR of participants on days 0 to 5, excluding all participants who were also administered anti-hypertensive medications.* Boxplots represent the median, interquartile range and interdecile range of the values. *Day 0* represents measurements taken before the first injection of betamethasone, while *day 1* represents 24 hours after the first injection, *day 2* represents 48 hours after the first injection, etc. * represents a statistically significant finding with $p < 0.05$. The number of measurements incorporated in each day is displayed at the top of the graph.

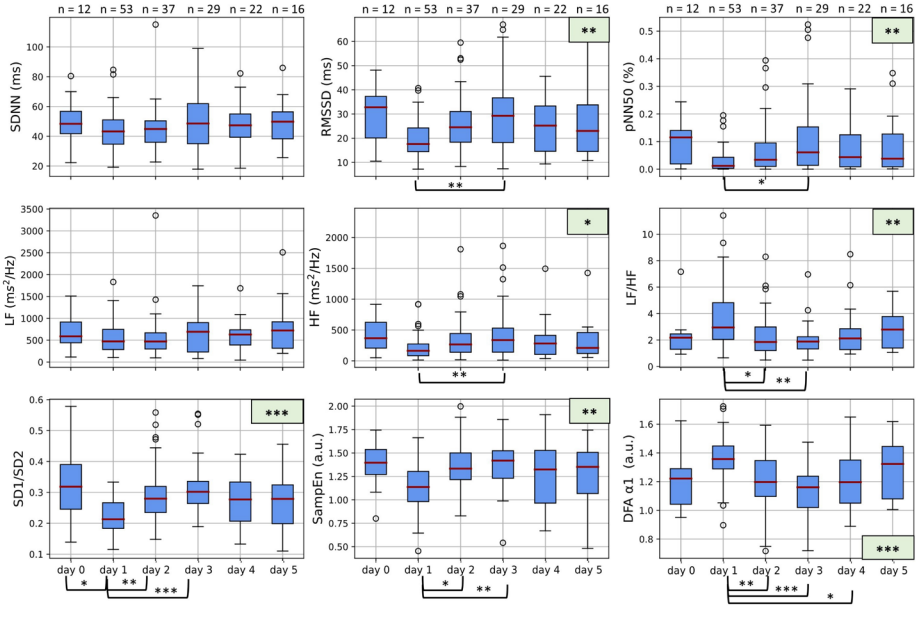

Figure S4: *Boxplots of maternal HRV on days 0 to 5, excluding all participants who were also administered anti-hypertensive medications.* Boxplots represent the median, interquartile range and interdecile range of the values. *Day 0* represents measurements taken before the first injection of betamethasone, while *day 1* represents 24 hours after the first injection, *day 2* represents 48 hours after the first injection, etc. * represents a statistically significant finding with $p < 0.05$, while ** presents $p < 0.01$ and *** represents $p < 0.001$. The number of measurements incorporated in each day is displayed at the top of the graph.

References

[1] C. Liggins and R. Howie, "A controlled trial of antepartum glucocorticoid treatment for prevention of the respiratory distress syndrome in premature infants," *Pediatrics*, vol. 50, no. 4, pp. 515–525, 1972, Accessed: Jul. 16, 2019. [Online]. Available: https://philips.tdnetdiscover.com/discover/result?logSearchID=30009867&pubid=PrimoCentral_medline4561295

[2] M. W. Kemp, J. P. Newnham, J. G. Challis, A. H. Jobe, and S. J. Stock, "The clinical use of corticosteroids in pregnancy," *Hum. Reprod. Update*, p. dmv047, Nov. 2015, doi: 10.1093/humupd/dmv047.

[3] A. L. Shanks, J. L. Grasch, S. K. Quinney, and D. M. Haas, "Controversies in antenatal corticosteroids," *Seminars in Fetal and Neonatal Medicine*, vol. 24, no. 3, pp. 182–188, Jun. 2019, doi: 10.1016/j.siny.2019.05.002.

[4] S. Hantoushzadeh, M. Saleh, and A. Maleki, "Effects of antenatal corticosteroids on maternal cardiovascular system, an underestimated notion in pregnant women," *BJOG*, vol. 129, no. 5, pp. 834–835, Apr. 2022, doi: 10.1111/1471-0528.16995.

[5] P. Tsai, "Re: Effects of antenatal corticosteroids on maternal cardiovascular system, an underestimated notion in pregnant women," *BJOG*, vol. 129, no. 5, pp. 835–836, Apr. 2022, doi: 10.1111/1471-0528.17020.

[6] S. Timmermans, J. Souffriau, and C. Libert, "A General Introduction to Glucocorticoid Biology," *Front. Immunol.*, vol. 10, p. 1545, Jul. 2019, doi: 10.3389/fimmu.2019.01545.

[7] F. Cottin *et al.*, "Effect of oral glucocorticoid intake on autonomic cardiovascular control," *SpringerPlus*, vol. 4, no. 1, p. 622, Dec. 2015, doi: 10.1186/s40064-015-1378-8.

[8] S. Haddad, R. Souza, J. Cecatti, and the WHO Intrapartum Care Algorithms Working Group, "Management of maternal pulse and blood pressure abnormalities during labour and childbirth: evidence-based algorithms for intrapartum care decision support," *BJOG*, pp. 1471–0528.16776, Apr. 2022, doi: 10.1111/1471-0528.16776.

[9] L. E. Shields, S. Wiesner, C. Klein, B. Pelletreau, and H. L. Hedriana, "Use of Maternal Early Warning Trigger tool reduces maternal morbidity," *American Journal of Obstetrics and Gynecology*, vol. 214, no. 4, p. 527.e1-527.e6, Apr. 2016, doi: 10.1016/j.ajog.2016.01.154.

[10] E. M. K. Ekholm, S. J. Piha, R. U. Erkkola, and K. J. Antila, "Autonomic cardiovascular reflexes in pregnancy. A longitudinal study," *Clinical Autonomic Research*, vol. 4, no. 4, pp. 161–165, Aug. 1994, doi: 10.1007/BF01826181.

[11] S. Moors *et al.*, "Heart rate variability in hypertensive pregnancy disorders: a systematic review," *Pregnancy Hypertension*, Mar. 2020, doi: 10.1016/j.preghy.2020.03.003.

[12] E. Täufer Cederlöf, M. Lundgren, B. Lindahl, and C. Christersson, "Pregnancy Complications and Risk of Cardiovascular Disease Later in Life: A Nationwide Cohort Study," *JAHA*, vol. 11, no. 2, p. e023079, Jan. 2022, doi: 10.1161/JAHA.121.023079.

[13] L. M. Reyes, C. W. Usselman, M. H. Davenport, and C. D. Steinback, "Sympathetic Nervous System Regulation in Human Normotensive and Hypertensive Pregnancies.," *Hypertension (Dallas, Tex. : 1979)*, vol. 71, no. 5, pp. 793–803, May 2018, doi: 10.1161/HYPERTENSIONAHA.117.10766.

[14] F. Shaffer and J. P. Ginsberg, "An Overview of Heart Rate Variability Metrics and Norms,"

Front. Public Health, vol. 5, p. 258, Sep. 2017, doi: 10.3389/fpubh.2017.00258.

[15] S. P. Rowan, C. L. Lilly, E. A. Claydon, J. Wallace, and K. Merryman, "Monitoring one heart to help two: heart rate variability and resting heart rate using wearable technology in active women across the perinatal period," *BMC Pregnancy Childbirth*, vol. 22, no. 1, p. 887, Nov. 2022, doi: 10.1186/s12884-022-05183-z.

[16] S. Rang, H. Wolf, G. A. Montfrans, and J. M. Karemaker, "Non–invasive assessment of autonomic cardiovascular control in normal human pregnancy and pregnancy- associated hypertensive disorders: a review," *Journal of Hypertension*, vol. 20, no. 11, pp. 2111–2119, 2002.

[17] G. K. Pal, P. Shyma, S. Habeebullah, P. Shyjus, and P. Pal, "Spectral Analysis of Heart Rate Variability for Early Prediction of Pregnancy-Induced Hypertension," *Clinical and Experimental Hypertension*, vol. 31, no. 4, pp. 330–341, Jan. 2009, doi: 10.1080/10641960802621333.

[18] M. Bester *et al.*, "Changes in Maternal Heart Rate Variability in Response to the Administration of Routine Obstetric Medication in Hospitalized Patients: Study Protocol for a Cohort Study (MAMA-Heart Study)," *Clinics and Practice*, vol. 11, no. 1, pp. 13–25, Jan. 2021, doi: 10.3390/clinpract11010004.

[19] K. M. J. Verdurmen *et al.*, "The influence of betamethasone on fetal heart rate variability, obtained by non-invasive fetal electrocardiogram recordings," *Early Human Development*, vol. 119, pp. 8–14, Apr. 2018, doi: 10.1016/j.earlhumdev.2018.02.011.

[20] L. Noben, K. M. J. Verdurmen, G. J. J. Warmerdam, R. Vullings, S. G. Oei, and J. O. E. H. van Laar, "The fetal electrocardiogram to detect the effects of betamethasone on fetal heart rate variability," *Early Human Development*, vol. 130, pp. 57–64, 2019, doi: 10.1016/j.earlhumdev.2019.01.011.

[21] K. Verdurmen, L. J. Van, and S. Oei, "Corticosteroids and fetal heart rate variability," *Journal of Maternal-Fetal and Neonatal Medicine*, vol. 27, pp. 361–361, 2014, doi: 10.3109/14767058.2014.924236.

[22] M. J. Rooijakkers *et al.*, "Influence of Electrode Placement on Signal Quality for Ambulatory Pregnancy Monitoring," *Computational and Mathematical Methods in Medicine*, vol. 2014, pp. 1–12, 2014, doi: 10.1155/2014/960980.

[23] M. J. Rooijakkers, C. Rabotti, M. Bennebroek, J. van Meerbergen, and M. Mischi, "Low-complexity R-peak detection in ECG signals: A preliminary step towards ambulatory fetal monitoring," in *2011 Annual International Conference of the IEEE Engineering in Medicine and Biology Society*, Boston, MA: IEEE, Aug. 2011, pp. 1761–1764. doi: 10.1109/IEMBS.2011.6090503.

[24] M. Bester, R. Joshi, M. Mischi, J. O. E. H. van Laar, and R. Vullings, "Longitudinally Tracking Maternal Autonomic Modulation During Normal Pregnancy With Comprehensive Heart Rate Variability Analyses," *Front. Physiol.*, vol. 13, p. 874684, May 2022, doi: 10.3389/fphys.2022.874684.

[25] C. Peters, R. Vullings, J. Bergmans, G. Oei, and P. Wijn, "The effect of artifact correction on spectral estimates of heart rate variability," in *2008 30th Annual International Conference of the IEEE Engineering in Medicine and Biology Society*, Vancouver, BC: IEEE, Aug. 2008, pp. 2669–2672. doi: 10.1109/IEMBS.2008.4649751.

[26] C. H. L. Peters, R. Vullings, M. J. Rooijakkers, J. W. M. Bergmans, S. G. Oei, and P. F. F.

Wijn, "A continuous wavelet transform-based method for time-frequency analysis of artefact-corrected heart rate variability data," *Physiol. Meas.*, vol. 32, no. 10, pp. 1517–1527, Oct. 2011, doi: 10.1088/0967-3334/32/10/001.

[27] L. M. Campana, R. L. Owens, G. D. Clifford, S. D. Pittman, and A. Malhotra, "Phase-rectified signal averaging as a sensitive index of autonomic changes with aging," *Journal of Applied Physiology*, vol. 108, no. 6, pp. 1668–1673, Jun. 2010, doi: 10.1152/japplphysiol.00013.2010.

[28] Task Force of The European Society of Cardiology and The North American Society of Pacing and Electrophysiology, "Heart rate variability. Standards of measurement, physiological interpretation, and clinical use.," *European heart journal*, vol. 17, no. 3, pp. 354–381, Mar. 1996.

[29] A. H. Khandoker, C. Karmakar, M. Brennan, M. Palaniswami, and A. Voss, *Poincaré Plot Methods for Heart Rate Variability Analysis*. Boston, MA: Springer US, 2013. doi: 10.1007/978-1-4614-7375-6.

[30] C. -K. Peng, S. Havlin, H. E. Stanley, and A. L. Goldberger, "Quantification of scaling exponents and crossover phenomena in nonstationary heartbeat time series," *Chaos*, vol. 5, no. 1, pp. 82–87, Mar. 1995, doi: 10.1063/1.166141.

[31] J. S. Richman and J. R. Moorman, "Physiological time-series analysis using approximate entropy and sample entropy," *American Journal of Physiology-Heart and Circulatory Physiology*, vol. 278, no. 6, pp. H2039–H2049, Jun. 2000, doi: 10.1152/ajpheart.2000.278.6.H2039.

[32] A. Bakhchina, K. Arutyunova, A. Sozinov, A. Demidovsky, and Y. Alexandrov, "Sample Entropy of the Heart Rate Reflects Properties of the System Organization of Behaviour," *Entropy*, vol. 20, no. 6, p. 449, Jun. 2018, doi: 10.3390/e20060449.

[33] R.-G. Yeh, J.-S. Shieh, G.-Y. Chen, and C.-D. Kuo, "Detrended fluctuation analysis of short-term heart rate variability in late pregnant women," *Autonomic Neuroscience*, vol. 150, no. 1–2, pp. 122–126, Oct. 2009, doi: 10.1016/j.autneu.2009.05.241.

[34] L. J. Green *et al.*, "Gestation-Specific Vital Sign Reference Ranges in Pregnancy," *Obstetrics & Gynecology*, vol. 135, no. 3, pp. 653–664, Mar. 2020, doi: 10.1097/AOG.0000000000003721.

[35] P. Castiglioni, G. Parati, M. Di Rienzo, R. Carabalona, A. Cividjian, and L. Quintin, "Scale exponents of blood pressure and heart rate during autonomic blockade as assessed by detrended fluctuation analysis: Cardiovascular scale exponents and autonomic blockade," *The Journal of Physiology*, vol. 589, no. 2, pp. 355–369, Jan. 2011, doi: 10.1113/jphysiol.2010.196428.

[36] J. L. Rojo-Alvarez *et al.*, "Analysis of physiological meaning of detrended Fluctuation Analysis in Heart Rate Variability using a lumped parameter model," in *2007 Computers in Cardiology*, Durham, NC, USA: IEEE, Sep. 2007, pp. 25–28. doi: 10.1109/CIC.2007.4745412.

[37] M. W. Schweizer *et al.*, "Heart rate variability in time and frequency domains: effects of gallopamil, nifedipine, and metoprolol compared with placebo.," *Heart*, vol. 70, no. 3, pp. 252–258, Sep. 1993, doi: 10.1136/hrt.70.3.252.

[38] M. A. Sarumi, J. W. Hole, and R. B. Gherman, "Maternal Bradycardia Associated with Betamethasone Administration During Pregnancy," *Case Reports in Obstetrics and Gynecology*, vol. 2019, pp. 1–3, Oct. 2019, doi: 10.1155/2019/6873057.

[39] S. V. Koenen, C. A. Mecenas, G. S. Smith, S. Jenkins, and P. W. Nathanielsz, "Effects of maternal betamethasone administration on fetal and maternal blood pressure and heart rate in the baboon at 0.7 of gestation," *American Journal of Obstetrics and Gynecology*, vol. 186, no. 4, pp. 812–817, Apr. 2002, doi: 10.1067/mob.2002.121654.

[40] R. M. Sapolsky, L. M. Romero, and A. U. Munck, "How Do Glucocorticoids Influence Stress Responses? Integrating Permissive, Suppressive, Stimulatory, and Preparative Actions," vol. 21, no. 1, p. 35, 2000.

[41] M. G. Matera, B. Rinaldi, L. Calzetta, P. Rogliani, and M. Cazzola, "Pharmacokinetics and pharmacodynamics of inhaled corticosteroids for asthma treatment," *Pulmonary Pharmacology & Therapeutics*, vol. 58, p. 101828, Oct. 2019, doi: 10.1016/j.pupt.2019.101828.

[42] S. V. Koenen, E. J. H. Mulder, L. D. Wijnberger, and G. H. A. Visser, "Transient Loss of the Diurnal Rhythms of Fetal Movements, Heart Rate, and Its Variation after Maternal Betamethasone Administration," *Pediatr Res*, vol. 57, no. 5 Part 1, pp. 662–666, May 2005, doi: 10.1203/01.PDR.0000159762.50504.1F.

[43] A. Agorastos *et al.*, "Vagal effects of endocrine HPA axis challenges on resting autonomic activity assessed by heart rate variability measures in healthy humans," *Psychoneuroendocrinology*, vol. 102, pp. 196–203, Apr. 2019, doi: 10.1016/j.psyneuen.2018.12.017.

[44] A. H. Jobe, M. A. Milad, T. Peppard, and W. J. Jusko, "Pharmacokinetics and Pharmacodynamics of Intramuscular and Oral Betamethasone and Dexamethasone in Reproductive Age Women in India.," *Clinical and translational science*, Dec. 2019, doi: 10.1111/cts.12724.

[45] MSD, "Celestone Chronodose, suspensie voor injectie 5,7 mg/ml," Merck Sharp & Dohme B.V., Haarlen, Netherlands, Samenvatting van de productkenmerken RVG 05399, Apr. 2018.

[46] J. F. Thayer and E. Sternberg, "Beyond Heart Rate Variability: Vagal Regulation of Allostatic Systems," *Annals of the New York Academy of Sciences*, vol. 1088, no. 1, pp. 361–372, Nov. 2006, doi: 10.1196/annals.1366.014.

[47] E. Mazgelytė *et al.*, "Association of salivary steroid hormones and their ratios with time-domain heart rate variability indices in healthy individuals," *J Med Biochemistry*, vol. 40, no. 2, pp. 173–180, 2021, doi: 10.5937/jomb0-26045.

[48] S. Pellissier *et al.*, "Relationship between Vagal Tone, Cortisol, TNF-Alpha, Epinephrine and Negative Affects in Crohn's Disease and Irritable Bowel Syndrome," *PLoS ONE*, vol. 9, no. 9, p. e105328, Sep. 2014, doi: 10.1371/journal.pone.0105328.

[49] N. T. Berry, C. K. Rhea, and L. Wideman, "Cardio-Hypothalamic-Pituitary Coupling during Rest and in Response to Exercise," *Entropy*, vol. 24, no. 8, p. 1045, Jul. 2022, doi: 10.3390/e24081045.

[50] A. G. Bechtold and D. A. Scheuer, "Glucocorticoids act in the dorsal hindbrain to modulate baroreflex control of heart rate," *American Journal of Physiology-Regulatory, Integrative and Comparative Physiology*, vol. 290, no. 4, pp. R1003–R1011, Apr. 2006, doi: 10.1152/ajpregu.00345.2005.

[51] L. Ballard and A. Ballard, "Scientific basis and therapeutic regimens for use of antenatal glucocorticoids," vol. 173, no. 1, p. 9, 1995.

Chapter 7

Changes in maternal heart rate variability in response to the administration of routine obstetric medications in hospitalized patients; study protocol for a cohort study (MAMA-heart study)

Reproduced after: M Bester*, S Moors*, R Joshi, TJ Nichting, MB van der Hout-van der Jagt, M Mischi, R Vullings, JOEH van Laar. Changes in maternal heart rate variability in response to the administration of routine obstetric medications in hospitalized patients; study protocol for a cohort study (MAMA-heart study). *Clinics and Practice*. 2021. *Equal contribution

Abstract

Pregnancy is a period of continuous change in the maternal cardiovascular system, partly mediated by the autonomic nervous system. Insufficient autonomic adaptation to increasing gestation is associated with pregnancy complications such as hypertensive disorders of pregnancy and preterm birth (both major causes of perinatal morbidity and mortality). Consequently, maternal heart rate variability (mHRV), a proxy measure for autonomic activity, is increasingly assessed in these cohorts to investigate the pathophysiology of their complications. A better pathophysiological understanding could facilitate early detection of these complications, which remains challenging. However, such studies (typically performed in pregnancies leading to hospitalization) have generated conflicting findings. A probable reason for these conflicting findings is that these study cohorts were likely administered routine obstetric medications during the study period of which the effects on mHRV are largely unknown. Subsequently, we design a longitudinal, observational study to quantify the effect of these medications – particularly corticosteroids, which are known to affect fetal HRV – on mHRV to improve the interpretation of past and future studies. We will enroll 61 women admitted to a tertiary obstetric unit with an indication to receive corticosteroids antenatally and continuously acquire mHRV throughout their hospitalization with wrist-worn photoplethysmography to facilitate a within-patient comparison of the effect of corticosteroids on mHRV.

1. Introduction

Pregnancy is a period of continuous anatomical and physiological change in both mother and fetus [1]. During this period, most maternal physiological systems undergo considerable adaptation to support the growing fetus. Some of the most prominent changes needed to sustain the increasing metabolic demands of the maternal-fetal dyad occur in the maternal cardiovascular system [1]–[3].

These maternal cardiovascular adaptations involve, amongst others, changes in blood pressure and heart rate (HR) [1]. The main mechanisms mediating these changes are related to the endocrine and the autonomic nervous systems (ANS) [2], [4]. However, in some cases, the ANS does not sufficiently adapt to support the increasing demands of pregnancy – a scenario that is associated with various pregnancy complications [5]. Two prominent examples are hypertensive disorders of pregnancy (HDP) and preterm birth (PTB), both of which are leading causes of worldwide perinatal and maternal morbidity and mortality [6]–[9].

Alleviating the burden of HDP and PTB (i.e. birth before 37 weeks of gestation) remains an important challenge in perinatology, in large part because early detection of these complications is challenging. Early detection of these conditions is important and actionable since effective risk-mitigating interventions do exist [10]–[12]. Although their exact etiologies remain uncertain, studies indicate that both complications are associated with dysfunctional autonomic regulation [5], [13]–[16]. A prominent theory is that this autonomic dysfunction results in insufficient placental development in early pregnancy, which in turn results in the development of such complications [17]–[19]. Therefore, assessing ANS activity during pregnancy is relevant as it can allow for the tracking of developing pathophysiologies, potentially enabling early detection.

Since changes in HR are closely modulated by the ANS, studying HR and, in particular, its variability offers a window into changes in autonomic activity [17], [20]–[22]. Consequently, maternal heart rate variability (mHRV) has been increasingly studied to assess autonomic dysfunction in complicated pregnancies [5], [17], [19], [20], [23]–[25]. However, such studies, which are typically performed in pregnancies leading to hospitalization, have generated conflicting findings [17], [19].

The onset of HDP and PTB is typically sudden, resulting in swift hospitalization to obstetric care units (OCUs) where patients frequently receive routine obstetric med-

ications. A probable reason for these conflicting findings is that – during the study period – these study cohorts were likely administered obstetric medications that potentially confounded measures of mHRV.

Typically, soon after admission to an OCU, corticosteroids and tocolytics are administered to the patient. Corticosteroids are aimed at maturing the fetal respiratory system in case of premature delivery [26], while tocolytics attenuate maternal contractions to reduce the risk of preterm delivery [11]. Additionally, magnesium sulfate ($MgSO_4$) and antihypertensive drugs may be administered as needed. These medications offer maternal and fetal neuroprotection in cases of HDP and PTB respectively [11], [12], [27].

Consequently, studies assessing mHRV in hospitalized cohorts with complications such as HDP and threatened PTB likely also capture the potential confounding effects of obstetric medications. While some researchers avoid this problem by only conducting short measurements before the administration of medications [5], [20], several studies do not discuss the administration of corticosteroids or tocolytics, even though their study populations would typically have received these [5], [11], [12], [23], [24], [27]–[29]. Others note the potential confounding effects of these medications as an unavoidable part of their study design [30], [31]. In fact, some even urge investigation into the effects of obstetric medications on mHRV [19], [24]. Quantifying these changes would not only enhance our understanding of how obstetric medications affect maternal physiology but may also improve the interpretation of past and future studies.

To our knowledge, only two studies have investigated the changes in mHRV in response to the administration of routinely used obstetric medications. Koenen et al. found no changes to the diurnal rhythm of mHRV in response to betamethasone administration (n=16), although it should be noted that only short and long-term variability (STV and LTV) were assessed [32]. Additionally, Weissman et al. found that a tocolytic drug (atosiban) did not affect mHRV in hospitalized patients [33]. Even though little is known regarding mHRV, the effect of obstetric medications on fetal HRV (fHRV) has been more widely investigated. Similar to Weissman's findings on mHRV, administering tocolytic drugs did not significantly alter fHRV [34]. However, corticosteroids are known to significantly affect fHRV [35]–[38]. Therefore, we investigate whether mHRV changes in response to administering corticosteroids.

Investigating the effect of routine obstetric medications such as corticosteroids and tocolytic drugs on mHRV should contribute to understanding the impact of these

medications. Subsequently, in this paper, we describe a study to investigate changes in mHRV in response to administering routinely administered obstetric medications in a cohort of patients hospitalized with pregnancy complications.

2. Methods

2.1 Aim of the study

This study aims to investigate the effect of routinely administered obstetric medications on mHRV in patients hospitalized due to pregnancy complications.

2.2 Clinical setting

This longitudinal, observational cohort study will be conducted at the OCU of Máxima Medical Center (Máxima MC), Veldhoven, The Netherlands. The study cohort will comprise patients admitted to the OCU between 23 5/7 and 33 6/7 weeks of gestation with an indication to receive corticosteroids antenatally. Since Máxima MC is a tertiary obstetric referral center, the majority of the study cohort will comprise high-risk patients transferred to Máxima MC from neighboring secondary care hospitals.

2.3 Clinical data acquisition

Longitudinal PPG measurements will be continuously acquired with the Philips Data Logger (PDL, Philips Research, Eindhoven, the Netherlands, where two of the authors are affiliated). The PDL – shown in Figure 1 – is a non-invasive wrist-worn device (CE-marked) that acquires PPG data (sampled at 32 Hz) through optical sensing that measures changes in blood volume. Previous studies have used and validated a predecessor of this device to collect PPG measurements in free-living conditions [39]–[41].

Figure 1. The Philips Data Logger (worn on the author's hand). This device will be employed in this study to acquire PPG and accelerometer data. The device does not display this PPG and accelerometer data, it only displays the time.

PPG measurements capture the time intervals between pulses resulting from subsequent heartbeats, serving as a measure of HR, from which HRV can be calculated [42]. Furthermore, the PDL also records movement data using a tri-axial accelerometer (range: ± 8 G, sampled at 32 Hz), which can aid in filtering out motion artifacts. The PDL offloads acquired data to a mobile phone via Bluetooth. Data are not displayed on either the PDL or the mobile phone, ensuring that acquired data cannot influence clinical decision-making.

In addition to PPG measurements, the study utilizes patient data routinely collected in electronic patient files. These data – detailed in the Study Parameter section – include maternal-fetal health parameters and routine measurements.

2.4 Routinely administered medications in obstetric care settings

Owing to their clinical state, the patient cohort participating in this study will be administered one or more obstetric medications as part of their standard clinical care. All medications administered during this study are part of standard care and not influenced by study participation.

When pregnancy complications are diagnosed before 34 weeks of gestation, patients receive corticosteroids (specifically betamethasone) [11]. Owing to its frequent use and its effects on fHRV, our study design focuses on this medication. A course of

betamethasone (Celestone Chrondose®, Schering AG, Berlin, Germany) consists of two 11.4 mg injections administered intramuscularly, each consisting of 50% betamethasone phosphate for quick uptake (≈ 1 hour) and 50% betamethasone acetate for slow release to facilitate sustained exposure [43]–[45]. Although the pharmacokinetics of betamethasone in the maternal system is not fully known, the maximum effect and terminal half-life of betamethasone (i.e. time until the drug concentration in plasma reduces by 50%) are believed to lie within 0.5-3 hours and within 6-12 hours after administration, respectively [45]–[48]. Betamethasone's biological half-life – which relates to its effect on the hypothalamus-pituitary-adrenal axis – is 36-59 hours [49], [50], and is cleared from the maternal system within 48 hours [46].

Patients will typically receive other obstetric medications in addition to corticosteroids; this is unavoidable in these cohorts [11], [12], [27]. In cases of threatened PTB, patients are likely to receive tocolytic drugs such as nifedipine or atosiban to attenuate uterine contractions [11]. Furthermore, patients in the study population can also receive $MgSO_4$, which is prescribed for either fetal neuroprotection (in case of PTB <30 weeks' gestation) or maternal neuroprotection (in case of severe HDP) [11], [12], [27]. Patients with HDP might also be administered anti-hypertensive medications such as labetalol, methyldopa, nifedipine, or nicardipine.

2.5 Study design

The study comprises two periods of PPG measurements in the same study population. The primary phase will assess the effect of obstetric medications on mHRV, based on PPG data gathered throughout subjects' hospitalization in the OCU. The secondary phase – added to compare cardiovascular features between the antenatal and postpartum periods – consists of 24-hour PPG measurements at six weeks postpartum, acquired in free-living conditions at home.

2.5.1. Primary phase:

We specify a series of measurement epochs from our continuous measurements as visualized in Figure 2. Our active measurement epochs (i.e. measurements to capture the effect of betamethasone) are defined on day 1 and day 2 (dark red in Figure 2). Similar studies assessing fHRV have typically found a slight increase in variability parameters on day 1, followed by a significant decrease in parameters on day 2. Hence, we will assess both active epochs against baseline measurements. We will exclude and replace subjects for whom reliable PPG data is not available in both active epochs.

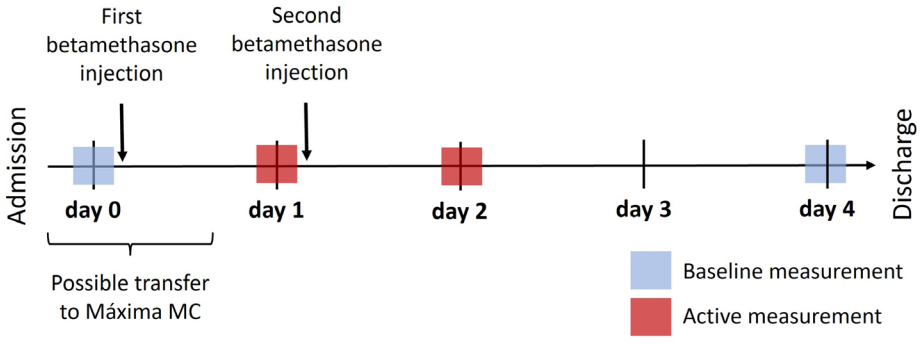

Figure 2: Baseline and active measurements epochs acquired in the primary phase of the study. The baseline measurements epochs are defined on day 0 and/or day 4 (light blue), while active measurements epochs are defined on day 1 and day 2 (dark red).

We define possible baseline measurements on day 0 (i.e. before betamethasone administration) and day 4 (i.e. 72 hours after the second betamethasone injection), depicted as light blue in Figure 2. Due to the typically speedy administration of betamethasone after admission, PPG measurements with the PDL will start as soon as possible to capture premedication measurements on day 0. However, many subjects will only be included on day 1 since the majority of our cohort will comprise transfers who have already received their first injection. Subsequently, we specify an additional baseline measurement on day 4 when the pharmacological effects of betamethasone will have diminished [45]–[50]. We will also exclude and replace subjects for whom no baseline epoch with reliable PPG data is available.

If baseline measurements from both day 0 and day 4 are available, the mean of these is taken as the baseline [38], [51]. Epochs that are compared for the primary analysis will be 24 (±4) hours apart to minimize diurnal effects [38]. Selected epochs will contain at least 5 minutes of PPG data of quality that is sufficient to continuously determine HR [52]. Additionally, epochs will be selected from rest periods (i.e. periods without motion artefacts) where possible, since PPG is most reliable under these conditions [41], [53].

2.5.2. Secondary phase:

Participants will wear the PDL at six weeks postpartum for a 24-hour monitoring period in free-living conditions at home. Participants are not excluded if they refuse to participate in the secondary phase.

2.6 Primary and secondary analyses

2.6.1. Primary phase:

The primary analysis will determine the effect of administering betamethasone on mHRV. Secondary analyses will, insofar as possible, explore the effect of other medications on mHRV, compare cardiovascular parameters between subgroups (e.g. stratified by diagnosis), assess cardiovascular parameters during delivery, and evaluate similarities between trends in PPG and routinely acquired CTG measurements.

2.6.2. Secondary phase:

PPG measurements acquired in the secondary phase will further facilitate secondary analyses, including a within-patient comparison of cardiovascular parameters between the antenatal and postpartum periods. If the eventual sample population allows, we will also compare postpartum parameters between subgroups (stratified by diagnosis).

2.7 Study parameters

We will assess cardiovascular parameters derived from the PPG measurements to perform our analyses. These include HR, HRV features (e.g. SDNN, RMSSD, HF, LF, and pNN50) and features based on the morphology of the PPG waveform (e.g. pulse area and large artery stiffness index [54]). To describe the study cohort, we will also collect the following data from patient records:

- Maternal condition:
  - patient characteristics, including age, BMI, and ethnicity
  - pregnancy characteristics, including gestational age, results of prenatal screening, and complications in pregnancy
  - obstetric history, including gravidity, parity, and previous pregnancy or labor complications
  - family history, including genetic or congenital diseases or a history of hypertension or preeclampsia
  - medical condition, including preexisting diseases (i.e. cardiovascular disease, pre-existing hypertension, autoimmune disorders, neurologic disorders)
  - routine measurements, including blood pressure, laboratory test results, physical examination results, ultrasound results.
- Fetal/neonatal condition, including fetal growth, congenital diseases, birth weight, APGAR score, CTG measurements, and umbilical cord blood gases.

- Labor and delivery, including mode of delivery and clinical notes.
- Administration of medications, including timing, dosage, and reasons for administration.

The electronic medical records from the hospital only contain information relevant to a patient's hospitalization or appointments at Máxima MC. Subsequently, we will contact subjects who did not deliver at Máxima MC to retrieve basic details of their delivery (i.e. birth weight and gestational age).

For subjects who participate in the secondary phase and have their postpartum appointments at Máxima MC, information on their postpartum condition (e.g. postpartum complications and standard checkup measurements) will also be collected from their electronic medical records.

2.8 Subject inclusion and exclusion criteria

Patients admitted to the OCU at Máxima MC who are going to receive one or both dosages of betamethasone injection(s) are eligible for inclusion. Table 1 outlines the entire inclusion and exclusion criteria.

Table 1: Inclusion and exclusion criteria for MAMA-heart study

Inclusion criteria	Exclusion criteria
• Age 18 years and above • Gestational age 23 5/7 to 33 6/7 weeks • Yet to receive the second betamethasone injection • Proficient in Dutch or English	• History of severe arrhythmia and/or maternal congenital heart disease • Diseases with known effects on ANS Known allergies to hard plastic (e.g. used in sport watches) or elastic band material • Wounds, injuries, or infectious diseases on the wrist where the PDL will be worn • Tattoo location on the wrist that interferes with the positioning of the PDL • Both wrists are unavailable for wearing the PDL (e.g. owing to intravenous lines) • Dexamethasone (another brand of corticosteroid) was administered instead of betamethasone

PDL= Philips Data Logger

Retrospectively, if subjects are identified to be incorrectly enrolled (i.e., not meeting the full eligibility criteria), they will be excluded from the study analysis and replaced with a new subject.

2.9 Sample size

We designed the study to detect the differences in mHRV indices between the active and baseline measurement epochs (in line with our primary analysis). Since we will assess multiple HRV indices, we base our sample size calculation on detecting a difference in mean NN-intervals (i.e. the time between heartbeats). NN-intervals form the basis for calculating HRV indices and are also a less sensitive measure than HRV, therefore resulting in a conservative sample size estimation. Subsequently, we calculated the sample size using a two-sided T-test for a confidence interval of 95% and a power assumption of 80%. The expected variation in NN-interval measurements was estimated from studies assessing NN-intervals in pregnant populations [14], [55], [56]. No prior research was available to guide the decision concerning effect size but given the heterogeneity of the cohort, we would like to be able to detect a small effect. Subsequently, we selected an effect size of 10%.

Based on these parameters, we calculated a sample size of 43 using the built-in power function for a paired t-test in R (version 3.5.3, RStudio Inc., Boston, MA, USA). Adding in a safety margin of 20% to the expected variation, the sample size increases to 61. We will perform an interim analysis after including 43 subjects to assess whether further inclusions are necessary. The study is powered for the primary analysis, and not specifically powered for secondary analyses.

2.10 Statistical analysis

Our study cohort has various diagnoses, which can result in different baseline measurements for mHRV. Owing to this, a within-subject comparison of mHRV features will be performed for the primary analysis to minimize the effect of this heterogeneity. For each participant, the active measurement epochs on day 1 and day 2 will respectively be compared to the baseline measurement epoch.

Since the treatment of this study cohort is guided by standard clinical management, the co-administration of medications is unavoidable [11], [12], [27]. To this end, we will perform variance analyses to understand whether this co-administration affects our results. For secondary analyses in both phases, we will perform within-subject as well as between-group comparisons.

We will test normality assumptions with a Shapiro-Wilk test and subsequently compare continuous variables using a paired T-test or a Wilcoxon matched-pairs test, and categorical variables using a $\chi 2$-test or Fisher's exact test, chosen as appropriate.

P<0.05 is considered significant for a two-tailed test. Effect sizes will be reported along with the P values [57].

2.11 Data handling and storage

We will adhere to the European General Data Protection Regulation (GDPR) and the Dutch Personal Data Protection Act ("Uitvoeringswet AVG") for data processing and analyses. Subsequently, subject data will be de-identified.

We will use Research Manager (version 5.51.0, Research Manager, Deventer, The Netherlands) for the case report form and data handling. Personal data will be stored in accordance with Good Clinical Practice guidelines. Analyses are carried out under the Eindhoven MedTech Innovation Center framework, in collaboration between Máxima MC, Philips Research, and the Eindhoven University of Technology.

2.12 Ethics and dissemination

The Medical Ethics Committee of Máxima MC, Veldhoven, The Netherlands, confirmed that the study neither imposes any changes in general practice nor does it burden participants. Therefore, in line with the Declaration of Helsinki, a waiver for ethical approval was granted (N19.112; 02/12/2019). The study is registered in the Dutch Trial Register (NL8204; 06/12/2019).

All investigators agree to publish the study results in an international peer-reviewed journal, regardless of whether the outcomes align with the stated hypotheses. The full study protocol is available upon request.

3. Discussion

The autonomic dysfunction associated with pregnancy complications has increasingly been studied by investigating mHRV [17], [19]. However, mHRV measures in these cohorts are possibly confounded by routinely administered obstetric medications, in particular corticosteroids. This likely impedes the accurate interpretation of such results and could explain why they are often conflicting. Therefore, quantifying changes in mHRV in response to obstetric medications would not only enhance our understanding of how these medications affect maternal physiology but also improve the interpretation of past and future studies.

Our study is one of only a few to explore the effect of administering routine obstetric medications on mHRV [33], [58], and the first to focus on investigating changes in mHRV resulting from antenatal administration of corticosteroids (betamethasone). Apart from a small number of human and animal studies [32], [59]–[61], research has focused on assessing changes in fHRV – demonstrating that administering betamethasone significantly decreases fHRV parameters [35], [62], [63]. Since fHRV is not continuously monitored in cohorts hospitalized due to pregnancy complications, these fetal studies (such as Verdurmen et al.'s) had to deliberately incorporate fHRV measurements into clinical workflow, which can be logistically challenging [63]. Since our clinical setting and protocol are comparable to theirs, we implement unobtrusive monitoring to ensure that our study fits more seamlessly into standard clinical workflow.

For collecting mHRV in our study, we selected a wristwatch-like device (the PDL) based on its ease of use and limited interference with clinical workflow. The traditional alternative would be an ECG Holter monitor, as it might offer higher accuracy in determining mHRV. However, this approach is more obtrusive and cumbersome for both the patient and clinical staff. Furthermore, in addition to high participant compliance in wrist-worn monitoring in pregnant populations [64], HRV determined from PPG measurements sampled above 25 Hz (PDL: 32 Hz) can be as reliable as that calculated from ECG [65]. Epochs used for analyses will be selected from rest periods where possible since this is when PPG measures are generally most reliable. Still, frequency domain features could be less reliable when calculated from PPG measurements and subsequently we will interpret these features with caution [53].

The unobtrusive nature of wrist-worn PPG measurements also offers opportunities for additional exploratory analyses: firstly, a continuous dataset representing the complete period of hospitalization of participants can be collected; secondly, it enables us to collect 24 hours of postpartum at-home measurements for these same participants (i.e. the secondary phase). Incorporating all these measurements could allow for analysis of mHRV throughout the perinatal period (i.e. antepartum, intrapartum, and postpartum), which – to our knowledge – has not yet been assessed. Insights into the postpartum period could be particularly useful since literature on how autonomic regulation changes in this period is limited [66]–[68].

Defining a baseline measurement epoch is another important challenge in assessing the effect of betamethasone on mHRV. The presumptive ideal is the epoch leading up

to the first betamethasone injection (i.e. day 0 in Figure 2), but this is impractical given that most of our study cohort will be transfers who have already received their first injection. Furthermore, since admission is typically urgent and unexpected, patients are likely physiologically stressed during day 0, which can affect HRV parameters [69]. Therefore, an alternative baseline measurement is necessary. Guided by available literature and the pharmacokinetics of betamethasone, we define our alternative baseline measurement on day 4. Koenen et al. found that while administering betamethasone suppresses the diurnal rhythm of maternal cortisol and ACTH levels, this rhythm returns by day 4 [32]. This aligns with what is known on the pharmacokinetics of the medication in the maternal system, with studies showing the maternal terminal half-life of betamethasone as 6 to 12 hours [45]–[48], and the corresponding biological half-life as 36 to 59 hours [49], [50]. Several studies have also shown that the effect of betamethasone on fHRV ceases by day 4 [37], [38], [51]. Factoring in that Ballard et al. have demonstrated that the medication's terminal half-life in the maternal system is half of that in the fetus [46], it is reasonable to assume that day 4 is a conservative baseline measurement. In the case that both baseline epochs are available, we use their mean [38], [51].

For the results of the study to be applicable in clinical practice, participants will represent a cohort of women who typically receive corticosteroids, i.e. patients with varying characteristics and diagnoses (e.g. HDP, threatened PTB), and who subsequently receive multiple medications. The heterogeneity in characteristics and diagnoses could serve as limitations, as they will likely also influence mHRV. We account for this heterogeneity by focusing on within-patient comparisons when assessing the effect of betamethasone on mHRV, emphasizing the relative change between the active and baseline epochs, and averaging results across subjects. Hence, the effect of the heterogeneity on the study results will be reduced.

Another limitation is the possible confounding effect of co-administration of medications. This is unavoidable in this study design and cohort [11], [12], [27]. As previously mentioned, little literature exists on the effect of obstetric medications on mHRV, aside from one study which determined that a tocolytic drug had no significant effect on mHRV [33]. We aim to assess the impact of this co-administration by doing variance analyses when multiple medications have been administered.

Still, the most prominent knowledge gap concerns betamethasone, and we subsequently focus on investigating the effect of this medication on mHRV. Results from

this study could identify the possible confounding effect of betamethasone on mHRV, thereby improving the interpretation of existing and future studies assessing the autonomic dysregulation associated with pregnancy complications such as HDP or threatened PTB. An improved interpretation of the changes in mHRV in these cohorts could facilitate earlier diagnosis through tracking deteriorations in mHRV. In turn, early detection could enable the prevention or better management of these complications, alleviating some of the burdens they place on women, families, and society.

References

[1] E. K. Tan and E. L. Tan, "Alterations in physiology and anatomy during pregnancy," *Best Practice and Research: Clinical Obstetrics and Gynaecology*, vol. 27, no. 6, pp. 791–802, Dec. 2013, doi: 10.1016/j.bpobgyn.2013.08.001.

[2] Q. Fu, "Hemodynamic and Electrocardiographic Aspects of Uncomplicated Singleton Pregnancy.," *Advances in experimental medicine and biology*, vol. 1065, pp. 413–431, 2018, doi: 10.1007/978-3-319-77932-4_26.

[3] P. Soma-Pillay, C. Nelson-Piercy, H. Tolppanen, and A. Mebazaa, "Physiological changes in pregnancy.," *Cardiovascular journal of Africa*, vol. 27, no. 2, pp. 89–94, 2016, doi: 10.5830/CVJA-2016-021.

[4] L. May, "Cardiac Physiology of Pregnancy," in *Comprehensive Physiology*, R. Terjung, Ed., Hoboken, NJ, USA: John Wiley & Sons, Inc., 2015, pp. 1325–1344. doi: 10.1002/cphy.c140043.

[5] S. V. Khlybova, V. I. Tsirkin, S. A. Dvoryanskii, I. A. Makarova, and A. N. Trukhin, "Heart rate variability in normal and complicated pregnancies," *Hum Physiol*, vol. 34, no. 5, pp. 625–632, Sep. 2008, doi: 10.1134/S0362119708050113.

[6] H. A. Frey and M. A. Klebanoff, "The epidemiology, etiology, and costs of preterm birth," *Seminars in Fetal and Neonatal Medicine*, vol. 21, no. 2, pp. 68–73, Apr. 2016, doi: 10.1016/j.siny.2015.12.011.

[7] M. Umesawa and G. Kobashi, "Epidemiology of hypertensive disorders in pregnancy: prevalence, risk factors, predictors and prognosis," *Hypertension research : official journal of the Japanese Society of Hypertension*, vol. 40, no. 3, pp. 213–220, 2017, doi: 10.1038/hr.2016.126.

[8] S. Saleem *et al.*, "A prospective study of maternal, fetal and neonatal deaths in low- and middle-income countries," *Bull. World Health Organ.*, vol. 92, no. 8, pp. 605–612, Aug. 2014, doi: 10.2471/BLT.13.127464.

[9] K. S. Khan, D. Wojdyla, L. Say, A. M. Gulmezoglu, and P. F. V. Look, "WHO analysis of causes of maternal death: a systematic review," *Lancet (London, England)*, vol. 367, no. 9516, pp. 1066–1074, Apr. 2006.

[10] Y. Cui, B. Zhu, and F. Zheng, "Low-dose aspirin at ≤16 weeks of gestation for preventing preeclampsia and its maternal and neonatal adverse outcomes: A systematic review and meta-analysis," *Exp Ther Med*, vol. 15, no. 5, pp. 4361–4369, May 2018, doi: 10.3892/etm.2018.5972.

[11] "ACOG practice bulletin no. 127: Management of preterm labor.," *Obstetrics and gynecology*, vol. 119, no. 6, pp. 1308–1317, Jun. 2012, doi: 10.1097/AOG.0b013e31825af2f0.

[12] "ACOG Practice Bulletin No. 202: Gestational Hypertension and Preeclampsia," *Obstetrics & Gynecology*, vol. 133, no. 1, p. e1, Jan. 2019, doi: 10.1097/AOG.0000000000003018.

[13] L. M. Reyes, C. W. Usselman, M. H. Davenport, and C. D. Steinback, "Sympathetic Nervous System Regulation in Human Normotensive and Hypertensive Pregnancies," *Hypertension*, vol. 71, no. 5, pp. 793–803, 2018, doi: 10.1161/HYPERTENSIONAHA.117.10766.

[14] C. A. Brown, C. T. Lee, S. M. J. Hains, and B. S. Kisilevsky, "Maternal heart rate variability and fetal behavior in hypertensive and normotensive pregnancies," *Biol Res Nurs*, vol. 10, no. 2, pp. 134–144, Oct. 2008, doi: 10.1177/1099800408322942.

[15] P. G. Guyenet, “The sympathetic control of blood pressure,” *Nat. Rev. Neurosci.*, vol. 7, no. 5, pp. 335–346, May 2006, doi: 10.1038/nrn1902.

[16] S. Julius and S. Majahalme, “The changing face of sympathetic overactivity in hypertension,” *Annals of Medicine*, vol. 32, no. 5, pp. 365–370, Jan. 2000, doi: 10.3109/07853890008995939.

[17] D. Yousif *et al.*, “Autonomic Dysfunction in Preeclampsia: A Systematic Review,” *Front. Neurol.*, vol. 10, Aug. 2019, doi: 10.3389/fneur.2019.00816.

[18] P. G. Nelson and K. B. Nelson, “Innervation of the placenta and uterus: Competition between cytotrophoblasts and nerves?,” *Placenta*, vol. 34, no. 6, pp. 463–466, Jun. 2013, doi: 10.1016/j.placenta.2013.03.004.

[19] S. Moors *et al.*, “Heart rate variability in hypertensive pregnancy disorders: A systematic review.,” *Pregnancy hypertension*, vol. 20, pp. 56–68, Mar. 2020, doi: 10.1016/j.preghy.2020.03.003.

[20] S. Musa, “Sympathetic activity in preeclampsia, a study of heart rate variability,” *Journal of hypertension*, vol. 36, pp. e5–e5, 2018, doi: 10.1097/01.hjh.0000548004.87380.fa.

[21] Task Force of The European Society of Cardiology and The North American Society of Pacing and Electrophysiology, “Heart rate variability. Standards of measurement, physiological interpretation, and clinical use.,” *European heart journal*, vol. 17, no. 3, pp. 354–381, Mar. 1996.

[22] S. Massaro and L. Pecchia, “Heart Rate Variability (HRV) Analysis: A Methodology for Organizational Neuroscience,” *Organizational Research Methods*, vol. 22, no. 1, pp. 354–393, Jan. 2019, doi: 10.1177/1094428116681072.

[23] M. Chaswal, R. Kapoor, A. Batra, S. Verma, and B. S. Yadav, “Heart Rate Variability and Cardiovascular Reflex Tests for Assessment of Autonomic Functions in Preeclampsia,” *International journal of hypertension*, vol. 2018, pp. 8163824–8163824, Sep. 2018, doi: 10.1155/2018/8163824.

[24] T. M. Weber *et al.*, “Heart rate variability and baroreceptor reflex sensitivity in early- versus late-onset preeclampsia,” *PLoS ONE*, vol. 12, no. 10, p. e0186521, Oct. 2017, doi: 10.1371/journal.pone.0186521.

[25] N. Heiskanen *et al.*, “Cardiovascular autonomic responses to head-up tilt in gestational hypertension and normal pregnancy,” *Blood pressure*, vol. 20, no. 2, pp. 84–91, 2011, doi: //dx.doi.org/10.3109/08037051.2010.532313.

[26] D. Roberts, J. Brown, N. Medley, and S. R. Dalziel, “Antenatal corticosteroids for accelerating fetal lung maturation for women at risk of preterm birth,” *Cochrane Database of Systematic Reviews*, Mar. 2017, doi: 10.1002/14651858.CD004454.pub3.

[27] “ACOG Practice Bulletin No. 188: Prelabor Rupture of Membranes.,” *Obstetrics and gynecology*, vol. 131, no. 1, pp. e1–e14, Jan. 2018, doi: 10.1097/AOG.0000000000002455.

[28] E. Tejera, M. J. Areias, A. I. Rodrigues, J. M. Nieto-Villar, and I. Rebelo, “Blood Pressure and Heart Rate Variability Complexity Analysis in Pregnant Women with Hypertension,” *Hypertension in Pregnancy*, vol. 31, no. 1, pp. 91–106, Feb. 2012, doi: 10.3109/10641955.2010.544801.

[29] R. Faber, M. Baumert, H. Stepan, N. Wessel, A. Voss, and T. Walther, “Baroreflex sensitivity, heart rate, and blood pressure variability in hypertensive pregnancy disorders,” *J Hum Hypertens*, vol. 18, no. 10, pp. 707–712, Oct. 2004, doi: 10.1038/sj.jhh.1001730.

[30] D. Casati *et al.*, "Maternal cardiac deceleration capacity: a novel insight into maternal autonomic function in pregnancies complicated by hypertensive disorders and intrauterine growth restriction," *European Journal of Obstetrics & Gynecology and Reproductive Biology*, vol. 206, pp. 6–11, Nov. 2016, doi: 10.1016/j.ejogrb.2016.08.007.

[31] A. Seeck, M. Baumert, C. Fischer, A. Khandoker, R. Faber, and A. Voss, "Advanced Poincaré plot analysis differentiates between hypertensive pregnancy disorders," *Physiol. Meas.*, vol. 32, no. 10, pp. 1611–1622, Oct. 2011, doi: 10.1088/0967-3334/32/10/009.

[32] S. V. Koenen, E. J. H. Mulder, L. D. Wijnberger, and G. H. A. Visser, "Transient Loss of the Diurnal Rhythms of Fetal Movements, Heart Rate, and Its Variation after Maternal Betamethasone Administration," p. 5.

[33] A. Weissman, R. S. Tobia, Y. Z. Burke, O. Maxymovski, and A. Drugan, "The effects of oxytocin and atosiban on the modulation of heart rate in pregnant women," *The Journal of Maternal-Fetal & Neonatal Medicine*, vol. 30, no. 3, pp. 329–333, Feb. 2017, doi: 10.3109/14767058.2016.1172564.

[34] K. M. J. Verdurmen, A. D. J. Hulsenboom, J. O. E. H. van Laar, and S. G. Oei, "Effect of tocolytic drugs on fetal heart rate variability: a systematic review," *The Journal of Maternal-Fetal & Neonatal Medicine*, vol. 30, no. 20, pp. 2387–2394, Oct. 2017, doi: 10.1080/14767058.2016.1249844.

[35] L. Noben, K. M. J. Verdurmen, G. J. J. Warmerdam, R. Vullings, S. G. Oei, and J. O. E. H. van Laar, "The fetal electrocardiogram to detect the effects of betamethasone on fetal heart rate variability," *Early Human Development*, vol. 130, pp. 57–64, Mar. 2019, doi: 10.1016/j.earlhumdev.2019.01.011.

[36] A. Nensi *et al.*, "Effect of magnesium sulphate on fetal heart rate parameters: a systematic review," *Journal of obstetrics and gynaecology Canada : JOGC = Journal d'obstetrique et gynecologie du Canada : JOGC*, vol. 36, no. 12, pp. 1055–1064, Dec. 2014.

[37] K. M. Verdurmen, J. Renckens, J. O. van Laar, and S. G. Oei, "The influence of corticosteroids on fetal heart rate variability: a systematic review of the literature," *Obstetrical & gynecological survey*, vol. 68, no. 12, pp. 811–824, Dec. 2013, doi: 10.1097/OGX.0000000000000009 [doi].

[38] K. M. J. Verdurmen *et al.*, "The influence of betamethasone on fetal heart rate variability, obtained by non-invasive fetal electrocardiogram recordings," *Early Human Development*, vol. 119, pp. 8–14, Apr. 2018, doi: 10.1016/j.earlhumdev.2018.02.011.

[39] L. M. Eerikäinen *et al.*, "Comparison between electrocardiogram- and photoplethysmogram-derived features for atrial fibrillation detection in free-living conditions," *Physiol Meas*, vol. 39, no. 8, p. 084001, 08 2018, doi: 10.1088/1361-6579/aad2c0.

[40] M. Radha *et al.*, "Estimating blood pressure trends and the nocturnal dip from photoplethysmography," *Physiol. Meas.*, vol. 40, no. 2, p. 025006, Feb. 2019, doi: 10.1088/1361-6579/ab030e.

[41] F. Sartor, J. Gelissen, R. van Dinther, D. Roovers, G. B. Papini, and G. Coppola, "Wrist-worn optical and chest strap heart rate comparison in a heterogeneous sample of healthy individuals and in coronary artery disease patients," *BMC Sports Sci Med Rehabil*, vol. 10, no. 1, p. 10, Dec. 2018, doi: 10.1186/s13102-018-0098-0.

[42] J. Allen, "Photoplethysmography and its application in clinical physiological measurement," *Physiol. Meas.*, vol. 28, no. 3, pp. R1–R39, Mar. 2007, doi: 10.1088/0967-3334/28/3/R01.

[43] M. W. Kemp, J. P. Newnham, J. G. Challis, A. H. Jobe, and S. J. Stock, "The clinical use of corticosteroids in pregnancy," *Hum. Reprod. Update*, p. dmv047, Nov. 2015, doi: 10.1093/humupd/dmv047.

[44] A. L. Shanks, J. L. Grasch, S. K. Quinney, and D. M. Haas, "Controversies in antenatal corticosteroids," *Seminars in Fetal and Neonatal Medicine*, vol. 24, no. 3, pp. 182–188, Jun. 2019, doi: 10.1016/j.siny.2019.05.002.

[45] I. I. Salem and N. M. Najib, "Pharmacokinetics of Betamethasone After Single-Dose Intramuscular Administration of Betamethasone Phosphate and Betamethasone Acetate to Healthy Subjects," *Clinical Therapeutics*, vol. 34, no. 1, pp. 214–220, Jan. 2012, doi: 10.1016/j.clinthera.2011.11.022.

[46] L. Ballard and A. Ballard, "Scientific basis and therapeutic regimens for use of antenatal glucocorticoids," vol. 173, no. 1, p. 9, 1995.

[47] T. J. M. Moss, D. A. Doherty, I. Nitsos, R. Harding, and J. P. Newnham, "Pharmacokinetics of betamethasone after maternal or fetal intramuscular administration," *American Journal of Obstetrics and Gynecology*, vol. 189, no. 6, pp. 1751–1757, Dec. 2003, doi: 10.1016/S0002-9378(03)00825-1.

[48] C. He *et al.*, "Pharmacokinetics of betamethasone and betamethasone 17-monopropionate in Chinese healthy volunteers after intramuscular injection of betamethasone phosphate/betamethasone dipropionate.," *Arzneimittel-Forschung*, vol. 61, no. 7, pp. 417–420, 2011, doi: 10.1055/s-0031-1296220.

[49] A. H. Jobe, M. A. Milad, T. Peppard, and W. J. Jusko, "Pharmacokinetics and Pharmacodynamics of Intramuscular and Oral Betamethasone and Dexamethasone in Reproductive Age Women in India," *Clin Transl Sci*, p. cts.12724, Dec. 2019, doi: 10.1111/cts.12724.

[50] MSD, "Celestone Chronodose, suspensie voor injectie 5,7 mg/ml," Merck Sharp & Dohme B.V., Haarlen, Netherlands, Samenvatting van de productkenmerken RVG 05399, Apr. 2018.

[51] L. Noben, K. M. J. Verdurmen, G. J. J. Warmerdam, R. Vullings, S. G. Oei, and J. O. E. H. van Laar, "The fetal electrocardiogram to detect the effects of betamethasone on fetal heart rate variability," *Early Human Development*, vol. 130, pp. 57–64, 2019, doi: 10.1016/j.earlhumdev.2019.01.011.

[52] R. Castaldo, L. Montesinos, P. Melillo, S. Massaro, and L. Pecchia, "To What Extent Can We Shorten HRV Analysis in Wearable Sensing? A Case Study on Mental Stress Detection.," in *EMBEC & NBC 2017*, H. Eskola, O. Väisänen, J. Viik, and J. Hyttinen, Eds., in IFMBE Proceedings, vol. 65. Singapore: Springer Singapore, 2018, pp. 643–646. doi: 10.1007/978-981-10-5122-7_161.

[53] N. Pinheiro *et al.*, "Can PPG be used for HRV analysis?," presented at the 2016 38th Annual International Conference of the IEEE Engineering in Medicine and Biology Society (EMBC), IEEE, 2016, pp. 2945–2949.

[54] M. Elgendi, "On the Analysis of Fingertip Photoplethysmogram Signals," *CCR*, vol. 8, no. 1, pp. 14–25, Jun. 2012, doi: 10.2174/157340312801215782.

[55] A. Voss *et al.*, "Baroreflex sensitivity, heart rate, and blood pressure variability in normal pregnancy," *American Journal of Hypertension*, vol. 13, no. 11, pp. 1218–1225, Nov. 2000, doi: 10.1016/S0895-7061(00)01199-7.

[56] T. Alam, A. Choudhary, and S. D, "Maternal heart rate variability during different tri-

mesters of pregnancy," *Natl J Physiol Pharm Pharmacol*, vol. 8, no. 9, p. 1475, 2018, doi: 10.5455/njppp.2018.8.0723327072018.

[57] D. S. Quintana, "Statistical considerations for reporting and planning heart rate variability case-control studies: Reporting heart rate variability studies," *Psychophysiol*, vol. 54, no. 3, pp. 344–349, Mar. 2017, doi: 10.1111/psyp.12798.

[58] Q. Zhou, J. Shen, G. Zhou, L. Shen, S. Zhou, and X. Li, "Effects of magnesium sulfate on heart rate, blood pressure variability and baroreflex sensitivity in preeclamptic rats treated with L-NAME," *Hypertension in Pregnancy*, vol. 32, no. 4, pp. 422–431, Nov. 2013, doi: 10.3109/10641955.2013.824978.

[59] F. Cottin *et al.*, "Effect of oral glucocorticoid intake on autonomic cardiovascular control," *SpringerPlus*, vol. 4, no. 1, p. 622, Dec. 2015, doi: 10.1186/s40064-015-1378-8.

[60] S. V. Koenen, C. A. Mecenas, G. S. Smith, S. Jenkins, and P. W. Nathanielsz, "Effects of maternal betamethasone administration on fetal and maternal blood pressure and heart rate in the baboon at 0.7 of gestation," *American Journal of Obstetrics and Gynecology*, vol. 186, no. 4, pp. 812–817, Apr. 2002, doi: 10.1067/mob.2002.121654.

[61] D. J. Brotman *et al.*, "Effects of Short-Term Glucocorticoids on Cardiovascular Biomarkers," *The Journal of Clinical Endocrinology & Metabolism*, vol. 90, no. 6, pp. 3202–3208, Jun. 2005, doi: 10.1210/jc.2004-2379.

[62] K. Verdurmen, L. J. Van, and S. Oei, "Corticosteroids and fetal heart rate variability," *Journal of Maternal-Fetal and Neonatal Medicine*, vol. 27, pp. 361–361, 2014, doi: 10.3109/14767058.2014.924236.

[63] K. M. J. Verdurmen *et al.*, "The influence of betamethasone on fetal heart rate variability, obtained by non-invasive fetal electrocardiogram recordings," *Early Human Development*, vol. 119, pp. 8–14, Apr. 2018, doi: 10.1016/j.earlhumdev.2018.02.011.

[64] K. Grym *et al.*, "Feasibility of smart wristbands for continuous monitoring during pregnancy and one month after birth," *BMC Pregnancy Childbirth*, vol. 19, no. 1, p. 34, Dec. 2019, doi: 10.1186/s12884-019-2187-9.

[65] A. Choi and H. Shin, "Photoplethysmography sampling frequency: pilot assessment of how low can we go to analyze pulse rate variability with reliability?," *Physiol. Meas.*, vol. 38, no. 3, pp. 586–600, Mar. 2017, doi: 10.1088/1361-6579/aa5efa.

[66] J. W. Samways *et al.*, "Maternal heart rate during the first 48 h postpartum: a retrospective cross sectional study," *European Journal of Obstetrics & Gynecology and Reproductive Biology*, vol. 206, pp. 41–47, Nov. 2016, doi: 10.1016/j.ejogrb.2016.08.040.

[67] A. A. Mahendru, T. R. Everett, I. B. Wilkinson, C. C. Lees, and C. M. McEniery, "A longitudinal study of maternal cardiovascular function from preconception to the postpartum period:," *Journal of Hypertension*, vol. 32, no. 4, pp. 849–856, Apr. 2014, doi: 10.1097/HJH.0000000000000090.

[68] M. W. Groer, C. M. Jevitt, F. Sahebzamani, J. W. Beckstead, and D. L. Keefe, "Breastfeeding Status and Maternal Cardiovascular Variables Across the Postpartum," *Journal of Women's Health*, vol. 22, no. 5, pp. 453–459, May 2013, doi: 10.1089/jwh.2012.3981.

[69] H.-G. Kim, E.-J. Cheon, D.-S. Bai, Y. H. Lee, and B.-H. Koo, "Stress and Heart Rate Variability: A Meta-Analysis and Review of the Literature," *Psychiatry Investig*, vol. 15, no. 3, pp. 235–245, Mar. 2018, doi: 10.30773/pi.2017.08.17.

Chapter 8

Change in maternal heart rate variability and photoplethysmography morphology in response to corticosteroid administration

8

Reproduced after: M Bester, TJ Nichting, R Joshi, L Aissati, SG Oei, M Mischi, JOEH van Laar, R Vullings. Change in maternal heart rate variability and photoplethysmography morphology in response to corticosteroid administration; a prospective, observational study. *Under review*. 2023.

Abstract

Background: Owing to the association between dysfunctional maternal autonomic regulation and pregnancy complications, assessing non-invasive features which reflect autonomic activity – such as heart rate variability (HRV) and the morphology of the photoplethysmography (PPG) pulse wave – may be useful for tracking maternal health. Consequently, research into the autonomic regulation of women with pregnancy complications is ongoing. However, women with early pregnancy complications typically receive medication, such as corticosteroids. The effect of this medication on maternal HRV and PPG pulse wave morphology is not well-researched. In this work, we performed a dedicated study to assess the effect of betamethasone (a commonly used corticosteroid) on non-invasively assessed features.

Methods: A prospective, observational study was performed at a tertiary care hospital. A total of 61 women with an indication for corticosteroids for fetal lung maturation (specifically, betamethasone, which is administered intramuscularly via two injections given 24 hours apart) were enrolled. These women wore a wrist-worn PPG device for at least four days. Five-minute measurements were selected for analysis from these data. Specifically, a baseline measurement was selected either before betamethasone administration or sufficiently thereafter (i.e., three days after the last injection). Furthermore, measurements were selected 24, 48, and 72 hours after betamethasone administration. HRV features in the time domain and frequency domain, as well as those describing heart rate (HR) complexity, were calculated. Furthermore, features describing the morphology of the PPG pulse wave were calculated, e.g., the area under the curve of the pulse wave. These features were compared between the different days.

Results: Maternal HR was significantly higher and HRV features linked to parasympathetic activity were significantly lower 24 hours after betamethasone administration. Features linked to sympathetic activity remained stable. Furthermore, betamethasone appears to have a vasoconstrictor effect on the morphology of the PPG pulse wave.

Conclusions: The administration of betamethasone affects maternal autonomic regulation and cardio-vasculature. Researchers assessing maternal HRV in women with pregnancy complications should take care to schedule measurements before or sufficiently after corticosteroid administration. Further investigation is needed to understand whether the administration of these drugs has long-term effects on maternal physiology.

Trial registration: NL8204; 06/12/2019

1. Introduction

The detection of pregnancy complications before the onset of their detrimental symptoms is a persistent challenge in perinatology. The early detection of complications allows for pharmaceutical or lifestyle interventions, as well as improved monitoring, which leads to improved perinatal outcomes [1], [2].

A promising monitoring tool for detecting the early onset of deterioration in maternal health is the assessment of maternal heart rate variability (mHRV) [3]–[5]. Given that changes in heart rate (HR) are regulated by the autonomic nervous system (ANS) [6] – and further considering that women with pregnancy complications have altered ANS activity compared to their healthy counterparts [7]–[9] – abnormalities in mHRV may be predictive of pregnancy complications. The use of mHRV to screen for abnormalities requires a clear understanding of how mHRV is altered during complicated pregnancies. Consequently, several researchers have investigated how mHRV is altered in women with pregnancy complications [3], [9], [10].

However, investigations into the mHRV of women with complicated pregnancies have been hindered by the routine administration of obstetric medications, such as tocolytics, beta-blockers, and corticosteroids, which are administered to women upon the diagnosis of complications. As the effect of these medications on mHRV is largely unknown, it is uncertain to which degree changes in HRV in this population reflect autonomic dysregulation associated with pregnancy complications, as opposed to merely reflecting the confounding effect of these medications [10]–[13].

While the impact of all routine obstetric medications warrants investigation, the drug most administered to pregnant women with complications is corticosteroids. Corticosteroids – specifically, betamethasone – are maternally administered for fetal lung maturation in anticipation of preterm labor, which is a typical concern in cases of early pregnancy complications [14]. Researchers have already shown that administering betamethasone invokes changes in fetal HR and HRV [15]–[17]. Furthermore, betamethasone is a glucocorticoid, with the latter being a class of drugs known to activate the cardiac stress response [18]. Therefore, we hypothesize that mHRV also changes in response to betamethasone administration.

Consequently, we set out to quantify the effect of antenatally administered corticosteroids (specifically, betamethasone, which is commonly used in antenatal care)

on mHRV based on continuous photoplethysmography (PPG) recordings performed in women hospitalized with pregnancy complications. Furthermore, as a sub-analysis analysis, we also examine the changes in the morphology of the PPG pulse-wave signal after betamethasone administration to gain further insight into the effect of corticosteroids on maternal physiology.

2. Methods

The Methods section details the prospective, observational study performed to collect PPG data from women who were administered betamethasone (Section 2.1). Thereafter, the analyses performed in this paper are detailed, specifically, a main analysis and a sub-analysis to determine the effect of corticosteroids on mHRV (Section 2.2) and the morphology of the maternal PPG pulse wave (Section 2.3), respectively. Finally, the statistical analysis of the data is described (Section 2.4). All processing is done in Python (PSF, USA).

2.1 Study design

Pregnant women admitted to the obstetric high care unit at Máxima Medical Center (Máxima MC) who had an indication for betamethasone (Celestone Chronodose®, Schering AG, Berlin, Germany; 2 doses of 12 mg intramuscularly, 24 h apart) but had not yet received their second injection, were invited to participate in this study. Such admissions are typically done with urgency as these patients are at risk of preterm birth. Consequently, this study – of which the protocol has been published [19] – was designed to have a low impact on clinical workflow. To this end, enrolled women received a wristband-like device to wear for the duration of their hospitalization which recorded PPG and tri-axial accelerometer data. This device (Philips Data Logger, Philips Research, Eindhoven, the Netherlands) continuously recorded the data at 32 Hz and offloaded it via Bluetooth to an accompanying mobile phone kept in the patient's room, which served as a data storage device. All women were at least 18 years old and without medical equipment or tattoos on their wrists that could obstruct data collection with the PPG device.

Patient metadata (e.g., complication, age, and medications along with the timing of their administration) were collected from patient medical records. The co-administration of medications was unavoidable since this was part of the standard treatment protocol [20]–[22]. To attenuate contractions in cases of threatened preterm labor,

tocolytics such as nifedipine or atosiban were administered. Antibiotics such as azithromycin or penicillin were administered to prevent infections, for example in the case of preterm rupture of membranes. Additionally, women with hypertensive disorders of pregnancy could receive antihypertensive medications; specifically, methyldopa or labetalol. Magnesium sulfate can also be administered in cases of preeclampsia or for fetal neuroprotection.

All participants gave oral consent followed by delayed written consent. A waiver was granted for the study by the Máxima MC (N19.112; 02/12/2019) and the study is registered in the Dutch Trial Register (NL8204; 06/12/2019).

2.2. Main analysis: the effect of administering betamethasone on mHRV

The main purpose of this work is to determine the effect of betamethasone on mHRV using a within-subject (paired) analysis. We compare HRV features at baseline (i.e., without the influence of betamethasone) against HRV in the days following betamethasone administration, as outlined in Figure 1. Since women who receive corticosteroids in the antenatal period are heterogeneous in terms of their pregnancy complications, age, gestational age, etc., a within-subject analysis was chosen to minimize the effect of these differing characteristics [9], [23]. Moreover, this choice was also made to reduce the impact of circadian rhythms on the analysis [24]; since betamethasone can be administered at any time, one participant may receive their first betamethasone injection at noon while another receives theirs at midnight.

In the following sections, we outline the timing and selection of the PPG segments used for this analysis, the preprocessing of these segments for determining HRV, and the calculation of the HR and HRV features, with the latter comprising time-domain, frequency-domain, and non-linear features.

2.2.1 Timing of measurements

For calculating HRV, five-minute PPG segments were identified from the continuous PPG recordings for each day, as outlined in the next section (2.2.2). Acquiring a baseline measurement before the participant receives betamethasone is challenging, partly because corticosteroids are typically urgently administered. Moreover, given that Máxima MC (the study site) is a tertiary teaching hospital, women are often transferred here after initial diagnosis and treatment at their primary hospital. Consequently, most women would have already received their first betamethasone injection before arriving at Máxima MC. To this end, for the main analysis concerning

mHRV, we defined the baseline measurement as either before the first betamethasone injection (noted as *day 0* in Figure 1), or sufficiently thereafter. In the latter case, *day 4* was used as the baseline measurement, based on the pharmacokinetics of betamethasone (a biological half-life of 36 – 59 hours [25], [26]) and the duration of the drug's effect on fetal HR and HRV (approximately 48 hours [15]–[17]). This decision is further detailed in the study protocol [19]. Additionally, active measurements are acquired approximately 24 hours, 48 hours, and 72 hours after the first injection (± 4 hours), i.e., *days 1, 2*, and *3*. Note that measurements on *day 0* and *day 1* had to precede the first and second injections of betamethasone, respectively.

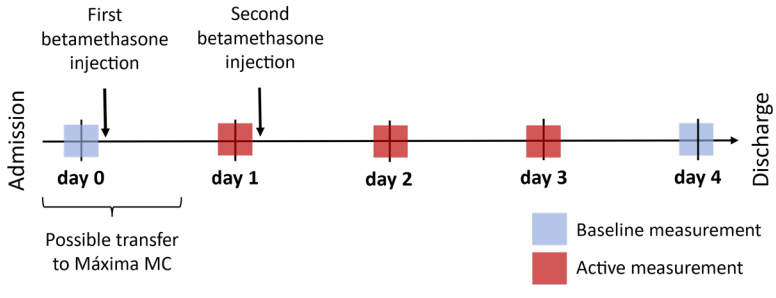

Figure 1: Five-minute measurements are selected preceding (if possible) and following the administration of betamethasone to assess the effect of this medication on mHRV and PPG pulse wave morphology. This figure illustrates the timing of the measurements on *days 0* to *4*. The measurement from *day 0* is the baseline measurement; if not available, the measurement from day 4 can be used as a baseline measurement. Note that measurements on *day 0* and *day 1* have to precede the first and second injections of betamethasone, respectively.

2.2.2 Segment selection

Furthermore, even though participants in this study were hospitalized for its duration, the study setup resembled a study with free-living conditions as the women were free to move their extremities as well as remove and reattach the PPG wristband. Consequently, motion artifacts and periods of sensor detachment were common in the data. Considering these limitations, as well as the constraints regarding the timing of the measurements, the data segments to be included were manually selected through exploratory data analysis. A single, contiguous five-minute segment was chosen for each *day*. Segments used for the analysis had to have no more than 20% of the inter-pulse intervals (IPI) discarded during preprocessing, as defined in Section 2.2.3.

In cases where a measurement for *day 0* was available, the measurement moment was chosen to be as close to one hour before the first betamethasone injection as

possible, considering the timing constraints for the subsequent measurements (i.e., within 24 hours, ± 4 hours) as well as the requirement for data quality discussed in the preceding paragraph. If *day 0* was not available, *day 1* was similarly chosen with regards to the second betamethasone injection, again with the consideration of the timing of subsequent measurements and data quality.

2.2.3 Preprocessing of PPG measurements for HRV analysis

For the HRV analysis, the IPI values are calculated as the difference between two contiguous waveform troughs, which are detected using a published algorithm [27]. IPIs were disregarded when considered physiologically implausible, i.e., when shorter or longer than 0.4 or 2.0 seconds, respectively, or when differing from their preceding interval by more than 20%. For the calculation of HRV features that relate to the frequency domain or complexity, a continual time series is needed, and subsequently, missing IPIs are replaced with cubic spline interpolation when calculating these features.

2.2.4 Determining HR and HRV features

First, the average of all the IPIs from each segment was determined and then converted to beats per minute (bpm) to obtain the HR. Thereafter, several HRV features were calculated. In the time domain, the standard deviation of the IPIs (SDNN) is calculated to capture overall HRV. Additionally, two features that capture parasympathetic activity were calculated, namely, the root mean square of the successive differences of the IPIs (RMSSD), and the percentage of consecutive IPIs differing by more than 50 ms (pNN50) [6], [28].

Furthermore, HRV can also be assessed in the frequency domain. To this end, we calculate the following features: the total power (TP) in the frequency domain, the power in the high-frequency band of 0.15–0.40 Hz (HF), the power in the low-frequency band of 0.04–0.15 Hz, and the ratio between the two (LF/HF). While LF is influenced by both branches of the ANS (i.e., both parasympathetic and sympathetic activity), HF captures mainly parasympathetic activity. Consequently, LF/HF provides information on the balance between the two branches by capturing what is referred to as the sympathovagal balance [6], [28].

We further determine some non-linear features of HRV. We use a Poincaré plot, which is a scatter plot of each IPI plotted against its predecessor. An ellipse is then fitted to this plot and two standard descriptors, namely SD1 and SD2, are calculated to represent the short- and long-term HRV, respectively. Similar to LF/HF, the ratio of these

– SD1/SD2 – offers a window into sympathovagal balance [6], [29], as short-term and long-term variability are primarily modulated by parasympathetic and sympathetic activity, respectively. Additionally, we assess the complexity of the signal represented by the IPIs with Sample entropy (SampEn) [30], [31]. SampEn quantifies the conditional probability that two epochs, which are similar within a tolerance r for a window length m, will remain similar when including the next data point (i.e., the next IPI). The parameters m and r were set to 2 and 0.2 times the standard deviation of the IPIs. Lower SampEn indicates a more predictable time series, i.e., a time series with higher regularity. Finally, we use detrended fluctuation analysis (DFA) [32], which is used to quantify the self-similarity of IPIs over time. A healthy HR pattern is not completely random. However, a healthy HR is also not fully predictable, rather, the HR time series contains trends that will repeat over different timescales. Using α_1, the short-term fractal scaling exponent of the DFA, which represents the correlation in the IPIs over 4–16 heartbeats, we can capture this characteristic of the HR. An α_1 of 1 suggests a high level of self-similarity. As α_1 decreases, the HR time series becomes more predictable [30], [33].

2.3. Sub-analysis: the effect of administering betamethasone on the morphology of the PPG pulse wave

The effect of betamethasone on the morphology of the PPG pulse wave (hereafter referred to as morphological features) has not previously been investigated to our knowledge. Consequently, for the sub-analysis – i.e., investigating the impact of betamethasone on maternal morphological features – no prior information is available to support the use of *day 4* as a suitable baseline measurement (as seen in Figure 1). Subsequently, we do not group *day 0* and *day 4* as baseline measurements but rather perform an unpaired analysis across all five *days* to examine the impact of betamethasone on the pulse wave. The same segments used in the HRV analysis (see Sections 2.2.1 and 2.2.2) are also used for this analysis.

2.3.1 Preprocessing of PPG measurements for analysis of morphological features

To determine the PPG features assessed in this study, the PPG pulse wave needs to be segmented to identify the relevant fiducial points, namely the initial trough (IT), systolic peak (SP), and final trough (FT), as seen in Figure 2. To this end, NeuroKit2 – a publicly available Python package for analyzing physiological signals [34] – was used. Pulses for which these fiducial points were not detected were excluded from the analysis, as these points are needed to calculate the features described in Section 2.3.2.

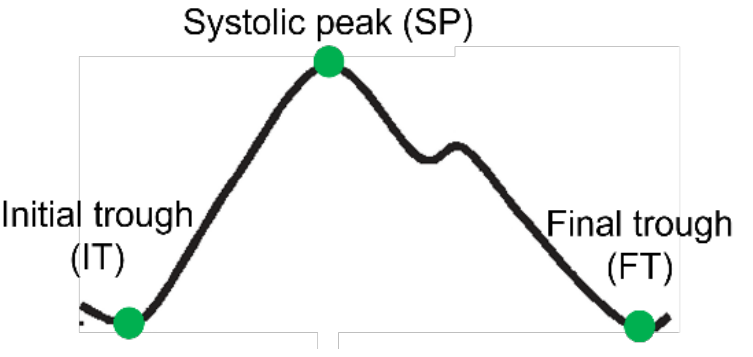

Figure 2: PPG pulse wave with relevant fiducial points

2.3.2 PPG-morphology features

The PPG pulse wave is a reflection of the blood flow through the vascular bed [35]. The initial rising edge of the pulse wave (i.e, from IT to SP, Figure 2) reflects the systolic phase of the heartbeat, while the falling edge corresponds to the diastolic phase (SP to FT). By assessing features describing the morphology of this pulse wave, we gain insight into vascular tone and by proxy its regulation via the ANS. While the exact mechanisms originating the different components of the PPG pulse wave are not known, these features are generally considered to provide valuable physiological information [35]. The features that are used to describe the waveform are shown in Figure 3 with corresponding descriptions in Table 1 [36]–[38]. Note that in addition to describing the geometry of the PPG pulse wave, features detailing the first – and second derivatives of the PPG pulse wave are also often used.

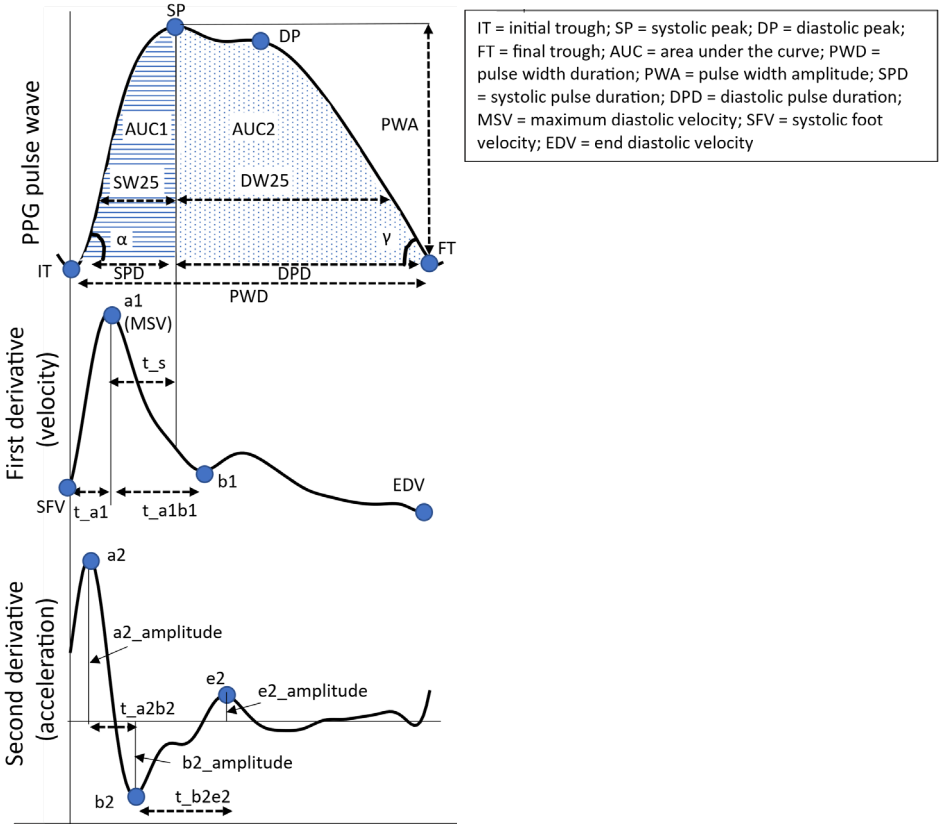

Figure 3: The top figure represents the PPG waveform, followed by the first and second derivatives of the waveform. Aspects of these waveforms relevant to the PPG morphology features listed in Table 1 are indicated in the figures.

Table 1: Description of the morphological features. The fiducial points on the PPG pulse wave discussed in the table can be found in Figure 3. Note that in Figure 1, DW25 and SW25 can be found, which represent the diastolic and systolic widths at 25% of the amplitude. Where features such as DW are mentioned in the table, these are similar to DW25, but at 10% instead of 25%.

Features		Explanation
Amplitude	PWA	Pulse width amplitude, i.e., the difference between SP and IT.
	b2_ amplitude	The absolute value of the amplitude of the deepest trough of the second derivative signal (b2)
Time differences	PWD	Pulse width duration; time interval between IT and FT.
	SPD	Systolic phase duration; time interval between IT and SP
	DPD	Diastolic phase duration; time interval between SP and FT
	t_a1	Time interval between IT and a1 on the first derivative signal
	t_a1b1	Time interval between the a1 and the first valley of the first derivative signal (b1)
	t_a2b2	Time interval between points a2 and b2 on the second derivative signal
	t_b2e2	Time interval between points b2 and e2 on the second derivative signal
AUC	AUC_total	AUC of the full pulse wave, i.e., between IT and FT
	AUC1	AUC of systolic phase, i.e., between IT and SP
	AUC2	AUC of diastolic phase, i.e., between SP and FT
Velocity and acceleration	mean(V)	Mean velocity, i.e., mean of the first derivative signal
	IDR(V)	Interdecile range of velocity, i.e., interdecile range of the first derivative signal
	Mean (Acc)	Mean of the second derivative signal
	MSV	Max systolic velocity; a1 on the first derivative
	SFV	Systolic foot velocity, i.e., value of the point on the first derivative signal corresponding to IT of the pulse wave

Ratio	DW10/SW10	The ratio of systolic width to diastolic width at 10% of the pulse wave amplitude; similar features are calculated at 25%, 50%, and 60%.
	t_s/PWD	The ratio between the time interval between a1 and SP (i.e., t_s), and the pulse width duration (PWD), which is the time interval between IT and FT.
	t_a1/PWD	The ratio of the time interval between the IT and a1 (i.e., t_a1) to PWD
	t_a1b1/PWD	The ratio of t_a1b1 to PWD
	t_a2b2/ PWD	The ratio of t_a2b2 to PWD
	t_b2e2/ PWD	The ratio of t_b2e2 to PWD
	b2/a2	The ratio of b2_amplitude to a2_amplitude, found on the second derivative signal
	e2/a2	The ratio of e2_amplitude to a2_amplitude, found on the second derivative signal
	SPD/PWD	The ratio of SPD to PWD
	SP/SPD	The ratio of the value of SP to SPD
	Pulsatility index	(Max systolic velocity (i.e., a1 on the first derivative) – end diastolic velocity (i.e., EDV on the first derivative) / (mean of the first derivative)
Slope	slope_IT_SP	The slope of line that connects IT and SP
	slope_SP_FT	The slope of line that connects SP and FT
Angle	α	The angle of the slope between IT and SP
	γ	The angle of the slope between SP and FT

2.4 Statistical analysis

A sample size of 61 was calculated using a two-sided t-test for a confidence interval of 95% and a power assumption of 80% (see protocol for further details [19]). As physiological data is typically non-parametrically distributed, we perform a nonparametric analysis throughout. As discussed in Section 2.2, a within-subject analysis is performed to compare HRV across the different *days* using Friedman's test with Dunn's post-hoc test. The prior provides information as to whether statistically significant changes occur across the four *days* analyzed while the latter reveals whether statistically significant differences exist between specific *days*, e.g., *day 1* and *day 3*. Bonferroni correction was implemented to control for family-wise error. Furthermore, an unpaired analysis was performed to investigate changes in morphological features

using a Kruskal-Wallis test with a Dunn's post-hoc test and Bonferroni correction to control for family-wise error. Note that the statistical analysis that was presented in the protocol has been updated in this work; the authors believe the analysis presented here is the more appropriate one. A value of $p < 0.05$ was considered statistically significant. Furthermore, effect sizes are reported along with statistical significance using Cohen's d, where 0.2 amounts to a small effect, 0.5 to a medium effect, and 0.8 to a large effect. We further perform a bootstrapping procedure (10,000 iterations) and report the subsequent mean d-value along with the 95% confidence intervals (CI), as is appropriate in non-parametric analyses [39].

3. Results

First, we describe the included participants in the study (Section 3.1). Thereafter, we present the results from the within-subject analysis performed to determine the effect of administering betamethasone on mHRV (Section 3.2). Following this, the results from the sub-analysis which investigates the effect of this drug on morphological features are given (Section 3.3). Results are presented as plots of the median values and interquartile ranges of the features; appropriate statistics are displayed on the figures.

3.1 Study group

A total of 143 women were enrolled in the study between July 2020 and January 2022. Of these, 61 women had sufficient measurements to be included in the analysis. Participant demographics are outlined in Table 2. Eight women had a *day 0* measurement to use for the baseline measurement, while *day 4* was used for the others.

Table 2: Characteristics of the patients included in the study. Where applicable, values are presented as median with interquartile range.

Characteristic	
Indication for betamethasone (no. of participants)	
Threatened preterm labor	31
Vaginal bleeding	4
Preterm rupture of membranes	8
Preeclampsia and/or HELLP syndrome*	13
Pregnancy induced hypertension	1

Fetal growth restriction	2
Non-obstetric operation	1
Suspicion of twin anemia polycythemia sequence	1
Gestational age at first betamethasone injection	28 weeks (26 weeks 3 days – 30 weeks)
BMI (pre-pregnancy)	24.95 (22.05 – 27.70) kg/m^2
Age	31 (27 – 33) years
Nulliparous	59.7%
Pregnancy with multiples	24.2%
Co-administration of medications during study period (no. of participants)	
Atosiban	11
Azitromycin	11
Nifidipine	19
Penicillen	2
Magnesium sulphate	19
Methyldopa	5
Labetalol	7

*HELLP = Hemolysis, Elevated Liver enzymes and Low Platelets

3.2 Main analysis: the effect of administering betamethasone on mHRV

The results of the HR and the three sets of HRV features corresponding to the *baseline*, *day 1*, *day 2*, and *day 3*, are plotted in Figures 4 to 6. The medians of the values are plotted, and the shaded area represents the interquartile ranges. The *p*-value of the overall significance of changes across the *days* is presented in the top-left corner of the graphs, while the statistical significance and effect size of differences between specific *days* are indicated with arrows at the bottom of the graphs. Of the included participants, 57 had data available for each *day* and were included in this section of the analysis. For the *baseline*, a median of 2.4% of IPIs was removed as specified in Section 2.2.3, while for *day 1*, *day 2*, and *day 3*, 3.6%, 3.2%, and 2.8% were removed, respectively.

3.2.1 Mean HR and time-domain HRV features

From Figure 4, we see that all time-domain features are significantly affected. HR increases significantly by about 10 bpm in the 24 hours after the first betamethasone injections, with a mean d of 0.7 (note: *day 1* is the time point preceding the second injection being administered). RMSSD and pNN50, which are features linked to parasympathetic activity, show medium to large decreases on *day 1* compared to the baseline and a statistically significant decrease compared to *day 3*.

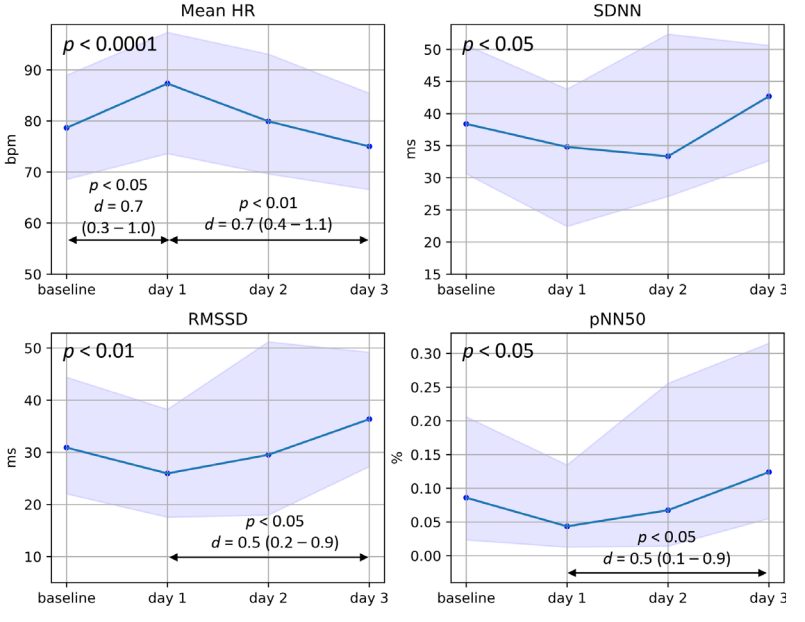

Figure 4: Plots of the median and interquartile ranges of maternal HR, SDNN, pNN50, and RMSSD in the days following betamethasone administration. The baseline represents measurements taken before the first injection of betamethasone or 96 hours thereafter, while *day 1* represents 24 hours after the first injection, and *days 2* and *3* represent 48 and 72 hours thereafter, respectively. The statistical significance (p-value) for changes across the four days is presented in the top-left corner of each graph, while differences between specific *days* are represented with arrows and corresponding p-values and d-values.

3.2.2 Frequency-domain HRV features

In Figure 5, we see that TP, HF, and LF/HF change significantly change across the four *days*, while LF (which is linked to sympathetic activity) is not significantly altered. HF, which is parasympathetically modulated, was specifically significantly reduced on *day 1* as compared to *day 3*.

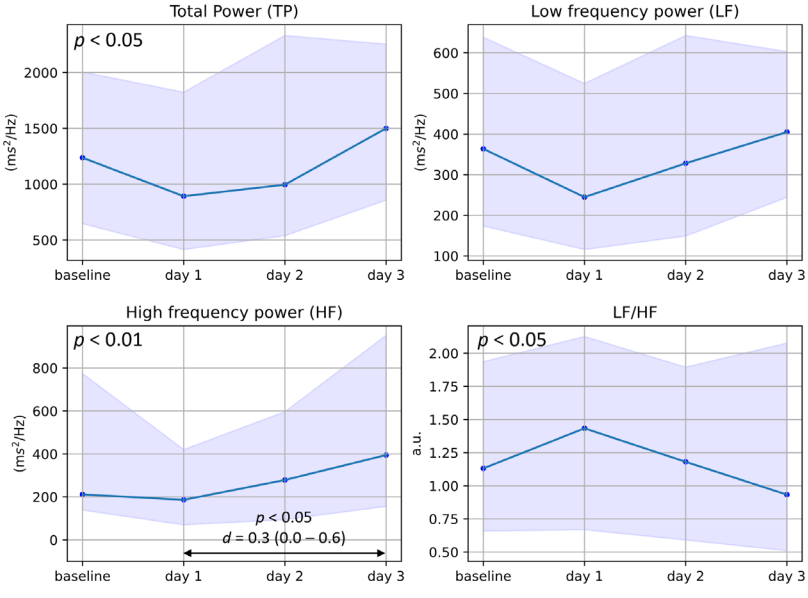

Figure 5: Plots of the median and interquartile ranges of maternal TP, LF, HF, and LF/HF in the days following betamethasone administration. The baseline represents measurements taken before the first injection of betamethasone or 96 hours thereafter, while *day 1* represents 24 hours after the first injection, and *days 2* and *3* represent 48 and 72 hours thereafter, respectively. The statistical significance (p-value) for changes across the four days is presented in the top-left corner of each graph, while differences between specific days are represented with arrows and corresponding p-values and d-values.

3.2.3 Non-linear HRV features

Of the non-linear or complexity features (Figure 6), only SD1/SD2 was found to change significantly across the four *days*, with a decrease on *day 1* compared to baseline followed by an increase on *day 2*. Furthermore, SampEn shows a significant difference between *day 1* and *day 2*. Note that a decrease in SD1/SD2 indicates similar physiological changes as an increase in LF/HF, namely increased long-term variation and/or decreased short-term variation.

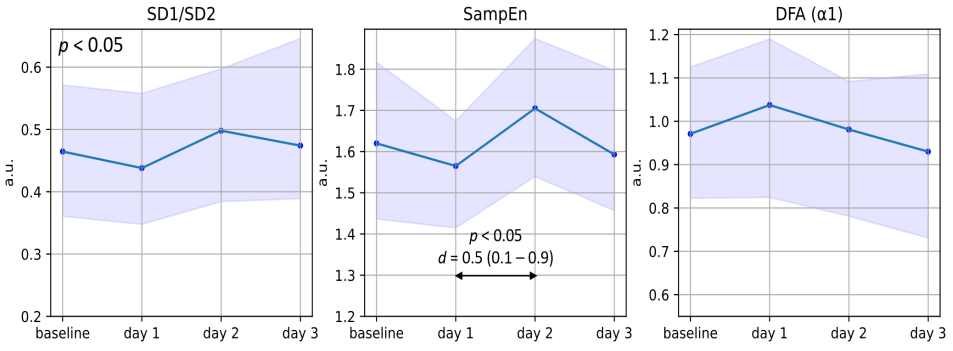

Figure 6: Plots of the median and interquartile ranges of maternal SD1/SD2, SampEn, and DFA α_1 in the days following betamethasone administration. The baseline represents measurements taken before the first injection of betamethasone or 96 hours thereafter, while *day 1* represents 24 hours after the first injection and *days 2* and *3* represent 48 and 72 hours thereafter, respectively. The statistical significance (p-value) for changes across the four days is presented in the top-left corner of each graph, while differences between specific days are represented with arrows and corresponding p-values and d-values.

3.3 Changes in maternal morphological features

The results from the unpaired analysis of the effect of betamethasone on morphological features are reported in this section. Note that an unpaired analysis was performed. The number of participants from which measurements (as defined in Section 2.3) were available for each *day* was as follows: eight for *day 0*, 60 for *day 1*, 60 for *day 2*, 56 for *day 3*, and 53 for *day 4*.

In Figure 7, the ensemble averages of all analyzed PPG pulse waves are plotted per *day*. Notice that the waveform becomes noticeably smaller from *day 0* to *day 4*. However, the difference between day 0 and the other days may be overestimated as measurements from only eight participants are included for *day 0*, while over 50 are included for the other *days*. While no significant differences were found in the morphological features describing the area or amplitude of the PPG waveform, several other features had significant changes in the days following betamethasone administration. The angle between the IT and SP (α), SP/SPD, b2_amplitude, dw10/sw10, dw25/sw25, PSV, and FSV all decrease significantly across the five days, while t_a1 and t_a1/PWD increase significantly. The SPD also changes significantly, specifically with a statistically significant increase from *day 1* to *day 3* and *day 4*. The overall effect sizes of these changes were small to medium. Other features introduced in Table 1 showed no significant changes.

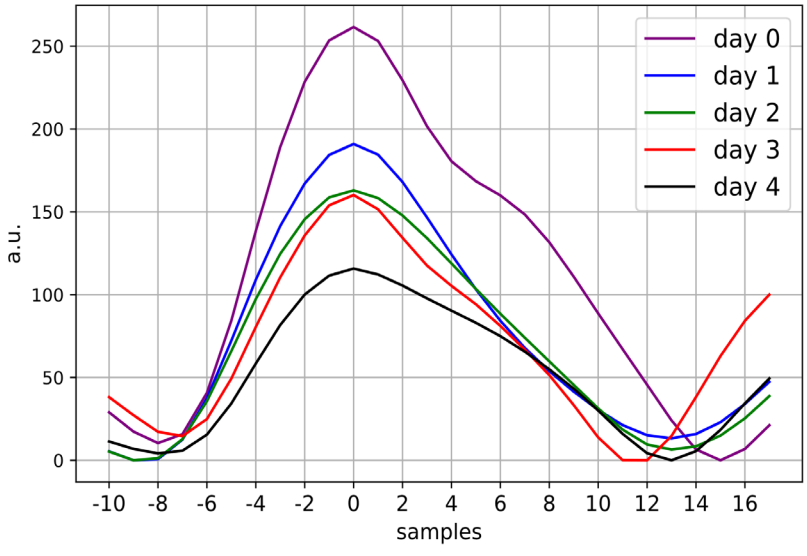

Figure 7: Ensemble averages of the PPG pulse waves analyzed for each day. The waveform becomes increasingly smaller from *day 0* to *day 4*, with *day 0* corresponding to the measurement before betamethasone is administered. *Day 1*, *day 2*, *day 3*, and *day 4* correspond to measurements taken 24, 48, 72, and 96 hours after the first betamethasone injection.

4. Discussion

Monitoring mHRV during pregnancy may offer novel opportunities for assessing maternal health and in doing so, aid in the early detection of pregnancy complications. Facilitating such assessments requires not only an understanding of how pregnancy complications affect mHRV but also how other confounding factors may alter mHRV. A potential confounder that is often present when assessing mHRV in complicated pregnancies is the effect of antenatal corticosteroids. In this work, we show that corticosteroids – specifically, betamethasone – indeed affect mHRV by increasing HR and decreasing HRV features linked to parasympathetic activity. Furthermore, we demonstrate for the first time, to our knowledge, how the PPG pulse wave morphology changes in response to corticosteroid administration.

Accurately assessing mHRV in women with pregnancy complications can be challenging. Women with complications such as threatened preterm birth, preterm rupture of membranes, or preeclampsia are typically admitted to the hospital upon diagnosis where they are administered medications such as corticosteroids with urgency.

Therefore, acquiring measurements without the influence of such medications is not trivial. Some researchers avoid this by performing short measurements before corticosteroids are administered [9], [40], while others mention these obstetric medications as potential confounders in their limitations [11], [12]. Others still make no mention of corticosteroids, even though according to standard treatment protocols it is likely that their population would have been administered these medications [13], [41]–[43].

Based on the results presented in this paper, we see that the effects of corticosteroids are not negligible, particularly up to the 72 hours following the first injection of betamethasone. Although the results on mHRV in complicated pregnancies are conflicting at times – potentially in part due to the influence of obstetric medications such as corticosteroids [10] – on average, pregnancy complications seem to be characterized by increased maternal sympathetic activity and decreased parasympathetic activity [44]–[46]. As corticosteroids seem to not affect sympathetic activity (see LF, Figure 5), likely, the increased sympathetic activity as captured by mHRV in complicated pregnancies is accurate. This increase is also confirmed by microneurography investigations, which directly measure sympathetic nerve activity [7], [8]. However, care should be taken when interpreting studies showing reduced parasympathetic activity, as this could also result from or at least be amplified by the administration of corticosteroids. Considering the results of this study, along with the 36 – 59 hours biological half-life of betamethasone [25], [26], i.e., the half-life of its suppression of the hypothalamus-pituitary-adrenal (HPA) axis, we suggest that assessments of mHRV in complicated pregnancies should be done either before or at least 72 hours after the second betamethasone injection to minimize the confounding effect of this medication. However, it should be noted that we could not confirm how similar measurements are on *day 0* and *day 4*, as only two participants had both measurements available.

In addition to the reduced parasympathetic activity, we also find that maternal HR is elevated by about 10 bpm (Figure 4) in the 24 hours after the first betamethasone injection. Note that the measurement on *day 1* is taken before the second injection of betamethasone is given; therefore, the increased HR is not a response to pain due to the injection. In recent work, we investigated the effect of corticosteroids on mHRV as determined from abdominal ECG measurements in a smaller group of hospitalized pregnant women [46]. In this previous work, we also found decreased parasympathetic activity along with a 10 bpm increase in HR in the 24 hours after betamethasone administration – similar to the results observed in this work [46]. As vital signs such as

maternal HR informs clinical decision-making [47]–[49], clinicians need to consider recent corticosteroid administration when evaluating maternal tachycardia.

In evaluating the results from the PPG pulse wave analysis (Figure 7), we find that several features reduce in the days following betamethasone administration. The effect of corticosteroids on the PPG pulse wave has not been previously demonstrated but the decreasing size of the waveform seen in Figure 7 after betamethasone administration does appear to correspond to the vasoconstrictive effect of glucocorticoids – the class of steroids to which corticosteroids belong – on blood vessels [50]. Whether this has a wider impact on maternal physiology – for example, a corresponding increase in blood pressure – is currently unknown. But as in the case of HRV, the effects of corticosteroids on the PPG pulse wave are not negligible.

The effects observed in mHRV, and maternal PPG morphology likely result from the pharmacodynamics of betamethasone, specifically how this drug interacts with the human stress response. During the body's stress response – typically partly mediated by the sympathetic nervous system – natural glucocorticoids are synthesized and these are perceived as cortisol which binds to glucocorticoid receptors, resulting in increased blood pressure (by way of vasoconstriction), increased HR, and decreased vagal tone [18]. Here, betamethasone (a synthetic glucocorticoid) administration leads to the same effect (Figures 4 and 7), but the sympathetic response is subverted (see LF in Figure 5) since there is no internal stimulus for the cardiac stress response but rather an external one via the injection medication. Once this increased level of glucocorticoids is detected in the bloodstream, the HPA-axis is suppressed. The biological half-life of this suppression is 36 – 59 hours [25], [26]; subsequently, the effect of betamethasone should start to diminish on day 2 and day 3, as is confirmed by the decreasing HR and the increase in HRV features linked to parasympathetic activity (Figures 4 and 5). Future work is needed to understand why HR seems to decrease and HRV seems to increase past the baseline on *day 3*. We speculate that on *day 3* the effects of the HPA-axis suppression may have worn off while the impact of the newly secreted cortisol is not yet seen in the HR and HRV features.

Furthermore, it is interesting that the opposite effect is observed in the mother than in the fetus. The literature reports that fetal HR typically decreases and HRV increases in the first 24 hours after betamethasone administration [15]–[17]. However, it should be noted that the half-life of betamethasone in the mother is half of that in the fetus [51], meaning that the effects on the maternal and fetal systems are potentially occur-

ring at different timescales. Still, future work is needed to understand whether this is indeed the case or whether the mother and fetus in fact have different physiological reactions to betamethasone administration.

This study has some limitations. Firstly, it is not possible to quantify the effect of the stress of the participants' hospitalization on the results. Moreover, several medications were co-administered to the participants as part of their standard treatment; this is unavoidable. Evaluating the impact of these medications on mHRV and PPG morphology in this study group is not feasible, as they are administered at different times and in different dosages. A dedicated study would be necessary to determine the effect of these co-administered medications. However, the fact that we see a clear impact of corticosteroids on the outcome measures despite the heterogeneity of the participants increases our confidence that corticosteroids indeed affect maternal physiology. Furthermore, these results largely confirm those of previous work in our group, where we assessed the impact of corticosteroids on mHRV in a similar population, as calculated from abdominal ECG recordings [46]. In this previous work, we performed sub-analyses to explore the impact of additional obstetric medications. We did so by repeating our analysis, first excluding women who received nifedipine, which was the most commonly co-administered medication, and second, excluding those using anti-hypertensives, which are known to affect mHRV [46]. In both cases, the trends in mHRV in the days following betamethasone administration were similar to those observed in the main analyses, which included all participants [46].

Furthermore, using wrist-worn PPG data for such an analysis comes with some inherent limitations. These data are very prone to motion artifacts and therefore, despite the large amount of data collected, only five-minute measurements were used for this analysis. Furthermore, measurements were collected at different times of the day since corticosteroids are administered at varying times. To this end, we performed a within-subject analysis for the mHRV analysis to minimize the effect of circadian rhythms on the results. However, these differences will still affect the values of the HRV features presented in Figures 4 to 6, as well as the results of the PPG pulse wave analysis. It should also be noted that posture changes can affect the amplitude of the PPG pulse wave, which may influence some of the features reported in Section 3.3. As this study setup mimics free-living conditions, we have no knowledge concerning the posture of the participants at the times of the measurements. However, these participants were on bed rest, meaning that likely they were in a semi-recumbent or supine position. Furthermore, any differences in posture are likely averaged out

between participants during the analysis. Additionally, HRV features may be less accurate when assessed with PPG. However, the fact that significant changes across the days are still detected provides additional evidence supporting our confidence on the effects of corticosteroids. Additionally, using wrist-worn PPG data further allows for studying the PPG pulse wave.

In conclusion, we believe this novel work is an important step towards a better understanding of how routine pharmaceuticals aimed at treating the fetus also affect maternal physiology. We demonstrate that administering corticosteroids increases maternal HR, decreases parasympathetic activity, and reduces indices that describe the morphology of the PPG pulse wave. The impact of corticosteroids on maternal physiology must be considered when investigating these features in the pregnant population.

References

[1] A. Mate, C. Reyes-Goya, Á. Santana-Garrido, and C. M. Vázquez, "Lifestyle, Maternal Nutrition and Healthy Pregnancy," *Current Vascular Pharmacology*, vol. 19, no. 2, pp. 132–140, Mar. 2021, doi: 10.2174/1570161118666200401112955.

[2] Y. Cui, B. Zhu, and F. Zheng, "Low-dose aspirin at ≤16 weeks of gestation for preventing preeclampsia and its maternal and neonatal adverse outcomes: A systematic review and meta-analysis," *Exp Ther Med*, vol. 15, no. 5, pp. 4361–4369, May 2018, doi: 10.3892/etm.2018.5972.

[3] S. Rang, H. Wolf, G. A. Montfrans, and J. M. Karemaker, "Non–invasive assessment of autonomic cardiovascular control in normal human pregnancy and pregnancy- associated hypertensive disorders: a review," *Journal of Hypertension*, vol. 20, no. 11, pp. 2111–2119, 2002.

[4] G. K. Pal, P. Shyma, S. Habeebullah, P. Shyjus, and P. Pal, "Spectral Analysis of Heart Rate Variability for Early Prediction of Pregnancy-Induced Hypertension," *Clinical and Experimental Hypertension*, vol. 31, no. 4, pp. 330–341, Jan. 2009, doi: 10.1080/10641960802621333.

[5] S. P. Rowan, C. L. Lilly, E. A. Claydon, J. Wallace, and K. Merryman, "Monitoring one heart to help two: heart rate variability and resting heart rate using wearable technology in active women across the perinatal period," *BMC Pregnancy Childbirth*, vol. 22, no. 1, p. 887, Nov. 2022, doi: 10.1186/s12884-022-05183-z.

[6] F. Shaffer and J. P. Ginsberg, "An Overview of Heart Rate Variability Metrics and Norms," *Front. Public Health*, vol. 5, p. 258, Sep. 2017, doi: 10.3389/fpubh.2017.00258.

[7] L. M. Reyes, C. W. Usselman, M. H. Davenport, and C. D. Steinback, "Sympathetic Nervous System Regulation in Human Normotensive and Hypertensive Pregnancies.," *Hypertension (Dallas, Tex. : 1979)*, vol. 71, no. 5, pp. 793–803, May 2018, doi: 10.1161/HYPERTENSIONAHA.117.10766.

[8] L. M. Reyes *et al.*, "Sympathetic nervous system activity and reactivity in women with gestational diabetes mellitus," *Physiol Rep*, vol. 8, no. 13, Jul. 2020, doi: 10.14814/phy2.14504.

[9] S. V. Khlybova, V. I. Tsirkin, S. A. Dvoryanskii, I. A. Makarova, and A. N. Trukhin, "Heart rate variability in normal and complicated pregnancies," *Hum Physiol*, vol. 34, no. 5, pp. 625–632, Sep. 2008, doi: 10.1134/S0362119708050113.

[10] S. Moors *et al.*, "Heart rate variability in hypertensive pregnancy disorders: a systematic review," *Pregnancy Hypertension*, Mar. 2020, doi: 10.1016/j.preghy.2020.03.003.

[11] A. Seeck, M. Baumert, C. Fischer, A. Khandoker, R. Faber, and A. Voss, "Advanced Poincaré plot analysis differentiates between hypertensive pregnancy disorders," *Physiol. Meas.*, vol. 32, no. 10, pp. 1611–1622, Oct. 2011, doi: 10.1088/0967-3334/32/10/009.

[12] D. Casati *et al.*, "Maternal cardiac deceleration capacity: a novel insight into maternal autonomic function in pregnancies complicated by hypertensive disorders and intrauterine growth restriction," *European Journal of Obstetrics & Gynecology and Reproductive Biology*, vol. 206, pp. 6–11, Nov. 2016, doi: 10.1016/j.ejogrb.2016.08.007.

[13] T. M. Weber *et al.*, "Heart rate variability and baroreceptor reflex sensitivity in early-

versus late-onset preeclampsia," *PloS one*, vol. 12, no. 10, p. e0186521, 2017, doi: 10.1371/journal.pone.0186521 [doi].

[14] R. L. Goldenberg, J. F. Culhane, J. D. Iams, and R. Romero, "Epidemiology and causes of preterm birth.," *Lancet (London, England)*, vol. 371, no. 9606, pp. 75–84, Jan. 2008, doi: 10.1016/S0140-6736(08)60074-4.

[15] K. M. Verdurmen, J. Renckens, J. O. van Laar, and S. G. Oei, "The influence of corticosteroids on fetal heart rate variability: a systematic review of the literature," *Obstetrical & gynecological survey*, vol. 68, no. 12, pp. 811–824, Dec. 2013, doi: 10.1097/OGX.0000000000000009 [doi].

[16] K. M. J. Verdurmen *et al.*, "The influence of betamethasone on fetal heart rate variability, obtained by non-invasive fetal electrocardiogram recordings," *Early Human Development*, vol. 119, pp. 8–14, Apr. 2018, doi: 10.1016/j.earlhumdev.2018.02.011.

[17] L. Noben, K. M. J. Verdurmen, G. J. J. Warmerdam, R. Vullings, S. G. Oei, and J. O. E. H. van Laar, "The fetal electrocardiogram to detect the effects of betamethasone on fetal heart rate variability," *Early Human Development*, vol. 130, pp. 57–64, 2019, doi: 10.1016/j.earlhumdev.2019.01.011.

[18] R. M. Sapolsky, L. M. Romero, and A. U. Munck, "How Do Glucocorticoids Influence Stress Responses? Integrating Permissive, Suppressive, Stimulatory, and Preparative Actions," vol. 21, no. 1, p. 35, 2000.

[19] M. Bester *et al.*, "Changes in Maternal Heart Rate Variability in Response to the Administration of Routine Obstetric Medication in Hospitalized Patients: Study Protocol for a Cohort Study (MAMA-Heart Study)," *Clinics and Practice*, vol. 11, no. 1, pp. 13–25, Jan. 2021, doi: 10.3390/clinpract11010004.

[20] "ACOG Practice Bulletin No. 188: Prelabor Rupture of Membranes.," *Obstetrics and gynecology*, vol. 131, no. 1, pp. e1–e14, Jan. 2018, doi: 10.1097/AOG.0000000000002455.

[21] "ACOG practice bulletin no. 127: Management of preterm labor.," *Obstetrics and gynecology*, vol. 119, no. 6, pp. 1308–1317, Jun. 2012, doi: 10.1097/AOG.0b013e31825af2f0.

[22] "ACOG Practice Bulletin No. 202: Gestational Hypertension and Preeclampsia," *Obstetrics and gynecology*, vol. 133, no. 1, p. e-e25, Jan. 2019, doi: 10.1097/AOG.0000000000003018.

[23] M. Bester, R. Joshi, A. Linders, M. Mischi, J. O. E. H. van Laar, and R. Vullings, "Characterizing the effect of demographics, cardiorespiratory factors, and inter-subject variation on maternal heart rate variability in pregnancy with statistical modeling: a retrospective observational analysis," *Sci Rep*, vol. 12, no. 1, p. 19305, Nov. 2022, doi: 10.1038/s41598-022-21792-2.

[24] E. M. K. Ekholm, J. Hartiala, and H. V. Huikuri, "Circadian rhythm of frequency-domain measures of heart rate variability in pregnancy," *BJOG:An international journal of O&G*, vol. 104, no. 7, pp. 825–828, Jul. 1997, doi: 10.1111/j.1471-0528.1997.tb12027.x.

[25] A. H. Jobe, M. A. Milad, T. Peppard, and W. J. Jusko, "Pharmacokinetics and Pharmacodynamics of Intramuscular and Oral Betamethasone and Dexamethasone in Reproductive Age Women in India.," *Clinical and translational science*, Dec. 2019, doi: 10.1111/cts.12724.

[26] MSD, "Celestone Chronodose, suspensie voor injectie 5,7 mg/ml," Merck Sharp & Dohme B.V., Haarlen, Netherlands, Samenvatting van de productkenmerken RVG 05399, Apr. 2018.

[27] L. M. Eerikäinen *et al.*, "Comparison between electrocardiogram- and photoplethysmogram-derived features for atrial fibrillation detection in free-living conditions," *Physiol Meas*, vol. 39, no. 8, p. 084001, 08 2018, doi: 10.1088/1361-6579/aad2c0.

[28] Task Force of The European Society of Cardiology and The North American Society of Pacing and Electrophysiology, "Heart rate variability. Standards of measurement, physiological interpretation, and clinical use.," *European heart journal*, vol. 17, no. 3, pp. 354–381, Mar. 1996.

[29] A. H. Khandoker, C. Karmakar, M. Brennan, M. Palaniswami, and A. Voss, *Poincaré Plot Methods for Heart Rate Variability Analysis*. Boston, MA: Springer US, 2013. doi: 10.1007/978-1-4614-7375-6.

[30] J. S. Richman and J. R. Moorman, "Physiological time-series analysis using approximate entropy and sample entropy," *American Journal of Physiology-Heart and Circulatory Physiology*, vol. 278, no. 6, pp. H2039–H2049, Jun. 2000, doi: 10.1152/ajpheart.2000.278.6.H2039.

[31] A. Bakhchina, K. Arutyunova, A. Sozinov, A. Demidovsky, and Y. Alexandrov, "Sample Entropy of the Heart Rate Reflects Properties of the System Organization of Behaviour," *Entropy*, vol. 20, no. 6, p. 449, Jun. 2018, doi: 10.3390/e20060449.

[32] C. -K. Peng, S. Havlin, H. E. Stanley, and A. L. Goldberger, "Quantification of scaling exponents and crossover phenomena in nonstationary heartbeat time series," *Chaos*, vol. 5, no. 1, pp. 82–87, Mar. 1995, doi: 10.1063/1.166141.

[33] R.-G. Yeh, J.-S. Shieh, G.-Y. Chen, and C.-D. Kuo, "Detrended fluctuation analysis of short-term heart rate variability in late pregnant women," *Autonomic Neuroscience*, vol. 150, no. 1–2, pp. 122–126, Oct. 2009, doi: 10.1016/j.autneu.2009.05.241.

[34] D. Makowski *et al.*, "NeuroKit2: A Python toolbox for neurophysiological signal processing," *Behav Res*, vol. 53, no. 4, pp. 1689–1696, Aug. 2021, doi: 10.3758/s13428-020-01516-y.

[35] J. Allen, "Photoplethysmography and its application in clinical physiological measurement," *Physiol. Meas.*, vol. 28, no. 3, pp. R1–R39, Mar. 2007, doi: 10.1088/0967-3334/28/3/R01.

[36] C. Fischer, B. Domer, T. Wibmer, and T. Penzel, "An Algorithm for Real-Time Pulse Waveform Segmentation and Artifact Detection in Photoplethysmograms," *IEEE J. Biomed. Health Inform.*, vol. 21, no. 2, pp. 372–381, Mar. 2017, doi: 10.1109/JBHI.2016.2518202.

[37] F. Li, L. Yang, H. Shi, and C. Liu, "Differences in photoplethysmography morphological features and feature time series between two opposite emotions: Happiness and sadness," *ARTRES*, vol. 18, no. C, p. 7, 2017, doi: 10.1016/j.artres.2017.02.003.

[38] C. El Hajj and P. A. Kyriacou, "Recurrent Neural Network Models for Blood Pressure Monitoring Using PPG Morphological Features," in *2021 43rd Annual International Conference of the IEEE Engineering in Medicine & Biology Society (EMBC)*, Mexico: IEEE, Nov. 2021, pp. 1865–1868. doi: 10.1109/EMBC46164.2021.9630319.

[39] K. Kelley, "The Effects of Nonnormal Distributions on Confidence Intervals Around the Standardized Mean Difference: Bootstrap and Parametric Confidence Intervals," *Educational and Psychological Measurement*, vol. 65, no. 1, pp. 51–69, Feb. 2005, doi: 10.1177/0013164404264850.

[40] S. Musa, "Sympathetic activity in preeclampsia, a study of heart rate variability," *Journal of hypertension*, vol. 36, pp. e5–e5, 2018, doi: 10.1097/01.hjh.0000548004.87380.fa.

[41] M. Chaswal, R. Kapoor, A. Batra, S. Verma, and B. S. Yadav, "Heart Rate Variability and Cardiovascular Reflex Tests for Assessment of Autonomic Functions in Preeclampsia," *International journal of hypertension*, vol. 2018, pp. 8163824–8163824, Sep. 2018, doi: 10.1155/2018/8163824.

[42] E. Tejera, M. J. Areias, A. I. Rodrigues, J. M. Nieto-Villar, and I. Rebelo, "Blood Pressure and Heart Rate Variability Complexity Analysis in Pregnant Women with Hypertension," *Hypertension in Pregnancy*, vol. 31, no. 1, pp. 91–106, Feb. 2012, doi: 10.3109/10641955.2010.544801.

[43] R. Faber, M. Baumert, H. Stepan, N. Wessel, A. Voss, and T. Walther, "Baroreflex sensitivity, heart rate, and blood pressure variability in hypertensive pregnancy disorders," *J Hum Hypertens*, vol. 18, no. 10, pp. 707–712, Oct. 2004, doi: 10.1038/sj.jhh.1001730.

[44] V. L. Brooks, "Autonomic control during pregnancy," in *Primer on the Autonomic Nervous System*, Elsevier, 2023, pp. 273–277. doi: 10.1016/B978-0-323-85492-4.00084-3.

[45] V. L. Brooks, Q. Fu, Z. Shi, and C. M. Heesch, "Adaptations in autonomic nervous system regulation in normal and hypertensive pregnancy," in *Handbook of Clinical Neurology*, Elsevier, 2020, pp. 57–84. doi: 10.1016/B978-0-444-64239-4.00003-5.

[46] M. Bester, R. Joshi, J. H. A. M. van Dooren, M. Mischi, R. Vullings, and J. O. E. H. van Laar, "Changes in Maternal Heart Rate and Autonomic Regulation following the Antenatal Administration of Corticosteroids: A Secondary Analysis," *JCM*, vol. 12, no. 2, p. 588, Jan. 2023, doi: 10.3390/jcm12020588.

[47] S. Haddad, R. Souza, J. Cecatti, and the WHO Intrapartum Care Algorithms Working Group, "Management of maternal pulse and blood pressure abnormalities during labour and childbirth: evidence-based algorithms for intrapartum care decision support," *BJOG*, pp. 1471–0528.16776, Apr. 2022, doi: 10.1111/1471-0528.16776.

[48] L. E. Shields, S. Wiesner, C. Klein, B. Pelletreau, and H. L. Hedriana, "Use of Maternal Early Warning Trigger tool reduces maternal morbidity," *American Journal of Obstetrics and Gynecology*, vol. 214, no. 4, p. 527.e1-527.e6, Apr. 2016, doi: 10.1016/j.ajog.2016.01.154.

[49] KwaZulu-Natal Department of Health *et al.*, "Persistent maternal tachycardia: A clinical alert for healthcare professionals providing maternity care in South Africa," *SAMJ*, vol. 112, no. 6, pp. 403–404, Jun. 2022, doi: 10.7196/SAMJ.2022.v112i6.16394.

[50] S. V. Koenen, E. J. H. Mulder, L. D. Wijnberger, and G. H. A. Visser, "Transient Loss of the Diurnal Rhythms of Fetal Movements, Heart Rate, and Its Variation after Maternal Betamethasone Administration," *Pediatr Res*, vol. 57, no. 5 Part 1, pp. 662–666, May 2005, doi: 10.1203/01.PDR.0000159762.50504.1F.

[51] L. Ballard and A. Ballard, "Scientific basis and therapeutic regimens for use of antenatal glucocorticoids," vol. 173, no. 1, p. 9, 1995.

Section IV

Coupling between physiological systems during pregnancy

Chapter 9

Cardiorespiratory coupling is altered during healthy pregnancy

9

Reproduced after: M Bester, G Perciballi, P Fonseca, M van der Gilst, M Mischi, JOEH van Laar, R Vullings, R Joshi. Cardiorespiratory coupling is altered during healthy pregnancy. *Under review*. 2023.

Abstract

Pregnancy complications are associated with abnormal regulation of the maternal autonomic nervous system. Subsequently, thoroughly understanding maternal autonomic regulation during healthy pregnancy may enable the earlier detection of complications, in turn allowing for the prevention of complications or at least improved management thereof. Under healthy autonomic regulation, reciprocal interactions occur between the cardiac and respiratory systems, referred to as cardiorespiratory coupling (CRC). In this work, we investigate for the first time the differences in CRC between healthy pregnant and non-pregnant women. We apply two algorithms – namely, synchrograms and bivariate phase rectified signal averaging – to nighttime recordings of ECG and respiratory (thoracic band) signals. We find that CRC is present in both groups. Significantly less ($p < 0.01$) cardio-respiratory synchronization occurs in pregnant women (11% versus 15% occurring in non-pregnant women). Moreover, there is a smaller response in the heart rate of pregnant women corresponding to inhalations and exhalations. Additionally, we stratified these analyses by sleep stages. Since each sleep stage is governed by different autonomic states, this stratification not only amplified some of the differences between groups but also brought out differences that remained hidden when analyzing the full-night recordings. Most prominently, CRC in pregnant women remains comparable across sleep stages, while CRC increases significantly in deep sleep for non-pregnant women. We hypothesize this difference is due to the known positive correlation between CRC and parasympathetic activity. Deep sleep is a parasympathetically dominant autonomic state while pregnancy is associated with parasympathetic withdrawal and sympathetic dominance. Furthermore, the anatomical changes to the maternal respiratory system during pregnancy may also contribute to changes in CRC. Likely, the physiological stress of pregnancy may also force the cardiac and respiratory systems to uncouple and function more independently. This work offers novel insight into the physiology of healthy pregnancy and forms part of the base knowledge needed to detect abnormalities in pregnancy.

1. Introduction

The maternal autonomic nervous system (ANS) plays an important role in maintaining perinatal health during pregnancy [1]. Since the ANS is responsible for regulating the function of and interaction between involuntary physiological processes such as heartbeats and respiration, this system is essential in enabling the adaptation of maternal physiology to adapt to the growing demands of pregnancy [2]. Correspondingly, dysfunctional maternal autonomic regulation has been found in women with pregnancy complications such as hypertensive disorders of pregnancy (HDP) and gestational diabetes mellitus (GDM) [3]. Pregnancy complications occur in up to 15% of pregnancies and can result in maternal and fetal morbidity and mortality [4]–[6].

A major hurdle in reducing the impact of pregnancy complications is the inability to detect these complications before the ideal window for medical intervention has passed. Owing to the link between pregnancy complications and autonomic dysfunction, assessing maternal autonomic activity may elucidate subclinical signatures of disease and aid in the early detection of these complications [7]. In essence, by identifying when autonomic activity deviates from what is considered normal in a healthy pregnancy, it may be possible to identify high-risk pregnancies earlier [7], [8].

However, while researchers have typically focused on the autonomic dysfunction seen in pregnancy complications [3], [9], the normal autonomic state in a healthy pregnancy is still only partly understood. Non-invasive assessments of autonomic regulation are most often performed by studying heart rate variability (HRV) [10]; recent work from our group has shown that there are large, statistically significant differences in a variety of HRV features between healthy pregnant and non-pregnant women [11]. However, while HRV is a powerful tool to assess autonomic regulation owing to its relative simplicity and the easy availability of heart rate (HR) measurements [10], such assessments capture only a part of the bigger picture of maternal autonomic regulation.

A coherent picture of maternal autonomic regulation may be further illuminated by not focusing solely on the HR but rather on the interaction between the cardiac system and the respiratory system. This interaction – referred to as cardiorespiratory coupling (CRC) – is modulated by the ANS [12] and is present in healthy autonomic states, but weakens or even disappears under diseased or stressed states [13]. Correspondingly, the results of two studies indicate altered CRC in pregnant women

with preeclampsia (a hypertensive disorder of pregnancy) when compared to healthy pregnant women [14], [15]. Yet, surprisingly little is known about CRC in healthy pregnant women and whether this differs from that in non-pregnant women. One study has shown that CRC strength reduces with progressing pregnancy and others have used HRV analyses to show a decrease in high-frequency (HF) cardiac activity [16], which is traditionally linked to the influence of respiration on cardiac activity [10], [17]. However, to our knowledge, no previous work has investigated whether there are differences in CRC between pregnant and non-pregnant women.

Subsequently, in the work presented in this paper, we compare CRC between pregnant and non-pregnant women. We do so using two methods: one addressing the potential synchronization between the cardiac and respiratory systems (synchrogram analysis), the other addressing a potential modulatory effect between the two systems (bivariate phase rectified signal averaging analysis). This analysis is performed on data from polysomnography (PSG) studies, which include long periods of synchronized ECG and respiratory (thoracic band) signals. Furthermore, as a sub-analysis, we stratify the investigation by sleep stages. As CRC is linked to autonomic regulation and each sleep stage is linked to a particular autonomic state [18], this stratification may bring out differences between the groups which may be unobservable if measured over the entire sleep cycle. This work illuminates a relatively unknown physiological aspect of pregnancy. Furthermore, quantifying this aspect of maternal autonomic regulation may offer another avenue to explore for the early detection of pregnancy complications.

2. Methods

In this section, we detail the datasets used in the analysis and the preprocessing of both the cardiac and respiratory signals. Furthermore, we describe the two methods that we used to assess CRC. The first method is a phase-locking analysis using the synchrogram method. While there is currently no standard method for assessing CRC, synchrograms are commonly used [19]. Second, we use bivariate phase rectified signal averaging (BPRSA). With this method, the effects of changes in one signal are observed in the other; for example, which activity is observed in the respiratory signal when the HR decelerates. This method, which was developed fairly recently, has previously been used to capture CRC in newborns [20], [21]. It has also been used more widely in coupling assessments, for example in assessing baroreflex sensitivity [22]–[25] as

well as capturing the coupling between uterine contractions, and both fetal HR and maternal HR, respectively [26]–[28]. All analyses were performed in Python (PSF, USA).

2.1 Datasets

The pregnancy group comprises healthy volunteers with singleton pregnancies. These women were recruited for an at-home polysomnography (PSG) study, which was conducted in 2015 to validate internal algorithms at Philips Research, Eindhoven, the Netherlands. Participants underwent two full nights of recordings with approximately eight weeks between subsequent sessions. Researchers visited the participants on the eve of recording to set up the Alice PDx PSG device which recorded ECG at 200 Hz and respiration at 100 Hz using a thoracic band. No abdominal band was attached. Forty-five women were recruited for this study; of these, 20 had recordings for both nights, 15 had recordings only for night 1 (N1), and two had recordings only for (N2). Eight participants had no recordings available. Participant characteristics are detailed in Table 1.

For the control group, female participants of childbearing age (i.e., 18 – 45 years old) were selected from the Healthbed dataset [29]. This dataset comprises 110 healthy volunteers who were recruited for a study performed between 2017 and 2018 to collect data for the development of new technologies for sleep assessment. The study was originally approved by the medical ethics committee of Maxima Medical Center, Veldhoven, the Netherlands (W17.128). The current data analysis protocol (CSG_2022_007) was approved by the medical ethics committee of Sleep Medicine Center Kempenhaeghe, the Netherlands. Pregnancy served as an exclusion criterion for this study. Furthermore, included subjects showed no indications of depression, anxiety, neurologic or psychiatric disorders, nor used any medication except birth control. One night of PSG recordings was done per participant at a sleep clinic (Kempenhaeghe, Heeze, the Netherlands), with ECG at 512 Hz and thoracic band respiration at 128 Hz. Characteristics of the 41 women who met the criteria for this analysis are detailed in Table 1.

Table 1: Patient characteristics for both groups presented as median and interquartile range.

	Pregnant group	**Non-pregnant group**
Age	31 (28 – 33) years	24 (21– 28)
(Pre-pregnancy) BMI (kg/m^2)	23.0 (20.7 – 25.5)	23.1 (22.1 – 24.6)

Gestational age (all recordings)	24 (20 – 28) weeks	
Gestational age (N1)	21 (18 – 23) weeks	
Gestational age (N2)	28 (26 – 32) weeks	
Average HR	74.6 (68.6 – 79.1) bpm	62.2 (57.5 – 67.3) bpm
Average BR	15.5 (14.5 – 16.8) brpm	15.3 (13.4 – 16.5) brpm
Time duration of measurement	07:58:12 (07:11:00 – 08:43:26)	08:38:23 (08:30:12 – 08:46:56)

BMI = body mass index; N1 = night 1; N2 = night 2; HR = heart rate; BR = breathing rate; bpm = beats per minute; brpm = breaths per minute

2.2 Signal preprocessing and fiducial point detection

Data for the pregnant group were recorded at home, i.e., in free-living conditions. Subsequently, there were several regions with sensor detachment and clear motion artifacts. These were removed based on visual inspection during exploratory data analysis. Thereafter, for both groups, a second-order notch filter was used to remove the 50 Hz powerline interference for both ECG and respiration. Respiration was further band-pass filtered between 0.05 and 0.6 Hz (corresponding to 3 to 36 breaths per minute) to remove noise and facilitate peak and trough detection. Respiratory peaks and troughs were detected using a published algorithm [30] from NeuroKit2, a toolbox designed for neurophysiological signal processing in Python [31]. Furthermore, the respiratory signals were normalized by subtracting the mean value of the signal from itself and thereafter dividing the signal by the median of its absolute values [20]. ECG R-peaks were also detected using a published peak detector [32] and, subsequently, the corresponding tachograms were calculated. RR-intervals were rejected if they fell outside the range of 0.5 to 2 seconds or differed from the preceding interval by more than 20%.

2.3 CRC assessment with synchrograms

Synchrograms are used to visualize and detect periods where a fixed relative phase relationship exists between two oscillatory signals, such as the ECG and respiratory signals. This type of CRC is referred to as cardiorespiratory phase synchronization (CRPS). We provide a brief, contextualized overview of this method here. However, for further details please see the original introduction of the method [33], as well as additional articles providing detailed examples of using synchrograms [34], [35].

The synchrogram provides a stroboscopic view of the phase of the respiration signal at the times of the R-peaks of the ECG waveform. As an example, assume that four (n = 4) R-peaks occur within one respiration cycle (m = 1). Each of these R-peaks would then occur at a certain phase relative to the corresponding respiratory cycle. If in the successive respiratory cycles, sets of four R-peaks again occur at the same fixed phases relative – within a threshold defined based on the literature – to their corresponding respiratory cycles, then phase locking is present at a ratio of 4:1 (n:m) for that period. This phase lock needs to be present for a minimum of two cycles of m (in this example, for two respiratory cycles) for CRPS to occur.

The fixed integer relationship of n:m is referred to as the phase locking ratio (PLR). We investigate the following PLRs: 3:1, 4:1, 5:1, 6:1, 7:1, 5:2, 7:2, 9:2, and 11:2, expecting based on literature that 3:1, 4:1, 5:1, and 6:1 would occur most frequently [18], [36], [37]. CRPS results are presented as the percentage of time in which CRPS occurs to ensure the results are independent of recording length and sleep architecture; the latter is elaborated upon in Section 2.5. To further illustrate CRPS, an example from one of the study participants is presented in Figure 1.

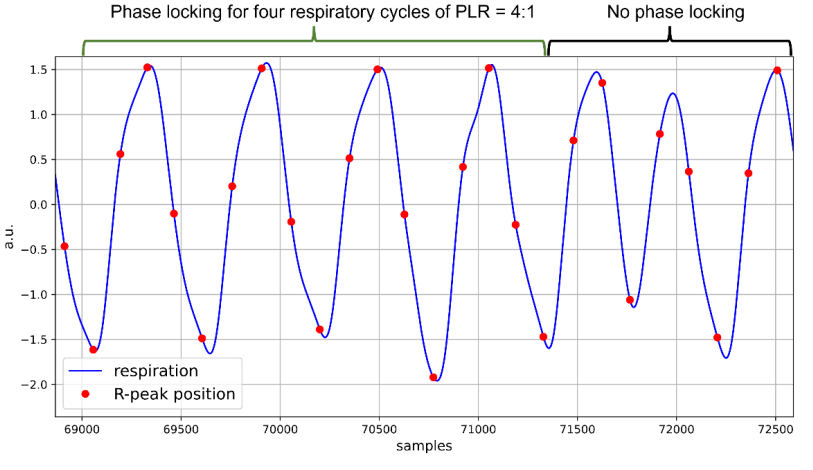

Figure 1: Illustration of a period of CRPS, with instances of the R-peaks plotted in red on the respiratory signals. Notice that for the first four respiratory cycles, phase locking of PLR 4:1 occurs. This is evident from the fact that the R-peaks (in red) occur at similar fixed positions relative to the respiratory cycles. Thereafter, no phase locking occurs.

Notice that each of the first four respiratory cycles has four red points, which correspond to the occurrence of the R-peak from the time-synchronized ECG signal, at similar relative positions. This pattern breaks down for the subsequent three respiratory cycles. Therefore, for the first four respiratory cycles, a phase locking of a 4:1 PLR occurs, while no phase locking occurs thereafter.

2.4 CRC assessment with BPRSA

BPRSA is the bivariate version of phase rectified signal averaging (PRSA). The latter is a technique that is used to elucidate quasi-periodicities in physiological signals which may otherwise be obscured by noise. This method, as well as its bivariate version discussed in the next paragraph, is presented in detail elsewhere [38]–[40]; here we give a brief overview pertaining to the analyses presented in this paper. Note that when using BRPSA to capture coupling, the PRSA and BPRSA results are typically both presented to better illustrate the coupling between the two signals. Hence, we describe both the PRSA and BPRSA analysis here [20], [26], [27], [38], [41].

The PRSA analysis is performed by first identifying the events or phases of interest – referred to as anchor points (APs) – in the relevant signal. Following this, a signal segment of length $2L + 1$ is isolated around each AP, with L empirically chosen to allow for visualizing the slowest oscillation of interest. Next, all signal segments are aligned by their APs and averaged. This averaging ensures that only periodicities that have a fixed relationship with the AP remain. Subsequently, we can observe the typical behavior of the signal around each AP.

An extension of this method allows for studying the coupling between two signals. BPRSA, i.e., the bivariate version of PRSA, captures if and how specific events or phases in one signal (the trigger signal) might correspond to or result in changes in another signal (the target signal). This is done by identifying the APs in the trigger signal and translating them in time to the target signal. From here, the rest of the analysis – as specified for PRSA – is performed on the target signal. If the resulting BPRSA waveform resembles a flatline, no coupling is present (as assessed by this specific method). However, if periodicities are present in the BPRSA waveform, this indicates that some activity in the target signal corresponding to the AP event in the trigger signal survives the averaging. Therefore, in such a case coupling is observed. Specifically, in the terminology used for BPRSA analysis, the coupling is observed *from* the trigger signal *to* the target signal. While we use this language throughout, it should be noted that causality is not necessarily implied.

2.4.1 PRSA of tachogram and respiration

We identify HR accelerations and HR decelerations as the two sets of APs for the tachogram, meaning that each HR deceleration and HR acceleration is identified as an AP, respectively. For the respiratory signal, inhalations and exhalations serve as APs. Note that for inhalation we use the point halfway in terms of time between the trough and the peak of the respiratory cycle; similarly, for exhalation, we use the halfway point between the peak and the trough. This halfway point was preferred, as the inhalation peak and exhalation through already represent the transition from inhalation to exhalation and exhalation to inhalation, respectively.

The following features are calculated to characterize the PRSA waveform of the tachogram, using HR decelerations as APs:

- Deceleration capacity (DC) [40]: This feature captures the response in HR to decelerations and is calculated in the following way:
  $DC = [X(0) + X(1) - X(-1) - X(-2)/4$,
  With X representing the PRSA waveform, X(0) representing the AP, X(1) is the value following the AP, while X(−1) and X(−2) precede the AP.
- Immediate deceleration response (IDR) [20]: the difference between the maximum and minimum value within the neighborhood of five RRi preceding the AP and five thereafter, including the AP.
- Slope of the deceleration response (SDR) [20]: The slope between the maximum and minimum value as defined for the IDR.

These features are also calculated in the case where HR accelerations are the APs and correspondingly named: acceleration capacity (AC), immediate acceleration response (IAR), and slope of the acceleration response (SAR). As these features capture the beat-to-beat information of the tachogram, they mainly reflect parasympathetic activity. Note that for the PRSA of the tachogram, the waveform's relationship to the time domain is units of RR values (specified here as RR_i) and not in seconds.

The PRSA waveform of the respiratory signal, both when inhalations and exhalations are APs, is characterized using the following features:

- Maximum respiratory amplitude (MRA) [20]: the difference between the maximum and minimum value of the PRSA within five seconds preceding or following the AP. This feature captures the maximum response to the AP.

- Sample entropy (SampEn) [20]: The sample entropy is calculated for the PRSA waveform. A small value corresponds to higher regularity, whereas a higher value implies more randomness in the oscillations of the waveform. The tolerance was set to 0.2 times the standard deviation of the waveform, while the embedding dimension was set to 4.

2.4.2 BPRSA of the tachogram and respiratory signal from cardiac activity to respiration

To quantify CRC *from cardiac activity to respiration*, we perform the BPRSA analysis with the tachogram as the trigger signal and the respiratory signal as the target signal. We use HR decelerations and HR accelerations as APs, respectively. Conversely, we use respiration as the trigger signal and the tachogram as the target signal to quantify CRC *from respiration to cardiac activity*.

We quantify the resulting BPRSA waveforms with SampEn as described in the previous section (Section 2.4.1). Furthermore, we calculate the maximum BPRSA amplitude (MBA) in the same manner as MRA is calculated (Section 2.4.1). Additionally, we also calculate the slope at the AP (SAP) [20] to identify the phase of tachogram or respiration at the AP (a negative value corresponds to HR acceleration or the expiratory phase, respectively, whereas a positive value corresponds to HR deceleration or the inspiratory phase, respectively). Finally, we also calculate the peak delay (PD), i.e., the delay between the peak/trough of the BPRSA waveform aligning with the AP and the x-axis, essentially capturing the time offset between the AP and the peak/through.

2.5 Sub-analysis: stratification by sleep stages

Since the data from both groups were recorded during the night and sleep stages are characterized by different autonomic tones [42], we stratify our analysis by sleep stage. Sleep can be characterized in three states of increasing depth (N1, N2, and N3), as well as rapid eye movement (REM). Sleep scoring is done on both datasets using a PSG-based automated sleep stager, Somnolyzer, which is detailed elsewhere [43]. For the pregnant group, ten recordings did not have the relevant signals to determine the sleep stages and were not included here, resulting in the inclusion of 47 recordings.

To illustrate this stratification, the N2 sleep stage is used. All segments of N2 sleep are isolated from the recording. Segments of less than 1-minute are disregarded for the synchrogram analysis and those less than three minutes long are discarded for the BPRSA analysis, based on the minimum length needed for these methods. (Note that

sleep staging is done in 30-second increments.) The synchrogram analysis, detailed in Section 2.3, is performed on each N2 segment. The results from all segments are weighted according to the length of the relevant segment as a fraction of the total length of the signal spent in N2. Concerning the BPRSA analysis (Section 2.4), only data from the N2 sleep stage is used for the analysis. Apart from this change, the analysis stays identical. The same process is repeated for all sleep stages, as well as for the sections where participants were identified as awake (Wake = W).

2.6 Sub-analysis: stratification by gestational age

Using both methods for CRC assessment, we perform an additional sub-analysis in the pregnant group to explore the effects of gestational age (i.e., the number of weeks participants had been pregnant) on CRC. We investigate whether CRC differs with gestational age, both by doing a pairwise comparison between the women who had two measurement sessions approximately eight weeks apart and by performing a simple regression analysis between the CRC indices and gestational age.

2.7 Statistical analysis

Almost all data and results were non-normally distributed and, subsequently, non-parametric analyses were performed. Statistical significance for changes between the pregnant and non-pregnant group was tested using the Mann–Whitney U test. When comparing differences between the sleep stages (i.e., differences between more than two groups), the Kruskal–Wallis test was used. Additionally, Cohen's d was calculated to determine effect size. The effect size is presented with the 95% confidence interval, obtained via bootstrapping with 10,000 iterations, which is appropriate for data that is not normally distributed [44]. A d-value of 0.8 suggests a large effect size, while $d = 0.5$ and $d = 0.3$ correspond to a medium and small effect size, respectively.

3. Results

The results for the synchrogram and BRPSA analyses are presented below, first when calculated over the full recordings, followed by the findings from the sub-analysis in which the analyses are stratified by sleep stages. Note that when stratifying CRC by gestational age (the sub-analysis described in Section 2.6), we found no significant or remarkable results. As such, these results are not further presented here.

Concerning the sleep stage stratification, we broke down the full recordings into the

different stages to contextualize the results relative to the time spent in each stage (Figure 2). The values displayed in Figure 2 are based on the synchrogram analysis, for which sleep stage segments shorter than one minute were discarded. Note that for the BPRSA analysis, these values differ slightly as segments of at least three minutes in length are needed. Still, the proportional time spent in each stage remains similar.

For pregnant women, a larger section of the recording time is spent in Wake (15.0% vs 5.1% in non-pregnant women). While pregnant women are known to have more wakeful periods than non-pregnant women [45], [46], this difference is likely partly a result of the differences in study setups; at-home PSG recordings are used for the pregnant group, while recordings for the non-pregnant group were done in a sleep clinic.

Considering the time spent in sleep, both groups spent most of their sleep in N2 (> 50%) and little time in N1 (< 5%). Both groups also spent comparable time in REM sleep (23.0% and 22.3%). However, the proportion of time pregnant women spent in N3 sleep is remarkably less than that of non-pregnant women (13.5% vs 24.8%), which is expected from the literature [45], [46]. Further aligning with the literature, pregnant women then spent almost 10% more of their sleep in N2 than their non-pregnant counterparts [46].

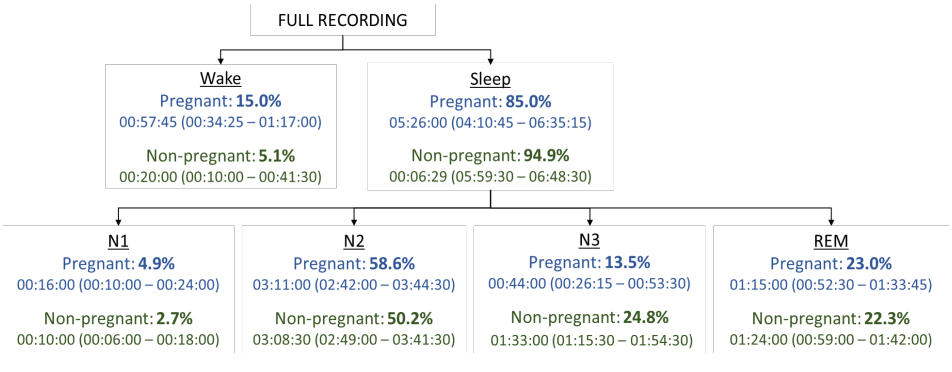

Figure 2: Data were recorded during the nighttime. The split of these recordings between Wake and Sleep is presented on the first tier, adding up to 100% per group. In the second tier, the time spent in Sleep is broken up into the four sleep stages (N1, N2, N3, and REM). Again, these proportions add up to 100% per group. The proportions presented here are calculated based on the median times spent in each stage per group. The median and interquartile range of the times spent in each stage are presented as hours: minutes:seconds.

3.1 CRC assessment with synchrograms

First, the synchrogram analysis was performed on the full recordings. Figure 3 visualizes the results for all the PLRs (i.e., phase locking ratios) combined, as well as 3:1, 4:1, and 5:1 – the most commonly occurring PLRs – with boxplots. The median and interquartile of the percentage of time spent in each PLR, along with the statistical significance (p) and effect sizes (d) of differences between the groups, are found in Table 2.

Overall, significantly less CRPS occurs during pregnancy (Figure 3, All ratios). In non-pregnant women, a median of 15% of the night is spent in CRPS, while in pregnant women CRPS occurs only a median of 11% of the time. Furthermore, significantly less CRPS of the PLRs 3:1 and 4:1 occur during pregnancy. However, there is a higher prevalence of the PLR of 5:1 in the pregnant group. In all cases $d \approx 0.6$, which corresponds to a medium effect size.

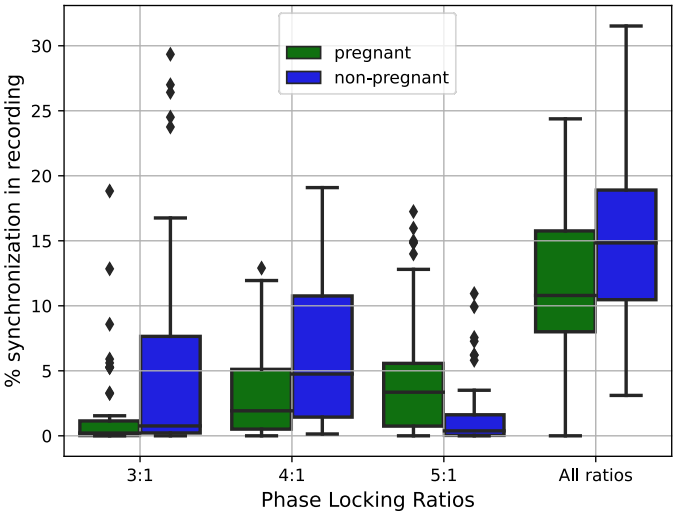

Figure 3: The percentage of synchronization for the pregnant (in green) and non-pregnant (in blue) group, presented for the most commonly occurring PLR (i.e., 3:1, 4:1, and 5:1), as well as for al ratios combined. For pregnant women, less synchronization occurs at 3:1, 4:1, and all ratios, while these women have more synchronization for 5:1 when compared to non-pregnant women.

When considering the additional PLRs such as 7:1 or 9:2 (Table 2), we see that these PLRs rarely occur in either of the groups. Still, there are mostly statistically significant differences between the groups, regardless of the PLR. Furthermore, PLRs with

a higher number of heartbeats per respiration cycle are more likely to occur in the pregnant group.

Table 2: Differences in CRPS between pregnant and non-pregnant women. CRPS values are presented as median and interquartile range.

Ratios	Pregnant	Non-pregnant	Significance	Effect size
All	10.79 (8.00 – 15.76)	14.84 (10.47 – 18.90)	$p < 0.01$	$d = 0.60$ (0.20 – 1.00)
3:1	0.21 (0.02 – 1.06)	0.76 (0.22 – 7.65)	$p < 0.01$	$d = 0.62$ (0.24 – 0.98)
4:1	1.88 (0.15 – 5.03)	4.75 (1.44 – 10.75)	$p < 0.01$	$d = 0.66$ (0.24 – 1.10)
5:1	3.26 (0.38 – 5.45)	0.38 (0.03 – 1.62)	$p < 0.01$	$d = 0.64$ (0.28 – 0.99)
6:1	0.20 (0.00 – 1.43)	0.00 (0.00 – 0.07)	$p < 0.001$	$d = 0.65$ (0.46 – 0.85)
7:1	0.00 (0.00 – 0.03)	0.00	$p = 0.01$	$d = 0.36$ (0.01 – 0.63)
5:2	0.00	0.00 (0.00 – 0.04)	$p < 0.001$	$d = 0.48$ (0.10 – 0.80)
7:2	0.39 (0.00 – 1.65)	0.00 (0.04 – 0.34)	$p < 0.01$	$d = 0.35$ (-0.06 – 0.78)
9:2	0.13 (0.00 – 0.44)	0.39 (0.18 – 0.45)	$p = 0.47$	$d = 0.05$ (-0.37 – 0.46)
11:2	0.06 (0.04 – 0.34)	0.00	$p = 0.01$	$d = 0.55$ (0.26 – 0.81)

3.1.1 Stratification by sleep stages

To investigate whether differences in autonomic regulation between the groups are driving their differences in CRC, the synchrogram analysis was stratified by the four sleep stages (N1, N2, N3, and REM) and Wake. The proportion of time each group spends in the different stages was previously outlined in Figure 2. In Figure 4, the percentage of time spent CRPS (combining all PLRs) is presented as stratified by sleep stages. The least amount of CRPS in sleep occurs during N1 and REM sleep (a median of approximately 5 – 7% for both groups in both stages), while the most occurs during N3 (a median of 13% and 20% for pregnant and non-pregnant women, respectively). Pregnant women have more CRPS during Wake, but it should be kept in mind that a larger proportion of Wake measurements are available for this group (Figure 2). When comparing overall CRPS between the different sleep stages, this differs significantly for both pregnant ($p = 0.0001$) and non-pregnant women ($p < 0.0001$).

Furthermore, there are significant ($p < 0.05$) and medium differences ($d = 0.62$) between the groups during N2, as well as large differences between the groups during

N3 ($p < 0.001$, $d = 0.93$), while for N1 and REM, the differences between groups are less evident and not significant. As sleep deepens, quantified by the progression from N1 to N3, the differences between the groups become more pronounced. For non-pregnant women, there is a delta of approximately 15% between the medium CRPS in N1 and N3, while for pregnant women this difference is only about 8%.

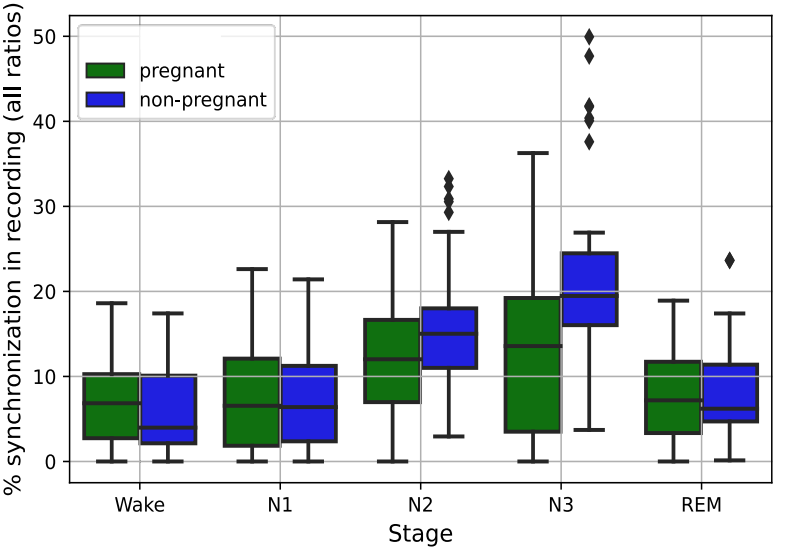

Figure 4: Synchronization periods stratified by sleep stages. The percentage of synchronization for the pregnant (in green) and non-pregnant (in blue) group, stratified by sleep stages. The results presented here are for all PLRs combined. Comparable synchronization occurs during Wake, N1, and REM, but pregnant women have reduced synchronization in N2 and N3 compared to non-pregnant women.

3.2 CRC assessment with BPRSA

The results from the BPRSA analysis are presented below, first performed using the entire signal and thereafter stratified by sleep stages. There are two overarching observations to notice from these results. First, from Figures 5 – 8, it is evident that there is a relationship between the cardiac and respiratory systems for both pregnant and non-pregnant women, regardless of whether HR accelerations, HR decelerations, inhalations, or exhalations are used as APs. Recalling Section 2.4, CRC is present if the resulting BPRSA waveform contains oscillations, i.e., not a flat line. The second observation is that while CRC is present in both groups, the nature of the CRC differs between pregnant and non-pregnant women.

3.2.1 Coupling from cardiac activity to respiration

We perform the BPRSA analysis with HR decelerations and accelerations as APs, respectively. The PRSA and BPRSA plots of the pregnant and non-pregnant groups, averaged per group, are presented in Figure 5. From the PRSA waveforms in this figure (Figures 5A and B), we can see a substantially larger response for non-pregnant women than for pregnant ones in both cases of APs. This is confirmed by the statistically significant ($p < 0.001$) and large ($d > 1.15$) differences in the features in Table 3 which capture the response observed in the PRSA waveforms (DC, AC, IDR, IAR, SDR, and SAR).

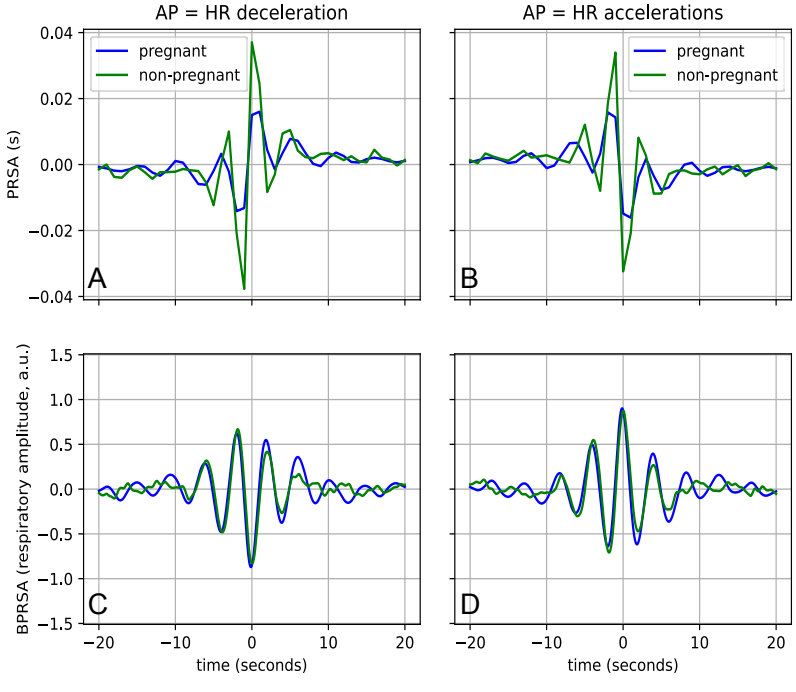

Figure 5: Coupling from cardiac activity to respiration, averaged across all participants. In the left panel (A and C), AP = HR deceleration, and in the right (B and D), AP = HR accelerations. The top row represents the result from the PRSA (A and B), while the bottom row is that of BPRSA (C and D). The means of the waveforms have been subtracted to facilitate comparison.

Considering now the PRSA waveforms along with the BPRSA waveforms; notice that the HR decelerations are clustered at the end of the expiratory phase, while HR accelerations cluster at the end of the inspiratory phase. Based on visual observation, the BPRSA waveforms of the two groups are similar (Figures 5C and D), apart from differences observed in the tail ends. However, based on the statistical analysis of the

features describing the BPRSA waveforms in Table 3, there are statistically significant differences between the BPRSA waveforms of the two groups, albeit with generally small to medium effects.

Table 3: Features describing the PRSA and BPRSA waveforms when CRC is assessed from cardiac activity to respiration. Features are presented as median and interquartile range.

		Feature	Pregnant	Non-pregnant	*p*	Effect size (d)
AP = HR deceleration	PRSA	IDR	0.035 (0.026 – 0.044)	0.067 (0.034 – 0.102)	< 0.001	1.28 (0.92 – 1.67)
		SDR (x 10^3)	12.1 (0.76 – 1.79)	5.82 (2.75 – 8.71)	< 0.001	1.42 (1.06 – 1.84)
		DC (x 10^2)	1.49 (1.14 – 1.81)	2.68 (1.48 – 3.67)	< 0.001	1.20 (0.87 – 1.57)
	BPRSA	MBA	1.37 (1.07 – 1.53)	1.55 (1.45 – 1.76)	< 0.001	0.25 (-0.25 – 1.07)
		PD (ms)	-11 (-19 – 0.5)	4 (-13 – 28)	0.03	0.39 (-0.04 – 0.84)
		SAP (x 10^3)	2.10 (0.00 – 3.91)	-0.31 (-2.96 – 1.33)	< 0.01	0.46 (-0.15 – 0.85)
		SampEn (x 10^2)	4.53 (3.99 – 4.84)	3.62 (3.08 – 4.08)	< 0.001	0.75 (0.26 – 1.33)
AP = HR acceleration	PRSA	IAR	0.035 (0.027 – 0.046)	0.062 (0.039 – 0.094)	< 0.001	1.27 (0.86 – 1.7)
		SAR (x 10^3)	-12.2 (-18.5 – -7.3)	-49.1 (-80.8 – -27.9)	< 0.001	1.43 (1.02 – 1.88)
		AC (x 10^2)	-1.50 (-1.87 – -1.21)	-2.64 (-3.24 – -1.61)	< 0.001	1.16 (0.75 – 1.6)
	BPRSA	MBA	1.46 (1.30 – 1.67)	1.67 (1.48 – 1.85)	< 0.01	0.22 (-0.25 – 0.93)
		PD (ms)	-11 (-18.5 – -1)	5 (-12 – 18)	< 0.01	0.41 (0.00 – 0.85)
		SAP (x 10^3)	-2.40 (-4.37 – -0.25)	0.51 (-1.94 – 2.75)	< 0.01	0.56 (0.28 – 1.01)
		SampEn (x 10^2)	4.49 (4.0 – 4.85)	3.52 (3.07 – 4.07)	< 0.001	0.75 (0.26 – 1.32)

MBA = maximum BPRSA amplitude; PD = peak delay; SAP = slope at the anchor point

3.2.2 Stratification by sleep stages: Coupling from cardiac activity to respiration

To delve further into the potential physiological drivers behind the differences in the groups, the BPRSA analysis from Section 3.2.1 was stratified by sleep stages. The PRSA graphs remained similar across sleep stages, with non-pregnant women always showing a larger response than their pregnant counterparts (results not shown). However, the BPRSA waveforms, which indicate the response in respiration corresponding to changes in HR, did differ per sleep stage. The average waveforms are presented in Figure 6. These waveforms are for the case of AP = HR decelerations; the BPRSA results of AP = HR accelerations were similar. The average waveforms for the N1 sleep stage are not presented here, as too little N1 data were available (Figure 2).

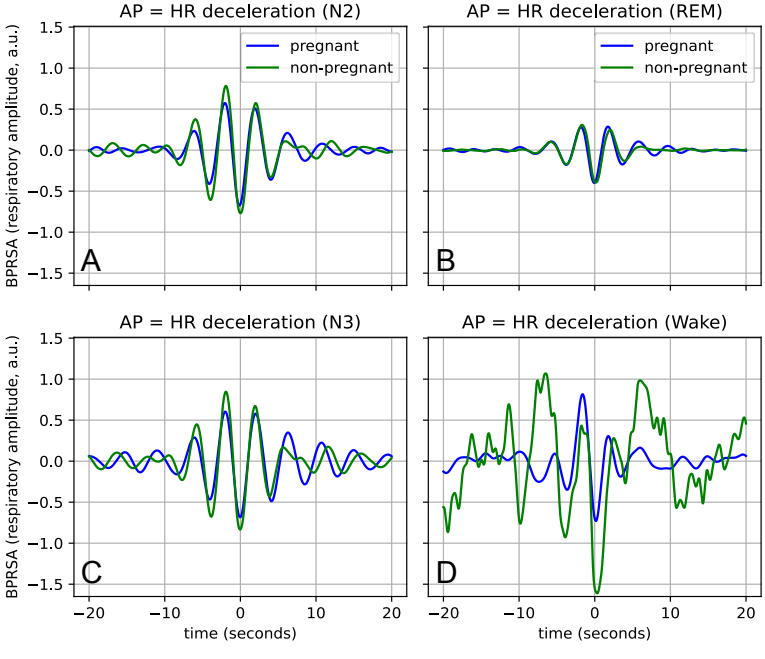

Figure 6: The average BPRSA waveforms representing coupling from cardiac activity to respiration during the N2 (A), N3 (C), REM (B), and Wake (D) for AP = HR decelerations. The means of the waveforms have been subtracted to facilitate comparison. Waveforms are averaged across all participants.

Notice that for N2 and N3 (Figures 6A and C), the difference in the maximum response (MBA), which is not visually obvious in Figure 5C, becomes apparent. Furthermore, in N2 the effect size of the difference is large (d = 0.88), while the effect size of the differences based on the full recordings is small (d = 0.25, Table 3). However, the

difference between the groups disappears when looking at data from the REM stage (Figure 6B). Furthermore, the amplitudes of both the BPRSA waveforms in the REM phase are reduced compared the that of N2 and N3, as well as to the BPRSA waveform based on the full recording (Figure 5C). Note that for the Wake results of the non-pregnant group (Figure 6D), the jagged appearance of the waveform likely results from the little Wake data available for this group (Figure 2) rather than physiological differences between the two groups.

3.2.3 Coupling from respiration to cardiac activity

Additionally, we performed the BPRSA analysis using inhalations and exhalations as APs, respectively. The average waveforms for both groups are presented in Figure 7, with the corresponding descriptive features found in Table 4. We see from the PRSA waveforms that there is a larger response for the pregnant group, although this difference is only significant ($p < 0.01$) for the case where exhalations are APs (see MRA for Table 4). However, looking at the BPRSA waveforms and features in Table 4, there is a clear difference in the amplitudes of the responses, with the larger response belonging to the non-pregnant group. These differences are echoed in the features in Table 4 for both inhalations and exhalations as APs: there are statistically significant ($p < 0.001$) and large ($d > 1.2$) differences in MBA, i.e., the amplitude of the response observed in the waveform. Furthermore, for both the PRSA and BPRSA waveforms, considering both sets of APs, there is significantly lower SampEn in the response of the pregnant women ($p < 0.001$, $d > 1$).

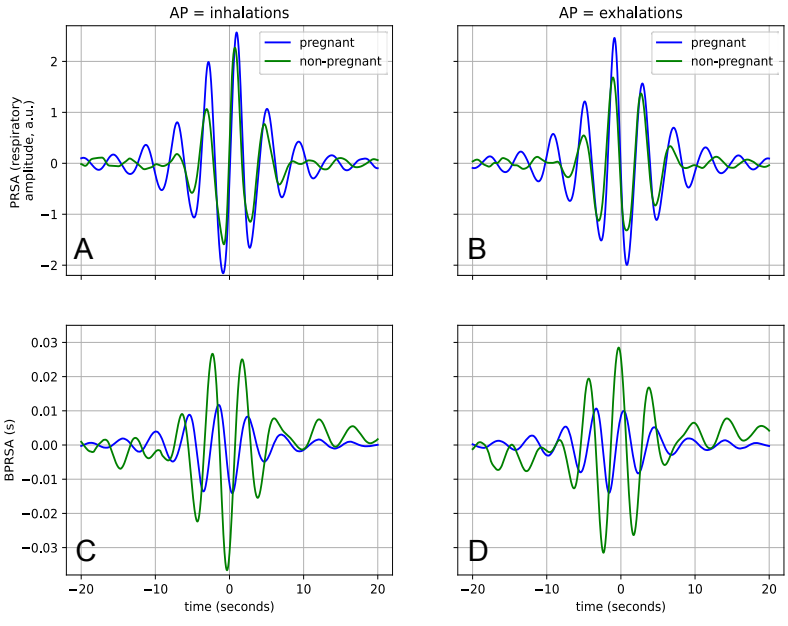

Figure 7: Coupling from respiration to cardiac activity. In the left panel (A, C), AP = inhalations, and in the right, AP = exhalations (B, D). The top row represents the result from the PRSA (A, B), while the bottom row is that of BPRSA (C, D). The means of the waveforms have been subtracted to facilitate comparison. Waveforms are averaged across all participants.

Table 4: Features describing the PRSA and BPRSA waveforms when CRC is assessed from respiration to cardiac activity. Features are presented as median and interquartile range.

		Feature	Pregnant	Non-pregnant	*p*	Effect size (*d*)
AP = INHALATION	PRSA	MRA	3.67 (3.41 – 4.12)	3.61 (3.34 – 3.77)	0.18	0.06 (-0.39 – 0.36)
		SampEn (x 10^2)	4.35 (3.98 – 4.84)	3.40 (2.92 – 3.71)	< 0.001	1.16 (0.71 – 1.70)
	BPRSA	MBA	0.036 (0.018 – 0.046)	0.068 (0.045 - 0.091)	< 0.001	1.28 (0.96 – 1.63)
		PD (ms)	36 (2 – 70)	12 (-47 – 58.25)	0.02	0.52 (0.09 – 0.95)
		SAP (x 10^3)	-0.108 (-0.304 – 0.000)	-0.069 (-0.243 – 0.105)	0.03	0.48 (0.07 – 0.88)
		SampEn (x 10^2)	4.69 (4.25 – 5.14)	3.26 (2.98 – 3.88)	< 0.001	1.48 (1.09 – 1.99)
AP = EXHALATION	PRSA	MRA	3.37 (3.19 – 3.87)	3.19 (3.04 – 3.36)	< 0.01	0.19 (-0.23 – 0.62)
		SampEn (x 10^2)	4.48 (3.98 – 4.88)	3.46 (3.07 – 3.98)	< 0.001	1.08 (0.62 – 1.64)
	BPRSA	MBA	0.034 (0.017 – 0.043)	0.066 (0.044 – 0.090)	< 0.001	1.35 (1.02 – 1.71)
		PD (ms)	42 (-11 – 79)	29 (-33.75 – 72.25)	0.20	0.23 (-0.2 – 0.65)
		SAP (x 10^3)	-0.056 (-0.025 – 0.180)	0.077 (-0.055 – 0.180)	0.44	0.29 (-0.15 – 0.68)
		SampEn (x 10^2)	4.76 (4.43 – 5.30)	3.31 (3.06 – 3.90)	< 0.001	1.31 (0.82 – 2.17)

MRA = maximum respiratory amplitude; MBA = maximum BPRSA amplitude; PD = peak delay; SAP = slope at the anchor point

3.2.4 Stratification by sleep stages: Coupling from respiration to cardiac activity

Next, the BPRSA analysis using respiration as the trigger signal and the tachogram as the target signal was stratified by sleep stages. The left panel of Figure 8 shows the average PRSA and BPRSA waveforms from the N2 sleep stage for AP = exhalations, which is when parasympathetic activity is dominant. The right panel shows that of

the REM sleep stage, where sympathetic activity is dominant [18]. The results of AP = inhalations are not shown as these are similar to those presented in Figure 8.

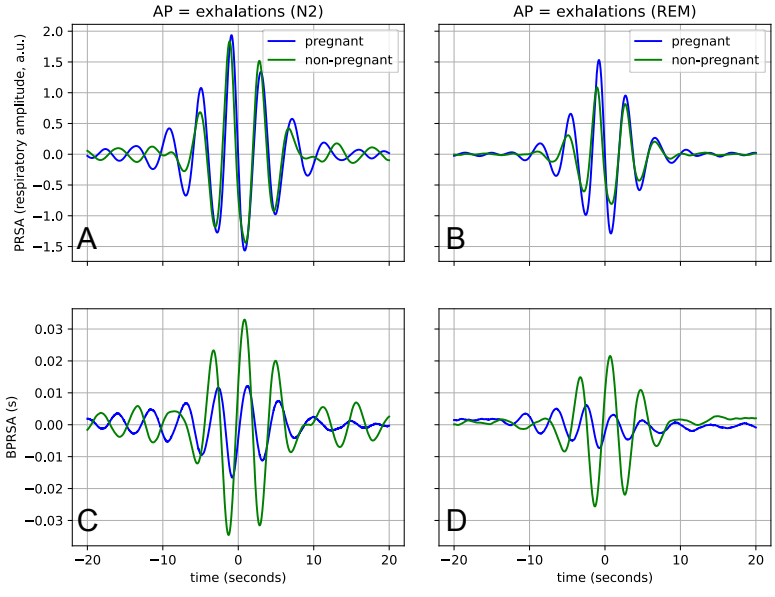

Figure 8: Coupling from respiration to cardiac activity during the N2 (left, A and C) and REM sleep stage (right, B and D), with AP = exhalations. The top row represents the result from the PRSA (A, B), while the bottom row is that of BPRSA (C, D). The means of the waveforms have been subtracted to facilitate comparison. Waveforms are averaged across all participants.

In Figures 7B and D, where the waveforms are based on the full night recordings, we can observe a difference in the amplitude of the PRSA waveforms with a small effect size (MRA from Table 4, $p < 0.01$, $d = 0.19$). From Figure 8, it seems that this difference is primarily driven by the large, significant differences in sympathetic states such as the REM stage ($p < 0.001$, $d = 1.61$). Considering now the BPRSA waveforms, we see that there is a substantially larger response for non-pregnant women, as compared to pregnant ones, for both N2 and REM. This is similar to the results seen in Figure 7D and this is also the case for N3 and Wake (not shown).

Furthermore, considering the values for SampEn for both the PRSA and the BPRSA waveforms for both sets of APs, there is significantly less regularity in the waveforms of the pregnant group, with a large effect ($d > 1$, $p < 0.001$), regardless of the sleep stage. This indicates that there is a higher level of randomness in the oscillations of the waveforms of the pregnant group, while the waveforms of non-pregnant women show more regularity.

4. Discussion

While it is known that pregnancy substantially impacts the cardiac, respiratory, and autonomic nervous systems of women, we show for the first time in this work that pregnant women have altered CRC when compared to their non-pregnant counterparts. Using two different CRC analyses, we find that the synchronization between the cardiac and respiratory systems (CRPS in Figure 2), as well as the effect of respiration on cardiac activity (Figure 7), are reduced during a healthy pregnancy. We further stratify these analyses by sleep stages. We find that when determining CRC per sleep stage, differences between the two groups are further enhanced as compared to the main analysis (CRPS in N3 in Figure 3; Figure 8). Furthermore, this stratification also reveals changes that are not apparent when comparing CRC based on the full recordings (Figure 6).

There are three physiological differences between pregnant and non-pregnant women which may contribute to the differences we see in CRC. The first is a difference in autonomic regulation; healthy pregnancy is an autonomic state characterized by increased sympathetic and decreased parasympathetic activity when compared to non-pregnant women of similar age [1], [11], [47]. This is also apparent from our results, as the reduced amplitude and slope of the PRSA waveforms of the tachogram for the pregnant group (Figure 5) can be explained by reduced parasympathetic activity [20], [40]. This is further confirmed by the fact that the features describing these waveforms (DC, AC, IDR, IAR, SDR, and SAR, Table 3) are significantly lower in pregnant women, with large effect sizes ($p < 0.001$, $d > 1$). We observed similar results in previous work done in our group [11], [48]. This reduced parasympathetic activity likely contributes to the lower levels of CRPS seen in the pregnancy group (blue boxplots in Figure 3) [18]. Note that CRPS is only higher for pregnant women for the PLR of 5:1 (Figure 3). This is probably because pregnant women have higher HRs and similar respiratory rates to non-pregnant women [11], [49]; this can also be seen for our subject cohorts in Table 1, indicating that a PLR with a high number of R-peaks within one respiratory cycle would be more likely to occur during pregnancy. The fact that non-pregnant have lower HRs likely contributes to the fact that more CRPS is seen for PLRs of 3:1 and 4:1; however, the total CRPS is also higher in non-pregnant women (Figure 3).

Researchers have found that the occurrence of CRPS increases as parasympathetic activity increases [18]. This is most prominent during N3 sleep, where parasympathetic activity is the highest and sympathetic activity is the lowest. During N3 sleep,

HR decreases and baroreceptors, which are stretch receptors in the aortic arch and carotid sinuses that help regulate blood pressure, become more sensitive. This further promotes a state of regular respiration and gas exchange, triggering higher levels of CRPS [50]. Tracking the statistically significant changes ($p < 0.001$) across sleep stages for the non-pregnant group (green boxplots in Figure 4) illustrates this phenomenon well, as CRPS increases progressively from N1 to N3, with a difference of 15% from N1 to N3. Furthermore, consider the coupling from respiration to cardiac activity, which is represented in Figure 8, where we see that the response in the BPRSA waveform is larger during N2 (Figure 8C) than during REM (Figure 8D), indicating reduced coupling under sympathetic dominant states such as REM.

This relationship between sleep architecture and CRPS is also described in the literature [18], [36]. Assessing CRPS in older subjects – who, similar to pregnant women, have higher sympathetic and lower parasympathetic activity – reveals that while the prevalence of CRPS decreases with age, the relationship between CRPS and sleep architecture remains intact [18]. We find that while this relationship is also present in healthy pregnant women, it is less prominent in this group when compared to the non-pregnant group (Figure 4).

The second physiological difference which may impact maternal CRC results from the anatomical changes that occur in the maternal respiratory system during pregnancy [51]. In a non-pregnant person, breathing is facilitated by the diaphragm and intercostal muscles, i.e., the muscles between the ribs. To inhale, the diaphragm flattens and the intercostal muscles contract to expand the ribcage, thereby creating a greater negative intrapleural pressure in the thoracic cavity and allowing air to fill the lungs. Thereafter, the diaphragm and intercostal muscles relax again, reducing the negative intrapleural pressure and forcing air out of the lungs [51]. However, as the fetus grows during pregnancy, it pushes up against the diaphragm and in doing so reduces the ability of the diaphragm to descend; correspondingly, there is less expansion of the lungs in the inferior direction (anatomically speaking) [51]. The maternal anatomy compensates for this by remodeling the ribcage to allow for more lateral expansion of the lungs during inspiration [51]. Considering that the respiration in this study was measured with a thoracic band, this increased lateral expansion may result in the higher amplitude of the differences in the PRSA response in pregnant women (as compared to non-pregnant women) when APs are inhalations or exhalations (Figures 7 and 8).

These changes in the thoracic cavity may also affect the blood flow to the heart, specifically, the venous return. The increase in negative intrapleural pressure during inspiration, along with the increased pressure that the descended diaphragm places on the abdominal cavity, increases the blood flow into the right atrium of the heart. This increased return to the right atrium and then ventricle results in increased stroke volume to the transpulmonary circulation (right ventricle pump). Thereafter, the increased preload to the left heart results in an increased stroke volume of the left ventricle. Correspondingly, HR also increases. This interaction facilitates respiratory sinus arrhythmia (RSA), a well-known coupling between the respiratory and cardiac systems, which is a measure of the amplitude of variation of the heartbeat intervals within respiratory cycles [18]. The changes in the maternal respiratory system – in particular, the increased lateral and decreased inferior expansion of the lungs – could reduce RSA. This is likely the reason for the difference in the response seen in the BPRSA analysis of CRC from respiration to cardiac activity (Figure 7). There is a larger response in the HR corresponding to inhalations and exhalations for non-pregnant women than for pregnant ones, which is confirmed by the large, statistically significant differences in MBA between the groups ($p < 0.001$, $d > 1.2$, Table 4). Furthermore, there is more regularity (confirmed by the significant differences in SampEn between the groups, Section 3.2.4) in the BPRSA waveforms of non-pregnant women, suggesting that this aspect of their CRC is more regular and predictable than that of pregnant women.

Third, and lastly, there is increased physiological stress during pregnancy. Pregnancy is often referred to as a nine-month stress test for the body [52], [53], and coupling between physiological systems reduces or even disappears under stress as the two sub-systems start functioning more independently. Subsequently, the stress that pregnancy places on the body likely contributes to both the reduced CRPS and smaller BPRSA response seen in pregnant women. However, it is important to note here that while coupling reduces during pregnancy, it still occurs. Therefore, it seems that the mother's body adapts well enough to the increased demands of pregnancy, including the physiological stress, altered autonomic state, and remodeled respiratory system, to still maintain CRC.

CRC is a complex physiological phenomenon that is not yet fully understood in healthy individuals [54], much less in pregnant women. The literature concerning the latter is very limited. One research group found that CRC changes with gestational age [16]. While we conversely found no relationship between CRC and progressing pregnancy

(Section 3), we should note that the gestational age range of our group is substantially smaller than theirs, which may be obscuring changes. Maternal CRC warrants further investigation. Investigating CRC provides additional insights into the physiology of pregnancy. Moreover, assessing CRC may offer opportunities for the early detection of pregnancy complications, as CRC is autonomically regulated and pregnancy complications are linked to autonomic dysfunction. The case for such assessments has already been made, as two investigations have demonstrated differences in CRC between healthy pregnant women and those with preeclampsia [14], [15].

When assessing CRC through the filter of a specific sleep stage, we find that not only are certain differences between pregnant and non-pregnant women greater than when assessed across the entire night recording (Figures 4 and 8), but this stratification also reveals changes that are not apparent when using the entire night's recording (Figure 6). Therefore, we postulate that differences between healthy and complicated pregnancies might be further illuminated by comparing CRC per sleep stage, rather than based on the recordings of an entire night. It should be remembered, however, that stratifying by sleep stages potentially eliminates the effect of short sleep stages (less than one minute in the case of the synchrogram and less than three minutes for BPRSA) as well as the impact of the transitions between the sleep stages. Further investigation is needed to understand the relationship between sleep stages transition and CRC.

A limitation of this work is that the measurement setup for the two groups differed; data from non-pregnant women were collected in a sleep lab, while those of pregnant women were collected at home. Stratifying the analyses by sleep stages aids in reducing the impact of these differing setups. However, it is not possible to reliably compare the Wake states between the groups. While the non-pregnant women would be in a supine position during Wake, no information is available on the posture or activities of the pregnant women during Wake.

To conclude, this work offers novel insights into the physiology of pregnancy. We show that while CRC is present in healthy pregnancy, it occurs less often than in non-pregnant women. The sensitivity of CRC to pregnancy suggests that it might be an additional tool for assessing maternal health. Additionally, assessing CRC per sleep stage will likely offer more meaningful information than assessing CRC across the entire night.

References

[1] V. L. Brooks, Q. Fu, Z. Shi, and C. M. Heesch, "Adaptations in autonomic nervous system regulation in normal and hypertensive pregnancy," in *Handbook of Clinical Neurology*, Elsevier, 2020, pp. 57–84. doi: 10.1016/B978-0-444-64239-4.00003-5.

[2] Q. Fu, "Hemodynamic and Electrocardiographic Aspects of Uncomplicated Singleton Pregnancy.," *Advances in experimental medicine and biology*, vol. 1065, pp. 413–431, 2018, doi: 10.1007/978-3-319-77932-4_26.

[3] S. Moors *et al.*, "Heart rate variability in hypertensive pregnancy disorders: a systematic review," *Pregnancy Hypertension*, Mar. 2020, doi: 10.1016/j.preghy.2020.03.003.

[4] K. S. Khan, D. Wojdyla, L. Say, A. M. Gulmezoglu, and P. F. V. Look, "WHO analysis of causes of maternal death: a systematic review," *Lancet (London, England)*, vol. 367, no. 9516, pp. 1066–1074, Apr. 2006.

[5] World Health Organization, United Nations Population Fund, Mailman School of Public Health. Averting Maternal Death and Disability, and United Nations Children's Fund (UNICEF), "Monitoring emergency obstetric care : a handbook," *Surveillance des soins obstétricaux d'urgence : manuel d'utilisation*, p. 152, 2009, Accessed: Jan. 18, 2023. [Online]. Available: https://apps.who.int/iris/handle/10665/44121

[6] Y. A. Barbitoff *et al.*, "A Data-Driven Review of the Genetic Factors of Pregnancy Complications," *IJMS*, vol. 21, no. 9, p. 3384, May 2020, doi: 10.3390/ijms21093384.

[7] S. Rang, H. Wolf, G. A. Montfrans, and J. M. Karemaker, "Non–invasive assessment of autonomic cardiovascular control in normal human pregnancy and pregnancy- associated hypertensive disorders: a review," *Journal of Hypertension*, vol. 20, no. 11, pp. 2111–2119, 2002.

[8] G. K. Pal, P. Shyma, S. Habeebullah, P. Shyjus, and P. Pal, "Spectral Analysis of Heart Rate Variability for Early Prediction of Pregnancy-Induced Hypertension," *Clinical and Experimental Hypertension*, vol. 31, no. 4, pp. 330–341, Jan. 2009, doi: 10.1080/10641960802621333.

[9] S. V. Khlybova, V. I. Tsirkin, S. A. Dvoryanskii, I. A. Makarova, and A. N. Trukhin, "Heart rate variability in normal and complicated pregnancies," *Hum Physiol*, vol. 34, no. 5, pp. 625–632, Sep. 2008, doi: 10.1134/S0362119708050113.

[10] F. Shaffer and J. P. Ginsberg, "An Overview of Heart Rate Variability Metrics and Norms," *Front. Public Health*, vol. 5, p. 258, Sep. 2017, doi: 10.3389/fpubh.2017.00258.

[11] M. Bester, R. Joshi, M. Mischi, J. O. E. H. Van Laar, and R. Vullings, "On the distinct differences in autonomic regulation between healthy pregnant and non-prengnant women - a HRV analysis," *Submitted*, 2023.

[12] J. M. Karemaker, "An introduction into autonomic nervous function," *Physiol. Meas.*, vol. 38, no. 5, pp. R89–R118, May 2017, doi: 10.1088/1361-6579/aa6782.

[13] A. J. Garcia, J. E. Koschnitzky, T. Dashevskiy, and J.-M. Ramirez, "Cardiorespiratory coupling in health and disease," *Autonomic Neuroscience*, vol. 175, no. 1–2, pp. 26–37, Apr. 2013, doi: 10.1016/j.autneu.2013.02.006.

[14] K. Berg, J. F. Kraemer, M. Riedl, H. Stepan, J. Kurths, and N. Wessel, "Increased cardiorespiratory coordination in preeclampsia," *Physiol. Meas.*, vol. 38, no. 5, pp. 912–924, May 2017, doi: 10.1088/1361-6579/aa64b0.

[15] M. Riedl, A. Suhrbier, H. Stepan, J. Kurths, and N. Wessel, "Short-term couplings of the cardiovascular system in pregnant women suffering from pre-eclampsia," *Phil. Trans. R. Soc. A.*, vol. 368, no. 1918, pp. 2237–2250, May 2010, doi: 10.1098/rsta.2010.0029.

[16] M. G. Moertl *et al.*, "Changes in haemodynamic and autonomous nervous system parameters measured non-invasively throughout normal pregnancy," *European Journal of Obstetrics & Gynecology and Reproductive Biology*, vol. 144, pp. S179–S183, May 2009, doi: 10.1016/j.ejogrb.2009.02.037.

[17] G. Speranza, G. Verlato, and A. Albiero, "Autonomic changes during pregnancy: Assessment by spectral heart rate variability analysis," *Journal of Electrocardiology*, vol. 31, no. 2, pp. 101–109, Apr. 1998, doi: 10.1016/S0022-0736(98)90040-1.

[18] R. P. Bartsch, A. Y. Schumann, J. W. Kantelhardt, T. Penzel, and P. Ch. Ivanov, "Phase transitions in physiologic coupling," *Proc. Natl. Acad. Sci. U.S.A.*, vol. 109, no. 26, pp. 10181–10186, Jun. 2012, doi: 10.1073/pnas.1204568109.

[19] V. Tonu, V. Vovc, and N. Enache, "Cardiorespiratory Coupling: A Review of the Analysis Methods," in *4th International Conference on Nanotechnologies and Biomedical Engineering*, I. Tiginyanu, V. Sontea, and S. Railean, Eds., in IFMBE Proceedings, vol. 77. Cham: Springer International Publishing, 2020, pp. 469–474. doi: 10.1007/978-3-030-31866-6_84.

[20] R. Joshi, D. Kommers, X. Long, L. Feijs, and S. V. Huffel, "Cardiorespiratory coupling in preterm infants," *J Appl Physiol*, vol. 126, pp. 202–213, doi: 10.1152/japplphysiol.00722.2018.

[21] M. Lucchini, W. P. Fifer, M. Ferrario, and M. G. Signorini, "Feasibility study for the assessment of cardio-respiratory coupling in newborn infants," in *2016 38th Annual International Conference of the IEEE Engineering in Medicine and Biology Society (EMBC)*, Orlando, FL, USA: IEEE, Aug. 2016, pp. 5509–5512. doi: 10.1109/EMBC.2016.7591974.

[22] M. W Rivolta and R. Sassi, "Comparison Between Bivariate Phase-Rectified Signal Averaging and Sequence Method in Assessing the Baroreflex Sensitivity," presented at the 2020 Computing in Cardiology Conference, Dec. 2020. doi: 10.22489/CinC.2020.444.

[23] B. De Maria *et al.*, "Separating arterial pressure increases and decreases in assessing cardiac baroreflex sensitivity via sequence and bivariate phase-rectified signal averaging techniques," *Med Biol Eng Comput*, vol. 56, no. 7, pp. 1241–1252, Jul. 2018, doi: 10.1007/s11517-017-1765-0.

[24] A. Bauer *et al.*, "Bivariate phase-rectified signal averaging for assessment of spontaneous baroreflex sensitivity: pilot study of the technology," *Journal of Electrocardiology*, vol. 43, no. 6, pp. 649–653, Nov. 2010, doi: 10.1016/j.jelectrocard.2010.05.012.

[25] A. Müller *et al.*, "Bivariate phase-rectified signal averaging for assessment of spontaneous baroreflex sensitivity: normalization of the results," *Journal of Electrocardiology*, vol. 45, no. 1, pp. 77–81, Jan. 2012, doi: 10.1016/j.jelectrocard.2011.07.010.

[26] J. E. Montero-Nava *et al.*, "Analysis of the fetal cardio-electrohysterographic coupling at the third trimester of gestation in healthy women by Bivariate Phase-Rectified Signal Averaging," *PLoS ONE*, vol. 15, no. 7, p. e0236123, Jul. 2020, doi: 10.1371/journal.pone.0236123.

[27] D. Casati *et al.*, "Assessment of Coupling between Trans-Abdominally Acquired Fetal ECG and Uterine Activity by Bivariate Phase-Rectified Signal Averaging Analysis," *PLoS ONE*, vol. 9, no. 4, p. e94557, Apr. 2014, doi: 10.1371/journal.pone.0094557.

[28] C. G. Esquivel-Arizmendi *et al.*, "Analysis of the Maternal Cardio-Electrohysterograph-

ic Coupling During Labor by Bivariate Phase-Rectified Signal Averaging," in *VIII Latin American Conference on Biomedical Engineering and XLII National Conference on Biomedical Engineering*, C. A. González Díaz, C. Chapa González, E. Laciar Leber, H. A. Vélez, N. P. Puente, D.-L. Flores, A. O. Andrade, H. A. Galván, F. Martínez, R. García, C. J. Trujillo, and A. R. Mejía, Eds., in IFMBE Proceedings, vol. 75. Cham: Springer International Publishing, 2020, pp. 21–27. doi: 10.1007/978-3-030-30648-9_3.

[29] F. B. van Meulen *et al.*, "Contactless Camera-Based Sleep Staging: The HealthBed Study," *Bioengineering*, vol. 10, no. 1, p. 109, Jan. 2023, doi: 10.3390/bioengineering10010109.

[30] D. Khodadad *et al.*, "Optimized breath detection algorithm in electrical impedance tomography," *Physiol. Meas.*, vol. 39, no. 9, p. 094001, Sep. 2018, doi: 10.1088/1361-6579/aad7e6.

[31] D. Makowski *et al.*, "NeuroKit2: A Python toolbox for neurophysiological signal processing," *Behav Res*, vol. 53, no. 4, pp. 1689–1696, Aug. 2021, doi: 10.3758/s13428-020-01516-y.

[32] M. J. Rooijakkers, C. Rabotti, M. Bennebroek, J. van Meerbergen, and M. Mischi, "Low-complexity R-peak detection in ECG signals: A preliminary step towards ambulatory fetal monitoring," in *2011 Annual International Conference of the IEEE Engineering in Medicine and Biology Society*, Boston, MA: IEEE, Aug. 2011, pp. 1761–1764. doi: 10.1109/IEMBS.2011.6090503.

[33] C. Schäfer, M. G. Rosenblum, H.-H. Abel, and J. Kurths, "Synchronization in the human cardiorespiratory system," *Phys. Rev. E*, vol. 60, no. 1, pp. 857–870, Jul. 1999, doi: 10.1103/PhysRevE.60.857.

[34] E. Toledo, S. Akselrod, I. Pinhas, and D. Aravot, "Does synchronization reflect a true interaction in the cardiorespiratory system?," *Medical Engineering*, p. 8, 2002.

[35] H. Krause, J. F. Kraemer, T. Penzel, J. Kurths, and N. Wessel, "On the difference of cardiorespiratory synchronisation and coordination," *Chaos*, vol. 27, no. 9, p. 093933, Sep. 2017, doi: 10.1063/1.4999352.

[36] R. Bartsch, J. W. Kantelhardt, T. Penzel, and S. Havlin, "Experimental Evidence for Phase Synchronization Transitions in the Human Cardiorespiratory System," *Phys. Rev. Lett.*, vol. 98, no. 5, p. 054102, Feb. 2007, doi: 10.1103/PhysRevLett.98.054102.

[37] R. Jerath, K. Harden, M. Crawford, V. A. Barnes, and M. Jensen, "Role of cardiorespiratory synchronization and sleep physiology: effects on membrane potential in the restorative functions of sleep," *Sleep Medicine*, vol. 15, no. 3, pp. 279–288, Mar. 2014, doi: 10.1016/j.sleep.2013.10.017.

[38] A. Bauer, P. Barthel, A. Müller, J. Kantelhardt, and G. Schmidt, "Bivariate phase-rectified signal averaging—a novel technique for cross-correlation analysis in noisy nonstationary signals," *Journal of Electrocardiology*, vol. 42, no. 6, pp. 602–606, Nov. 2009, doi: 10.1016/j.jelectrocard.2009.06.023.

[39] A. Y. Schumann, J. W. Kantelhardt, A. Bauer, and G. Schmidt, "Bivariate phase-rectified signal averaging," *Physica A: Statistical Mechanics and its Applications*, vol. 387, no. 21, pp. 5091–5100, Sep. 2008, doi: 10.1016/j.physa.2008.05.002.

[40] A. Bauer *et al.*, "Phase-rectified signal averaging detects quasi-periodicities in non-stationary data," *Physica A: Statistical Mechanics and its Applications*, vol. 364, pp. 423–434, May 2006, doi: 10.1016/j.physa.2005.08.080.

[41] S. M. Lobmaier *et al.*, "Fetal heart rate variability responsiveness to maternal stress,

non-invasively detected from maternal transabdominal ECG," *Arch Gynecol Obstet*, vol. 301, no. 2, pp. 405–414, Feb. 2020, doi: 10.1007/s00404-019-05390-8.

[42] A. Y. Schumann, R. P. Bartsch, T. Penzel, P. Ch. Ivanov, and J. W. Kantelhardt, "Aging Effects on Cardiac and Respiratory Dynamics in Healthy Subjects across Sleep Stages," *Sleep*, vol. 33, no. 7, pp. 943–955, Jul. 2010, doi: 10.1093/sleep/33.7.943.

[43] B. M. Wulterkens *et al.*, "It is All in the Wrist: Wearable Sleep Staging in a Clinical Population versus Reference Polysomnography," *NSS*, vol. Volume 13, pp. 885–897, Jun. 2021, doi: 10.2147/NSS.S306808.

[44] K. Kelley, "The Effects of Nonnormal Distributions on Confidence Intervals Around the Standardized Mean Difference: Bootstrap and Parametric Confidence Intervals," *Educational and Psychological Measurement*, vol. 65, no. 1, pp. 51–69, Feb. 2005, doi: 10.1177/0013164404264850.

[45] D. L. Wilson, M. Barnes, L. Ellett, M. Permezel, M. Jackson, and S. F. Crowe, "Decreased sleep efficiency, increased wake after sleep onset and increased cortical arousals in late pregnancy: Decreased sleep efficiency in late pregnancy," *Australian and New Zealand Journal of Obstetrics and Gynaecology*, vol. 51, no. 1, pp. 38–46, Feb. 2011, doi: 10.1111/j.1479-828X.2010.01252.x.

[46] B. Izci-Balserak, B. T. Keenan, C. Corbitt, B. Staley, M. Perlis, and G. W. Pien, "Changes in Sleep Characteristics and Breathing Parameters During Sleep in Early and Late Pregnancy," *Journal of Clinical Sleep Medicine*, vol. 14, no. 07, pp. 1161–1168, Jul. 2018, doi: 10.5664/jcsm.7216.

[47] L. M. Reyes, C. W. Usselman, M. H. Davenport, and C. D. Steinback, "Sympathetic Nervous System Regulation in Human Normotensive and Hypertensive Pregnancies.," *Hypertension (Dallas, Tex. : 1979)*, vol. 71, no. 5, pp. 793–803, May 2018, doi: 10.1161/HYPERTENSIONAHA.117.10766.

[48] M. Bester, R. Rizea, R. Joshi, M. Mischi, J. O. E. H. Van Laar, and R. Vullings, "Maternal Autonomic Responsiveness Is Attenuated in Healthy Pregnancy: A Phase Rectified Signal Averaging Analysis," presented at the EMBC, Jul. 2022.

[49] L. J. Green *et al.*, "Gestation-Specific Vital Sign Reference Ranges in Pregnancy," *Obstetrics & Gynecology*, vol. 135, no. 3, pp. 653–664, Mar. 2020, doi: 10.1097/AOG.0000000000003721.

[50] M. G. Miglis, "Sleep and the Autonomic Nervous System," in *Sleep and Neurologic Disease*, Elsevier, 2017, pp. 227–244. doi: 10.1016/B978-0-12-804074-4.00018-2.

[51] A. LoMauro and A. Aliverti, "Respiratory physiology of pregnancy: Physiology masterclass," *Breathe*, vol. 11, no. 4, pp. 297–301, Dec. 2015, doi: 10.1183/20734735.008615.

[52] T. D. Bilhartz, P. A. Bilhartz, T. N. Bilhartz, and R. D. Bilhartz, "Making Use of a Natural Stress Test: Pregnancy and Cardiovascular Risk," *Journal of Women's Health*, vol. 20, no. 5, p. 8, 2011, doi: 10.1089/jwh.2010.2291.

[53] L. Chasan-Taber, "It Is Time to View Pregnancy as a Stress Test," *JOURNAL OF WOMEN'S HEALTH*, vol. 25, no. 1, p. 2, 2016, doi: 10.1089/jwh.2015.5653.

[54] R. M. de Abreu, B. Cairo, and A. Porta, "On the significance of estimating cardiorespiratory coupling strength in sports medicine," *Front. Netw. Physiol.*, vol. 2, p. 1114733, Jan. 2023, doi: 10.3389/fnetp.2022.1114733.

Chapter 10

Evidence and clinical relevance of maternal-fetal cardiac coupling: a scoping review

10

Reproduced after: TJ Nichting*, M Bester*, R Joshi, M Mischi, M van der Ven, DAA van der Woude, SG Oei, JOEH van Laar, R Vullings. Evidence and clinical relevance of maternal-fetal cardiac coupling: a scoping review. *Accepted for publication, PLOS One.* 2023. *Equal contribution.

Abstract

Background: Researchers have long suspected a mutual interaction between maternal and fetal heart rhythms, referred to as maternal-fetal cardiac coupling (MFCC). While several studies have been published on this phenomenon, they vary in terms of methodologies, populations assessed, and definitions of coupling. Moreover, a clear discussion of the potential clinical implications is often lacking. Subsequently, we perform a scoping review to map the current state of the research in this field and, by doing so, form a foundation for clinically oriented future research on this topic.

Methods: A literature search was performed in PubMed, Embase, and Cochrane. After screening for the title and the abstract, a full-text evaluation of eligibility followed. All studies on MFCC were included which described coupling between heart rate measurements in both the mother and fetus, regardless of the coupling method used, gestational age, or the maternal or fetal health condition.

Results: 23 studies remained after a systematic evaluation of 6,672 studies. Of these, 21 studies found at least occasional instances of MFCC. Methods used to capture MFCC are synchrograms and corresponding phase coherence indices, cross-correlation, joint symbolic dynamics, transfer entropy, bivariate phase rectified signal averaging, and deep coherence. Physiological pathways regulating MFCC are suggested to exist either via the autonomic nervous system or due to the vibroacoustic effect, though neither of these suggested pathways has been verified. The strength and direction of MFCC are found to change with gestational age and with the rate of maternal breathing, while also being further altered in fetuses with cardiac abnormalities and during labor.

Conclusion: From the synthesis of the available literature on MFCC presented in this scoping review, it seems evident that MFCC does indeed exist and may have clinical relevance in tracking fetal well-being and development during pregnancy.

1. Introduction

Although the mother and fetus are physically distinct from each other, their cardiac systems are connected via the placenta to facilitate gas and nutrient exchange for the fetus [1]. Both cardiac systems are constantly adapting in response to external as well as internal stimuli [2].

For example, the mother's heart rate (HR) is influenced by the environmental temperature and the time of day but also changes in response to her stress levels [2], [3]. Similarly, the fetal HR will be regulated in response to internal triggers, for example, fetal blood oxygen levels [4], as well as external triggers such as lights and sounds sensed through the maternal abdomen [5]. However, since the external environment of the fetus is that of the maternal womb, the fetus also responds to changes in maternal physiology, for example changing maternal stress levels [6]. Moreover, the fetus forms part of the internal environment of the mother, and maternal HR has also been observed to change in response to fetal movement [7]. Researchers have suggested that maternal HR may respond to changes in fetal HR and vice versa – this mutual interaction is referred to as maternal-fetal cardiac coupling (MFCC) [8].

Since Hildebrandt et al. in 1979 first suggested that there may be an interaction between maternal and fetal heartbeats [9], researchers have investigated the potential existence and applications of MFCC [10]–[12]. Quantifying and understanding the presence, strength, and direction of MFCC is valuable. Not only could assessments of MFCC elucidate gestational cardiac physiology, but such assessments may also offer tools to track fetal development and screen for maternal and fetal complications [13]–[15].

The potential interaction between maternal and fetal heart rhythms is a complex and not yet clearly defined research field [8], [16]. Although more than 20 research studies have been published on the topic of MFCC, these studies not only employ different methods and study different populations but also define MFCC differently. Consequently, how to quantify and interpret MFCC remains unclear. Moreover, while clinical relevance is a common aim of research on physiological coupling, results of MFCC analyses are reported without a clear discussion of the potential clinical implications.

Therefore, an exploratory mapping of existing literature – presented in a clinically accessible manner – is a necessary foundation for future clinically motivated research in this field. As MFCC is an area of emerging research, this topic lends itself to a scop-

ing review. A scoping review provides a detailed overview of all research in the field and goes beyond answering a specific question, as is typically the motivation for a systematic review. In this manner, scoping reviews generate findings that help refine research priorities and inform future primary research [17], [18].

With this scoping review, we aim to ascertain the current state of research on MFCC and, in doing so, form a foundation for future clinically oriented research on this topic. To this end, we perform a search of all available research in this field. Thereafter, we synthesize the evolution of the methodologies employed to capture MFCC. Next, we summarize the results to determine whether MFCC exists and, if so, which physiological pathways may regulate MFCC. Finally, we discuss the potential clinical implications of MFCC.

2. Methods

The methodology for this scoping review followed the framework first suggested by Arksey and O'Malley [17] while incorporating further suggestions and insights from Levac et al. [19], Daudt et al. [20], Munn et al. [18], and Peters et al. [21]. The review was reported per the PRISMA guidelines extension for scoping reviews (PRISMA-ScR) [22]. The protocol for this review was preregistered before the literature search and data extraction on Open Science Framework (Registration DOI: **10.17605/OSF.IO/DYF34**).

2.1 Search strategies and study selection

The search strategy was developed in consultation with a clinical librarian and can be found in Appendix 1. Searches were carried out on 27 October 2022 in PubMed, Embase, and Cochrane. No date limits or other filters were applied, but the language was limited to English, Dutch, and German, owing to the language proficiency of the primary authors. Search results were downloaded and systematically sorted using Rayyan QCRI, a platform specifically designed to manage the review process (**https://rayyan.qcri.org/welcome**). Citations and references of the included studies were further searched to identify more potential studies. Additionally, publications from active researchers in the field of MFCC were tracked and included if relevant to this scoping review.

Studies had to meet certain criteria to be eligible for the review. All studies assessing MFCC – regardless of the coupling method used, gestational age (GA), or the

maternal-fetal health condition – which incorporated HR measurements from both the mother and fetus, were allowed for this scoping review. Studies measuring *only* other types of coupling, e.g. coupling between maternal HR and fetal movement, were excluded.

The review process comprised two levels of screening. First, the title and abstract of all the identified literature were screened. Thereafter, a full-text review of studies identified in the first level was carried out to assess eligibility. The review process was carried out independently by two researchers (MB, TN), blinded to each other's results [19]. After each level of screening, the identified studies were discussed. Disagreement was resolved by discussion. If necessary, an independent researcher was consulted to decide whether an article should be included.

In some cases, research was disseminated first as a conference paper and thereafter as a journal article. In these cases, when everything reported in the conference paper was encompassed in the journal article, the conference paper was excluded. Furthermore, if only a conference abstract was available for a study without an accompanying paper, the abstract was excluded.

3. Results

A total of 6,672 studies were identified by searching the indicated databases. An additional six studies were found through other resources; three were found by searching the references of studies included through the database search, while three were found via searches of publications from researchers active in the field of MFCC. The latter three were either conference papers from technically oriented conference proceedings [23] or articles from journals that are not listed in PubMed, Embase, or Cochrane [8], [12]. After removing the duplicate studies, 4,813 unique studies remained, of which 32 were found eligible for full-text screening. After this full-text assessment, 23 studies were included in this review. Figure 1 shows a flowchart of the selection process. The study characteristics and results are summarized in Table 1.

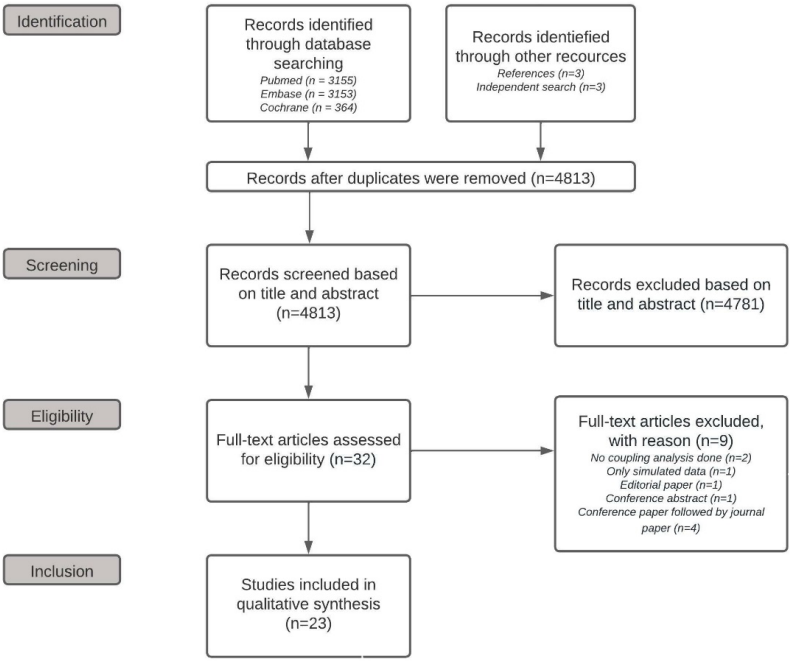

Figure 1: Flowchart of the selection process

Hereafter we will elaborate on four aspects of the results reported in the table, namely: the different methodologies that have been used to capture MFCC; the results on the existence and direction of MFCC; the physiological explanations offered for MFCC; and the potential clinical possibilities of MFCC suggested in the included studies.

3.1 MFCC: methodologies.

Broadly, MFCC analyses may be assigned to three groups: synchronization or coordination, describing a fixed relationship between two signals in either phase or time; pattern-matching, where the aim is to see if similar activity occurs in both signals; and modulation, which implies that changes in one signal results in or relates to changes in another [24]. The methodology of earlier studies investigating MFCC focused on finding periods of synchronization with synchrograms and corresponding phase coherence indices [9], [25]–[30], as well as corresponding patterns between maternal and fetal cardiac activity with cross-correlation [7], [31], [32]. In line with the latter, joint-symbolic dynamics was subsequently used to investigate whether maternal and fetal HR behavior corresponded to each other [8], [33], [34]. In more recent studies, the focus mostly shifted towards methods more closely associated with modulation [6], [10]–[12], [35]. A summary of these methods is presented here.

Table 1: Characteristics and main results of the included articles.

Author, year	Document type and study design	Population (nr. of recordings)	Gestational age, weeks (nr. of recordings)	In- and exclusion criteria	
Hildebrandt, 1979 [9]	Journal article. Longitudinal prospective cohort.	Total 2 (85)	Month 8 or 9 of pregnancy	× Inclusion: N/A × Exclusion: N/A	
Van Leeuwen, 2003 [25]	Journal article. Longitudinal prospective cohort.	Total 62 (177) × Healthy 35 (139) × FGR 21 (30) × Isolated ectopic beats or short-lived bradycardia 6 (8)	16-42 × 2nd trimester (49) × 3rd trimester (128)	× Inclusion: N/A × Exclusion: persistent arrhythmias	
DiPietro, 2004 [7]	Journal article. Longitudinal prospective cohort.	Total 137 (822)	20, 24, 28, 32, 36, 38	× Inclusion: non-smoking, uncomplicated singleton pregnancy. × Exclusion: preterm delivery, GDM, congenital malformation, fetal death in utero, nonviable delivery, FGR, loss to follow-up.	
DiPietro, 2006 [31]	Journal article. Longitudinal prospective cohort.	Total 195 (1170)	20, 24, 28, 32, 36, 38	× Inclusion: uncomplicated singleton. × Exclusion: preterm delivery, congenital malformations, fetal death in utero, nonviable delivery, condition of antepartum origin detected in the newborn, loss to follow-up.	
Van Leeuwen, 2009 [26]	Journal article. Prospective cohort.	Total 6 (7)	34-40	× Inclusion: N/A × Exclusion: N/A	

	Data acquisition methods	Coupling assessment method	Results (if coupling ratios are presented, these are M:F)	Presence of cardiac coupling	Direction of coupling	Clinical utility
	× Method: fetal and maternal ECG × Duration: continuous recording for 3 or 7 nights, respectively; recordings are broken up into 1-hour segments × Verification of results: N/A	Synchrograms and phase coherence	× 30/85 (35.3%) recordings with periods of synchronization. × Significant phase preference at 2:1.	Occasional	N/A	N/A
	× Method: magnetocardiography, × Duration: 5-minute recordings. × Verification of results: surrogate twin method	Synchrograms and phase coherence	× 164/177 recordings (92.6%) with periods of synchronization. × More synchronization periods in the 3rd trimester than in the 2nd trimester, × Significant phase preference at 3:5 and 4:7. × However, the number and duration of synchronization periods were similar to surrogate data.	Occasional	N/A	N/A
	× Method: fetal actocardiography and maternal ECG × Duration: 30-50 minutes × Verification of results: N/A	Cross-correlation	× No relationship between fetal heart rate and maternal heart rate.	No	N/A	N/A
	× Method: fetal actocardiograph and maternal ECG × Duration: 50 minutes × Verification of results: N/A	Cross-correlation	× No relationship between fetal heart rate and maternal heart rate.	No	N/A	N/A
	× Method: magnetocardigraphy × Duration: 40 minutes, which includes 5-minute recordings for 6 different maternal breathing paces (15 cpm, 10 cpm, 20 cpm, 12cpm, spontaneously) × Verification of results: surrogate twin method.	Synchrograms and phase coherence	× Synchronization periods in all recordings × Synchronization periods were more prevalent at higher breathing paces × Significant phase preference at 12 cpm: 2:3. × Significant phase preference at 20 cpm: 3:4 and 3:5.	Yes	N/A	Fetal surveillance and the detection of pathological conditions in pregnancy

Riedl, 2009 [35]	Journal article. Retrospective cohort study.	Total 3 (3)	End of pregnancy	× Inclusion: N/A × Exclusion: N/A	
Wang, 2013 [28]	Conference paper prospective cohort.	Total 37 (39)	16-40 × 16-26 (10) × 27-33 (13) × 34-40 (16)	× Inclusion: N/A × Exclusion: abnormal range of FHR.	
Van Leeuwen, 2014 [27]	Journal paper. Retrospective cohort study.	Total 40 (40) × Exercise 21 (21) × Control 19 (19)	36	× Inclusion: low-risk pregnancies, singleton, 20-35 years. Subjects in the exercise group exercised for a minimum of 30 minutes, 3 times a week (based on MPAQ questionnaire). × Exclusion: excessive artefacts (ectopic beats, preventricular or preatrial contractions)	
Khandoker, 2014 [33]	Conference paper. Longitudinal prospective cohort.	Total 45 (66)	× 16-25 (22) × 26-30 (22) × 32-41 (22)	× Inclusion: singleton pregnancies × Exclusion: N/A	
Mazbanrad, 2015 [10]	Journal paper Prospective cohort.	Total 65 (65) The same population as Khandoker 2016, but different coupling assessment method.	16-41 × 16-25 (25) × 26-31 (18) × 18-41 (22)	× Inclusion: normal, singleton pregnancies × Exclusion: N/A	
Khandoker, 2016 [12]	Journal paper. Prospective cohort	Total 66 (66) The same population as Mazbanrad 2015, but different coupling assessment method.	16-41 × 16-25 (22) × 26-31 (22) × 18-41 (22)	× Inclusion: normal, singleton pregnancies × Exclusion: N/A	

	× Method: magnetocardiography × Duration: 5-minute recording at a maternal breathing paces of 20 cpm. × Verification of results: surrogate twin method.	Phase locking, Partial Directed Coherence	× Only a few synchronization periods could not be explained by surrogate data × Significant phase preference at 3:5	Occasional	M→F	Detection of prenatal disease or deficit. Assessment of fetal neural integration
	× Method: abdominal fetal and maternal ECG × Duration: 1 minute. × Verification of results: N/A	Synchrograms and phase coherence	× Synchronization periods for all recordings × Significant phase preference at 1:2 and 4:5	Yes	N/A	Clinical markers for evaluating antenatal development
	× Method: magnetocardiography × Duration: 18 minutes × Verification of results: surrogate twin method.	Synchrograms and phase coherence	× Synchronization periods in all recordings × Less synchronization in the exercise group × Synchronization is more prevalent at higher breathing paces	Occasional	N/A	Marker for physiological health or development
	× Method: abdominal fetal and maternal ECG × Duration: 1 minute × Verification of results: N/A	Joint Symbolic Dynamics	× Results indicated significant differences in coupling between early- and mid-gestation as well as early- and late gestation × No differences were seen between mid and late gestation. A variety of coupling patterns can be used to differentiate between gestational groups	Yes	N/A	Clinical markers of healthy prenatal development and fetal cardiac anomalies
	× Method: abdominal fetal and maternal ECG × Duration: 1 minute × Verification of results: surrogate twin method.	Transfer Entropy	× Significant TE for 63/65 cases × Significant increase in TE (M→F) and a decreasing trend (F→M) with increasing GA × Decreased delay in TE (M→F)	Yes	Both directions	Assessment of fetal sensory and autonomic nervous system
	× Method: abdominal fetal and maternal ECG × Duration: 1-2 minutes × Verification of results: surrogate twin method.	Partial Directed Coherence	× MFCC (M→F) was weak during early gestation, became the strongest in mid-gestation and remained so in late gestation × MFCC (F→M) was the strongest during early gestation and gradually decreased with gestational age progression.	Yes	Both directions	Assessment of fetal well-being

Alangri, 2018 [29]	Conference paper. Prospective cohort	Total 70 (70) Cohort: 44 (44) × Healthy 37 (37) × CHD 7 (7) Added from another database 26 (26)	× <32: healthy (22), CHD (5). × >32: healthy (15), CHD (2). Added from another database (26) × >32 (26)	× Inclusion: N/A × Exclusion: N/A	
Avci, 2018 [11]	Conference paper. Prospective cohort	Total 74 (74)	28-38 × <32 (31) × >31 (43)	× Inclusion: low risk pregnant women × Exclusion: N/A	
Khandoker. 2019 [34]	Journal article. Prospective cohort The same population as Khandoker 2014 and 2019, but with different coupling assessment method and abnormal cases are added.	Total 85 (85) × Healthy 66 (66) Abnormal = fetal bradycardia fetal, tachycardia, premature atrial contraction, different types of CHD 19 (19)	16-41 Healthy: × 16-25 (22) × 26-30 (22) × 32-40 (22) Abnormal × 19-38 weeks (19)	× Inclusion: N/A × Exclusion: N/A	
Khandoker, 2019 [15]	Journal article. Prospective cohort Same population as Khandoker 2014 and 2019, but different coupling assessment method or abnormal cases are added.	Total 85 (85) × Healthy 66 (66) × Abnormal = fetal bradycardia fetal, tachycardia, premature atrial contraction, different types of CHD 19 (19)	16-41 Healthy: × 16-25 (22) × 26-30 (22) × 32-40 (22) Abnormal × 19-38 weeks (19)	× Inclusion: for healthy fetuses as per intrapartum monitoring guidelines (FIGO) × Exclusion: N/A	
Khandoker, 2020 [14]	Conference paper. Prospective cohort	Total 16 (16)	19-32 weeks	× Inclusion: No records of fetal abnormalities × Exclusion: N/A	

	× Method longitudinal cohort: abdominal fetal and maternal ECG × Method other database: Phonocardiography × Duration: 1 minute × Verification of results: N/A	Synchrogram and phase coherence	× Significant difference in phase coherence index in healthy pregnancies between early GA and late GA × Significant difference in phase coherence index between healthy pregnancies during early GA and fetuses with CHD	Yes	N/A	Marker for development of the autonomic nervous system and impairment of cardiac autonomic activity
	× Method: magnetocardiography × Duration: 6-11 minutes × Verification of results: N/A	Transfer Entropy	× TE (M→F) did not significantly change with increasing GA* × TE (F→M) showed a decreasing trend with increasing GA*	Yes	Both directions	N/A
	× Method: abdominal fetal and maternal ECG × Duration: 1 minute × Verification of results: N/A	Joint Symbolic Dynamics	× Significant differences in the occurrence of a variety of coupling patterns between early and mid/late gestation. × Coupling patterns do not capture differences between mid and late gestation × Some coupling indices were significantly different for the abnormal group in comparison to the healthy group	Yes	N/A	Marker for healthy prenatal development and fetal cardiac anomalies
	× Method: abdominal fetal and maternal ECG × Duration: 1 minute × Verification of results: surrogate twin method.	Phase locking, Partial Directed Coherence	× Synchronization (M→F) was increased with increasing GA, maximum during mid-gestation × Synchronization (F→M) was decreased with increasing GA × MFCC (F→M) was weaker in abnormal pregnancies and stronger MFCC (M→F) compared to healthy pregnancies	Yes	Both directions	Marker of healthy prenatal development and its deviation; detecting fetal hypoxia
	× Method: abdominal fetal and maternal ECG × Duration: 10 minutes × Verification of results: N/A	Phase coherence	× Incorporating coupling parameters improves the estimation of GA compared to using only maternal and fetal HRV features	Yes	N/A	Estimation of fetal gestational age

Khandoker, 2020 [23]	Conference paper. Prospective cohort, animal study	Total 6 mice, 10 fetuses (6)	17.5 days (21 days is full term for mice)**	× Inclusion: N/A × Exclusion: N/A	
Lobmaier, 2020 [6]	Journal paper. Prospective case-control	Total 104 (104) × Control 53 (53) × Case stressed 51 (51)	>28 weeks × Control 36.7 (53) × Case 36.4 (51)	× Inclusion: singleton pregnancies, 18-45 years old, third trimester of pregnancy × Exclusion: FGR, fetal malformations, maternal severe illness, maternal drug or alcohol abuse.	
DiPietro, 2021 [32]	Journal paper. Prospective cohort.	Total 84 (84)	36.2	× Inclusion: obese, singleton, non-smoking, normal pregnancies × Exclusion: N/A	
Wahbah, 2021 [30]	Journal paper. Prospective cohort	Total 60 (60)	20-41	× Inclusion: healthy singleton with no records of fetal abnormalities × Exclusion: N/A	
Tepichin-Castro, 2021[8]	Journal paper. Longitudinal prospective cohort	Total 22 (44)	× First measurement in third trimester 36.5 (22) × Second measurement during active labour 39.4 (22)	× Inclusion: low-risk pregnant women × Exclusion: N/A	

	× Method: needle ECG × Duration measurement: 15 minutes × Verification of results: N/A	Phase coherence	× No significant changes in synchronization during anesthesia	Yes	N/A	N/A
	× Method: abdominal fetal and maternal ECG × Duration: 40 minutes × Verification of results: N/A	BPRSA	× Fetal stress index was significantly higher in fetuses of stressed mothers when compared to controls.	Yes	M → F	Identification of children at risk for altered neurodevelopmental trajectories due to perinatal stress exposure to allow for early intervention.
	× Method: Polysomnography and abdominal maternal and fetal ECG × Duration: 5 minutes × Verification of results: N/A	Cross-correlation	× Synchronization was observed only during WASO (wakefulness after sleep onset)	Occasional	N/A	N/A
	× Method: abdominal fetal and maternal ECG × Duration: 10 minutes × Verification of results: N/A	Synchrograms and Phase coherence	× Synchronization changes with GA. × Significant phase preference at 2:3 and 2:4. × Incorporating coupling parameters improves the estimation of GA compared to using only maternal and fetal HRV features.	Yes	N/A	Estimation of fetal gestational age
	× Method: abdominal fetal and maternal ECG × Duration: 5 minutes × Verification of results: N/A	Joint Symbolic Dynamics	× Stronger coupling indices during active labour as compared to third trimester	Yes	N/A	Monitoring during labour to assess fetal well-being of both mother and fetus.

Alkhodori, 2022 [36]	Journal article. Prospective cohort (local dataset for testing and training AI model) and retrospective cohort (Physionet dataset for validation)	Total 114 (941) Local dataset: 109 (873) Physionet dataset: 5 (68)	× Local dataset: 20 – 40 (873) × Physionet dataset: 38 – 41 weeks (68)	× Inclusion: healthy fetal cardiac condition × Exclusion : maternal cardiovascular condition	
Khandoker, 2022 [37]	Journal paper Case-controlled animal study	Total 27 mice (27), 48 fetuses (48) - Atropine injection 9 mice (9), 14 fetuses (14) - Propranolol injection 9 mice (9), 17 fetuses (17) - Saline injection 9 mice (9), 17 fetuses (17)	17.5 days (21 days is full term for mice)	× Inclusion: N/A × Exclusion: N/A	

	× Method: fetal and maternal ECG, × Duration: 1 minute. × Verification of results: results from deep learning are compared to phase coherence index results (considered as the group truth)	Synchrograms and phase coherence index (as ground truth) Deep learning (termed deep coherence)	× The number of recordings with coupling is not specified. × Significant phase preference at 1:2, 2:3, and 3:5. × Deep coherence was 90% accurate in identifying the phase of coupling (AUROC > 0.93) × Phase preferences change with GA × Phase preferences are significantly associated with maternal BMI and age.	Yes	N/A	Continuous monitoring of fetal condition to improve triaging using lower-cost devices with less side-effect than those currently used.
	× Method: needle ECG × Duration: 20 minutes (injection after 10 minutes) × Verification of results: saline injection	Phase coherence	× Atropine injection increases ratio 1:4 and decreases ratios 1:2 and 1:3. × Atropine injection increases ratio 1:4 and 1:5, as well as decreases ratio 1:2. × Coupling ratios are not significantly affected by saline injection.	Yes	N/A	Understanding the role of maternal autonomic activity in fetal development and complications.

BPRSA: bivariate phase rectified signal averaging, **CHD**: congenital heart disease, **CPM**: cycles per minute, **F→M**: Fetal to Maternal Direction, **FGR**: Fetal growth restriction, **GA**: gestational age, **GDM**: Gestational diabetes mellitus, **HRV**: Heart Rate Variability, **M→F**: Maternal to Fetal Direction, **MFCC**: Maternal-Fetal Cardiac Coupling, **MPAQ**: Modifiable Physical Activity Questionnaire, **TE**: Transfer Entropy. P-values of 0.05 were used to indicate significance for all articles included in this review. *P-value of 0.01 (for all other analysis, a P-value of 0.05 was used to demonstrate significance). **Note that contrary to humans, maternal HR in mice is lower than fetal HR [38], [39].

3.1.1 Synchrograms and phase coherence index

Synchrograms are a visual representation of the relative phases of the maternal and fetal heartbeats. The more fixed the relationship between the relative phases of the maternal and fetal heartbeats are, the higher the coherence is between them. When periods of sufficient coherence occur (i.e., where the metric describing coherence exceeds a prespecified threshold), it is determined that phase locking occurs in this period of the signal. The expected ratio between the heartbeats needs to be defined a-priori. Periods where phase locking is detected are reported either as the number of occurrences of these phase locking periods or as their prevalence in the signals (e.g., phase synchronization of two fetal heartbeats to one maternal heartbeat, 2:1, was found in 8% of the signal). Such analyses do not address the potential directionality of MFCC.In other words, it does not say whether the fetal HR affects the maternal HR or the other way around. Additionally, the final study included in Table 1 uses an artificial intelligence method known as *Deep coherence* [36]. This method is a deep learning implementation of the phase coherence index, where the deep learning model seeks to identify phases of synchronization in correspondence with what would be found with the original method described above, but without any mathematical derivations, pre-processing steps, or signal transformations to the input data [36].

3.1.2 Cross-correlation

This method assesses the similarity of two signals as a function of the displacement of one signal relative to the other. Therefore, cross-correlation accounts for a possible lag in the relationship between the maternal and fetal heartbeats. Therefore, it is possible to see when a pattern in one signal precedes the pattern in the other which may offer some indication of the directionality of the coupling. A higher cross-correlation value, therefore, implies stronger coupling.

3.1.3 Joint-symbolic dynamics (JSD)

JSD is a processing technique where information in a complex signal is simplified by replacing it with symbols (known as course-graining). In the case of MFCC, for example, each heartbeat may be replaced with a symbol indicating that it is increased (I), constant (C), or decreased (D) to the previous beat. In this way, patterns are detected in the signal, for example, DDD would indicate a sustained decrease in HR. In JSD, both the maternal and fetal HR signals are replaced with such symbols. Thereafter, the overlap between the two signals is measured with for example cross-correlation methods or cross-sample entropy.

3.1.4 Transfer entropy (TE)

TE assesses whether having information about the past activity of signal 1 reduces the information needed to describe the current or future activity in signal 2. The more the past information of signal 1 reduces the uncertainty in describing signal 2, the higher the information flow, and therefore TE, is from signal 1 to signal 2. A higher TE value suggests stronger coupling. TE inherently assumes a direction between the interactions.

3.1.5 Granger causality and partial directed coherence (PDC)

Granger causality operates on a similar principle to TE. If past information from signal 1 is useful in *predicting* the current state of signal 2, signal 1 is said to cause signal 2. Granger causality therefore inherently presumes a directionality between the information flow of the two signals. PDC, which is said to determine the intensity of information flow, is based on the principle of Granger causality. However, while Granger causality is assessed in the time domain, PDC is calculated using the frequency information of the time series. A higher causality or coherence value indicates stronger coupling.

3.1.6 Bivariate phase rectified signal averaging (BPRSA)

BPRSA assumes that changes in signal 1 (the trigger signal) result in or correspond to changes in signal 2 (the target signal). Anchor points – which are defined as the location of certain signal phases of interest, such as where the HR decelerates – are identified on the trigger signal. A signal segment is isolated around each anchor point which is sufficiently long to capture the expected interactions. All identified signal segments are then aligned and averaged. This process is then repeated in the target signal, using the anchor points identified in the trigger signal. If no relationship exists between the two signals, then this averaging should result in a flatline signal. However, if a relationship indeed exists, there should be an observable response in both averaged-out signals, implying that activity in the trigger signal is in some way influencing the target signal. By specifying the trigger and target signal, a directional relationship is inherently being investigated, though it should be noted that changes in both trigger and target signals may be modulated by a tertiary mechanism. Subsequently, an observed relationship does not imply causality.

3.1.7 Occurrence of these methods in the papers included in this scoping review

Synchrograms and phase coherence index were used to investigate MFCC in 11 (47.9%) of the included studies, cross-correlation was used in three (13.0%) studies, JSD was

investigated in three (13.0%) studies, TE in two (8.7%) studies, Granger causality, and PDC in three studies (13.0%), and finally BPRSA was used to investigate MFCC in one study (4.4%).

3.2 MFCC: presence and directionality.

Of the included studies, 21 (91.3%) found that MFCC existed, at least, occasionally. The remaining two (8.3%) studies, which used cross-correlation to capture MFCC [7], [31], did not find any evidence of MFCC.

Studies investigating the phase locking between the maternal and fetal cardiac systems using synchrograms and phase coherence indices found occasional periods of synchronization. Using these methodologies, researchers demonstrated how the prevalence of these periods of synchronization increases or decreases under certain conditions such as different maternal respiration rates [26], [27], progressing GA [25], [29], or regular maternal exercise [27]. While epochs of synchronization were present in all recordings regardless of the maternal respiration rate, synchronization was more prevalent at higher rates of respiration. Mothers who exercised regularly had lower incidences of MFCC than their less active controls. GA seems to influence the synchronization ratio as it gradually reduces with progressing GA. However, another study could not demonstrate the influence of progressing GA on synchronization. Two studies using cross-correlation did not find MFCC. A third performed their analysis using nighttime recordings – owing to the reduced effect of motion artifacts and external stimuli during this period – and stratified their cross-correlation analysis by sleep stages. This study reported occasional MFCC in the period of wakefulness after sleep onset period [7], [31], [32].

The method of JSD was used in three studies, in each of which MFCC was captured and found to change with progressing GA. MFCC patterns were significantly different between the early- and mid-GA groups as well as between the early- and late-GA groups (16-25 weeks, 26-31 weeks, and 32-41 weeks GA, respectively) [33]. Furthermore, one of these studies compared MFCC in women between their third trimester and during labor, finding stronger MFCC patterns during labor as compared to the third trimester [8]. The third study found altered MFCC patterns in fetuses with cardiac abnormalities in comparison to healthy fetuses. The changes in the MFCC patterns of the complicated pregnancies compared to the healthy ones differed depending on the type of fetal cardiac anomaly [34].

Furthermore, MFCC was investigated with TE, and researchers found MFCC in both directions. We introduce the terminology of $MFCC_{M\rightarrow F}$ if information flows from the mother to the fetus and $MFCC_{F\rightarrow M}$ for the alternative. Please note that this directionality does not imply causality. $MFCC_{M\rightarrow F}$ was found to either stay constant or increase only slightly with progressing GA, while $MFCC_{F\rightarrow M}$ was found to reduce with advancing gestation [10], [11]. Studies using PDC or Granger causality similarly found MFCC to be present in both directions with the strength of $MFCC_{M\rightarrow F}$ increasing with GA while the strength of $MFCC_{F\rightarrow M}$ decreased with progressing GA [12], [15], [35].

3.3 MFCC: physiological pathways.

No studies included in this review described specific investigations into the physiological pathways that are responsible for MFCC. However, some researchers suggest that the maternal heart rhythm mechanically or vibroacoustically stimulates the fetal heart [25]–[27]. The pulsation of the maternal arteries causes vibrations that may be sensed or heard by the fetus. When the frequency of these vibrations approaches that of the fetal heart rhythm, the fetal heartbeat may become entrained to the maternal heart [9], [40], [41]. Furthermore, researchers suspect that the autonomic nervous system (ANS) serves as a pathway for MFCC. Consequently, small-scale studies performed on mice models were used to test this hypothesis. These studies revealed alterations in MFCC under maternal sympathetic or para-sympathetic blockade [37], although no clear conclusions could be drawn as to the role of the ANS in MFCC.

3.4 MFCC: Clinical relevance

Overall, researchers suggest that assessing MFCC may serve as a tool to assess fetal well-being during pregnancy and labor and to track fetal development. However, three clinical applications of MFCC have been specifically investigated: first, the potential for using MFCC indices to discriminate between normal and abnormal fetuses [15], [29], [34]; second, estimating GA based on MFCC indices in rural or remote setups where ultrasound technology or expertise is not available [14], [30]; and third, using MFCC as an index of prenatal exposure to maternal stress [6].

Three studies specifically investigated abnormal fetuses in comparison to healthy fetuses. Two of these studies investigated a heterogeneous group of pregnancies with fetal cardiac anomalies or fetal cardiac heart rhythm disorders such as fetal bradycardia, fetal tachycardia, or premature atrial contractions. The first study, using JSD, found stronger MFCC patterns for abnormal cases when compared to pregnancies with healthy fetuses [34]. The second study, using PDC, found decreased $MFCC_{F\rightarrow M}$,

while $MFCC_{M \to F}$ was increased compared to healthy fetuses [15]. Finally, one other study using phase locking found significant differences in phase coherence indices between fetuses affected by different types of congenital heart diseases and healthy fetuses [29].

Two other studies showed that incorporating synchronization and phase coherence parameters could improve the estimation of GA with regression models when compared against models using only maternal and fetal HR variability features. When compared against the gold standard of establishing GA from crown-rump length, the best-performing model had a mean root mean square error of 2.67 weeks [14], [30].

Finally, one study used BPRSA to investigate MFCC in fetuses with stressed mothers (as assessed with the Perceived Stress Scale index) [6]. Features from the BPRSA analysis were used to develop a fetal stress index (FSI). The FSI was significantly higher in fetuses with stressed mothers compared to controls.

4. Discussion

Although there is heterogeneity in methodologies used and populations assessed in the studies included in this scoping review, it seems that MFCC does indeed exist, both from the mother to her fetus ($MFCC_{M \to F}$) as well as from the fetus to its mother ($MFCC_{F \to M}$). Furthermore, there is potential clinical value in assessing MFCC for monitoring fetal well-being and tracking fetal development.

While analyses using cross-correlation did not yield convincing evidence for MFCC [7], [31], phase synchronization, along with its phase coherence index, captured occasional MFCC between the maternal-fetal pair [9], [14], [15], [25]–[27], [27]–[30], [35], [37]. It should be noted that using cross-correlation to investigate associations between time series data (such as maternal and fetal heart rhythms) often leads to an underestimation of the strength of the association [7]. Considering this limitation and further considering that most studies support the existence of MFCC, we conclude that cross-correlation is not an appropriate method for capturing MFCC.

The seemingly intermittent nature of MFCC motivated investigations into the conditions under which MFCC occurs. While regular maternal physical exercise resulted in less synchronization between maternal and fetal HR[27], higher instances of MFCC

were found at higher maternal respiration rates [26]. Furthermore, MFCC also varies with progressing pregnancy both in strength and direction. In early pregnancy, the influence is mainly from the fetus to the mother, while in later pregnancy $MFCC_{M \rightarrow F}$ is dominant [11], [15], [42], [43].

The etiology of MFCC is currently unknown. Some researchers suggest that this type of coupling may be mechanically or acoustically driven [25]–[27]. Similar to cardiac rhythms becoming entrained to locomotor actions in cardiac-locomotor coupling (i.e., when the frequency of a rhythmic activity such as walking becomes close to the frequency of the HR, or a fixed factor thereof, and the two synchronize to each other) [44], the fetal heart rhythm may become entrained to the forcing maternal cardiac oscillator, i.e., the maternal pulse waves [9]. Furthermore, the fetal HR changes in reaction to the mechanical energy from the maternal vessels may be enhanced by the fetus's auditory perception of the frequency range of the pulsating maternal arteries – a phenomenon called the vibroacoustic effect [25]–[27]. This could explain the increasing strength of $MFCC_{M \rightarrow F}$ with GA, as the fetal auditory system is only fully developed at 27 weeks of gestation [45]. The vibroacoustic effect has been observed in adults where a frequency-lock was found in reaction to an external acoustic signal, but only when the frequency was similar to that of the subject's HR [40]. The same might be happening to the fetal HR in the case of MFCC, although this would rarely be observed as the HR frequencies of the mother and fetus would be too far apart to induce MFCC under normal circumstances.

Subsequently, it stands to reason that a higher incidence of MFCC may be observed at higher maternal HR. This aligns with findings suggesting more periods of MFCC during quicker maternal respiration; increased respiration narrows the maternal interval between successive heartbeats, potentially encouraging the entrainment of the fetal rhythm to that of its mother [26]. However, it should also be noted that rather than changes in maternal cardiac rhythm modulating changes in the fetal rhythm (or vice versa), a third system may be driving changes in both these systems [32]. Specifically, it is feasible that maternal respiration acts as a common driving force, simultaneously modulating both the maternal and the fetal HR. This modulating effect of maternal respiration is yet to be directly investigated. However, a faster-paced maternal respiratory rate did induce higher instances of MFCC [26]. We propose that the movement of the maternal diaphragm may also play a role here, exhorting a vibroacoustic effect on both the maternal and fetal cardiac system, but this has not been investigated.

The increased strength of $MFCC_{M \to F}$ with progressing GA is likely linked to the maturation of the fetal ANS, reaching maturity around the transition from the second to the third trimester [46]. With gestational progression, the increasingly stable and finely tuned fetal ANS may lead to an enhanced fetal cardiac reaction to maternal input [10], [42], [47]. On the other hand, while respiratory sinus arrhythmia is typically present in the mother, in the fetus it is present in increasing strength from 32 weeks GA onwards [46]. Theoretically, the fetal HR would become more closely coupled with its own respiratory system from this point onward. Yet, this manifests as a decrease in $MFCC_{F \to M}$ with progressing GA rather than a decrease in $MFCC_{M \to F}$, further highlighting the complexity and dearth of knowledge concerning MFCC.

Additionally, the adrenergic innervation of the uterine wall may play an important role in $MFCC_{F \to M}$ [48], [49]. Fetal movements may stimulate the maternal sympathetic nervous system, resulting in higher maternal HR. Theoretically, this effect would increase with gestational progression as larger fetuses are capable of stronger movements. However, the opposite is observed; $MFCC_{F \to M}$ decreases with progressing pregnancy. This decrease is likely due to the maternal ANS becoming increasingly hypo-responsive to external stimuli, such as fetal movements, during healthily progressing pregnancy [42], [50], [51]. Small-scale studies using mice models also support the hypothesis of the ANS playing a central role in MFCC as indices of MFCC in pregnant mice reveal an antagonistic response to maternal sympathetic or para-sympathetic blockade [37]. However, these animal studies used phase coherence for the assessment of MFCC and were therefore not able to assess directionality.

Still, even though the etiology of MFCC is not yet clear, results do suggest that assessments of this coupling may have clinical relevance. Indices of MFCC are altered in pregnancies with fetuses affected by cardiac arrhythmias or fetal cardiac anomalies compared to healthy fetuses [15], [29], [34]. Furthermore, MFCC parameters have been used to estimate fetal GA fairly successfully against the gold standard. [14], [30].

Maternal stress during pregnancy has also been found to affect MFCC [6]. Based on this finding, researchers have developed an FSI (based on MFCC features) to identify infants at risk for altered neurodevelopmental trajectories due to perinatal stress exposure [6]. While no further clinical applications have been investigated, the most common suggestion for clinical applications is tracking fetal neurodevelopment to screen for abnormalities.

The effect of maternal complications on MFCC is yet to be explored. Such analyses are potentially interesting since, as previously discussed, MFCC seems to be affected by autonomic changes, and complications such as hypertensive disorders of pregnancy are associated with dysfunctional autonomic regulation [52]. Furthermore, assessments of maternal-infant cardiac coupling in the immediate postnatal period – preferably in preterm infants where the autonomic behavior is still similar to that of the fetus – may be illuminating. In such a study design, various possible influencing factors could be examined under controlled conditions, for example, changes in maternal respiration rate or HR. Additionally, synchronization under specific (patho) physiological conditions such as fetal behavioral state or fetal hypoxemia should be investigated. The latter might be particularly interesting. While the evolutionary driver behind MFCC is unknown, it may be in some way related to the oxygenation of the fetus; i.e., lower oxygenation levels in the fetal blood could trigger increases in maternal HR to increase gas exchange via the placenta [53]. On the other hand, when maternal oxygen levels decrease, the fetal HR responds by increasing the fetal HR [54].

Several limitations exist that affect the investigation of MFCC. While each of the studies in this scoping review is limited in some ways, there are also inherent difficulties in studying MFCC. First, since time-synchronized maternal and fetal HRs are needed, options for measurement technologies to capture MFCC are limited. While magnetocardiography can be used, it is impractical, owing to the size and expense of the equipment, therefore leaving abdominal electrocardiophysiology (ECG) as the pragmatic option. Fetal HR can be difficult to accurately detect from abdominal ECG and signals capturing the electrophysiological activity of the fetal heart are typically weak (i.e., of low signal-to-noise ratio). However, recent advancements in the field of fetal electrocardiography have greatly contributed to solving this problem by providing higher-quality fetal signals that enable more accurate MFCC investigation [55]. Second, the majority of methods used to assess the coupling between systems derive from different scientific domains and are not specifically designed to study the coupling between physiological systems, which might make them less effective. Third, the studies included in this review reveal that there is no consensus on the definition of MFCC. This is important since the definition of coupling determines the method by which researchers chose to study its potential occurrence; a presumption of fixed phase ratios between the maternal and fetal heartbeats would most likely lead to analysis via synchrograms, while hypothesizing that modulations in one signal lead to or correspond to changes in the other would likely result in a TE or BPRSA analysis.

Lastly, a deep learning approach called deep coherence was recently proposed in the field of MFCC research [36]. Deep learning methods like deep coherence may help to reduce the need for a priori assumptions and processing. However, from this review, it is clear that while MFCC does seem to exist, our understanding of MFCC is limited. Therefore, techniques that are not fully explainable to capture MFCC should be used with caution. Rather, it may be beneficial for future research to first directly compare known coupling techniques for the assessment of MFCC to narrow down those which are useful [56]. Furthermore, more research is necessary to probe the pathway behind and nature of MFCC.

5. Conclusion

We conclude that the studies included in this scoping review suggest that MFCC does exist and that its strength and direction change with progressing GA. Although the physiological pathways of MFCC are not yet sufficiently substantiated, assessing MFCC during pregnancy may offer opportunities to assess fetal development and well-being and may potentially aid in detecting fetal (cardiac) abnormalities.

References

[1] E. Maltepe and S. J. Fisher, "Placenta: The Forgotten Organ," *Annu. Rev. Cell Dev. Biol.*, vol. 31, no. 1, pp. 523–552, Nov. 2015, doi: 10.1146/annurev-cellbio-100814-125620.

[2] F. Shaffer, R. McCraty, and C. L. Zerr, "A healthy heart is not a metronome: an integrative review of the heart's anatomy and heart rate variability," *Front. Psychol.*, vol. 5, Sep. 2014, doi: 10.3389/fpsyg.2014.01040.

[3] H.-G. Kim, E.-J. Cheon, D.-S. Bai, Y. H. Lee, and B.-H. Koo, "Stress and Heart Rate Variability: A Meta-Analysis and Review of the Literature," *Psychiatry Investig*, vol. 15, no. 3, pp. 235–245, Mar. 2018, doi: 10.30773/pi.2017.08.17.

[4] A. K. Luttkus, W. Friedmann, C. Homm-Luttkus, and J. W. Dudenhausen, "Correlation of fetal oxygen saturation to fetal heart rate patterns, Evaluation of fetal pulse oximetry with two different oxisensors: Correlation of fetal oxygen saturation to fetal heart rate patterns, Evaluation of fetal pulse oximetry with two different oxisensors," *Acta Obstetricia et Gynecologica Scandinavica*, vol. 77, no. 3, pp. 307–312, Mar. 1998, doi: 10.1034/j.1600-0412.1998.770310.x.

[5] K. Sjöström, L. Valentin, T. Thelin, and K. Maršál, "Maternal anxiety in late pregnancy: effect on fetal movements and fetal heart rate," *Early Human Development*, vol. 67, no. 1–2, pp. 87–100, Apr. 2002, doi: 10.1016/S0378-3782(01)00256-0.

[6] S. M. Lobmaier *et al.*, "Fetal heart rate variability responsiveness to maternal stress, non-invasively detected from maternal transabdominal ECG," *Arch Gynecol Obstet*, vol. 301, no. 2, pp. 405–414, Feb. 2020, doi: 10.1007/s00404-019-05390-8.

[7] J. A. Dipietro, R. A. Irizarry, K. A. Costigan, and E. D. Gurewitsch, "The psychophysiology of the maternal-fetal relationship," *Psychophysiology*, vol. 41, no. 4, pp. 510–520, Jul. 2004, doi: 10.1111/j.1469-8986.2004.00187.x.

[8] C. A. Tepichín-Castro, C. I. Ledesma-Ramírez, M. Á. Peña-Castillo, G. Pacheco-López, J. C. Echeverría, and J. J. Reyes-Lagos, "Joint symbolic dynamics identifies differences in the maternal-fetal cardiac coupling between nonlaboring and laboring women," *Biomedical Signal Processing and Control*, vol. 68, p. 102769, Jul. 2021, doi: 10.1016/j.bspc.2021.102769.

[9] G. Hildebrandt and H. R. Klein, "Uber die Phasenkoordination von miitterlichem und foetalem Herzrhythmus wiihrend der Schwangerschaft," *Klin. Wochenschr*, vol. 57, pp. 87–91.

[10] F. Marzbanrad, Y. Kimura, M. Palaniswami, and A. H. Khandoker, "Quantifying the Interactions between Maternal and Fetal Heart Rates by Transfer Entropy," *PLoS ONE*, vol. 10, no. 12, p. e0145672, Dec. 2015, doi: 10.1371/journal.pone.0145672.

[11] R. Avci, D. Escalona-Vargas, E. R. Siegel, C. L. Lowery, and H. Eswaran, "Coupling Analysis of Fetal and Maternal Heart Rates via Transfer Entropy Using Magnetocardiography," in *2018 40th Annual International Conference of the IEEE Engineering in Medicine and Biology Society (EMBC)*, Honolulu, HI: IEEE, Jul. 2018, pp. 1–4. doi: 10.1109/EMBC.2018.8513053.

[12] A. H. Khandoker *et al.*, "Analysis of maternal–fetal heart rate coupling directions with partial directed coherence," *Biomedical Signal Processing and Control*, vol. 30, pp. 25–30, Sep. 2016, doi: 10.1016/j.bspc.2016.06.010.

[13] I. Lakhno, "Autonomic imbalance captures maternal and fetal circulatory response to pre-eclampsia," *Clin Hypertens*, vol. 23, no. 1, p. 5, Dec. 2017, doi: 10.1186/s40885-016-0061-x.

[14] A. H. Khandoker, M. Wahbah, R. Al Sakaji, K. Funamoto, A. Krishnan, and Y. Kimu-

ra, "Estimating Fetal Age by Fetal Maternal Heart Rate Coupling Parameters," in *2020 42nd Annual International Conference of the IEEE Engineering in Medicine & Biology Society (EMBC)*, Montreal, QC, Canada: IEEE, Jul. 2020, pp. 604–607. doi: 10.1109/EMBC44109.2020.9176049.

[15] A. H. Khandoker, S. Schulz, H. M. Al-Angari, A. Voss, and Y. Kimura, "Alterations in Maternal–Fetal Heart Rate Coupling Strength and Directions in Abnormal Fetuses," *Front. Physiol.*, vol. 10, p. 482, Apr. 2019, doi: 10.3389/fphys.2019.00482.

[16] S. Schulz *et al.*, "Cardiovascular and cardiorespiratory coupling analyses: a review," *Phil. Trans. R. Soc. A.*, vol. 371, no. 1997, p. 20120191, Aug. 2013, doi: 10.1098/rsta.2012.0191.

[17] H. Arksey and L. O'Malley, "Scoping studies: towards a methodological framework," *International Journal of Social Research Methodology*, vol. 8, no. 1, pp. 19–32, Feb. 2005, doi: 10.1080/1364557032000119616.

[18] Z. Munn, M. D. J. Peters, C. Stern, C. Tufanaru, A. McArthur, and E. Aromataris, "Systematic review or scoping review? Guidance for authors when choosing between a systematic or scoping review approach," *BMC Med Res Methodol*, vol. 18, no. 1, p. 143, Dec. 2018, doi: 10.1186/s12874-018-0611-x.

[19] D. Levac, H. Colquhoun, and K. K. O'Brien, "Scoping studies: advancing the methodology," *Implementation Sci*, vol. 5, no. 1, p. 69, Dec. 2010, doi: 10.1186/1748-5908-5-69.

[20] H. M. Daudt, C. van Mossel, and S. J. Scott, "Enhancing the scoping study methodology: a large, inter-professional team's experience with Arksey and O'Malley's framework," *BMC Med Res Methodol*, vol. 13, no. 1, p. 48, Dec. 2013, doi: 10.1186/1471-2288-13-48.

[21] M. D. J. Peters *et al.*, "Updated methodological guidance for the conduct of scoping reviews," *JBI Evidence Synthesis*, vol. 18, no. 10, pp. 2119–2126, Oct. 2020, doi: 10.11124/JBIES-20-00167.

[22] J. McGowan *et al.*, "Reporting scoping reviews—PRISMA ScR extension," *Journal of Clinical Epidemiology*, vol. 123, pp. 177–179, Jul. 2020, doi: 10.1016/j.jclinepi.2020.03.016.

[23] A. Khandoker, M. Wahbah, C. Yoshida, Y. Kimura, and Y. Kasahara, "Effect of Anesthesia on Fetal-Maternal Heart Rate Variability and Coupling in Pregnant Mice and Fetuses," presented at the 2020 Computing in Cardiology Conference, Dec. 2020. doi: 10.22489/CinC.2020.197.

[24] C. Schäfer, M. G. Rosenblum, H.-H. Abel, and J. Kurths, "Synchronization in the human cardiorespiratory system," *Phys. Rev. E*, vol. 60, no. 1, pp. 857–870, Jul. 1999, doi: 10.1103/PhysRevE.60.857.

[25] P. V. Leeuwen, D. Geue, S. Lange, D. Cysarz, H. Bettermann, and D. H. Grönemeyer, "Is there evidence of fetal-maternal heart rate synchronization?," *BMC Physiology*, p. 11, 2003.

[26] P. Van Leeuwen *et al.*, "Influence of paced maternal breathing on fetal-maternal heart rate coordination," *Proceedings of the National Academy of Sciences*, vol. 106, no. 33, pp. 13661–13666, Aug. 2009, doi: 10.1073/pnas.0901049106.

[27] P. Van Leeuwen, K. M. Gustafson, D. Cysarz, D. Geue, L. E. May, and D. Grönemeyer, "Aerobic Exercise during Pregnancy and Presence of Fetal-Maternal Heart Rate Synchronization," *PLoS ONE*, vol. 9, no. 8, p. e106036, Aug. 2014, doi: 10.1371/journal.pone.0106036.

[28] Wang, Qiangian *et al.*, "Investigating the beat by beat phase synchronization between maternal and fetal heart rates," in *2013 35th Annual International Conference of the IEEE*

Engineering in Medicine and Biology Society (EMBC), Osaka: IEEE, Jul. 2013, pp. 3821–3824. doi: 10.1109/EMBC.2013.6610377.

[29] H. M. Alangari, Y. Kimura, and A. H. Khandoker, "Preliminary Evaluation of Fetal Congenital Heart Defects Changes on Fetal-Maternal Heart Rate Coupling Strength," in *2018 40th Annual International Conference of the IEEE Engineering in Medicine and Biology Society (EMBC)*, Honolulu, HI: IEEE, Jul. 2018, pp. 251–254. doi: 10.1109/EMBC.2018.8512272.

[30] M. Wahbah, R. Al Sakaji, K. Funamoto, A. Krishnan, Y. Kimura, and A. H. Khandoker, "Estimating Gestational Age From Maternal-Fetal Heart Rate Coupling Parameters," *IEEE Access*, vol. 9, pp. 65369–65379, 2021, doi: 10.1109/ACCESS.2021.3074550.

[31] J. A. DiPietro, L. E. Caulfield, R. A. Irizarry, P. Chen, M. Merialdi, and N. Zavaleta, "Prenatal development of intrafetal and maternal-fetal synchrony.," *Behavioral Neuroscience*, vol. 120, no. 3, pp. 687–701, 2006, doi: 10.1037/0735-7044.120.3.687.

[32] J. A. DiPietro *et al.*, "Fetal heart rate during maternal sleep," *Dev Psychobiol*, vol. 63, no. 5, pp. 945–959, Jul. 2021, doi: 10.1002/dev.22118.

[33] A. H. Khandoker, "Investigating maternal-fetal heart rate coupling by high resolution joint symbolic dynamics," p. 4.

[34] A. H. Khandoker *et al.*, "Quantification of maternal-fetal cardiac couplings in normal and abnormal pregnancies applying high resolution joint symbolic dynamics," *Mathematical Biosciences and Engineering*, vol. 17, no. 1, pp. 802–813, 2020, doi: 10.3934/mbe.2020042.

[35] M. Riedl *et al.*, "Testing foetal–maternal heart rate synchronization via model-based analyses," *Phil. Trans. R. Soc. A.*, vol. 367, no. 1892, pp. 1407–1421, Apr. 2009, doi: 10.1098/rsta.2008.0277.

[36] M. Alkhodari *et al.*, "Deep learning identifies cardiac coupling between mother and fetus during gestation," *Front. Cardiovasc. Med.*, vol. 9, p. 926965, Jul. 2022, doi: 10.3389/fcvm.2022.926965.

[37] A. H. Khandoker *et al.*, "Investigating the effect of cholinergic and adrenergic blocking agents on maternal-fetal heart rates and their interactions in mice fetuses," *Biology Open*, vol. 11, no. 4, p. bio058999, Apr. 2022, doi: 10.1242/bio.058999.

[38] P. M. L. Janssen, B. J. Biesiadecki, M. T. Ziolo, and J. P. Davis, "The Need for Speed: Mice, Men, and Myocardial Kinetic Reserve," *Circ Res*, vol. 119, no. 3, pp. 418–421, Jul. 2016, doi: 10.1161/CIRCRESAHA.116.309126.

[39] Q. Yu, L. Leatherbury, X. Tian, and C. W. Lo, "Cardiovascular Assessment of Fetal Mice by In Utero Echocardiography," *Ultrasound in Medicine & Biology*, vol. 34, no. 5, pp. 741–752, May 2008, doi: 10.1016/j.ultrasmedbio.2007.11.001.

[40] V. S. Anishchenko, A. G. Balanov, N. B. Janson, N. B. Igosheva, and G. V. Bordyugov, "ENTRAINMENT BETWEEN HEART RATE AND WEAK NONINVASIVE FORCING," *Int. J. Bifurcation Chaos*, vol. 10, no. 10, pp. 2339–2348, Oct. 2000, doi: 10.1142/S0218127400001468.

[41] C. Porcaro *et al.*, "Fetal auditory responses to external sounds and mother's heart beat: Detection improved by Independent Component Analysis," *Brain Research*, vol. 1101, no. 1, pp. 51–58, Jul. 2006, doi: 10.1016/j.brainres.2006.04.134.

[42] F. Marzbanrad, Y. Kimura, M. Endo, M. Palaniswami, and A. H. Khandoker, "Transfer entropy analysis of maternal and fetal heart rate coupling," in *2015 37th Annual International Conference of the IEEE Engineering in Medicine and Biology Society (EMBC)*, Milan:

IEEE, Aug. 2015, pp. 7865–7868. doi: 10.1109/EMBC.2015.7320215.

[43] A. H. Khandoker *et al.*, "Analysis of maternal–fetal heart rate coupling directions with partial directed coherence," *Biomedical Signal Processing and Control*, vol. 30, pp. 25–30, Sep. 2016, doi: 10.1016/j.bspc.2016.06.010.

[44] D. De Bartolo *et al.*, "Effects of cognitive workload on heart and locomotor rhythms coupling," *Neuroscience Letters*, vol. 762, p. 136140, Sep. 2021, doi: 10.1016/j.neulet.2021.136140.

[45] P. G. Hepper and B. S. Shahidullah, "Development of fetal hearing," *Archives of Disease in Childhood - Fetal and Neonatal Edition*, vol. 71, no. 2, pp. F81–F87, Sep. 1994, doi: 10.1136/fn.71.2.F81.

[46] U. Schneider *et al.*, "Developmental milestones of the autonomic nervous system revealed via longitudinal monitoring of fetal heart rate variability," *PLoS ONE*, vol. 13, no. 7, p. e0200799, Jul. 2018, doi: 10.1371/journal.pone.0200799.

[47] B. S. Kisilevsky, D. W. Muir, and J. A. Low, "Maturation of Human Fetal Responses to Vibroacoustic Stimulation," *Society for Research in Child Development*, vol. 63, no. 6, pp. 1497–1508, 1992, doi: 131.155.214.110.

[48] J. A. DiPietro, K. M. Voegtline, K. A. Costigan, F. Aguirre, K. Kivlighan, and P. Chen, "Physiological reactivity of pregnant women to evoked fetal startle," *Journal of Psychosomatic Research*, vol. 75, no. 4, pp. 321–326, Oct. 2013, doi: 10.1016/j.jpsychores.2013.07.008.

[49] C. Owman, E. Rosenbren, and N. O. Sjoberg, "Adrenergic innervation of the human female reproductive organs: a histochemical and chemical investigation," *Obstet Gynecol*, vol. 30, no. 6, pp. 763–773, Dec. 1967.

[50] S. Entringer *et al.*, "Attenuation of maternal psychophysiological stress responses and the maternal cortisol awakening response over the course of human pregnancy," *Stress*, vol. 13, no. 3, pp. 258–268, May 2010, doi: 10.3109/10253890903349501.

[51] M. Bester, R. Joshi, M. Mischi, J. O. E. H. van Laar, and R. Vullings, "Longitudinally Tracking Maternal Autonomic Modulation During Normal Pregnancy With Comprehensive Heart Rate Variability Analyses," *Front. Physiol.*, vol. 13, p. 874684, May 2022, doi: 10.3389/fphys.2022.874684.

[52] S. Moors *et al.*, "Heart rate variability in hypertensive pregnancy disorders: a systematic review," *Pregnancy Hypertension*, Mar. 2020, doi: 10.1016/j.preghy.2020.03.003.

[53] D. J. Bekedam, E. J. H. Mulder, R. J. M. Snijders, and G. H. A. Visser, "The effects of maternal hyperoxia on fetal breathing movements, body movements and heart rate variation in growth retarded fetuses," *Early Human Development*, vol. 27, no. 3, pp. 223–232, Dec. 1991, doi: 10.1016/0378-3782(91)90196-A.

[54] T. Kutlu *et al.*, "Acute fetal heart rate tracing changes secondary to cigarette smoking in third trimester pregnancies," *The Journal of Maternal-Fetal & Neonatal Medicine*, vol. 30, no. 12, pp. 1407–1409, Jun. 2017, doi: 10.1080/14767058.2016.1214708.

[55] R. Vullings and J. O. E. H. van Laar, "Non-invasive Fetal Electrocardiography for Intrapartum Cardiotocography," *Front. Pediatr.*, vol. 8, p. 599049, Dec. 2020, doi: 10.3389/fped.2020.599049.

[56] A. Rozo *et al.*, "Benchmarking Transfer Entropy Methods for the Study of Linear and Nonlinear Cardio-Respiratory Interactions," *Entropy*, vol. 23, no. 8, p. 939, Jul. 2021, doi: 10.3390/e23080939.

Chapter 11

Conclusions and outlook

Every year, over 100 million pregnancies occur [1]. Of these, 15 to 20% will develop pregnancy complications [2]–[4]. In addition to the detrimental effect of these complications on the maternal-fetal pair during pregnancy, these complications place the mother and her offspring at risk for future diseases [4]–[15] and burden healthcare systems [16]. The impact of pregnancy complications can be reduced if these complications are detected early enough to allow for the use of existing interventions, such as lifestyle changes or pharmaceutical regimens [17]–[22]. However, early detection remains a persistent challenge in perinatology [23], [24]. Owing to the link between pregnancy complications and dysfunctional autonomic regulation, seemingly from as early as the first trimester [5], [25], tracking non-invasive measures of maternal autonomic activity may aid in the early detection of pregnancy complications [25], [26].

The availability and readiness of suitable technology further increase the attractiveness of these long-term monitoring solutions. The autonomic nervous system (ANS) regulates heart rate (HR); as such, assessing HR variability (HRV) serves as a proxy measure for non-invasively assessing the ANS [27]. There are a plethora of wearable HR monitors available, the most common, and most pragmatic, of which are smartwatches that use photoplethysmography (PPG) measurements to track the HR and derive the HRV. The use of such wrist-worn wearables for monitoring has been found to have a high acceptability in the pregnant population [28], [29]. However, while the technology required to implement such a monitoring solution exists, the necessary research on non-invasive measures of maternal autonomic activity and all the factors which might influence it does not. The work in this thesis focuses on filling multiple research gaps to move us closer to implementing such monitoring solutions for the early detection of pregnancy complications.

The thesis comprises four sections, that in turn contain a total of nine chapters (**Chapters 2 to 10**). Below the key findings of each chapter are presented, along with a takeaway message corresponding to each section. Additionally, important limitations are mentioned throughout. Thereafter, we discuss practical steps for future research. Finally, we describe how we envision the fit of this solution in the current antenatal care systems in middle- to high-income countries, before concluding with final remarks.

1. Section I: Maternal autonomic regulation during healthy pregnancy

In the first section, we investigate the impact of healthy pregnancy on non-invasive measures of autonomic activity. First, in **Chapter 2**, we perform the most comprehensive assessment of HRV in healthy pregnancy to date, using the largest study groups available in the literature. We use not only standard HRV features as is typically done in the literature [29] but also features assessing the non-linearity, responsiveness, and fragmentation of the HR. We find that there are significant differences in all HRV features between pregnant and non-pregnant women, usually with a large effect size. For context, the effect sizes for the differences between pregnant and non-pregnant women were generally larger than those between healthy men and women [30]. Consequently, the large basis of literature on HRV in women of childbearing age [31]–[33] cannot be readily translated to the pregnant population.

Results based on standard HRV features – of which the main purpose is to reflect the interplay between the sympathetic and parasympathetic branches of the ANS [27] – indicate decreased parasympathetic and increased sympathetic influence on the maternal heart. These results confirm conclusions drawn from studies using invasive or obtrusive methods (such as microneurography and cardiac reflex tests, respectively), namely that pregnancy is a state of sympathetic overactivation and vagal withdrawal [26], [34]. Furthermore, while the results from smaller HRV studies with similar methodologies vary [35], our results are in agreement with the majority of these studies. However, the additional HRV feature sets that we use offer new insights into gestational physiology, and we believe that two sets of these – non-linear features and those linked to autonomic responsiveness – should be included in all HRV-based models aimed at assessing perinatal health. The motivation behind this statement is that the largest differences between the pregnant and non-pregnant groups are observed for non-linear features, specifically α_1 from the detrended fluctuation analysis and SD1/SD2 from the Poincaré analysis (Figure 8, **Chapter 2**). Furthermore, in **Chapter 4** (*Section II*), we find that these features are particularly sensitive to progressing pregnancy. This may indicate that these features best capture the autonomic changes essential to healthy pregnancy; in turn, we hypothesize that non-linear HRV features may be most sensitive to capturing maternal autonomic dysfunction. Features connected to autonomic responsiveness, such as deceleration capacity [36], could additionally be useful as they may reflect the reduced neurocardiovascular transduction found in

healthy pregnancy, i.e., a state where sympathetic activity in the body has a reduced effect on cardiovascular end-points, such as HR [37]. Higher-than-expected autonomic responsiveness and neurocardiovascular responsiveness have been found in women with pregnancy complications [6], [38]. A limitation of this study was that the mean age of the pregnant group is approximately five years higher than that of the non-pregnant group. While age is known to affect HRV, based on the literature [39] as well as the results of **Chapter 5** of this thesis [40], it is unlikely that a difference of this magnitude can be attributed to a small difference in age.

While the work in **Chapter 2** is based on ECG recordings, which are the gold standard for HRV analysis, wrist-worn PPG is the most likely candidate for long-term monitoring. When analyzing PPG measurements, information on the morphology of the PPG pulse wave can be extracted in addition to HRV features. While the exact physiological meaning of features describing the pulse wave remains uncertain and its morphology has rarely been studied in pregnancy [41], these features provide information on autonomic regulation, as the vascular tone is regulated by the ANS [42]. Consequently, in **Chapter 3** we investigate differences in HRV features and features describing the morphology of the PPG pulse wave between healthy pregnant and non-pregnant women, based on wrist-worn PPG measurements. We find that the vast majority of features differed between these two groups, with the differences in HRV features mostly aligning with those found in **Chapter 2**. Furthermore, using a binary classification model as a tool, we find that the systolic pulse duration (as based on the PPG pulse wave) is the feature most impacted by pregnancy. Furthermore, using this model, we find that while we can discriminate between pregnant and non-pregnant women adequately based on HRV features alone (area under the receiver operating characteristic curve (AUROC), with standard deviation = 0.74 (0.03)), the performance of the model improves by incorporating features describing the PPG pulse wave (AUROC = 0.825 (0.03)). Therefore, there seems to be complementary information in the PPG morphology that can be used in future research toward early detection of autonomic dysregulation during pregnancy. Concerning the HRV features, we found that mean HR is most impacted by pregnancy and that additional HRV features only incrementally improved the performance of the model. However, this is likely owing to a lower accuracy in HRV features as a result of the low sampling rate of the PPG (32 Hz), which is the the main limitation of this study. Still, when considering the most important HRV features for the model (Table 3, **Chapter 3**), half of these were related to autonomic responsiveness, as hypothesized in **Chapter 2**.

However, PPG measurements are prone to motion artifacts, making it at times impossible to extract useful information from these data. Herein lies both a limitation and an opportunity. PPG measurements often need to be collected during sleep to minimize the impact of these motion artifacts, as for our data in **Chapter 3**. Sleep comprises different stages, each of which is governed by a different autonomic state [43]. These stages can be calculated based on PPG measurements [44]. As a subanalysis, we use these sleep stages as a type of filter and classify our two groups based only on measurements from specific sleep stages. We find that our model performed best (AUROC = 0.84 (0.05)) when using measurements from the N3 stage, which is parasympathetically dominated [43], and worst based on measurements from the sympathetically dominated REM (rapid eye movement) stage (AUROC = 0.77 (0.09)) [43]. Filtering by sleep stage approximates a controlled environment that the two groups have in common, even though their study setups are not identical, and removes the potentially confounding impact of differences in sleep architectures between groups. Therefore, if maternal autonomic regulation is assessed in free-living conditions, it may be beneficial to similarly filter assessments of indices based on sleep stages as such a design lends itself to repeatable measurements that are well suited to studying subjects longitudinally.

The takeaway message from Section I: Healthy pregnant women are autonomically distinct from healthy non-pregnant women. HRV features capturing HR non-linearity and autonomic responsiveness, as well as features describing the PPG pulse wave, provide additional value when assessing the impact of pregnancy on female physiology. Performing autonomic assessments in free-living conditions may benefit from stratifying assessments per sleep stage, as these approximate a controlled environment that allows for repeatable measurements.

2. Section II: Factors influencing maternal autonomic regulation during healthy pregnancy

From *Section I*, we gain insights into how noninvasive measures of autonomic function differ between healthy pregnant and non-pregnant women. However, using this knowledge to identify abnormal maternal autonomic regulation requires understanding factors outside of pregnancy complications that may be influencing maternal HRV

during pregnancy. The most apparent of such factors is gestational age (GA). Subsequently, in **Chapter 4**, we perform an in-depth investigation into how HRV changes with GA. Per participant, we assess a median of eight measurements across pregnancy to capture potentially dynamic changes in maternal HRV, rather than performing one assessment per trimester as is typically done in the literature [35]. The changes that are already observed when comparing pregnant women to their non-pregnant counterparts in **Chapter 2** generally intensify as GA progresses, i.e., parasympathetic activity, HR complexity, and HR responsiveness further decrease, while sympathetic activity further increases. Additionally, not only do non-linear HRV features such as α_1 differ most between pregnant and non-pregnant women (**Chapter 2**), but these features are also particularly sensitive to progressing pregnancy (Figure 8, **Chapter 4**).

We find two trends in maternal HRV which, to our knowledge, have not been reported before. First, there is a clear shift in maternal HRV occurring during the transition from the second to the third trimester, with features such as RMSSD, pNN50, and SampEn decreasing sharply. The physiological drivers behind the timing of this change are unclear; however, this autonomic shift does coincide with the most rapid period of fetal autonomic development [45]. Second, there is an uptick in overall variability (SDNN) and features assessing autonomic responsiveness in the weeks leading up to delivery, likely reflecting the maternal body preparing for the physiological challenge of labor. Both trends are recently confirmed by research from WHOOP (Boston, USA), a wearables company focused on fitness tracking, when they analyzed the HRV data of their members who had worn smartwatches throughout their pregnancies [46].

However, it is not just GA that affects maternal HRV in healthy pregnancies. While body mass index and parity are not found to affect maternal HRV, maternal age, as well as HR and breathing rate, do impact these features (**Chapter 5)**. Furthermore, inter-subject variability accounts for up to two-thirds of the variation observed in maternal HRV (Table 4, **Chapter 5**). Considering these findings alongside those of **Chapter 4**, personalized tracking of trends in maternal HRV would be more valuable for the early detection of pregnancy complications as opposed to spot checks at regular antenatal appointments.

The takeaway message from Section II: Owing to the impact of GA and maternal characteristics on maternal HRV, personalized tracking of maternal HRV across pregnancy to identify deviations in maternal HRV trends from expected norms is better suited for early detection of complications than spot measurements at antenatal appointments.

3. Section III: The effect of corticosteroids on maternal autonomic regulation in complicated pregnancies

Identifying abnormalities in maternal autonomic regulation requires insights into normal autonomic regulation during healthy pregnancy (*Section I*) as well as which factors may be affecting regulation (*Section II*). Similarly, identifying such autonomic abnormalities also requires an understanding of maternal autonomic regulation in complicated pregnancies and, in turn, which factors may be confounding measurements thereof. While more literature is available on maternal HRV in complicated pregnancies [26], [47], [48] than in healthy pregnancies [35], the reported results are often limited by the unknown, potentially confounding effects of corticosteroids. Antenatally administered corticosteroids – drugs that accelerate the maturation of the fetal physiology in anticipation of preterm birth [49] – are routinely administered to women admitted to the hospital with pregnancy complications such as preeclampsia. Assessments of maternal HRV in complicated pregnancies are often performed in such hospitalized groups, where the impact of these routine medications are listed as limitations [38], [47], [50], or, in many cases, not addressed. However, these medications do affect fetal HRV [51]–[53]; therefore, we investigate their potential effect on maternal HRV in **Chapters 6** to **8**.

As a first step, in **Chapter 6**, we perform a secondary analysis of abdominal ECG measurements collected with the initial purpose of assessing the effect of betamethasone, a commonly used corticosteroid, on fetal HRV. Our results show that maternal HRV indeed changes in response to the administration of this medication; primarily, HR is elevated and HRV features linked to parasympathetic activity are reduced for 24 to 48 hours after the first injection of betamethasone. The latter is particularly important, as pregnancy complications are also reported to reduce parasympathetic activity [47], [54]. However, to confirm these findings, we design and execute a dedicated, prospective study (**Chapter 7**). Here we collect data over four days in women with an indication for corticosteroids using wrist-worn PPG, enabling us to assess the effect of betamethasone on both maternal HRV and PPG pulse wave morphology (**Chapter 8)**. The changes observed in maternal HR and HRV in this chapter are similar to those seen in **Chapter 6**. Furthermore, corticosteroids are known to act as vasoconstrictors [55], which is reflected in the changes that we observe in the pulse wave morphology features, such as those describing the area under the pulse wave. Overall, we propose

that studies investigating maternal autonomic regulation in complicated pregnancies should do so before the administration of corticosteroids or sufficiently thereafter, i.e., at least three days after the last injection.

An interesting finding from both **Chapters 6** and **8** with bearing on clinical practice is that maternal HR is elevated by approximately 10 bpm for 24 hours after corticosteroids are administered. In a population with an already elevated HR [56], [57], such an increase may push the maternal HR past the threshold of tachycardia [58]. While guidelines for evaluating maternal HR recommend considering the recent administration of beta-blockers when detecting bradycardia, no pharmaceutical considerations are defined for maternal tachycardia. Consequently, we suggest that the administration of corticosteroids should be weighed when evaluating maternal tachycardia.

The main limitation of the research in this section is that the co-administration of medications such as anti-hypertensives or tocolytics, which may also influence HR and HRV, is common in the population investigated. This is unavoidable, as the administration of these medications is part of the standard treatment protocol [59]–[61]. While we do perform a sub-analysis to demonstrate that the changes observed in HR and HRV are indeed related to the administration of corticosteroids (Appendix, **Chapter 6**) further research is needed to establish the effects of other obstetric medications on maternal HR and HRV.

The takeaway message from Section III: The administration of corticosteroids impacts non-invasive indices of autonomic regulation in women with pregnancy complications. Studies investigating maternal autonomic regulation in this population should do so before corticosteroid administration or sufficiently long thereafter.

4. Section IV: Coupling between physiological systems during pregnancy

As assessing maternal HRV and PPG pulse wave morphology are the most pragmatic solutions to longitudinally tracking autonomic regulation, we devote *Sections I, II,* and *III* to performing research essential to the implementation of such solutions. Here, in the final section, we examine additional non-invasive indices of autonomic activity. Specifically, we consider physiological coupling relationships in the pregnancy period,

which are reflective of autonomic functioning [62], [63]. Assessing physiological coupling may, in the future, provide supplementary tools for evaluating perinatal health; in the present, such assessments offer novel insights into the physiology of pregnancy.

A well-known coupling relationship exists between the cardiac and respiratory systems, i.e., cardiorespiratory coupling (CRC). Yet, the understanding of maternal CRC is severely limited. While two studies have demonstrated that aspects of CRC differ between healthy and preeclamptic pregnant women, our work in **Chapter 9** is the first to investigate how CRC differs between healthy pregnant and non-pregnant women. We demonstrate that while CRC occurred in both groups, CRC reduces during pregnancy. We assess CRC with two methods. The first is a synchrogram analysis, which assesses the synchronization between the heartbeats and the respiratory signal. Results from this analysis show that less synchronization occurs in pregnant women. Secondly, we use bivariate phase rectified signal averaging. This method captures the modulations in HR corresponding to respiratory inhalations or exhalations, or, conversely, the modulations in the respiratory signal corresponding to accelerations or decelerations in HR. We see that the modulations in each signal corresponding to the other are dampened for pregnant women.

As CRC is known to reduce under periods of physiological stress [62], [64], it stands to reason that the stress of pregnancy on the maternal body results in reduced CRC. Still, the differences in autonomic regulation between the two groups (**Chapter 2**) may also be driving differences in CRC. As our analysis is based on nighttime recordings, we stratify our analysis by sleep stages. Since sleep stages are governed by different autonomic states [43], [63], this stratification allows us to investigate the impact of autonomic activity on CRC. We found that CRC increases for the non-pregnant group from N1 to N2 to N3 (which corresponds to increasing parasympathetic activity), while for the pregnant group, the prevalence of CRC remains similar across these stages. This leads us to conclude that the reduced vagal tone in pregnant women is at least partly responsible for the lower CRC seen in this group. Furthermore, not only does assessing autonomic activity per sleep stage approximate a controlled environment (**Chapter 3** in Section 11.1), but it seems to also elucidate differences between the groups which are not apparent when assessing the full night's recording.

Finally, in **Chapter 10**, we investigate a coupling that is only found during pregnancy. Almost 50 years ago, Hildebrandt et al. assessed the HR patterns of four maternal-fetal pairs and observed a relationship between the two [65]. In the last twenty

years, research into this relationship – referred to as maternal-fetal cardiac coupling (MFCC) – has accelerated, with researchers using a variety of methods to assess different populations. Owing to the inconsistencies in the literature, questions concerning MFCC remained. Mainly, does this coupling exist? If so, could we use it to assess perinatal health? Subsequently, we perform a scoping review of the literature to ascertain the state of this research field. Most of the reviewed papers (22 out of 24) found incidences of MFCC in their study groups, regardless of the methods employed; only cross-correlation proved to be a poor method for capturing MFCC. Furthermore, based on results from methods such as transfer entropy, information seems to flow in both directions. This means that not only does the maternal cardiac system influence that of the fetus, but the fetal cardiac system also influences that of the mother, which may seem less intuitive than the prior. However, as with all coupling relationships, it is important to note that these interactions may be a result of a third system regulating both maternal and fetal cardiac systems, rather than merely an interaction between the two.

Little work has been done concerning the clinical potential of MFCC indices. Since research shows that the nature of MFCC changes with progressing pregnancy, authors have suggested that MFCC may be useful in tacking fetal development. Furthermore, two studies have shown differences in MFCC indices between pregnant women with healthy fetuses and those with fetal congenital heart disease [66]–[68]. More research in this area is warranted as limited options are available for assessing the fetus in the womb. Furthermore, non-invasive ECG measurements are gaining popularity and this modality allows for the synchronized assessment of maternal and fetal HRs. Therefore, given that indices of MFCC may become relatively easy to acquire during antenatal care, it is worth investigating whether such indices would add value in assessing perinatal health.

The takeaway message from Section IV: CRC is weakened in healthy pregnant women compared to non-pregnant controls. Furthermore, a coupling relationship exists between the maternal and fetal cardiac systems (MFCC). Owing to the sensitivity of CRC to pregnancy and the evidence in the literature that suggests that MFCC varies in complicated pregnancies, assessments of coupling may play a future role in assessing perinatal health.

5. Future research

While the research presented in this thesis is not without its limitations, it is a necessary step toward the use of non-invasive assessments of autonomic activity for the early detection of pregnancy complications. While there are likely additional obstacles to address, the most pertinent next step is to determine the trends in maternal HRV in complicated pregnancies. Such an investigation, if done prospectively, would likely require several years and the cooperation of multiple institutions. Considering the incidences of the different types of pregnancy complications (for example, around 5% for preeclampsia [4], [69]–[71]) as well as the potentially high dropout rate due to the longitudinal nature of the study, hundreds if not thousands of participants would need to be included.

The size and logistic complexity of such a study could be reduced by focusing on a specific complication, such as preeclampsia, and only including women at risk for this complication. However, we would propose an alternative. In recent years, smartwatch companies have started using data from their users for research purposes. For example, Fitbit data (Fitbit, Inc, San Francisco, USA) from 8 million people were used to determine normative ranges for HRV values [72], while in the Apple Heart Study, over 400 000 participants who were already using Apple Watches (Apple Inc, Cupertino, USA) were included to provide data for the development of algorithms to detect abnormal heart rhythms [73], [74]. Furthermore, a recent study used data from over 5 000 smartwatch users who had been diagnosed with Covid-19 to retrospectively identify HRV signatures indicating the infection in the pre-symptomatic phase [75]. Similarly, we believe that the most pragmatic option for defining the HRV trajectory of women who develop pregnancy complications is to build a study around women who are already smartwatch users. Daily data would likely be available for the participants, which would hypothetically allow for identifying the GA at which the HRV trends between healthy (**Chapter 4)** and complicated pregnancies deviate. A similar approach has already been used by WHOOP, as discussed in Section 11.2. An additional benefit of our proposed analysis is that the collected data would also offer insights into how the maternal ANS adapts during the first weeks of pregnancy, which remains one of the most significant gaps in the literature. Furthermore, using PPG data would allow for tracking features describing the morphology of the pulse wave, which would likley offer additional benefit in tracking maternal health (**Chapter 3**). Finally, a large-scale, prospective study would be needed to validate whether tracking maternal autonomic regulation throughout pregnancy indeed improves perinatal outcomes.

6. Screening for maternal complications with non-invasive assessments of autonomic activity within the current antenatal framework

Assuming that non-invasive autonomic measures are useful for the early detection of pregnancy complications, we consider how implementing this solution may complement the current antenatal care system. In middle- to high-income countries, women typically have an intake appointment at 8 to 10 weeks of gestation to confirm the vitality of the pregnancy. Thereafter, they have regular antenatal appointments with increasing frequency, from monthly to weekly, as birth approaches. At the intake appointment, women's pregnancies are typically screened as either low- or high-risk, with the latter often receiving increased monitoring and testing throughout the gestational period. We envision that all women would wear a smartwatch throughout their pregnancy, at least during the night. HRV and PPG morphology features would be calculated nightly based on data from a specific sleep stage, likely N3. These features would then be tracked against normative trajectories of these features. If a pregnancy is low-risk and trends in maternal autonomic regulation deviate from the expected norms of healthy pregnancy, the woman would be moved to a high-risk pregnancy path for increased monitoring and testing. Additionally, if abnormal maternal regulation is found in women already at high risk for a complication, appropriate additional testing and monitoring could be performed. For example, if this woman is at risk for hypertensive disorders of pregnancy, she would be asked to perform daily BP checks using an ambulatory BP cuff.

7. Final remarks

The average woman will be pregnant twice in her lifetime. Considering how common pregnancies are, it can feel surprising that research gaps concerning healthy gestation persist. We believe that four reasons are contributing to gaps in the literature on non-invasive indices of maternal autonomic regulation. First, because pregnancy is so common, there may be the assumption that maternal HRV has been more extensively researched than it has. Second, healthy pregnant women are considered a vulnerable population from an ethical standpoint, and as such, there are additional barriers to

getting institutional approval to study them. Third, perinatal HRV research often focuses on the fetus. Understandably so, as the fetus is the more vulnerable of the maternal-fetal pair and the one whose health status is more difficult to assess. And fourth, if the research primarily concerns the mother, the focus tends to be on HRV in women with pregnancy complications. The motivation driving such research is clear, as reducing the impact of pregnancy complications is one of the overarching goals of obstetric research. However, this focus sometimes lacks recognition that knowing what is normal is essential to detecting what is abnormal. Consequently, in this thesis, we endeavored to comprehensively understand normal maternal autonomic regulation, as assessed with non-invasive methods. We envision that the work presented here will form the basis for future research into dysfunctional maternal autonomic regulation, especially for the early detection of pregnancy complications. Such early detection would not only reduce perinatal morbidity and mortality but, considering the life-long impact that these complications have on the mother and her offspring, would benefit the health of the society as a whole.

References

[1] "Number of births per year," *The world counts*, Feb. 2023. https://www.theworldcounts.com/populations/world/births

[2] World Health Organization, United Nations Population Fund, Mailman School of Public Health. Averting Maternal Death and Disability, and United Nations Children's Fund (UNICEF), "Monitoring emergency obstetric care : a handbook," *Surveillance des soins obstétricaux d'urgence : manuel d'utilisation*, p. 152, 2009, Accessed: Jan. 18, 2023. [Online]. Available: https://apps.who.int/iris/handle/10665/44121

[3] Y. A. Barbitoff *et al.*, "A Data-Driven Review of the Genetic Factors of Pregnancy Complications," *IJMS*, vol. 21, no. 9, p. 3384, May 2020, doi: 10.3390/ijms21093384.

[4] "Trends in pregnancy and childbirth complications in the U.S.," Blue Cross Blue Shield Association, Jun. 2020. [Online]. Available: https://www.bcbs.com/sites/default/files/file-attachments/health-of-america-report/HoA_Maternal_Health.pdf

[5] J. Qiu, L. Chen, X. Wang, and W. Zhu, "Early-pregnancy maternal heart rate is related to gestational diabetes mellitus (GDM)," *European Journal of Obstetrics & Gynecology and Reproductive Biology*, vol. 268, pp. 31–36, Jan. 2022, doi: 10.1016/j.ejogrb.2021.11.007.

[6] L. M. Reyes *et al.*, "Sympathetic nervous system activity and reactivity in women with gestational diabetes mellitus," *Physiol Rep*, vol. 8, no. 13, Jul. 2020, doi: 10.14814/phy2.14504.

[7] C. Phaloprakarn and S. Tangjitgamol, "Risk score for predicting primary cesarean delivery in women with gestational diabetes mellitus," *BMC Pregnancy Childbirth*, vol. 20, no. 1, p. 607, Dec. 2020, doi: 10.1186/s12884-020-03306-y.

[8] X. Zhang, A. Decker, R. W. Platt, and M. S. Kramer, "How big is too big? The perinatal consequences of fetal macrosomia," *American Journal of Obstetrics and Gynecology*, vol. 198, no. 5, p. 517.e1-517.e6, May 2008, doi: 10.1016/j.ajog.2007.12.005.

[9] W. Ying, J. M. Catov, and P. Ouyang, "Hypertensive Disorders of Pregnancy and Future Maternal Cardiovascular Risk," *JAHA*, vol. 7, no. 17, p. e009382, Sep. 2018, doi: 10.1161/JAHA.118.009382.

[10] H. R. Turbeville and J. M. Sasser, "Preeclampsia beyond pregnancy: long-term consequences for mother and child," *American Journal of Physiology-Renal Physiology*, vol. 318, no. 6, pp. F1315–F1326, Jun. 2020, doi: 10.1152/ajprenal.00071.2020.

[11] C. Huang *et al.*, "Maternal hypertensive disorder of pregnancy and offspring early-onset cardiovascular disease in childhood, adolescence, and young adulthood: A national population-based cohort study," *PLoS Med*, vol. 18, no. 9, p. e1003805, Sep. 2021, doi: 10.1371/journal.pmed.1003805.

[12] "Diabetes in pregnancy: management from preconception to the postnatal period," National Institue for Health and Care Excellence, Feb. 2015. [Online]. Available: https://www.nice.org.uk/guidance/ng3/chapter/Recommendations-for-research#postnatal-treatment-for-women-diagnosed-with-gestational-diabetes

[13] E. Sheiner, "Gestational Diabetes Mellitus: Long-Term Consequences for the Mother and Child Grand Challenge: How to Move on Towards Secondary Prevention?," vol. 1, 2020.

[14] M. S. Harrison and R. L. Goldenberg, "Global burden of prematurity," *Seminars in Fetal*

and Neonatal Medicine, vol. 21, no. 2, pp. 74–79, Apr. 2016, doi: 10.1016/j.siny.2015.12.007.

[15] B. Mbarak, C. Kilewo, S. Kuganda, and B. F. Sunguya, "Postpartum depression among women with pre-eclampsia and eclampsia in Tanzania; a call for integrative intervention," *BMC Pregnancy Childbirth*, vol. 19, no. 1, p. 270, Dec. 2019, doi: 10.1186/s12884-019-2395-3.

[16] S. O'Neil *et al.*, "The High Costs of Maternal Morbidity Show Why We Need Greater Investment in Maternal Health," Commonwealth Fund, Nov. 2021. [Online]. Available: https://doi.org/10.26099/nz8s-4708

[17] A. Mate, C. Reyes-Goya, Á. Santana-Garrido, L. Sobrevia, and C. M. Vázquez, "Impact of maternal nutrition in viral infections during pregnancy," *Biochimica et Biophysica Acta (BBA) - Molecular Basis of Disease*, vol. 1867, no. 11, p. 166231, Nov. 2021, doi: 10.1016/j.bbadis.2021.166231.

[18] A. C. De Kat, J. Hirst, M. Woodward, S. Kennedy, and S. A. Peters, "Prediction models for preeclampsia: A systematic review," *Pregnancy Hypertension*, vol. 16, pp. 48–66, Apr. 2019, doi: 10.1016/j.preghy.2019.03.005.

[19] Y. Cui, B. Zhu, and F. Zheng, "Low-dose aspirin at ≤16 weeks of gestation for preventing preeclampsia and its maternal and neonatal adverse outcomes: A systematic review and meta-analysis," *Exp Ther Med*, vol. 15, no. 5, pp. 4361–4369, May 2018, doi: 10.3892/etm.2018.5972.

[20] US Preventive Services Task Force *et al.*, "Screening for Preeclampsia: US Preventive Services Task Force Recommendation Statement," *JAMA*, vol. 317, no. 16, p. 1661, Apr. 2017, doi: 10.1001/jama.2017.3439.

[21] M. Murphy, S. McHugh, L. M. O'Keeffe, R. A. Greene, P. Corcoran, and P. M. Kearney, "Preventive health counselling during antenatal care using the pregnancy risk assessment monitoring system (PRAMS) in Ireland," *BMC Pregnancy Childbirth*, vol. 20, no. 1, p. 98, Dec. 2020, doi: 10.1186/s12884-020-2756-y.

[22] L. Huynh *et al.*, "Systematic Literature Review of the Costs of Pregnancy in the US," *PharmacoEconomics*, vol. 31, no. 11, pp. 1005–1030, Nov. 2013, doi: 10.1007/s40273-013-0096-8.

[23] C. E. Kleinrouweler *et al.*, "Prognostic models in obstetrics: available, but far from applicable.," *American journal of obstetrics and gynecology*, vol. 214, no. 1, pp. 79-90.e36, Jan. 2016, doi: 10.1016/j.ajog.2015.06.013.

[24] V. A. Danilack, A. P. Nunes, and M. G. Phipps, "Unexpected complications of low-risk pregnancies in the United States," *American Journal of Obstetrics and Gynecology*, vol. 212, no. 6, p. 809.e1-809.e6, Jun. 2015, doi: 10.1016/j.ajog.2015.03.038.

[25] G. K. Pal, P. Shyma, S. Habeebullah, P. Shyjus, and P. Pal, "Spectral Analysis of Heart Rate Variability for Early Prediction of Pregnancy-Induced Hypertension," *Clinical and Experimental Hypertension*, vol. 31, no. 4, pp. 330–341, Jan. 2009, doi: 10.1080/10641960802621333.

[26] S. Rang, H. Wolf, G. A. Montfrans, and J. M. Karemaker, "Non–invasive assessment of autonomic cardiovascular control in normal human pregnancy and pregnancy- associated hypertensive disorders: a review," *Journal of Hypertension*, vol. 20, no. 11, pp. 2111–2119, 2002.

[27] F. Shaffer and J. P. Ginsberg, "An Overview of Heart Rate Variability Metrics and Norms," *Front. Public Health*, vol. 5, p. 258, Sep. 2017, doi: 10.3389/fpubh.2017.00258.

[28] K. Grym *et al.*, "Feasibility of smart wristbands for continuous monitoring during pregnancy and one month after birth," *BMC Pregnancy Childbirth*, vol. 19, no. 1, p. 34, Dec. 2019, doi: 10.1186/s12884-019-2187-9.

[29] A. Maugeri, M. Barchitta, and A. Agodi, "How Wearable Sensors Can Support the Research on Foetal and Pregnancy Outcomes: A Scoping Review," *JPM*, vol. 13, no. 2, p. 218, Jan. 2023, doi: 10.3390/jpm13020218.

[30] M. Bester, R. Joshi, M. Mischi, J. O. E. H. Van Laar, and R. Vullings, "On the distinct differences in autonomic regulation between healthy pregnant and non-prengnant women - a HRV analysis," *Submitted*, 2023.

[31] J. Koenig and J. F. Thayer, "Sex differences in healthy human heart rate variability: A meta-analysis," *Neuroscience & Biobehavioral Reviews*, vol. 64, pp. 288–310, May 2016, doi: 10.1016/j.neubiorev.2016.03.007.

[32] J. Zhang, "Effect of Age and Sex on Heart Rate Variability in Healthy Subjects," *Journal of Manipulative and Physiological Therapeutics*, vol. 30, no. 5, pp. 374–379, Jun. 2007, doi: 10.1016/j.jmpt.2007.04.001.

[33] A. Dart, "Gender, sex hormones and autonomic nervous control of the cardiovascular system," *Cardiovascular Research*, vol. 53, no. 3, pp. 678–687, Feb. 2002, doi: 10.1016/S0008-6363(01)00508-9.

[34] V. L. Brooks, Q. Fu, Z. Shi, and C. M. Heesch, "Adaptations in autonomic nervous system regulation in normal and hypertensive pregnancy," in *Handbook of Clinical Neurology*, Elsevier, 2020, pp. 57–84. doi: 10.1016/B978-0-444-64239-4.00003-5.

[35] Z. Sharifiheris, A. Rahmani, J. Onwuka, and M. Bender, "The Utilization of Heart Rate Variability for Autonomic Nervous System Assessment in Healthy Pregnant Women: Systematic Review," *JMIR Bioinform Biotech*, vol. 3, no. 1, p. e36791, Nov. 2022, doi: 10.2196/36791.

[36] A. Bauer *et al.*, "Deceleration capacity of heart rate as a predictor of mortality after myocardial infarction: cohort study," *The Lancet*, vol. 367, no. 9523, pp. 1674–1681, May 2006, doi: 10.1016/S0140-6736(06)68735-7.

[37] L. M. Reyes, C. W. Usselman, M. H. Davenport, and C. D. Steinback, "Sympathetic Nervous System Regulation in Human Normotensive and Hypertensive Pregnancies.," *Hypertension (Dallas, Tex. : 1979)*, vol. 71, no. 5, pp. 793–803, May 2018, doi: 10.1161/HYPERTENSIONAHA.117.10766.

[38] D. Casati *et al.*, "Maternal cardiac deceleration capacity: a novel insight into maternal autonomic function in pregnancies complicated by hypertensive disorders and intrauterine growth restriction," *European Journal of Obstetrics & Gynecology and Reproductive Biology*, vol. 206, pp. 6–11, Nov. 2016, doi: 10.1016/j.ejogrb.2016.08.007.

[39] S. Sammito and I. Böckelmann, "Reference values for time- and frequency-domain heart rate variability measures," *Heart Rhythm*, vol. 13, no. 6, pp. 1309–1316, Jun. 2016, doi: 10.1016/j.hrthm.2016.02.006.

[40] M. Bester, R. Joshi, A. Linders, M. Mischi, J. O. E. H. van Laar, and R. Vullings, "Characterizing the effect of demographics, cardiorespiratory factors, and inter-subject variation on maternal heart rate variability in pregnancy with statistical modeling: a retrospective observational analysis," *Sci Rep*, vol. 12, no. 1, p. 19305, Nov. 2022, doi: 10.1038/s41598-022-21792-2.

[41] S. Fangming, L. Zhaoxi, S. Xiurong, H. Nan, W. Lei, and L. Xiaomin, "The Pulse Wave Analysis of Normal Pregnancy: Investigating the Gestational Effects on Photoplethysmographic Signals," *Bio-Medical Materials and Engineering*, no. 1, pp. 209–219, 2014, doi: 10.3233/BME-130801.

[42] Y. Sheng and L. Zhu, "The crosstalk between autonomic nervous system and blood vessels," *Int J Physiol Pathophysiol Pharmacol*, vol. 10, no. 1, pp. 17–28, 2018.

[43] M. G. Miglis, "Sleep and the Autonomic Nervous System," in *Sleep and Neurologic Disease*, Elsevier, 2017, pp. 227–244. doi: 10.1016/B978-0-12-804074-4.00018-2.

[44] B. M. Wulterkens *et al.*, "It is All in the Wrist: Wearable Sleep Staging in a Clinical Population versus Reference Polysomnography," *NSS*, vol. Volume 13, pp. 885–897, Jun. 2021, doi: 10.2147/NSS.S306808.

[45] F. Cerritelli *et al.*, "A Review on the Vagus Nerve and Autonomic Nervous System During Fetal Development: Searching for Critical Windows," *Front. Neurosci.*, vol. 15, p. 721605, Sep. 2021, doi: 10.3389/fnins.2021.721605.

[46] S. P. Rowan, C. L. Lilly, E. A. Claydon, J. Wallace, and K. Merryman, "Monitoring one heart to help two: heart rate variability and resting heart rate using wearable technology in active women across the perinatal period," *BMC Pregnancy Childbirth*, vol. 22, no. 1, p. 887, Nov. 2022, doi: 10.1186/s12884-022-05183-z.

[47] S. Moors *et al.*, "Heart rate variability in hypertensive pregnancy disorders: a systematic review," *Pregnancy Hypertension*, Mar. 2020, doi: 10.1016/j.preghy.2020.03.003.

[48] D. Yousif *et al.*, "Autonomic Dysfunction in Preeclampsia: A Systematic Review," *Front. Neurol.*, vol. 10, Aug. 2019, doi: 10.3389/fneur.2019.00816.

[49] M. W. Kemp, J. P. Newnham, J. G. Challis, A. H. Jobe, and S. J. Stock, "The clinical use of corticosteroids in pregnancy," *Hum. Reprod. Update*, p. dmv047, Nov. 2015, doi: 10.1093/humupd/dmv047.

[50] A. Seeck, M. Baumert, C. Fischer, A. Khandoker, R. Faber, and A. Voss, "Advanced Poincaré plot analysis differentiates between hypertensive pregnancy disorders," *Physiol. Meas.*, vol. 32, no. 10, pp. 1611–1622, Oct. 2011, doi: 10.1088/0967-3334/32/10/009.

[51] K. M. Verdurmen, J. Renckens, J. O. van Laar, and S. G. Oei, "The influence of corticosteroids on fetal heart rate variability: a systematic review of the literature," *Obstetrical & gynecological survey*, vol. 68, no. 12, pp. 811–824, Dec. 2013, doi: 10.1097/OGX.0000000000000009 [doi].

[52] K. M. J. Verdurmen *et al.*, "The influence of betamethasone on fetal heart rate variability, obtained by non-invasive fetal electrocardiogram recordings," *Early Human Development*, vol. 119, pp. 8–14, Apr. 2018, doi: 10.1016/j.earlhumdev.2018.02.011.

[53] L. Noben, K. M. J. Verdurmen, G. J. J. Warmerdam, R. Vullings, S. G. Oei, and J. O. E. H. van Laar, "The fetal electrocardiogram to detect the effects of betamethasone on fetal heart rate variability," *Early Human Development*, vol. 130, pp. 57–64, 2019, doi: 10.1016/j.earlhumdev.2019.01.011.

[54] S. V. Khlybova, V. I. Tsirkin, S. A. Dvoryanskii, I. A. Makarova, and A. N. Trukhin, "Heart rate variability in normal and complicated pregnancies," *Hum Physiol*, vol. 34, no. 5, pp. 625–632, Sep. 2008, doi: 10.1134/S0362119708050113.

[55] S. V. Koenen, E. J. H. Mulder, L. D. Wijnberger, and G. H. A. Visser, "Transient Loss of the

Diurnal Rhythms of Fetal Movements, Heart Rate, and Its Variation after Maternal Betamethasone Administration," *Pediatr Res*, vol. 57, no. 5 Part 1, pp. 662–666, May 2005, doi: 10.1203/01.PDR.0000159762.50504.1F.

[56] L. J. Green *et al.*, "Gestation-Specific Vital Sign Reference Ranges in Pregnancy," *Obstetrics & Gynecology*, vol. 135, no. 3, pp. 653–664, Mar. 2020, doi: 10.1097/AOG.0000000000003721.

[57] L. Loerup *et al.*, "Trends of blood pressure and heart rate in normal pregnancies: a systematic review and meta-analysis," *BMC Med*, vol. 17, no. 1, p. 167, Dec. 2019, doi: 10.1186/s12916-019-1399-1.

[58] S. Haddad, R. Souza, J. Cecatti, and the WHO Intrapartum Care Algorithms Working Group, "Management of maternal pulse and blood pressure abnormalities during labour and childbirth: evidence-based algorithms for intrapartum care decision support," *BJOG*, pp. 1471–0528.16776, Apr. 2022, doi: 10.1111/1471-0528.16776.

[59] "ACOG practice bulletin no. 127: Management of preterm labor.," *Obstetrics and gynecology*, vol. 119, no. 6, pp. 1308–1317, Jun. 2012, doi: 10.1097/AOG.0b013e31825af2f0.

[60] "ACOG Practice Bulletin No. 188: Prelabor Rupture of Membranes.," *Obstetrics and gynecology*, vol. 131, no. 1, pp. e1–e14, Jan. 2018, doi: 10.1097/AOG.0000000000002455.

[61] "ACOG Practice Bulletin No. 202: Gestational Hypertension and Preeclampsia," *Obstetrics and gynecology*, vol. 133, no. 1, p. e-e25, Jan. 2019, doi: 10.1097/AOG.0000000000003018.

[62] S. Schulz *et al.*, "Cardiovascular and cardiorespiratory coupling analyses: a review," *Phil. Trans. R. Soc. A.*, vol. 371, no. 1997, p. 20120191, Aug. 2013, doi: 10.1098/rsta.2012.0191.

[63] R. P. Bartsch, A. Y. Schumann, J. W. Kantelhardt, T. Penzel, and P. Ch. Ivanov, "Phase transitions in physiologic coupling," *Proc. Natl. Acad. Sci. U.S.A.*, vol. 109, no. 26, pp. 10181–10186, Jun. 2012, doi: 10.1073/pnas.1204568109.

[64] A. J. Garcia, J. E. Koschnitzky, T. Dashevskiy, and J.-M. Ramirez, "Cardiorespiratory coupling in health and disease," *Autonomic Neuroscience*, vol. 175, no. 1–2, pp. 26–37, Apr. 2013, doi: 10.1016/j.autneu.2013.02.006.

[65] G. Hildebrandt and H. R. Klein, "Uber die Phasenkoordination von miitterlichem und foetalem Herzrhythmus wiihrend der Schwangerschaft," *Klin. Wochenschr*, vol. 57, pp. 87–91.

[66] H. M. Alangari, Y. Kimura, and A. H. Khandoker, "Preliminary Evaluation of Fetal Congenital Heart Defects Changes on Fetal-Maternal Heart Rate Coupling Strength," in *2018 40th Annual International Conference of the IEEE Engineering in Medicine and Biology Society (EMBC)*, Honolulu, HI: IEEE, Jul. 2018, pp. 251–254. doi: 10.1109/EMBC.2018.8512272.

[67] A. H. Khandoker *et al.*, "Quantification of maternal-fetal cardiac couplings in normal and abnormal pregnancies applying high resolution joint symbolic dynamics," *Mathematical Biosciences and Engineering*, vol. 17, no. 1, pp. 802–813, 2020, doi: 10.3934/mbe.2020042.

[68] A. H. Khandoker, S. Schulz, H. M. Al-Angari, A. Voss, and Y. Kimura, "Alterations in Maternal–Fetal Heart Rate Coupling Strength and Directions in Abnormal Fetuses," *Front. Physiol.*, vol. 10, p. 482, Apr. 2019, doi: 10.3389/fphys.2019.00482.

[69] J. O. Lo, J. F. Mission, and A. B. Caughey, "Hypertensive disease of pregnancy and maternal mortality," *Current Opinion in Obstetrics & Gynecology*, vol. 25, no. 2, pp. 124–132, Apr. 2013, doi: 10.1097/GCO.0b013e32835e0ef5.

[70] B. W. J. Mol, C. T. Roberts, S. Thangaratinam, L. A. Magee, C. J. M. de Groot, and G. J. Hofmeyr, "Pre-eclampsia," *The Lancet*, vol. 387, no. 10022, pp. 999–1011, Mar. 2016, doi: 10.1016/S0140-6736(15)00070-7.

[71] M. Forrest *et al.*, "Arterial stiffness measurements in pregnancy as a predictive tool for hypertensive disorders of pregnancy and preeclampsia: Protocol for a systematic review and meta-analysis," *European Journal of Obstetrics & Gynecology and Reproductive Biology: X*, vol. 13, p. 100141, Jan. 2022, doi: 10.1016/j.eurox.2022.100141.

[72] A. Natarajan, A. Pantelopoulos, H. Emir-Farinas, and P. Natarajan, "Heart rate variability with photoplethysmography in 8 million individuals: a cross-sectional study," *The Lancet Digital Health*, vol. 2, no. 12, pp. e650–e657, Dec. 2020, doi: 10.1016/S2589-7500(20)30246-6.

[73] M. P. Turakhia *et al.*, "Rationale and design of a large-scale, app-based study to identify cardiac arrhythmias using a smartwatch: The Apple Heart Study," *American Heart Journal*, vol. 207, pp. 66–75, Jan. 2019, doi: 10.1016/j.ahj.2018.09.002.

[74] M. V. Perez *et al.*, "Large-Scale Assessment of a Smartwatch to Identify Atrial Fibrillation," *N Engl J Med*, vol. 381, no. 20, pp. 1909–1917, Nov. 2019, doi: 10.1056/NEJMoa1901183.

[75] T. Mishra *et al.*, "Pre-symptomatic detection of COVID-19 from smartwatch data," *Nat Biomed Eng*, vol. 4, no. 12, pp. 1208–1220, Dec. 2020, doi: 10.1038/s41551-020-00640-6.

Journal articles

[1] M. Bester, M.J. Almario Escorcia, P. Fonseca, M. Mollura, M.M. van Gilst, R. Barbieri, M. Mischi, J.O.E.H. van Laar, R. Vullings, and R. Joshi, "The impact of healthy pregnancy on features of heart rate variability and pulse wave morphology derived from wrist-worn photoplethysmography," *Submitted*, 2023.

[2] M. Bester, G. Perciballi, P. Fonseca, M.M. van der Gilst, M. Mischi, J.O.E.H. van Laar, R. Vullings, and R. Joshi, "Cardiorespiratory coupling is altered during healthy pregnancy," *Submitted*, 2023.

[3] M. Bester, T.J. Nichting, R. Joshi, L. Aissati, S.G. Oei, M. Mischi, J.O.E.H. van Laar, and R. Vullings, "Change in maternal heart rate variability and photoplethysmography morphology in response to corticosteroid administration," *Submitted*, 2023.

[4] T.J. Nichting*, M. Bester*, R. Joshi, M. Mischi, M. van der Ven, D.A.A. van der Woude, S.G. Oei, J.O.E.H. van Laar, and R. Vullings, "Evidence and clinical relevance of maternal-fetal cardiac coupling: a scoping review," *Accepted for publication, PLOS One*, 2023.

[5] M. Bester, R. Joshi, M. Mischi, J.O.E.H. van Laar, and R. Vullings, "On the distinct differences in autonomic regulation between pregnant and non-pregnant women - a heart rate variability analysis," *Physiol. Meas.*, vol. 44, no. 5, p. 055001, May 2023, doi: 10.1088/1361-6579/acce1e.

[6] M. Bester, R. Joshi, J.H.A.M. van Dooren, M. Mischi, R. Vullings, and J.O.E.H. van Laar, "Changes in Maternal Heart Rate and Autonomic Regulation following the Antenatal Administration of Corticosteroids: A Secondary Analysis," *JCM*, vol. 12, no. 2, p. 588, Jan. 2023, doi: 10.3390/jcm12020588.

[7] M. Bester, R. Joshi, A. Linders, M. Mischi, J.O.E.H. van Laar, and R. Vullings, "Characterizing the effect of demographics, cardiorespiratory factors, and inter-subject variation on maternal heart rate variability in pregnancy with statistical modeling: a retrospective observational analysis," *Sci Rep*, vol. 12, no. 1, p. 19305, Nov. 2022, doi: 10.1038/s41598-022-21792-2.

[8] M. Bester, R. Joshi, M. Mischi, J.O.E.H. van Laar, and R. Vullings, "Longitudinally Tracking Maternal Autonomic Modulation During Normal Pregnancy With Comprehensive Heart Rate Variability Analyses," *Front. Physiol.*, vol. 13, p. 874684, May 2022, doi: 10.3389/fphys.2022.874684.

[9] M. Bester*, S. Moors*, R. Joshi, T.J. Nichting, M.B. van der Hout-van der Jagt, M. Mischi, R. Vullings, and J.O.E.H. van Laar, "Changes in Maternal Heart Rate Variability in Response to the Administration of Routine Obstetric Medication in Hospitalized Patients: Study Protocol for a Cohort Study (MAMA-Heart Study)," *Clinics and Practice*, vol. 11, no. 1, pp. 13–25, Jan. 2021, doi: 10.3390/clinpract11010004.

* equal contribution

Conference talks and proceedings

[1] M. Bester, R. Rizea, R. Joshi, M. Mischi, J.O.E.H. Van Laar, and R. Vullings, “Maternal autonomic responsiveness is attenuated in healthy pregnancy: a phase rectified signal averaging analysis,” in *2022 44th Annual International Conference of the IEEE Engineering in Medicine & Biology Society (EMBC)*, Glasgow, Scotland, United Kingdom: IEEE, Jul. 2022, pp. 4982–4986. doi: 10.1109/EMBC48229.2022.9870894.

[2] M. Bester, R. Joshi, P.J.A. Snellings, M. Mischi, J.O.E.H. van Laar, and R. Vullings, “Longitudinal Assessment of Fetal Heart Rate Variability During Pregnancy,” in 2022 *Computing in Cardiology (CinC)*, Tampere, Finland: IEEE, Sep. 2022 doi: 10.22489/CinC.2022.271.

[3] M. Bester, R. Joshi, M. Mischi, J.O.E.H. Van Laar, and R. Vullings, “The Effects of Advancing Gestation on Maternal Autonomic Response,” in *2021 Computing in Cardiology (CinC)*, Brno, Czech Republic: IEEE, Sep. 2021, pp. 1–4. doi: 10.23919/CinC53138.2021.9662852.

[4] M. Bester, D. Van Den Heever, R. Joshi, and K. Dellimore, “A study of short cessations and temporal dynamics of breathing in preterm infants,” in *2018 3rd Biennial South African Biomedical Engineering Conference (SAIBMEC)*, Stellenbosch: IEEE, Apr. 2018, pp. 1–4. doi: 10.1109/SAIBMEC.2018.8363174.

Invited talk

M. Bester, "*Towards the early detection of pregnancy complications: Assessing autonomic dysregulation to identify high-risk pregnancies*", presented at the Nuffield Department of Women's & Reproductive Health, University of Oxford, UK, 2022.

Acknowledgements

Recently, I ran into a friend from high school. While catching up, I told him about the doctoral research that I have been pursuing over the last few years. He remarked that this was precisely in line with the plans I had for my future over a decade ago. I had long since forgotten the starting point of this road that I have been on for ten years and, suddenly, I had the wonderful and somewhat bewildering realization that I was now achieving a goal so long in the making. I first want to honor God for this, who provided me with these opportunities and enabled me far beyond my own abilities. In the end, this dissertation has become much more than I hoped it would be when I started in March 2019. It is certainly more than I thought it could be a year later when Covid brought the world – and with it, the clinical study intended to be the center point of this dissertation – to a grinding halt. Even though this book is surely a product of hard work and sound guidance by my supervisory team, it is also the result of what most people would see as several lucky breaks but which I know to be many answered prayers.

I was fortunate that this sound guidance was given to me by a multi-disciplinary team of four, working in three different sectors. The first of these is my first promotor, prof. dr. ir. Mischi. Massimo, your willingness to help was evident from your late-night emails with one last suggestion for a paper or rebuttal, as well as your willingness to always give me a few minutes of your time, even when I could see you were swamped with meetings and deadlines. The BM/d lab is a warm and friendly place to work, which is not always the case in academia. This environment would not be possible if you did not set the tone for it.

Secondly, my second promotor and daily supervisor, dr. ir. Vullings. Rik, thank you for your constant support during my PhD. You were a calm, sure presence in uncertain times, of which there were many in the last four years. You gave me a lot of freedom to explore different options and to learn from my own mistakes while also quickly pointing out when I have gone down the wrong path. I enjoyed working in such an environment and it allowed me to be productive. On a different note, I also respected how you prioritize your family and set the necessary boundaries with work. It was a refreshing attitude in an often work-obsessed environment and a lesson I will take with me into my career.

Third, my co-promotor and clinical supervisor, dr. van Laar. Judith, I enjoyed working with you and, as an engineer, was thankful for the experience of spending time in a clinical environment. I could learn clinical insights from you which no amount of literature research would provide. Moreover, despite your numerous clinical and academic obligations, you always made time to help me with what I needed, even to the point where you were translating medical files so I could gather the metadata for one of our papers. This was surely not part of a typical day for you but you always did what needed to be done with a joyful attitude and I sincerely appreciated it.

Last but in no way least, dr. ir. Joshi, my academic advisor at Philips Research. Rohan, people rightly say that a PhD is a lonely journey but you did your best to make sure that mine rarely was. When I started you told me that you viewed a PhD candidacy as one of the last true apprenticeships left in modern times and I can attest that you treated it as such. You were remarkably intentional in your role as advisor and taught me all that you could, which was surely limited by my ability to absorb information rather than your wealth of knowledge concerning everything from writing and reasoning to economics and agriculture. I'm thankful to end this journey with a new friend.

I would also like to extend my thanks to my committee members, prof. dr. Signorini, prof. dr. ir. van Pul, and dr. Georgieva, for reviewing my thesis. Due to some technical difficulties, this is a task you eventually had to perform under quite some time pressure. My sincerest thanks that you handled the situation with so much grace. Furthermore, dr. Georgieva, I was particularly thankful for the opportunity to present my work to your group in 2022. I will remember it as one of the highlights of the past four years.

This dissertation was done in collaboration between academic, clinical, and industrial partners. Between TU/e, Máxima MC, and Philips Research, there are too many people to thank individually. However, I would like to mention a few. Dr. Suzanne Moors and drs. Thomas Nichting, I am thankful to have been able to work with you and gain a clinical perspective on the work we were doing. At TU/e, a warm thank you to all my fellow BM/d PhDs over the years. The many talks over lunches and beers on a Thursday made the PhD that much more enjoyable. A special thank you to Iris Huijben and Elisabetta Peri; we started our post-graduate studies in the lab at approximately the same time and I always felt that I had a friend in you both. Finally, at Philips Research, a word of thanks to Mohammed Meftah and Sonja van Harten. Mohammed, you always provided some much-needed perspective when I felt overwhelmed by the small

world of my PhD. Sonja, thank you for offering up a large chunk of your time to help a bewildered first-year PhD student understand privacy law. When I think back to the early days of my study, I remember our meetings fondly. Furthermore, I am grateful to the two interns I supervised at Philips, Giulia Perciballi and María José Almario Escorcia. Working with you was one of my richest learning experiences. Ultimately, each of you was essential to a chapter in this book.

Finally, a thank you to the friends I have made here during my study; you know who you are. You were kind enough to listen to me when I felt overwhelmed and wise enough to tell me to stop complaining after a while and remember that there is so much more to life than this dissertation. A special thank you to André, Mariette, and Annika who patiently endured living with a doctoral student, with an extra thank you to Annika, who designed the cover and layout of this book. Finally, I am grateful to my family who value education and who never gave me reason to doubt that I can do what I set my mind to. 'Where there is a will, there is a way', as my mother likes to say.

Speaking of mothers, as a final note I want to express my gratitude to the hundreds of women who were willing to take part in the studies analyzed in this dissertation. I hope that the importance of maternal health during pregnancy is evident to the reader of this book and that the work presented here will be a meaningful step toward making pregnancies safer for women.

About the author

Maretha Bester was born on 18 April 1994 in Paarl, South Africa, where she obtained her high school diploma at Paarl Girls' High in 2012. In 2016, she graduated with her bachelor's degree in mechatronic engineering from the University of Stellenbosch, South Africa. Thereafter, she pursued a master's degree in mechatronic engineering at the same institution as part of the Biomedical Research Group. Her research focused on characterizing the respiratory dynamics of preterm infants. During this period, she also carried out a research internship in the Patient Care and Monitoring department at Philips Research in Eindhoven, the Netherlands. She graduated with her master's degree in 2019. In the same year, she relocated to Eindhoven, the Netherlands to start her doctoral degree as part of the Biomedical Diagnostics Lab within the group of Signal Processing Systems at the Eindhoven University of Technology. Her research centered on improving the monitoring of maternal health during pregnancy. The research, of which the results are presented in this dissertation, was performed in a collaborative framework between the Eindhoven University of Technology, Philips Research, and Máxima Medical Center – as part of the Eindhoven MedTech Innovation Centre.